UNIVERSITÉ DU QUÉBEC EN ABITIBI-TÉMISCAMINGUE

COMPORTEMENT HYDRO-BIO-GÉO-CHIMIQUE DE SYSTÈMES PASSIFS DE TRAITEMENT DU DRAINAGE MINIER ACIDE FORTEMENT CONTAMINÉ EN FER

THÈSE

PRÉSENTÉE

COMME EXIGENCE PARTIELLE

DU DOCTORAT EN SCIENCES DE L'ENVIRONNEMENT

PAR

THOMAS GENTY

FÉVRIER 2012

À mes parents, mon frère, ma famille, mes amis et surtout à Caroline.

« Lorsque nous nous livrons pour la première fois à l'étude d'une science, nous sommes par rapport à cette science, dans un état très-analogue à celui dans lequel sont les enfans, & la marche que nous avons à suivre est précisément celle que suit la nature dans la formation de leurs idées. De même que dans l'enfant l'idée est un effet de la sensation, que c'est la sensation qui fait naître l'idée ; de même aussi pour celui qui commence à se livrer à l'étude des sciences physiques, les idées ne doivent être qu'une conséquence, une suite immédiate d'une expérience ou d'une observation. »

Antoine Laurent de Lavoisier, Traité élémentaire de chimie : Discours préliminaire, 1789.

REMERCIEMENTS

Je tiens premièrement à remercier mon directeur de thèse, Bruno Bussière, pour m'avoir donné l'occasion de faire ce projet au sein de l'Université du Québec en Abitibi-Témiscamingue, ainsi que pour tout l'encadrement et le soutien nécessaire à cette aventure. Je tiens aussi à remercier mes co-encadrants, Mostafa Benzaazoua et Gérald Zagury, pour leur aide, notamment lors de la correction des articles, et les membres de mon comité de thèse, Vincent Cloutier et Isabelle Demers, pour leurs conseils lors de l'écriture du projet, de la synthèse environnementale et pour la correction de mon fameux « franglais ». Je remercie aussi les partenaires de la Chaire CRSNG-Poly-Uqat en Environnement et gestion des rejets miniers (particulièrement le MRNF pour avoir financé le projet de construction au site Lorraine) et la Chaire de Recherches du Canada en Restauration des sites miniers abandonnés pour avoir financer cette étude.

Je tiens également à saluer mes amis (ex-)étudiants à savoir Sylvette, Bruno, Hassan, Véronique, Samuel, Virginie, Marie-Pier, Jovette, Sabah, Geneviève, Thomas (ancien numéro 1), Drissa, Erol, Aissa, Nacim, Ichrak, Benoit, les collègues de foresterie et les stagiaires. Félicitations à tout ceux qui ont terminé leur stage, maîtrise ou thèse avec succès et bonne continuation aux autres. Je suis heureux de vous avoir côtoyé tout ce temps. Merci aussi à tous le personnel de l'URSTM et des chaires (Mélanie, Tikou, Karen, Caroline, Raphaël, David, Denis, Li, Nil, Mélinda, Janie, Louise, Karl, Abdel, Carmen, Mamert, Alain, Olivier, Yvan, Richard, Rachid, Evgénia et Mathieu, mon chimiste préféré, etc., avec qui j'ai aimé passé tout ce temps (plus de quatre ans en tout !). Merci aussi à Robin qui m'a initié aux joies des biofiltres et des drains calcaires. J'espère n'avoir oublié personne et merci à tous !

Je remercie aussi ma Caroline qui m'a supporté durant ces quatre années de doctorat ainsi que pour son aide lors des corrections.

Pour finir, je tiens à remercier tout spécialement notre cher vieil Antoine et ses confrères alchimistes, sans qui la chimie moderne n'aurait pas commencée. Je remercie aussi la pollution sans qui nous n'aurions pas de travail.

TABLE DES MATIÈRES

LISTE DES FIGURES

LISTE DES TABLEAUX

LISTE DES SYMBOLES ET ABRÉVIATIONS

a et A: aire (cm^2)

A_s : surface spécifique (m^2/m^3 or m^{-1})

ALD: drain anoxique calcaire

AMD: drainage minier acide

b: constante de Langmuir (L/mg)

BET: mesure de la surface spécifique selon le modèle de Brunauer, Emmett et Teller

BPSR: biofiltre passif sulfato-réducteur

BSR: bactérie sulfato-réductrice

C_e: concentration à l'équilibre (mg/g)

CEBC: couverture à effet de barrière capillaire

CEC: capacité d'échange cationique (meq/g)

C_i et C_o: concentration initiale (mg/g)

COD: carbone organique dissou (mg/L)

COT: carbone organique total (%)

$C_{surface}$: concentration à la surface du solide (mg/L).

C_t: concentration au temps t (mg/g)

CT: carbone total (%)

$C_{U:}$ coefficient d'uniformité

$\overline{d}$: moyenne des différences entre deux paires de valeurs

d_i: différences entre deux paires de valeurs

d_p : diamètre de la particule (m)

$\frac{dH}{dL}$: gradient hydraulique

DAC: drain anoxique calcaire

DCO : drain calcaire oxique

DMA: drainage minier acide

DOC: carbone organique dissou (mg/L)

DOL-X: drain dolomitique X

DSC: calorimétrie différentielle à balayage

DRX: diffraction des rayons X

D_x: diamètre passant à x %

e.g.: exempli gratia

EDS: spectrométrie à dispersion d'énergie

Eh: potentiel d'oxydoréduction corrigé par rapport à l'électrode standard à hydrogène (mV)

d_{i+1} et d_i : diamètre de deux tamis consécutifs (m)

$F_{a,b}^{0.05}$: valeur statistique de Fisher en fonction des degrés de liberté a et b de deux colonnes pour un intervalle de confiance de 95%

$f(d_p)$: fonction de fréquence d'apparition du diamètre d_p

FTIR: spectroscopie infrarouge à transformée de Fourrier

G_s: densité spécifique

HATR: réflection horizontale totale atténuée

HDPE: polyéthylène haute densité

HRT: temps de rétention hydraulique

h_x : charge de colonne d'eau (cm)

i.e.: id est

ICP-AES: inductively coupled plasma- spectroscopie d'émission atomique

J_{CaCO_3} : flux de carbonate dissous (mol/jour)

k_d: constante cinétique de diffusion interne ($mg.g^{-1}.s^{-1/2}$),

k_f: constante de Freundlich (mg/g)

k_{fe}: constante cinétique de diffusion externe (cm/s)

k_{sat} : conductivité hydraulique saturée (cm/s)

k_x: constante cinétique de 1er ou 2nd ordre (s^{-1}, $g.mg.s^{-1}$)

L: longueur (cm)

m_r: ratio entre la masse de sorbant et le volume de solution (g/L)

m et M: masse (g, kg)

m_i : masse retenue dans le tamis i (g)

$M_x(t)$: masse au temps t (kg)

MEB: microscopie électronique à balayage

MEND: mine environment neutral drainage program

MRNF: ministère des ressources naturelles et fauniques

n: constante de Freundlich

N: nombre de paire

n: porosité

NSERC: conseil de recherche en sciences naturelles et de génie du Canada

NTK: azote total Kjeldahl (%)

ORP: potentiel d'oxydoréduction non corrigé par rapport à l'électrode standard à hydrogène (mV)

Q: débit (L/jour)

q_e: quantité adsorbée à l'équilibre (mg/g)

$q_{e,Freundlich}$: quantité adsorbée à l'équilibre calculée avec l'équation de Freundlich (mg/g)

q_{max}: quantité maximale adsorbée (mg/g)

q_t: quantité adsorbée au temps t (mg/g)

$q_{t,\exp}$: quantité expérimentale adsorbée au temps t (mg/g)

$q_{t,theo}$: quantité adsorbée théorique calculée au temps t (mg/g)

R^2: coefficient de corrélation

rpm: tour par minute

s_d: déviation standard des différence de paires.

SEM: microscopie électronique à balayage

SEP: extraction séquentielle

SHE: électrode standard à hydrogène

SRB: bactérie sulfato-reductrice

SRPB: bioréacteur passive sulpfato-reducteur

S_s : surface spécifique (m^2/g)

SSE: somme des carrés des erreurs

t: valeur du test de Student

TC: carbone total (%)

TGA: analyse thermogravimétrique

TIC: carbone inorganique total

TKN: azote total Kjeldahl (%)

TOC: carbone organique total (%)

TRH: temps de rétention hydraulique

UQAT: université du Québec en Abitibi Témiscamigue

V: volume (mL, L, cm^3)

V_t: volume total (L)

V_v: volume de vide (L)

XPS : spectroscopie des photoélectrons X

XRD: diffraction des rayons X

μ: moyenne

τ: temps de séjour (s)

Γ : facteur de forme

$[X]$: concentration de l'élément X (mg/L)

$[X]_e$: concentration de X dans l'effluent (mol/L)

$[X]_i$: concentration initiale de X (mol/L)

% (v/v): pourcentage volumique

%(w/w) et %(wt): pourcentage massique

2D et 1D: 2 et 1 dimension

RÉSUMÉ

Le drainage minier acide (DMA) fortement concentré en fer (>500 mg/L) est fréquemment retrouvé dans les mines en activité et fermées, qui exploitent ou ont exploité des gisements riches en sulfures de fer. Le traitement de ce type de DMA ce fait traditionnellement dans des usines utilisant des méthodes actives. Toutefois, pour les mines fermées ou abandonnées, la construction et le maintien d'usines de traitement ne constituent pas une solution environnementale acceptable à long terme. Les traitements passifs, peu demandant en maintenance et en énergie, deviennent alors une alternative intéressante. De plus, les systèmes de traitements passifs utilisent des matériaux naturels ou des déchets et permettent, dans plusieurs cas, d'atteindre une qualité d'eau comparable à celle que l'on retrouverait en sortie d'usine de traitement.

Toutefois, dans le cas où des drainages miniers acides fortement contaminés en fer sont traités, les traitements passifs peuvent avoir des performances limitées. Des études récentes de Neculita (2008) et Potvin (2009) ont montré que les biofiltres passifs sulfato-réducteurs (BPSR) et les drains calcaires (oxiques ou anoxiques nommés DCO et DAC respectivement) ne permettent pas de traiter efficacement des DMA ayant des concentrations en fer de plus de 500 mg/L. Dans une de ces études, le biofiltre passif sulfato-réducteur s'est même colmaté à cause des précipités de fer.

Étant donné que l'utilisation seule de BPSR ou de drains calcaires ne permet pas d'atteindre un niveau de traitement acceptable, l'objectif principal de cette étude est donc de déterminer quelle serait la filière de traitement optimale afin de traiter un DMA fortement concentré en fer (autour de 4000 mg/L). L'objectif secondaire est aussi de transposer les résultats obtenus en laboratoire afin de construire une filière de traitement sur le terrain. Pour atteindre ces objectifs, le travail de laboratoire a été divisé en trois grandes thématiques. Dans un premier temps, les matériaux utilisés dans la filière de traitement (matériaux organiques et cendres de bois) ont été caractérisés de façon à connaître leurs propriétés physiques (capacité d'échange cationique, surface spécifique, densité, granulométrie, par exemple), chimiques (carbone organique total et azote total entre autres) et microbiologiques (dénombrement des bactéries sulfato-réductrices par exemple). Par la suite, des tests batch ont permis de déterminer leurs capacités de sorption du fer et les cinétiques de sorption. La seconde partie consiste ensuite à déterminer les efficacités de traitement des matériaux, ayant le plus grand potentiel selon les tests batch, dans des colonnes d'environ 10 L. Cette étape permet de comprendre l'efficacité de chaque type de traitement pris séparément. Le comportement hydraulique à long terme est aussi évalué grâce à la mesure de la conductivité hydraulique saturée. Suite à ces résultats, une filière de traitement a été proposée. Dans la troisième et dernière étape de laboratoire, la filière de traitement est testée dans un réacteur de 2 m^3. Ce dernier essai permet de valider la solution testée en colonne pour traiter le DMA fortement chargé en fer. Les résultats du test en réacteur de 2 m^3 permettent également de concevoir la filière de traitement sur le terrain.

Les essais en laboratoire ont permis de proposer une filière de traitement qui serait composée de trois parties. Premièrement, un biofiltre passif sulfato-réducteur (fumier de volaille,

copeaux et sciure de feuillus, compost végétal, sédiments, urée et 50% en masse de calcite finement broyée) permettrait de neutraliser l'acidité et de retenir une partie des métaux dissous. La seconde section de traitement serait composée par des cendres de bois de cogénération en raison de leurs forts pouvoirs de sorption du fer. Enfin, un second biofiltre passif sulfato-réducteur serait placé en dernier afin d'agir comme étape de polissage et pour éliminer les métaux résiduels. L'étude hydraulique a aussi montré que le système n'a pas vu sa conductivité hydraulique saturée réellement diminuer durant les essais en laboratoire. Ceci tend à démontrer que les phénomènes de colmatage seraient limités dans les conditions de laboratoire. L'essai en réacteur de 2 m^3 permet aussi de valider la solution proposée dans les essais en colonne. Enfin, les résultats obtenus en laboratoire ont permis de construire une filière de traitement de 160 m^3 environ (pour un temps de rétention hydraulique de 12 jours et pour un traitement de 5 L/min) sur le site minier Lorraine (Témiscamingue, Québec) qui est un site minier restauré mais générateur d'un DMA riche en fer (2500 mg/L en octobre 2011).

Le présent projet a donc permis d'approfondir les connaissances liées au traitement des DMA fortement concentrés en fer (>500 mg/L) avec des filières de traitement passif. De plus, l'utilisation des cendres de bois dans la filière de traitement est aussi un apport scientifique non négligeable. Enfin, les connaissances et la méthodologie acquises lors de cette étude seront applicables à d'autres sites miniers abandonnés ou fermés.

Mots clés : drainage minier acide, fer, systèmes passifs, filière de traitement, biofiltre passif sulfato-réducteur, cendres de bois.

CHAPITRE 1

INTRODUCTION

L'activité minière soutenue au Québec laisse et a laissé de nombreux sites de stockage de stériles (haldes à stériles) et de résidus miniers (parcs à résidus) à travers le territoire. On estime à plus de 1420 hectares l'aire totale des sites miniers abandonnés dans la région Abitibi-Témiscamingue-Nord-du-Québec (Bussière, 2010). Ces rejets peuvent s'avérer chimiquement instables lorsqu'exposés aux conditions atmosphériques. L'effluent résultant des réactions chimiques et biologiques avec l'eau et l'oxygène s'appelle le drainage minier (e.g. Aubertin et al., 2002, Bussière et al., 2005). Ce drainage minier peut être redéfini en trois catégories suivant le pH de l'eau : le drainage minier acide si le pH est inférieur à 6, le drainage neutre contaminé si le pH est compris entre 6 et 9 et le drainage alcalin si le pH est supérieur à 9 (Aubertin et al., 2002).

1.1 Problématique du drainage minier acide

Les stériles ou résidus sont habituellement stockés dans des aires d'entreposage situées à proximité de la mine et peuvent couvrir des superficies de plusieurs dizaines d'hectares (Bussière et al., 2005). Lorsqu'il y a présence de minéraux sulfureux dans les rejets (la pyrite par exemple), les éléments atmosphériques (eau, air) conduisent à l'oxydation des résidus. Il y a alors production d'acide sulfurique (H_2SO_4), d'où une diminution du pH favorisant également la lixiviation de métaux toxiques présents dans les résidus (Akcil et Koldas., 2006). Ce phénomène s'appelle le drainage minier acide (DMA).

Le DMA est le fruit d'une série de réactions chimiques et biochimiques (e.g. Kleinmann et al., 1981; Ritcey, 1989; Blowes and Ptacek, 1994; Evangelou, 1995; Perkins et al., 1995; Morin et Hutt, 1997). On peut résumer la formation du DMA en combinant toutes les réactions chimiques et biologiques dans l'équation [1-1] suivante (Kleinmann et al. 1981):

[1-1] $$FeS_2 + 15/4 O_2 + 7/2 H_2O \rightarrow Fe(OH)_3 + 2H_2SO_4$$

Le DMA est une source importante de pollution des eaux et peut avoir des effets dévastateurs sur l'environnement. Il peut entraîner l'acidification de lacs et de rivières (Espana et al., 2006), compromettant ainsi la vie des plantes aquatiques et des autres organismes vivants dans l'eau ou sur les rives (Grout and Levings, 2001). Par lessivage acide, certains métaux lourds peuvent être relâchés (Lei et al., 2010) et devenir biodisponibles dans la chaîne trophique, menaçant ainsi la santé et même la vie des organismes biologiques (Zis et al., 2004, El Khalil et al., 2008, Alvarez-Valero et al., 2009).

Le DMA constitue un problème à long terme, car il peut persister dans l'environnement jusqu'à l'épuisement des minéraux sulfureux présents dans les rejets miniers. Lorsque le processus est amorcé, il devient presque impossible de l'arrêter, d'où l'intérêt de trouver des méthodes de traitement des effluents et de contrôle des réactions menant au DMA (Bussière et al., 2005).

1.2 Traitement du drainage minier acide

Dans le cas où le drainage minier acide n'est pas commencé, il est possible de prévenir sa formation à la source (Johnson et Hallberg, 2005). Les solutions envisagées ont pour but principal de limiter l'apport d'un ou plusieurs des éléments constitutifs de la réaction de génération du DMA, soit l'oxygène, l'eau ou les sulfures (voir Aubertin et al., 2002, pour plus d'informations sur les méthodes de contrôle du DMA). Ainsi l'oxydation des sulfures reste contrôlée.

Dans le cas de sites générateurs de DMA où l'on n'a pas limité le problème à la source, il faut recueillir les effluents miniers et les traiter afin de minimiser les impacts sur l'environnement. La réglementation au Québec impose les limites suivantes aux effluents finaux par la Directive 019 sur l'industrie minière : 0.2 mg/L pour As, 0.3 mg/L pour Cu, 3 mg/L pour Fe, 0.5 mg/L pour Ni et Zn, 0.2 mg/L pour Pb et un pH compris entre 6 et 9 (les valeurs données ici sont des moyennes annuelles, Directive 019, 2005).

Il existe deux principaux types de traitement des eaux minières contaminées par le DMA (Johnson et Hallberg, 2005): les systèmes actifs et passifs. Chacun de ces deux types de traitement est ensuite subdivisé en traitement biologique et abiotique tel que présenté à la Figure 1.1.

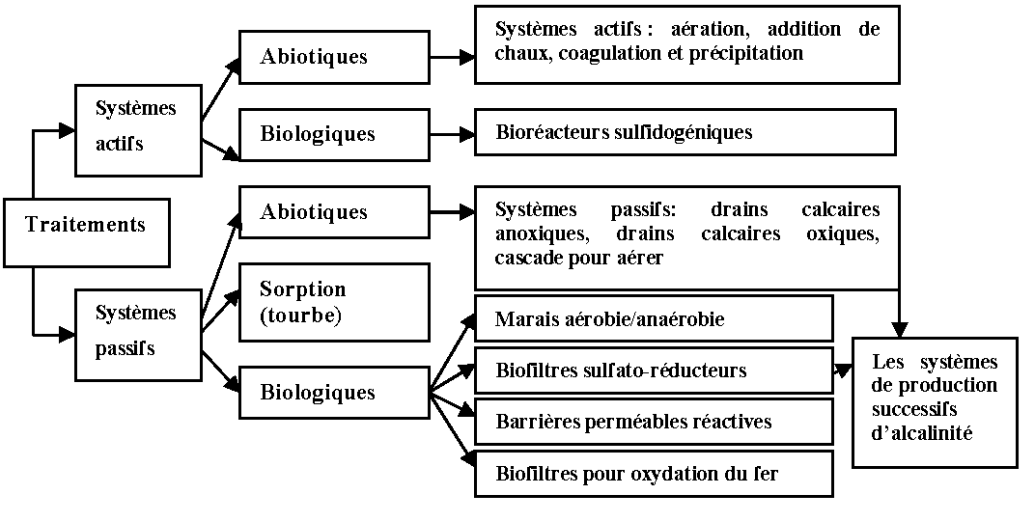

Figure 1.1. Stratégies biologiques et abiotiques de traitement du DMA (adapté de Johnson et Halberg, 2005)

À la fermeture d'une mine, il devient difficile de justifier le traitement actif à perpétuité, particulièrement dans le contexte du développement durable. C'est pourquoi les systèmes de traitement passif deviennent de plus en plus une alternative intéressante. En effet, ces systèmes sont peu gourmands en énergie, utilisent des matériaux naturels ou des déchets et représentent un coût d'investissement en capital faible en comparaison des usines actives (Melanson, 2006). Ce type de traitement se base sur des réactions chimiques et biologiques que l'on trouve dans la nature et est opéré sans ajout de réactifs en continu (Gazea et al., 1995). Les traitements passifs peuvent être subdivisés en deux catégories que sont les traitements abiotiques (drains calcaires par exemples) et biologiques (marécages a/ana-érobies et les biofiltres passifs sulfato-réducteurs BPSR par exemples) (Johnson et Hallberg, 2005, Neculita et al., 2007). Les traitements passifs sont présentés sommairement dans le Tableau 1.1. Quant aux traitements actifs (qui ne font pas partie des sujets traités dans cette thèse), le lecteur intéressé peut consulter les références suivantes : Aubertin et al., 2002, Akcil et Koldas, 2005, Johnson et Hallberg, 2005, Kalin et al., 2006, Silveira et al., 2009.

Tableau 1.1. Fonctionnement des différents traitements passifs du DMA

Traitement	Mode d'action	Effets
Drain anoxique calcaire	Dissolution du calcaire en conditions anoxiques	Augmentation de l'alcalinité, diminution de l'acidité, formation de précipités métalliques en sortie du drain
Drain calcaire oxique et chenal calcaire	Dissolution du calcaire en conditions aérobies	Augmentation de l'alcalinité, diminution de l'acidité, formation de précipités métalliques dans le drain
Cascade pour aération	Aération de l'effluent	Oxydation et précipitation des métaux
Marais aérobie	Aération de l'effluent par les plantes, adsorption et bioaccumulation	Diminution de la quantité de métaux en solution par des mécanismes d'oxydation et d'hydrolyse
Marais anaérobie	Milieux réducteur favorisé par la présence de matière organique dans le marais (Idem bioréacteur)	Précipitation des métaux en sulfures métalliques par des bactéries sulfato-réductrices
Bioréacteur sulfato-réducteur	Dégradation concomitante de la matière organique contenue dans le réacteur et réduction des sulfates de l'effluent en sulfure d'hydrogène	Augmentation de l'alcalinité, diminution de l'acidité, précipitation des métaux en sulfures métalliques par des bactéries sulfato-réductrices associées à la matière organique, sorption, coprécipitation, échange d'ions
Barrière perméable sulfato-réductrice	Dégradation concomitante de la matière organique contenu dans le réacteur et réduction des sulfates de l'eau souterraine en sulfure d'hydrogène	La différence réside dans la conception, la barrière perméable sera plutôt utilisée dans le cas de contaminations souterraines
Les systèmes de production successifs d'alcalinité	Combinaison du drain anoxique et du bioréacteur sulfato-réducteur. Constitués d'une couche de calcaire et d'une couche de matière organique	Le terme successif est utilisé étant donné que le calcaire va augmenter le pH et l'alcalinité et la matière organique, par l'intermédiaire des BSR, va précipiter les métaux et produire de l'alcalinité
Sorption (tourbe)	Adsorption, chélation, échange d'ions	Diminution des métaux en solution

Adapté de Gazea et al., 1995, Cravotta et Trahan, 1999, MEND, 1999, Gusek, 2001, URS Report, 2003, Luptakova et Kusnierova, 2005, Champagne et al., 2005, Johnson et Halberg, 2005, Skousen et Ziemkiewicz, 2005, Neculita et al., 2007, Neculita et al., 2008a.

1.3 Sites miniers typiques québécois générant du drainage minier acide

Les aires de stockage de rejets de mine de métaux de base et de métaux précieux contiennent très souvent au Québec des sulfures de fer. Par conséquent, si aucune précaution n'est prise lors du stockage, ces rejets peuvent générer, dans certains cas, du DMA très contaminé notamment en fer, entraînant dès lors une très forte acidité métallique.

Beaucoup de sites miniers québécois à restaurer ou déjà restaurés se situent dans la région de l'Abitibi-Témiscamingue. Par exemple, les sites Manitou (200 ha), Aldermac (76 ha), Lorraine (22 ha), Barvue (40 ha) et East Malartic (500 ha) représentent plus de 50% de la superficie totale des sites miniers abandonnés du Québec (Cyr, 2005). Dans la suite de cette sous-partie, on présente succinctement trois de ces sites miniers abandonnés[1] abitibiens, soit les sites Lorraine, Manitou et Aldermac (Tableau 1.2).

La principale observation qui ressort à la lecture du Tableau 1.2 est que les concentrations en fer et en sulfates sont très importantes (plus de 1450 mg/L pour le fer et plus 3150 mg/L pour les sulfates); ces concentrations sont typiques des sites miniers sulfureux en Abitibi-Témisacamingue.

[1] Un site minier inactif est qualifié d'abandonné en vertu de la Loi sur les mines lorsque aucun responsable n'est en mesure d'en entreprendre la restauration, soit parce que les responsables n'existent plus légalement ou qu'ils n'ont plus les ressources financières nécessaires (Cyr, 2008).

Tableau 1.2. Synthèse des qualités de DMA (concentration en fer et sulfate en mg/L) provenant de trois sites miniers abandonnés en Abitibi-Témisacamingue

Nom du site	Abandon	Principaux sulfures des résidus	Qualité du DMA			Restauration	Références
			pH	Fer	Sulfate		
Lorraine	1968	Chalcopyrite pyrite pyrrhotite pentlandite	3	3150 (en 1999)	8100 (en 1999)	Couverture à effet de barrière capillaire et drains dolomitiques en 1998	Dagenais et al. (2005), Potvin (2009), Bussière et al. (2009)
Manitou	1978	pyrite	2-3	20 000 (essai en cellule sur le terrain de 11m x11m*)	110 000 (essai en cellule sur le terrain de 11m x11m *)	Recouvrement monocouche avec résidus non générateurs depuis 2007	Cyr (2005), Gosselin (2007), *Molson et al. (2008)
Aldermac	1943	pyrite pyrrhotite	2-5	8493 (en 1997)	1450 (en 1997)	Stockage des résidus sous membranes étanches ou en conditions de saturation en eau, en 2008	Bédard et al. (1997), Cyr (2005 et 2008)

1.4 Synthèse de travaux récents sur les systèmes de traitement passif

Au cours des dernières années, les systèmes passifs de traitement du DMA ont fait l'objet de nombreuses études. Toutefois, les DMA très chargés en fer restent peu étudiés malgré les défis techniques qu'ils comportent. Dans cette sous-section, des travaux récents sur le traitement de DMA fortement chargés en fer (ce qualificatif est utilisé ici pour des concentrations >500 mg/L) dans des systèmes de traitement passif sont présentés.

1.4.1 Traitement de DMA fortement chargés en fer par biofiltres passifs sulfato-réducteurs

Les biofiltres passifs sulfato-réducteurs (BPSR) contiennent un substrat biodégradable, habituellement des produits agricoles comme le compost de feuille, la sciure de bois de feuillus, le fumier de volaille, qui favorise la croissance des microorganismes responsables du traitement des eaux, ainsi qu'un support stable (comme le sable) pour le développement des bactéries (Cocos, 2000, Neculita et al., 2007). En conditions anaérobies, les sucres libres formés par la dégradation de la matière organique sont transformés par fermentation en acides organiques à courte chaîne ou en acides gras, qui sont des substrats favorables à la croissance des bactéries sulfato-réductrices (BSR). En effet, le métabolisme des BSR demande une source d'électrons qui provient de ces molécules à courtes chaînes comme le lactate, et un accepteur d'électrons en la présence des sulfates contenus dans le DMA. Les BSR réduisent alors les sulfates en sulfure d'hydrogène (Luptakova et Kusnierova, 2005, Neculita et al., 2007, Jong et Parry, 2006). La dégradation de la matière organique va aussi induire une production d'hydrogénocarbonates qui augmentera l'alcalinité de l'eau. La génération de sulfures d'hydrogène fait alors précipiter les ions métalliques sous forme de sulfures métalliques peu solubles.

Les études récentes montrent que la précipitation des sulfures métalliques n'est pas la seule voie de traitement des eaux contaminées par le DMA (Neculita et al., 2008b, Potvin, 2009). Les métaux peuvent être stabilisés par sorption, précipitation ou co-précipitation d'hydroxydes et carbonates (Neculita et al., 2008b, Teclu et al., 2008). De plus, les phénomènes de sorption semblent être les plus importants dans les premiers temps de vie du biofiltre (Sheoran et al., 2010). Toutefois, bien que la sorption des métaux est largement décrite dans la littérature dans le cadre du traitement conventionnel des eaux industrielles (e.g. Blais et al., 1999) et observée dans des extractions séquentielles (Neculita, 2008, Potvin, 2009), peu ou pas d'articles traitent des propriétés de sorption des métaux sur les matériaux constituant un BPSR pour traiter le DMA.

Le Tableau 1.3 présente quelques exemples de traitement de DMA par des biofiltres sulfato-réducteurs. Il est possible de remarquer que la rétention du fer est généralement efficace pour

des concentrations inférieures à 500 mg/L. On peut également observer que les recherches ne traitent que rarement de la capacité des biofiltres à traiter des DMA ayant des concentrations en fer supérieures à 500 mg/L et encore moins des concentrations supérieures à 1 000 mg/L comme celles que l'on retrouve au Tableau 1.2.

Dans le cas de DMA chargés en fer (autour de 500 mg/L), les biofiltres passifs sulfato-réducteurs pourraient néanmoins être utilisés selon deux autres études récentes réalisées par Neculita (2008) et Potvin (2009). En effet, des bioréacteurs colonnes (3,5 L), suivi durant une période de 11 à 15 mois à deux temps de rétention hydraulique (TRH) de 7,3 jours et 10 jours, ont été efficaces pour le traitement d'un DMA contaminé ayant 500 mg/L de fer (Neculita, 2008, Neculita et al., 2008a). De plus, il a été remarqué que la qualité de l'effluent traité a toujours été meilleure à un TRH de 10 jours. Toutefois, la diminution de la perméabilité du mélange réactif pour 10 jours de TRH suggère que des problèmes hydrauliques pourraient affecter le système de traitement et ainsi limiter l'efficacité durant l'exploitation à long-terme (Neculita, 2008). C'est pourquoi, un compromis entre l'efficacité de traitement de l'eau et le comportement hydraulique doit être fait pour le dimensionnement d'un BPSR efficace à long terme (Neculita, 2008, Sheoran et al., 2010).

Une seconde étude a été réalisée par Potvin (2009), dans un réacteur compartimenté de 2000 L avec écoulement horizontal, pour traiter le même DMA et avec le même mélange réactif que Neculita (2008). La diminution des concentrations de la plupart des métaux est supérieure à 90%. Dans le cas du fer, la diminution est de plus de 69% alors que pour le Mn, la diminution est de moins de 57%. Le dénombrement des BSR, la génération d'alcalinité ainsi que les diminutions des concentrations en sulfates et en certains métaux suggèrent que la sulfato-réduction était bien présente dans le BPSR. Les résultats montrent aussi que d'autres mécanismes de traitement participent à l'amélioration de la qualité d'eau telles la sorption, la précipitation de minéraux carbonatés et d'hydroxydes de fer. Ces mécanismes seraient responsables de la réduction significative des teneurs en métaux à l'effluent. En plus d'être efficace pour le traitement d'un DMA fortement contaminé, le reacteur testé dans cette étude n'a pas vu son comportement hydrogéologique changer de façon significative durant la période de test (contrairement à ce qui avait été observé dans l'étude en colonne de Neculita, 2008).

Tableau 1.3. Exemples de performances de traitement de DMA

Mélange BPSR	DMA	Performances	Références
Déchets forestiers, boues municipales, sédiments, dolomite	pH = 1,6 Fe = 400 mg/L SO_4^{2-}= 2500 mg/L	pH = 5-6 Fe = 5 mg/L SO_4^{2-}= 20-40 mg/L	Tassé et Germain (2002)
Rejets de l'industrie du vin, éthanol, calcite et sable	pH = 2,5 Fe = 550 mg/L SO_4^{2-}= 2 g/L	pH = 6 61-91% de réduction Fe 90% de réduction SO_4^{2-}	Costa et al. (2009)
Argile, boues de station d'épuration, herbe coupée	pH= 2,3 Fe = 1800 mg/L S = 2700 m g/L	pH = 6,5 Fe = 70 mg/L S = 1330 mg/L	Harris et Ragusa (2001)
Compost, calcite, sédiments	pH = 3 Fe = 10 mg/L SO_4^{2-}= 1000 mg/L	pH = 7 Fe < 0,1 mg/L SO_4^{2-}= 1000 mg/L	Gibert et al. (2005)
Gravier, dolomite, boues de station dépuration, fumier de vache, compost	pH = 2,9 Fe = 279 mg/L	pH = 5-7 99% de réduction Fe	La et al. (2003)
Sable, sédiments, chitine de carapaces de crabe	pH = 3,5 Fe = 1-10 mg/L	pH = 7,5 100% réduction Fe	Robinson-Lora et Brennan (2009)
Gravier, compost de champignon, calcite	pH = 2,6 Fe = 363 mg/L SO_4^{2-}= 2362 mg/L	pH = 6-7 90% de réduction Fe 23% de réduction SO_4^{2-}	Ji et Kim (2008)
Pulpe de bois, sciure, écorces, feuilles érable, paille, tourbe, fumier de vache, grains, orge, mélasse, acide lactique, calcaire, sable, sédiments, phosphates	pH = 2,5 Fe = 160 mg/L SO_4^{2-}= 4000 mg/L	pH = 6-7 Fe < 1 mg/L SO_4^{2-}= 1170-3450 mg/L	Kuyucak et St-Germain (1994)
Compost, écorces, copeaux de pin, calcite, coquilles de moule	pH = 4,5 Fe = 65,8 mg/L SO_4^{2-}= 608 mg/L	pH = 6-7 94% de réduction Fe 99% de réduction SO_4^{2-}	Mc Cauley et al. (2009)
Sciure de bois, foin, fumier de bétail	pH = 4 Fe = 50-70 mg/L	pH = 5,5 Fer = 25 mg/L	Johnson et Hallberg (2005)
Matériaux organiques, calcite, fumiers	pH = 3,3 Fe = 8 mg/L	pH = 6-7 Fe < 1 mg/L	Zaluski et al. (2003)
Copeaux de bois, calcite, compost, foin	pH = 2-3 Fe = 15-33 mg/L SO_4^{2-}= 661-887 mg/L	pH = 6,5 Fe < 1 mg/L SO_4^{2-}= 360 mg/L	Kuyucak et al. (2006)
Copeaux, sciure, tourbe, compost, fumier, éthanol, sédiments, urée, sable, calcite	pH = 3.9-4.2 Fe = 1683 mg/L SO_4^{2-}= 2944-4608 mg/L	pH = 6,5-8,5 100% de réduction Fe SO_4^{2-}= 163-5575 mg/L	Zagury et al., 2006

1.4.2 Traitement de DMA fortement chargés en fer par drains calcaires

Les drains calcaires font partie des systèmes de traitements chimiques passifs du DMA. Le but principal de ce système est de neutraliser l'acidité des effluents miniers contaminés à de faibles coûts en capital et d'opération (Johnson et Hallberg, 2005). On distingue principalement deux configurations pour ces types de drains calcaires: le drain anoxique et le drain oxique (Potvin, 2009).

Les drains calcaires anoxiques (DAC) sont fondamentalement des tranchées remplies de calcaire (par exemple $CaCO_3$) concassé, isolées sous un plastique et un géotextile et recouvertes de terre ou d'une couche d'argile pour garantir l'étanchéité (Bernier, 2002, Melanson, 2006). Au fur et à mesure de leur écoulement dans le système, les eaux de drainage minier acide dissolvent le calcaire avec un dégagement de calcium et de bicarbonates, ce qui entraîne une augmentation du pH et de l'alcalinité (Bernier, 2002). Le milieu anoxique d'un DAC prévient l'oxydation des métaux dissous à l'intérieur du drain. Les précipités métalliques se forment donc uniquement à la sortie du drain, c'est-à-dire à la rencontre de l'oxygène. On observe donc en sortie de drain des réactions d'oxydation et d'hydrolyse des métaux (Hedin et al., 1994, Cravotta et Trahan, 1999, Ulrich, 1999).

La conception des drains calcaires oxiques (DCO) est très proche de celle des DAC. La différence réside dans le fait que la tranchée n'est pas recouverte d'un matériel étanche. Tout comme la version anoxique, le chenal calcaire et les DCO augmentent aussi le pH et l'alcalinité de l'effluent grâce à la dissolution du calcaire. Cependant, en raison des conditions oxiques du système, les métaux, et particulièrement le fer, précipitent sous forme d'hydroxydes et d'oxydes dans le drain (URS Report, 2003).

Le type de roche utilisé dans les drains calcaires peut être de différents types telles la serpentinite (Bernier, 2005), la dolomite (St Arnault et al., 2004) et la calcite (Genty, 2007, Hosten et Gulsun, 2004, Cravotta, 2003, Hedin et al., 1994). La réactivité des minéraux vis-à-vis de la neutralisation est différente et l'on préfèrera si possible l'utilisation de calcite avec un haut degré de pureté en carbonate de calcium (Genty et al., 2008 - voir aussi l'Appendice B de la thèse). Toutefois, il est possible de noter que des précipités d'oxyhydroxydes et fer et de gypse peuvent se former à la surface des grains dans le drain et peuvent donc diminuer la

réactivité de ce dernier (Hedin et al, 1994). Dans certains cas, cet enrobage n'est pas un facteur limitant (Santomartino et Webb, 2007, Genty et al., 2008). Enfin, le dimensionnement des drains calcaires anoxiques est principalement basé sur la détermination du temps de rétention hydraulique, c'est-à-dire le temps que met une goutte d'eau pour parcourir le drain en entier (Genty et al., 2008, Potvin, 2009).

Le choix d'un drain calcaire anoxique ou oxique est-il adéquat avec le défi du traitement de DMA fortement chargés en fer (> 500 mg/L) typique des DMA au Québec ? Dans les paragraphes précédents, il a été mentionné que les précipités de fer peuvent enrober les carbonates et donc diminuer l'efficacité du traitement. Dans une étude récente, Potvin (2009) a utilisé un réacteur compartimenté de 2000 L pour traiter un DMA fortement chargé en fer (6900 mg/L) avec un drain dolomitique anoxique et oxique. L'efficacité de traitement a été faible. En effet, le fer, le soufre, le cobalt, le manganèse, le nickel et le zinc sont faiblement retenus ou faiblement remis en solution par le DAC et le DCO. Les indices de saturation minéralogique, la quantification par diffraction des rayons X (DRX) et les observations au microscope électronique à balayage (MEB) montrent que le fer et le soufre précipitent dans les systèmes de traitement (Potvin, 2009). En résumé, les DAC et les DCO montrent peu d'efficacité pour le traitement des métaux d'un DMA fortement contaminé. Pour les matériaux et conditions testés, ils ne peuvent augmenter le pH à des valeurs légèrement supérieures à 5 et ce, même pour un TRH nettement supérieur à 15 heures. Bien que ces deux types de système de traitement permettent de générer de l'alcalinité, ils ne peuvent pas être recommandés comme solution unique pour traiter les métaux d'un DMA fortement chargé en fer (Potvin, 2009).

1.5 Traitement du DMA par des filières de traitements passifs

Les DMA fortement chargés en fer sont particulièrement difficiles à traiter par les méthodes de traitement passif conventionnelles. Dans ces cas, l'utilisation des systèmes combinés ou des filières de traitement (utilisations de plusieurs procédés classiques de traitement passif en série) semble plus appropriée que l'utilisation d'une seule méthode (Potvin, 2009).

Il a été montré dans la littérature que l'utilisation des filières de traitement montre une bonne efficacité dans le traitement d'un DMA moyennement chargé en fer. En effet, Champagne et

al. (2005) ont démontré que l'utilisation d'une filière de traitement est nécessaire pour traiter un DMA ayant une concentration en fer de seulement 189 mg/L; ce qui est faible par rapport aux drainages miniers provenant des sites Lorraine, Manitou et Aldermac présentés précédemment (Tableau 1.2). Le traitement de cette eau se fait par l'intermédiaire d'une étape d'aération-décantation pour prétraiter le fer (oxydation de fer ferreux en fer ferrique suivi de la précipitation d'hydroxydes ferriques), d'une étape de filtration sur de la tourbe (sorption des métaux et diminution du potentiel d'oxydoréduction afin d'obtenir des conditions anoxiques), d'une étape de filtration sur biofiltre sulfato-réducteur (augmentation de l'alcalinité, diminution des métaux) et enfin d'une étape de polissage dans un drain anoxique calcaire afin d'augmenter l'alcalinité (Rouhani et al., 2003, Champagne et al., 2005) . Dans cette étude, l'importance des procédés de sorption dans une filière de traitement est mise en lumière. En effet, la sorption sur tourbe est souvent utilisée dans le traitement des effluents pour adsorber les métaux (e.g. Brown et al., 2000, Ma et Tobin, 2004, Gupta et al., 2009). Les performances de rétention des métaux du filtre de tourbe, pour un temps de rétention hydraulique de 4,8 jours, sont alors pour le fer, l'aluminium et le cuivre respectivement de 95%, 87% et 99% (Champagne et al., 2005). Enfin, en sortie de la filière, les concentrations en métaux, exceptée pour le cadmium, sont diminuées au delà de 99% (Champagne et al., 2005).

Une seconde étude de Figueroa et al. (2007) traite d'une filière de traitement d'un DMA chargé en fer à hauteur de 40 mg/L par des drains calcaires oxiques suivis de biofiltres sulfato-réducteurs. Les temps de rétention hydraulique varient de 0.3 à 0.6 jours dans le DCO et de 5 à 10 jours dans le BPSR. Le DCO permet alors une bonne élimination de fer par précipitation (autour de 97%) et augmente le pH de l'effluent jusqu'à 5-6 afin d'assurer des conditions optimales pour le biofitre. Par la suite, le BPSR permet de traiter adéquatement le zinc présent dans les eaux de drainage (de 65-75 mg/L dans le DMA à des valeurs <0,1 mg/L à l'effluent).

Kuyucak et al. (2006) ont installé un bioréacteur sulfato-réducteur suivi d'un aérateur et d'un drain calcaire oxique sur le site de Cadillac Molybdenite, en Abitibi-Témiscamingue. La concentration en fer à traiter est de l'ordre de 32,3 mg/L et le pH du DMA varie de 2,7 à 5,4. Au cours de l'année 2005, la concentration moyenne en fer à la sortie de la filière était de

0,12 mg/L (99% de rétention) et le pH autour de 6,7 ; ce qui respecte les directives du gouvernement du Québec.

Parmi les autres exemples, il est aussi possible de citer Wilmoth (2002) qui décrit le fonctionnement de trois filières de traitement du DMA (pH de 3,3 et une concentration en fer de 8,6 mg/L) sur le site Calliope aux États Unis. Les filières comprennent différents compartiments : un premier contenant de la matière organique pour diminuer le potentiel d'oxydoréduction du DMA et nourrir les BSR, un second contenant de la calcite pour augmenter le pH et l'alcalinité, une autre section contient de la matière organique et la dernière intègre un support de graniodorite pour permettre aux BSR de se développer sur une surface stable. Le temps de rétention hydraulique dans la filière y est d'environ 4 à 5 jours. Le pH de l'effluent de la filière est augmenté à environ 7-8 et la concentration moyenne en sortie de l'effluent est de 0,1 mg/L pour le fer (soit plus de 98% de rétention).

Les exemples précédents montrent bien que le fer n'est pas un paramètre limitant pour le traitement par des systèmes combinés de DMA peu chargés (<500 mg/L). Toutefois, dans le cas de DMA plus chargés en fer, les étapes d'aération et décantation souvent préconisées pour la diminution du fer sont peu efficaces. En effet, une étude d'une filière comprenant un drain anoxique calcaire, une aération et une décantation, pour traiter des DMA ayant une concentration fer de 1600 à 6900 mg/L, n'a pas permis la rétention efficace du fer (Genty et al., 2008[2]). En effet, bien que le DAC permet d'augmenter le pH, la précipitation du fer dans l'étape d'aération décantation fait rechuter le pH autour de 3 et donc inhibe l'oxydation chimique et la précipitation du fer dans le décanteur.

1.6 Limites et défis actuels du traitement de drainages miniers acides fortement contaminés

Les systèmes de traitement passif tels les DAC et les BPSR ont démontré leur efficacité dans le cas de DMA acides mais peu chargés en métaux provenant de mines de charbon (e.g. Hedin et al., 1994, Cravotta et Trahan 1999, Cravotta 2003, Bhattacharya et al., 2008). Cependant dans le cas de DMA plus acides et plus concentrés en métaux dissous, il peut

[2] Voir Appendice B

s'avérer nécessaire de combiner plusieurs méthodes de traitement entres elles. La filière de traitement idéale serait alors une série de procédés traitant chacun à leur tour (ou simultanément) les composantes de la pollution tout en minimisant le coût de construction et l'espace occupé (Trumm, 2006).

Cela est encore plus important quand la charge en métaux est élevée, notamment pour le fer, puisqu'à ce moment, les DAC et les BPSR ont de la difficulté à traiter l'eau contaminée (Rouhani et al., 2003, Genty et al., 2008; Neculita, 2008). En effet, il peut se former des hydroxydes métalliques en entrée de biofiltre, diminuant ainsi l'activité des BSR et modifiant le comportement hydraulique du système. De plus, le fer à la sortie des BPSR peut entraîner de la toxicité à l'effluent (Neculita et al., 2008b). Une forte charge en fer peut aussi entraîner un enrobage de minéraux secondaires ferriques sur les matériaux calcaires constituant le DAC (Genty et al., 2008), ce qui peut mener éventuellement au colmatage du drain. Enfin, si les concentrations en fer demeurent élevées à l'effluent, même si le pH a pu être relevé près de la neutralité, la précipitation du fer lorsqu'exposé aux conditions atmosphériques va refaire chuter ce dernier à des valeurs nettement acides (Genty et al., 2011[3]). Le fer est donc un paramètre limitant l'efficacité des BPSR et des DAC si sa concentration est trop élevée. Le Tableau 1.4 résume les phénomènes positifs et les problèmes rencontrés dans le cas d'une utilisation seul pour traiter un DMA très contaminé en fer pour les systèmes de traitement de type DAC, aération-décantation, BPSR et sorption.

[3] Voir aussi l'Appendice B

Tableau 1.4. Fonctionnement de systèmes passifs et les problèmes rencontrés lorsque les concentrations en fer sont élevées (Adapté de Neculita, 2008, Genty et al., 2008 et Potvin, 2009)

Type de traitement	Fonctionnement positif	Problèmes rencontrés
DAC	Neutralisation, augmentation de l'alcalinité, rétention du Cr, Pb, Cd, Al	Pas de rétention du fer, possibilité de diminution de la réactivité par enrobage du calcaire par des précipités secondaires
Aération décantation	Oxydation du fer	Oxydation du fer entraînant une acidification du décanteur et donc une resolubilisation du fer
BPSR	Neutralisation, augmentation de l'alcalinité, rétention de la plupart des métaux	Problème de colmatage du système, rétention moyenne du fer si ce dernier est en grande concentration, diminution de l'efficacité pour des pH <5, ou des potentiels d'oxydoréduction trop élevés.
Sorption	Sorption des métaux	Saturation des sites de sorption plus ou moins rapide

De plus, la connaissance de l'hydrodynamique des drains calcaires et des BPSR a été peu étudiée et ce, autant à l'échelle des modèles au laboratoire que sur le terrain. Cet aspect est particulièrement sensible dans le contexte où il y a précipitation massive du fer (ou d'autres minéraux secondaires) dans les pores de la matrice du système de traitement passif, ce qui pourrait modifier les propriétés hydrogéologiques (conductivité hydraulique saturée par exemple) du système.

Enfin, la mise en place d'un système de traitement sur le terrain serait une belle opportunité pour comprendre le fonctionnement des BPSR pendant l'hiver et pour voir l'importance de la température sur le traitement du DMA. En effet, la plupart des études en laboratoire ne testent pas l'influence de ce dernier paramètre. Sur le terrain, une étude de Wilmoth (2002), montre que l'efficacité des BPSR est plus grande à 16°C qu'à 2°C, mais aussi que les BSR restent présentes aux basses températures. Plusieurs études montrent aussi que les basses températures n'affectent pas le redémarrage des processus de traitement lors de la fonte des

neiges. En effet, les biofitres contenant de la tourbe semblent ne pas être affectés pendant les hivers tempérés (Rouhani et al., 2003, Champagne et al., 2005).

1.7 Objectifs et hypothèses

A l'heure actuelle, la plupart des études sur les systèmes de traitement passif du DMA visent à démontrer l'efficacité chimique d'un seul traitement pour des DMA peu chargés en fer (<500 mg/L). L'objectif principal de ce présent projet est de mieux comprendre le comportement hydro-bio-géo-chimique de différents systèmes de traitement passif et de les combiner dans une filière de traitement pour un DMA fortement chargé en fer (>500 mg/L).

Pour atteindre cet objectif, quatre hypothèses principales seront postulées :

a) Les systèmes de traitements passifs doivent être couplés entre eux pour traiter des DMA très acides et fortement chargés en fer;

b) Pour bien concevoir une filière de traitement, il est essentiel de bien comprendre le comportement de chaque composante de la filière;

c) Les phénomènes de sorption sont essentiels pour retenir le fer dans la filière de traitement;

d) Les changements d'échelle au laboratoire (10L et 2000L) et sur le terrain ont une importance sur les résultats du traitement.

Ces hypothèses permettent alors de dégager les objectifs spécifiques du projet :

a) Caractériser les propriétés de sorption du fer sur les matériaux utilisés dans les systèmes passifs;

b) Tester les traitements passifs de façon indépendante (à l'échelle batch et en colonne) puis les combiner entre eux (en colonne et dans un modèle d'environ 2000 L) pour obtenir une filière de traitement capable de traiter un DMA riche en fer;

c) Caractériser les mécanismes de rétention des métaux des différentes étapes de traitement par diverses approches (chimiques et minéralogiques principalement);

d) Concevoir une filière de traitement pour les eaux acides du site Lorraine au Témiscamingue;

e) Faire le lien entre les résultats produits aux différentes échelles au laboratoire.

1.8 Contenu de la thèse

Étant donné les nombreuses revues de littérature réalisées récemment sur les traitements passifs (e.g. Neculita et al., 2007, Potvin, 2009, Sheroan et al., 2010), il n'a pas été considéré nécessaire de refaire une nouvelle revue de littérature spécifiquement pour cette thèse. Toutefois, le présent chapitre contient de nombreuses informations résumant le fonctionnement de ces systèmes de traitement du DMA. De plus, chaque chapitre de la thèse comprend une partie introduction faisant un état de l'art sur le type de traitement étudié.

Pour répondre adéquatement aux objectifs fixés dans le cadre de cette étude, la thèse sera composée de cinq chapitres majeurs. Les chapitres 2, 3 et 4 seront orientés sur la sélection des matériaux utilisés dans les systèmes de traitement. Plus spécifiquement, ces chapitres discuteront des caractéristiques physico-chimiques des matériaux, propriétés des matériaux vis-à-vis de la sorption du fer, les propriétés hydrauliques et les performances de traitement du DMA des différents matériaux utilisés (ou du mélange de matériaux) de façon indépendante.

Le chapitre 5 traitera quant à lui de l'étude d'une filière de traitement du DMA composée des procédés étudiés dans les chapitres précédents. Cette étude sera tout d'abord réalisée dans des colonnes afin de vérifier l'efficacité de traitement de la filière. Ensuite, basé sur les résultats précédents, un test plus représentatif des conditions réelles sera réalisé dans un réacteur compartimenté de 2000 L. La filière de traitement utilisée dans les colonnes sera reproduite et les performances de traitement seront évaluées pour une période d'un an. De plus, l'effet du changement d'échelle sera quantifié en comparant les résultats de qualité d'eau et grâce à une caractérisation des mécanismes de rétention des métaux dans les systèmes de traitement (colonnes et réacteur).

Le chapitre 6 discutera ensuite de la conception d'une filière de traitement d'un DMA riche en fer pour un site réel. Les calculs seront basés sur les performances observées dans le réacteur de 2000 L (présenté dans le chapitre 5). L'instrumentation proposée pour le système sera aussi présentée. La construction ayant été réalisée à la fin des travaux de thèse, les résultats liés à l'efficacité de traitement ne sont pas encore disponibles au moment de la finalisation du document. Toutefois, il nous est apparu indispensable de présenter ces travaux afin de décrire la démarche utilisée pour transférer les connaissances acquises lors des essais en laboratoire vers un projet de plus grande ampleur.

1.9 Originalité et principales contributions de la thèse

Comme il a été présenté précédemment, les systèmes passifs utilisés seuls peuvent avoir une performance limitée en raison des fortes charges en métaux dans les DMA. De plus, les études portant sur les DMA fortement contaminés en fer sont peu nombreuses. Ainsi, les principales contributions de cette étude sont donc le traitement d'un DMA considéré comme fortement contaminé en fer (de 2000 à 4000 mg/L) grâce à la combinaison de plusieurs procédés de traitement passif. En outre, l'efficacité des cendres de bois de cogénération (encore peu utilisées dans les systèmes passifs) dans une filière de traitement pour retenir les métaux (et principalement le fer), a été démontrée. La construction sur le terrain de la filière de traitement donne l'opportunité d'étudier dans des conditions réalistes l'efficacité de traitement. L'influence des conditions climatiques, des débits, et l'effet d'échelle pourront être ainsi évalués.

L'originalité de cette thèse repose aussi sur l'utilisation de nombreuses techniques de caractérisation afin de comprendre le fonctionnement des systèmes de traitement. Ainsi, des tests batch ont pu confirmer le rôle important de la sorption des matériaux utilisés dans les BPSR et dans les filtres contenant de la cendre de bois. De plus, les nombreuses analyses chimiques et minéralogiques des échantillons post-démantèlement permettent aussi de comprendre les mécanismes de rétention des métaux. Enfin, une nouvelle approche utilisant des essais de traceur a permis de déterminer les TRH opérationnels et de diagnostiquer les problèmes hydrauliques à l'intérieur des réacteurs (les écoulements préférentiels par exemple).

Enfin, la conception de la filière de traitement *in situ* pour le site Lorraine se base principalement sur les résultats en laboratoire. Ce projet a permis de développer une méthodologie concrète de restauration des eaux polluées par le DMA. Ces outils permettront alors d'appliquer une démarche similaire sur d'autres sites à restaurer en Abitibi-Témiscamingue et ailleurs. Cette méthode est basée sur les caractéristiques de l'effluent, la sélection des matériaux et le choix d'une filière de traitement.

CHAPITRE 2

TREATMENT OF ACID MINE DRAINAGE WITH HIGH IRON CONCENTRATION USING SULPHATE REDUCING PASSIVE BIOREACTOR: I. MIXTURES CHARACTERIZATION, IRON SORPTION CAPACITY AND BATCH TESTS ASSAYS

Cet article a été soumis à Applied Geochemistry, en novembre 2011.

Auteurs

Thomas Genty[1], Bruno Bussière[1], Mostafa Benzaazoua[2], Gérald J. Zagury[3]

[1]Industrial Chair CRSNG Polytechnique-UQAT: Environment and mining wastes management, University of Québec in Abitibi-Témiscamingue, Rouyn-Noranda, Québec, Canada

[2]Laboratoire de Génie Civil et d'Ingénierie Environnementale, INSA de Lyon, Villeurbanne, France

[3]Industrial Chair CRSNG Polytechnique-UQAT : Environment and mining wastes management, École Polytechnique, Québec, Canada

Abstract

The use of active water treatment to treat acid mine drainage (AMD) in abandoned mine sites is not desirable. Passive treatment systems are an attractive alternative to active treatments since they do not use much energy, they can be built with natural materials or wastes and they usually involve low investment costs compared to active treatment plants. Sulphate-reducing passive biofilters (SRPB) are considered to be the best option to treat AMD with high iron concentration. In this study, materials used to design the mixture used in SRPB treating a high iron concentrated AMD were properly characterized and iron sorption onto the material was investigated. Sorption tests showed mainly that organic materials (manures,

municipal wastewater sludges and compost) were the performing substrate to remove iron. Eight different biofilter mixtures were then compared for their capacity to treat a high iron acid mine drainage (pH 3.5 and [Fe] = 4000 mg/L) using batch tests for 40 days. For most mixtures tested, the pH increased up to 6.5, the redox potential decreased below 0 mV after 10 days of testing, and dissolved metal concentrations were reduced by more than 99%. Results showed also that mixtures based on chicken, cow, or sheep manures give similar results, and mixtures containing 50% of calcite or sand performed well.

Keywords: acid mine drainage, sulphate-reducing passive bioreactor, batch tests, sorption tests.

2.1 Introduction

The main water pollution source in mining operations comes from the interaction between water, air, and sulphidic mine wastes; this environmental problem is known as acid mine drainage (AMD) (Aubertin and al., 2002). AMD generation results from a series of chemical and biochemical oxidation reactions of sulphide minerals (e.g. Kleinmann and al., 1981; Blowes and Ptacek, 1994; Evangelou and Zhang, 1995; Perkins and al., 1995; Morin and Hutt, 1997) that lead to acidity as well as dissolved metals concentration increases, if the neutralization potential from carbonate or silicate minerals is absent or exhausted (Benzaazoua et al. 2004).

Mining companies often use conventional active treatment plants to treat the contaminated effluents when AMD cannot be controlled at its source. The approach consists of adding lime to neutralize acidity, leading to metals precipitation (MacDonald et al., 1989, Aubertin and al., 2002, Brown et al., 2002, Aubé, 2005). However, the treatment plants become expensive to manage when mines are closed. Passive treatment systems, which require less energy and use natural or waste materials, are preferred as treatment method for these closed sites (Gazea and al., 1995, Morin and Hutt, 1997, Skousen and Ziemkiewicz, 2005, Neculita et al., 2007). There are different types of passive systems. The first category includes chemical approaches like anoxic limestone drains that increase pH and alkalinity by carbonate dissolution (Cravotta and Trahan, 1999, Genty et al., 2011). The second category integrates biological

systems that use sulphate reducing bacteria (SRB) to treat AMD effluents (Neculita et al., 2007); this paper focuses on this second category.

Sulphate reducing passive bioreactor (SRPB) uses SRB metabolism to reduce metal concentration and increase pH and alkalinity. The degradation of a carbon source coupled with the sulphate reduction allows the formation of hydrogen sulphide and hydrogenocarbonate ions. Equation [2-1] represents the organic material degradation (Luptakova and Kusnierova, 2005, Jong and Parry, 2006, Neculita et al., 2007).

[2-1] $$2CH_2O + SO_4^{2-} \rightarrow 2HCO_3^- + H_2S$$

Then, hydrogen sulphide precipitates with metal (M^{2+}) as show in equation [2-2].

[2-2] $$M^{2+} + H_2S \rightarrow MS + 2H^+$$

However, previous studies show that the precipitation of metal sulphides is not the only removal metal mechanism. Metals can be also fixed by many others phenomena: sorption, biosorption, precipitation, coprecipitation with hydroxides and carbonates, and physical filtration (Neculita et al., 2007, Karathanasis et al., 2010). Sorption is an important phenomenon of metal retention particularly at the beginning of SRPB operation (Neculita et al., 2008b, Karathanasis et al., 2010).

A key component of SRPB reactors is the carbon mixture (Beaulieu, 2001, Cocos et al., 2002, Neculita et al., 2007). Significant sulphate-reduction rates have been obtained with reactive mixtures containing more than one organic carbon source (Waybrant et al., 1998). The organic mixture must ensure a good availability of carbon and nutrients for bacteria growth. Typically, SRPB mixtures contain organic materials (cow, chicken, sheep manures or wastewater sludges), cellulosic wastes (compost, maple sawdust and wood chips), SRB inoculum (ex. river or stream sediments), a neutralizing agent (calcite, carbonates), a structural agent (sand), and nitrogen source (urea) (Cocos et al., 2002, Zagury et al., 2006, Costa et al,. 2008, Neculita and Zagury, 2008). The roles of the main SRPB components can be summarized as follows: organic material and cellulosic wastes are degraded by bacteria which produce alkalinity; the neutralizing agent allows an increase of the pH (at values more

optimal for SRB activity), the structural agent prevents clogging phenomena, and the nutrients like urea support SRB development. Performances of SRB bioreactors mainly depend on the carbon source and on the contact time between sulphates contained in the AMD solution and the bacteria. Many authors worked on mixture optimization (e.g. Cocos et al., 2002, Waybrant et al., 1998, Neculita and Zagury, 2008). Recent works by Potvin (2009) and Neculita et al. (2008a) proved that a mixture based on manure, wood chips, sawdust, compost, carbonate, sand, sediments, and urea allows treating AMD with an iron concentration of approximately 500 mg/L for a hydraulic retention time of 10 days.

Prior to biofilter process design, it is necessary to optimize the carbon mixture and hydraulic parameter in laboratory (Gusek, 2001). This is done mainly through three main steps. The first step is called a batch test (around 1 L) (Waybrant et al., 1998, Cocos et al., 2002, Beaulieu, 2001, Tassé and Germain, 2002, Gibert et al., 2004, Zagury et al., 2006), and allows preselecting the most promising mixture. Indeed, the choice of an effective substrate mixture is dependent on the composition of the AMD and the types of substrates available at low cost. During the second step, column tests (around 10 L) can be carried out to verify the effectiveness of the treatment (Beaulieu, 2001, Gibert et al., 2004, Gibert et al., 2005, Jong and Parry, 2006, Neculita et al., 2008a, Costa et al., 2008). This step also allows adjusting the hydraulic retention time. Finally, medium scale tests (50 litres and more) allow verifying the scale effect (Kuyucak and St-Germain, 1994, Gusek, 2001, Dann et al., 2009, Potvin, 2009). Once all these steps are optimized, full size SRPB can be constructed (Germain and Cyr, 2003, Zaluski et al., 2003, Kuyucak et al., 2006).

In the present paper and in the companion paper (Genty et al. 2011), the first two steps of SRPB design approach are presented (batch and column tests). This study focuses on AMD with high iron concentration (approximately 4000 mg/L) typical of those frequently found close to abandoned Canada base metal mine sites (Aubertin et al., 2002, Molson et al., 2008, Potvin, 2009). The main originality of this study was the treatment with SRPB of AMD with high iron concentration because SRPB tend to have lower efficiency when iron concentration is higher than 1000 mg/L (Neculita et al., 2008a, Potvin, 2009). In this paper, the emphasis is on material characterization and batch test results. Sorption tests are also performed to

characterize sorption phenomena which occur at the beginning of SRPB operation. Iron sorption testing is the second original part of this paper.

2.2 Materials and Methods

2.2.1 Synthetic acid mine drainage quality

The water treatment tests were carried out using a synthetic AMD solution having characteristics given in Table 2.1. The metallic salts used for the preparation of AMD were dissolved in tap water. AMD had a pH of 3.5, a high concentration of iron (approximately 4320 mg/L), and a sulphate concentration above 11878 mg/L. Chemical conditions (low pH, high Eh) in AMD tank caused some precipitation of iron hydroxide, but metal concentrations stayed relatively stable.

Table 2.1 Concentrations of the synthetic acid mine drainage (in mg/L except pH)

Elements	Initial	Salt used
Al	6.24	$Al_2(SO_4)_3,18H_2O$
Cd	2.15	$CdSO_4,8H_2O$
Cr	1.35	$CrK(SO_4)_2,12H_2O$
Fe	4320	$FeSO_4,7H2O$
Mg	9.95	$MgSO4,7H_2O$
Mn	42.8	$MnSO_4,H_2O$
Ni	3.46	$NiSO_4,6H_2O$
Pb	0,58	$Pb(NO_3)_2$
SO_4^{2-}	11878	$Na_2SO_4,10H_2O$
Zn	49.2	$ZnSO_4,7H_2O$
pH	3,5	HCl 1N

2.2.2 Physical, mineralogical, bacterial and chemical characterization of solids

Each material and mixtures used in this study were fully characterized. Water content was evaluated in duplicate by drying samples at 40°C during 2 days. Relative density of the grains was measured by a helium pycnometer Micromeritics Accupyc 1330 and the specific surface area by a surface analyser Micromeritics Gimini III 2375 (on dry material). Particle size was determined as per Aitcin et al. (1983). Paste pH was determined in deionized water using a solid to liquid ratio of 1:10 (ASTM, 1995).

Total organic carbon (TOC) was measured by adding potassium dichromate and sulphuric acid and measurement of excess of potassium dichromate; the total Kjeldahl nitrogen (TKN) was evaluated by mineralization of organic matter by sulphuric acid (into ammonium, carbon dioxide and water), and measurement of ammonium formed. Water extracts (1:10 solid liquid ratio) were also analyzed for dissolved organic carbon (DOC) using a heated tube at 680°C with a catalyser and an infra-red detector of carbon dioxide emitted.

Solids were digested in HNO_3, Br_2, HCl, and HF to determine chemical composition of each material (Potts, 1987). Then, the liquid resulting from this treatment was analysed for metal content by Inductively Coupled Plasma-Atomic Emission Spectrometry using a Perkin Elmer OPTIMA 3100 RL (ICP-AES; relative precision of 5%, Villeneuve, 2004). The method to evaluate cation exchange capacity (CEC) was adapted from Zagury et al. (2004). A positive CEC indicates that cation exchange is one of the sorption mechanisms of iron retention. This method consisted in saturating all matrix exchange sites with sodium ions (with a sodium acetate solution 1N) and to desorb it with a solution of ammonium acetate 1N. Then, sodium concentration was analysed using a Metrohm 881 compact IC pro ions chromatograph (column Metrosep C 4 150/4.0, elluent: 1.7 mmol HNO3 and 0.7 mmol dipicolinic acid, flow rate: 0.9 mL/min, 25°C). The mineralogy of the crystallized mineral fraction was determined by an X-ray diffractometer (XRD; Bruker axs D8 ADVANCE). The instrument is equipped with a Cu anticathode and scintillation counter. Data treatment was done using Bruker A.X.S. EVA and TOPAS software package. The proportion of minerals is estimated by the Rietveld method (relative precision of 0.5%, Raudsepp and Pani, 2003).
Finally, sulphate reducing bacteria (SRB) enumerations within the solid organic materials and the tested sediments were performed using the Most Probable Number according to ASTM (1990) and Beaulieu (2001).

2.2.3 Analytical method for water quality evaluation and geochemical modeling

The pH of samples was determined with an Orion Triode sensor coupled with a Benchtop pH/ISE Meter Orion model 920 (relative precision +/- 0.01 pH) and the Eh (redox potential) was measured by a Pt/Ag/AgCl sensor linked to a Benchtop pH/ISE Meter Orion 920 (relative precision +/- 0.2 mV), values were corrected relative to the standard hydrogen

electrode (SHE). Filtered samples (with a 0.45 µm filter) used for the metal analysis were acidified with 2% volume with nitric acid (70%) before analysis. Sulphate concentration was evaluated on filtered sample using a nephelometric method based on the precipitation of barium sulphate (AFNOR, 1986). Then, the absorbance of the solution was measured at 650 nm with an Ultraspec 2100 pro spectrophotometer (relative precision of +/- 0.5%).

Saturation indices of the main minerals susceptible to precipitate were calculated using a thermodynamic chemical equilibrium model (Vminteq v 2.53) using the activity correction SIT model (KTH, 2010). Geochemical modelling helps in the assessment of metal retention mechanisms during the batch tests. However, this model does not take into account the sulphate reducing bacteria activity.

2.2.4 Batch experiments

Eight mixtures were investigated in this study. The mixture proportions (%, dry weight) are given in Table 2.2. These mixtures contained organic materials (cow, chicken, sheep manures or waste water sludges, compost), cellulosic wastes (maple sawdust and wood chips), SRB inoculum (river sediments), a neutralizing agent (calcite mineral or a calcium carbonate powder grad 99% ACS), a structural agent (sand), and nitrogen source (urea powder 99% ACS). Maple chips and sawdust came from P.W.I. industries, Canada, chicken manure from Fertilo de Fafard, Canada; sheep manure and cow manure from Canadian Tire Corporation, Canada; leaf compost from Compost du Québec, Canada; the waste water sludges from the municipality of Rouyn-Noranda, Canada; fine calcite with a particle size smaller than 0.625 cm from Calcite du Nord, Canada; and finally sediment came from the Osisko lake, Rouyn-Noranda, Canada.

The composition of mixture #1 is mainly inspired from previous studies of Cocos et al. (2002) and Neculita and Zagury (2008). Mixtures #2, #3 and #5 were selected to evaluate the possibility of using different sources of easily degradable carbon (Cocos et al., 2002, Costa et al, 2008). Mixture #6 allows comparing the efficiency of similar mixtures with or without sediment SBR inoculums. Mixtures #4 and #7 were tested to investigate the effect of an increase of the granular material percentage on the treatment performance. A higher saturated hydraulic conductivity for these bioreactors was expected thanks to an increased of granular

material percentage (Benner et al., 1997, Rötting et al., 2008). Finally, mixture #8 was similar to mixture #1, but without urea.

Table 2.2 Composition of the eight mixtures for BSR biofilter (composition given in dry mass %)

Mixture	#1	#2	#3	#4	#5	#6	#7	#8
Celullosic wastes								
Maple chips	10	10	10	5	10	10	6	10
Sawdust	20	20	20	10	20	20	11	20
Organic wastes								
Chiken manure	10			5		10	8	10
Sheep manure		10						
Cow manure			10					
Waste water sludges					10			
Leaf compost	20	20	20	10	20	20	12	20
Inoculum								
River sediment	15	15	15	8	15		8	15
Inert structural agent								
Sand	20	20	20	10	20	35	50	20
Nutriment (Nitrogen)								
Urea	3	3	3	2	3	3	3	
Neutralizing agent								
Calcium carbonate	2	2	2		2	2	2	
Calcite				50				5

Batch tests were performed in 1L glass flasks[4], at room temperature (21°C) under nitrogen atmosphere and placed on a shaking table (150 rpm). As per Neculita and Zagury (2008), the ratio between mixture and AMD was 200 g dry mixture for 600 mL of AMD. pH, Eh, sulphate and metals were measured every week during 40 days. After the end of the test, the chemical composition of the solid matrix was determined and geochemical modeling was performed for durations of 0, 10, 24, and 40 days.

[4] Des photographies de chaque essai (batch, colonnes, réacteur de 2000 L, terrain et démantellement) peuvent être consultées à l'Appendice D.De plus, des études précédentes ont permis de statuer sur le fait que les essais étaient répétables (e.g. Cocos et al., 2002, Neculita and Zagury, 2008) et donc aucun duplicata n'a été fait dans le cadre de la présente étude

2.2.5 Sorption experiment description

Iron retention capacity of each mixture component (manure, waste water sludges, compost, maple sawdust and chips, and river sediments.) was assessed. Iron was monitored because it has been previously demonstrated that there is a decrease of SRPB efficiency when iron concentration in AMD is high (Neculita et al., 2008a).

2.2.5.1 Sorption isotherm experiments

Isotherm studies were performed at 21°C in a 200 mL Erlenmeyer filled with 100 mL of aqueous solution and 2 g of dry material at pH of 3 and 6 (pH adjustment with NaOH 1N or HCl 1N). The agitation speed was set at 200 rpm. The ratio of solid material to solution (and consequently the quantity of iron in solution) should ensure that equilibrium conditions are reached quickly (Gupta et al., 2009). Metal concentration within the aqueous solutions varied from the common AMD loads to AMD concentration diluted fifty times. Diluted AMD solution was used in isotherm sorption tests although only iron concentration was measured. Iron was the most concentrated metal to remove, and other metals were not considered problematic with the concentrations used (Neculita et al., 2008a). Indeed, since ionic competition can occur on sorption sites, it was considered more representative to use AMD solution with numerous metal salts instead of deionised water with iron only (Limousin et al., 2007). After reaching equilibrium in 24 hours, water samples were filtered for metal content analysis. Sorption capacity, q_e (mg/g) of the sorbent was calculated using the mass balance equation (Al-Degs et al., 2006):

[2-3] $$q_e = [C_i - C_e].\frac{V}{m}$$

where C_i, C_e, V, and m are respectively initial metal concentration (mg/L), metal concentration at equilibrium (mg/L), total volume (L) and mass (g) of the sorbent.

2.2.5.2 Kinetic sorption experiments

Kinetic sorption studies of iron were carried out in agitated batch sorption systems, which consisted of a 200 mL Erlenmeyer filled with 100 mL aqueous solution of AMD diluted

twenty times (this concentration was chosen to observe a significant iron decrease during 24 hours), and 2 g of dry material. The agitation speed was fixed at 200 rpm. This test was performed at pH 3 and 6 by adjustment with NaOH 1N or HCl 1N. Water samples were taken regularly to determine the evolution of iron concentration during the first 24 hours (0, 2, 4, 8, and 24 hours).

The instant iron uptake q_t (mg/g) of the sorbent was calculated by the mass balance equation (Al-Degs et al., 2006):

[2-4] $$q_t = [C_i - C_t] . \frac{V}{m}$$

where C_i, C_t, V, and m are respectively initial metal concentration (mg/L), metal concentration at time t (mg/L), total volume (L) and weight (g) of sorbent.

2.2.5.3 Sorption tests interpretation approaches

It is usually assumed in the literature that sorption isotherm and sorption kinetic characterize the sorption capacity of a material towards an ion. To describe equilibrium phenomena, two of the most commonly isotherm theories were used: the Langmuir and Freundlich equilibrium isotherms. The linear form of Langmuir equation can be represented by the following equation (Ayari et al., 2004, Al-Degs et al., 2006, Jha et al., 2008, Garcia-Mendieta t al., 2009):

[2-5] $$\frac{C_e}{q_e} = \frac{1}{b.q_{max}} + \frac{C_e}{q_{max}}$$

where C_e is the equilibrium concentration of remaining metal in the solution (mg/L), q_e is the amount of a metal adsorbed per unit mass of sorbent at equilibrium (mg/g), q_{max} is the amount of sorbate at complete monolayer coverage (mg/g), and b (L/mg) is a constant related to the heat of adsorption. The Langmuir model assumes that the removal of a metal ion occurs on a homogenous surface by a monolayer sorption (Jha et al., 2008). In other words, sorption sites are identical, retain only one molecule and are energetically and sterically independent of the adsorbed quantity (Limousin et al., 2007).

Freundlich linear isotherm can be described by the following equation (Ayari et al., 2004, Al-Degs et al., 2006, Jha et al., 2008, Garcia-Mendieta et al., 2009):

[2-6] $$\log q_e = \log k_f + n.\log C_e$$

with C_e in mg/g, q_e in mg/g. k_f is the equilibrium constant (mg/g) indicative of adsorption capacity and n represents the sorption equilibrium constant. The Freundlich model assumes that sorption occurs on a heterogeneous surface (due mainly to the complex composition of natural material) and an exponential distribution of active sites (Jha et al., 2008, Garcia-Mendieta et al., 2009).

Sorption processes begin by diffusion of metal ion onto the surface (external and internal diffusion) and then the metal ion links to the surface. Numerous models have been proposed to describe sorption kinetic tests. They can be divided into two main types: reaction-based models and diffusion-based models (Ho et al., 2000, Al-Degs et al., 2006). In this study, the first type of models represents more accurately the sorption kinetic and thus diffusion based models are not presented.

If the sorption mechanism is controlled by the surface reaction where the metal ion was linked to the material, kinetic models using pseudo first order or pseudo second order can be used. Equations [2-6] and [2-7] represent two models of pseudo first and second rate (Ho et al., 2000, Al-Degs et al., 2006, Jha et al., 2008, Garcia-Mendieta et al., 2009):

[2-6] pseudo first order : $$\log(q_e - q_t) = \log q_e - k_1.\frac{t}{2.303}1$$

[2-7] pseudo second order : $$\frac{t}{q_t} = \frac{1}{k_2.q_e^{\,2}} + \frac{t}{q_e}$$

where q_e is the amount of a metal adsorbed per unit mass of sorbent at equilibrium (mg/g), q_t is the amount of a metal adsorbed per unit mass of sorbent (mg/g) at the time t (s), k_1 is the pseudo first order rate constant (s^{-1}), and k_2 the pseudo second order rate constant ($g.mg.s^{-1}$). Several other models can be found in the literature (Ho et al., 2000) and have been compared

with experimental data, but the two selected models (equation [2-6] and [2-7]) were found to be the more efficient to fit the experimental data.

2.3 Results and interpretations

2.3.1 Initial materials and mixtures characteristics

Table 2.3 presents the main characterization results of organic materials and river sediments. Organic material can be divided into cellulosic (maple chips and sawdust) and organic wastes (manure, sludge and compost).

As observed by Neculita and Zagury (2008), the cellulosic materials paste pH measurements were more acidic than those of the organic wastes (between 6.2-5.6 and 6.0-7.3 respectively). The total organic carbon (TOC) was higher for the cellulosic wastes than for the organic wastes (49-51% and 21-30% respectively) while the total Khejdahl nitrogen (TKN) values varied from 1.1 to 2.6% except for the maple chips (0.1%) and the river sediments (0.04%). Dissolved organic carbon (DOC) values for the cellulosic wastes were significantly higher than those of the organic wastes (respectively 280 and 450 mg/L for wood chips and sawdust and below 57 mg/L for manure, municipal sludges and sediments). The presence of sulphate reducing bacteria (SRB) inoculums in materials used in biofilter mixture is significant. The data presented in Table 2.4 show that manures, compost, and sediments contain a minimum of 450 to 2300 SRB cell/100mL. These results confirmed that the source of SRB in the tested mixtures is not only sediments. Moreover, urea is a nitrogen source for bacteria (Neculita and Zagury, 2008). The TKN percentage of urea was approximately 47%.

The particle size analysis of calcite showed a grain size D_{10} (D_x being the effective diameter, corresponding to x% passing on the cumulative grain-size distribution curve) of 0.53 mm and a uniformity coefficient ($C_U = D_{60}/D_{10}$) of 3.5. The XRD analysis confirmed that the calcite used was relatively pure (96.5 wt.% calcite) and contained a small proportion of quartz and hornblende. The mineralogical composition of the river sediment estimated by XRD was: albite (24%), tremolite (20%), quartz (17%), microcline (14%), chlorite (7%), talc (6%), anorthite (5%) muscovite (5%) and traces of kaolinite, wurtzite, hematite, and magnetite.

Sorption of iron onto organic material surface is complex (Vizier, 1987). Numerous mechanisms can occur, such as adsorption (physical or chemical), cation exchange, mechanical trapping, and surface precipitation. Isotherms test characterizations allow describing the sorption mechanism (sorption onto a homogeneous surface or a heterogeneous surface) and while kinetic tests allow determining which step (diffusion, reaction at the surface) is limiting the sorption. However, sorption mechanisms cannot be specifically identified. Cation exchange capacity (CEC) was determined for all materials to get an idea of the quantity of metals that can be removed by ionic exchange for 1 g of sample. The CEC results were: 18.4 meq/100g (dry) for sediments, 38.8 meq/100g (dry) for cow manure, 47.7 meq/100g (dry) for maple chips, 52.7 meq/100g (dry) for leaf compost, 52.9 meq/100g (dry) for sheep manure, 55.5 meq/100g (dry) for chicken manure, 66.2 meq/100g (dry) for waste water sludge, and 72.7 meq/100g (dry) for sawdust. The positive results for CEC for all materials highlighted that ion exchange could be one of the metal sorption phenomena that occurred onto organic materials and sediments surfaces. These results were not unexpected since the tested sediments contain clay minerals, known to have an important ion exchange capacity (e.g. Garcıa-Sanchez et al., 1999, Coles and Yong, 2002, Ayari et al., 2004, Fonseca et al., 2006, Plante, 2010). Organic materials are also known for having a significant CEC (Volesky and Hollan, 1995, Asadi et al., 2009, Yurtsever and Sangil, 2009).

Table 2.4 presents the characterization of the biofilter mixture prepared with the materials previously presented. The eight mixtures tested are also characterized with the TOC/TKN and DOC/sulphate ratios. It is usually assumed that ratios TOC/TKN near 10 and DOC/sulphate near approximately 0.4 are optimal for sulphate reducing biofilter to reach good performances (Neculita and Zagury, 2008). These ratios allowed a good availability of nutrients for SRB development. For mixtures used in this study, the most favourable ratio TOC/TKN was obtained with mixture #1 (13); for mixtures #2, #3, #4, #6 and #7, the ratio varied between 24 and 28. The ratio for mixture #5 was 5 (lack of carbon in comparison with nitrogen). For mixture #8, the value obtained (94) was significantly higher than the target of 10, and can be explained by a lack of nitrogen due mainly to the absence of urea in the mixture. Values of DOC/sulphate ratio varied from $1.2x10^{-2}$ to $5.7x10^{-2}$ for mixtures #1 to #7, and the ratio was $3.3x10^{-3}$ for mixture #8. This result indicated that easily degradable organic

carbon represented by DOC was less available for the last mixture. Values were globally lower than the targeted optimal ratio of 0.4 because of the high sulphate concentration used in AMD (9000 mg/L).

Table 2.3 Characterization of organic materials and river sediments used in this study[5]

Material	Maple chips	Maple sawdust	Chicken manure	Cow manure	Sheep manure	Municipal sludges	Leaf compost	River Sediments
Physical parameters								
Paste pH	6.2	5.6	6.0	7.0	7.1	7.3	6.7	7.1
Water content (%w/w)	4	3	55	62	58	74	56	27
Relative density of grains	1.45	1.48	1.57	1.69	1.64	2.04	1.80	2.66
Specific surface area (m^2/g)	0.58	0.86	1.15	0.96	1.10	15.75	1.67	13.02
CEC (meq/100g)	47.7	72.7	55.5	38.8	52.9	66.2	52.7	18.4
Biodegradation parameters								
TOC (%w/w dry weight)	51	49	26	27	30	21	24	1.5
TKN (%w/w dry Weight)	0.1	0.2	2.6	1.4	1.1	1.9	1.3	0.04
DOC water extract (mg/L)	280	450	57	35	32	5.6	48	6.4
TOC/TKN	510	272	10	19	27	11	18	38
Sulphate reducing parameters								
SRB (cells/100 mL)	<2	<2	450	780	2300	2300	780	1300
DOC/SO_4^{2-}	3.2×10^{-2}	5.0×10^{-2}	6.3×10^{-3}	3.9×10^{-3}	3.6×10^{-3}	3.9×10^{-4}	5.3×10^{-3}	7.1×10^{-4}

[5] Le contenu en métaux des matériaux et des mélanges peut être consulté en Appendice F.

Table 2.4 Characterization of sulphate reducing biofilter mixtures #1 to #8

Biofilter mixture	#1	#2	#3	#4	#5	#6	#7	#8
Physical parameters								
Water content (%w/w)	27	24	30	20	34	27	22	27
Relative density of grains	2.04	2.09	1.97	2.26	1.94	1.66	2.16	1.89
Biodegradation parameters								
TOC (%w/w dry weight)	13	24	28	11	20	23	23	29
TKN (%w/w dry Weight)	1.0	0.9	1.1	0.4	6.2	1.0	0.9	0.3
DOC water extract (mg/L)	110	120	310	140	170	310	510	30
TOC/TKN	13	26	25	28	3	24	24	94
Sulphate reducing parameters								
DOC/SO_4^{2-}	$1.2x10^{-2}$	$1.3x10^{-2}$	$3.4x10^{-2}$	$1.6x10^{-2}$	$1.9x10^{-2}$	$3.4x10^{-2}$	$5.7x10^{-2}$	$3.3x10^{-3}$

2.3.2 Batch experiment results

Results of the evolution of the main chemical parameters determined during anaerobic batch tests are presented in Figure 2.1. Figure 2.1a shows that the solution pH for each flask rose up to 7 over 10 days, except for mixture #8 (lowest DOC content of all mixtures) which needed 30 days to reach pH-neutrality. The Eh in most flasks decreased below 0 mV and thus promoted reducing conditions; mixtures #4 and #8 remained at values of approximately 150 to 210 mV (Figure 2.1b). Each mixture allowed removing more than 99% of iron over less than 20 days as showed in Figure 2.1c. With regards to sulphate concentrations (Figure 2.1d), there was no significant decrease before 18 days, which approximately corresponds to the latency period for SRB activity (Neculita and Zagury, 2008), except for mixture #8 where a progressive decrease was observed. The initial value of sulphate concentration was higher than expected in the original AMD because some components of the organic mixtures (mainly manure and compost) contained and released sulphate during the test (Zagury et al., 2006). After 40 days testing, sulphate decreased by 64% for mixture #1 and #2, 63% for mixture# 3, 29% for mixture #4, 39% for mixture #5, 34% for mixture# 6, 65% for mixture #7, and 73% for mixture #8.

Cadmium, chromium, nickel, lead, and zinc removal were higher than 99% for all mixtures after 40 days. The removal for manganese reached 99% for all mixture except for mixture #8. Aluminum removal was 54% for mixture #1, 78% for mixture #3, 92% for mixture #5 and 99% for the other mixtures. Moreover, mixtures analyses in terms of metal contents showed an increase of Cd, Fe, Mn, Ni, Pb and Zn after 40 days.

Retentions of most of these metals (not shown here) occurred between 0 and 10 days. The same observation was made by Cocos et al. (2002). Considering this last observation and the fact that the sulphate reduction mainly began after 20 days, the mechanisms of metal removal during the first days was essentially attributed to sorption mechanisms, hydroxide and carbonate precipitation, and not to sulphide precipitation (as stated elsewhere by Karathanasis et al., 2010). Sorption properties of the materials studied will be discussed in section 3.3.

Sulphate removal rates can also be calculated for the 40-day period and during the period between 18 and 40 days. This last period may correspond to the initiation of bacterial

sulphate reduction. Sulphate removal rates for the eight reactive mixtures varied from 102 to 217 mg/L/day for the entire testing, and between 59 and 278 mg/L/days for the period between 18 and 40 days. Values estimated for the second period (18 to 40 days) were comparable to those obtained in previous works by Neculita and Zagury (2008). However, depending on pH and Eh conditions, sulphate removal could be attributed to sulphate reduction (sulphide formation) or to sulphate precipitation (Neculita and Zagury, 2008, Potvin, 2009). For the day 0, Vminteq modeling predicted only the precipitation of H-jarosite and Geothite-lepidochrocite, which is common in AMD (Potvin, 2009). For all mixtures, Vminteq predicted precipitation of aluminium hydroxide, goethite and lepidochrocite for days 10, 14 and 40. For mixture #1, #3, #5, #6, and #7, precipitation of iron, nickel and zinc sulphides could occur while for mixture #2, #4 and #8 gypsum precipitation was probable. Thus, sulphate can be removed trough two phenomena by the studied mixtures: gypsum or metal sulphide precipitation.

Considering that mixtures #1, #2, #3, #5 gave similar results for metal removal and neutralization, different easily degradable organic carbon sources can be used in SRPB, such as chicken, cow, sheep manure or municipal sludge. Mixture #6 results demonstrated that a SRB inoculums coming from sediment were not essential since results were equivalent to mixture #1. Mixtures #4 and #7 performed also well and are comparable in terms of performance to mixture #1. Mixture #8 performed worse than the others (lower sulphate removal during the period 18 to 40 days, lower iron retention kinetic, lower neutralization). Consequently, three original mixtures (#1, #4 and #7) emerged from these batch tests and were selected for the column test investigation (see the companion paper).

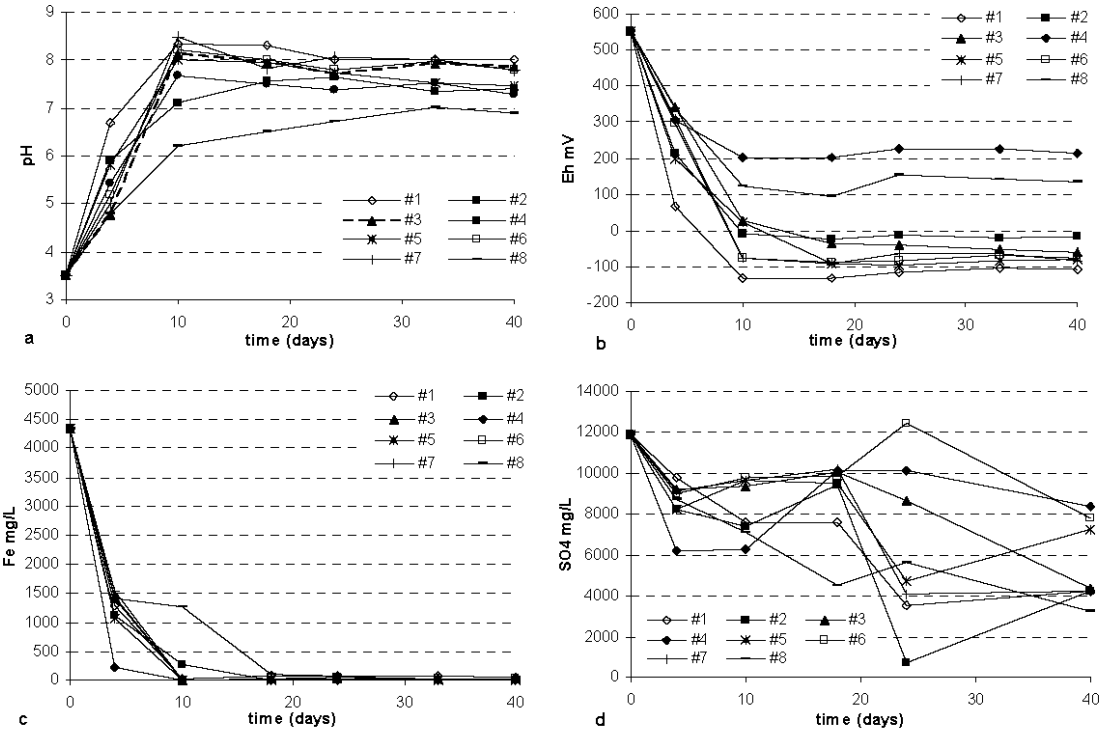

Figure 2.1 Chemical parameters measured in batch tests for the 8 mixtures: pH (a), Eh (b), iron concentration (c) and sulphates concentration (d).

2.3.3 Sorption experiment results

2.3.3.1 Sorption isotherm test results

The purpose of the adsorption isotherms is to relate at equilibrium the adsorbate concentration (at the solid surface) to the metal concentration in solution. A classification of the sorption phenomena for liquid/solid systems is given by Limousin et al. (2007) and García-Mendieta et al. (2009), which distinguish four classes of isotherm: high affinity (H), Langmuir (L), constant-partition (C) and sigmoidal shaped (S) isotherm.

In this study, isotherms (see Figure 2.2) with a convex shape (equivalent to L type) were obtained for all materials at pH 3 and isotherms with sigmoidal form (equivalent to S type) were obtained for all material at pH 6 (except for maple chips where the curve is more of L-type). Thus, two mechanisms could represent sorption phenomena. At pH 3, the solid was

progressively saturated and micropores were filled by a monocover of iron linked with high interaction like chemisorption. At pH 6, a monocover was first formed and then several other covers were created. This type of observation is also presented by García-Mendieta et al. (2009) for the sorption of iron on clinoptilolite (ion exchanger) at pH 6. Table 2.5 presents the main results of isotherm data compared with the Langmuir and Freundlich models. However, Freundlich model was more appropriate to model isotherm data for most materials at pH 3 and 6, except for compost at pH 6 where Langmuir model was more adapted.

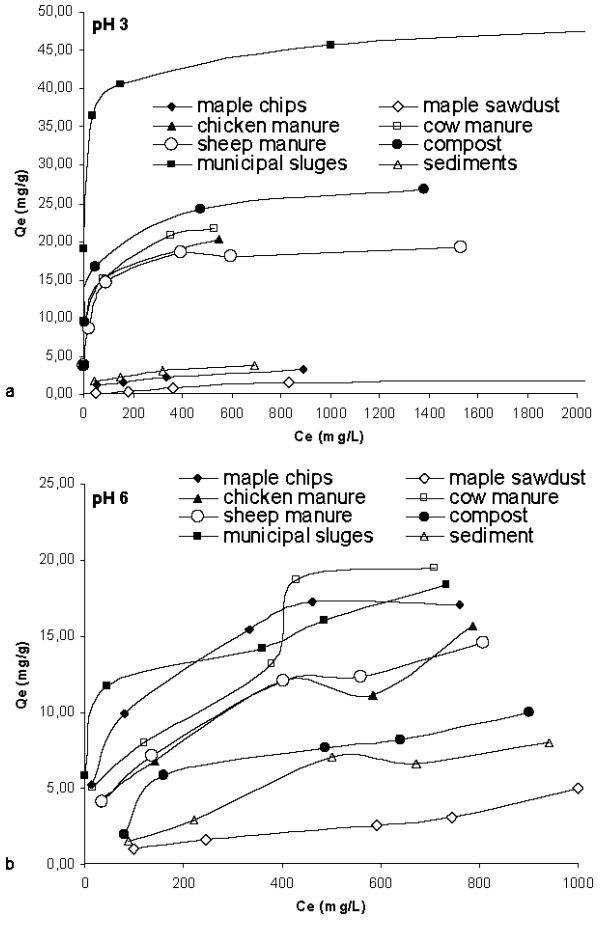

Figure 2.2 Iron sorption isotherms at pH 3 (Fig. 2a) and pH 6 (Fig. 2b) for the different materials

The maximum iron sorption capacity q_{max} (mg/g) could be estimated graphically for each material. The order from the most adsorbing to the less adsorbing material at pH 3 was: municipal sludges (q_{max} = 48.5 mg/g) > compost (q_{max} = 26.7 mg/g) > cow manure (q_{max} = 21.5 mg/g) > chicken manure (q_{max} = 20.3 mg/g) > sheep manure (q_{max} = 19.3 mg/g) > sediments (q_{max} = 3.8 mg/g) > maple chips (q_{max} = 3.0 mg/g) > maple sawdust (q_{max} = 2.0 mg/g). At pH 6, this order is different: cow manure (q_{max} = 19.5 mg/g) > municipal sludges (q_{max} = 18.4 mg/g) > maple chips (q_{max} = 17.1 mg/g) > chicken manure (q_{max} = 15.6 mg/g) > sheep manure (q_{max} = 14.6 mg/g) > compost (q_{max} = 10.0 mg/g) > sediments (q_{max} = 8.0 mg/g) > maple sawdust (q_{max} = 5.0 mg/g). Hence, iron sorption behaviour of materials depends on the solution pH. At pH 3, most of the materials had a higher iron sorption capacity than at pH 6, except for sediments, maple sawdust and chips.

Isotherm results also showed that iron removal seemed to be more important (k_f values were higher; this parameter represents the adsorbed quantity of iron in mg per gram of material for an iron equilibrium concentration of 1 mg/L) at pH 3 than at pH 6 for all materials, except for maple chips and cow manure. These results show that materials tested were able to uptake iron directly from AMD (neutralization was not a factor to improve the uptake capacity of a material). However, at near neutral pH, iron surface–enhanced precipitation could improve iron retention (Limousin et al., 2007); this was probably the case for cow manure, maple sawdust and chips which have paste pH between 6 and 7. This hypothesis of iron precipitation was validated by Vminteq modeling that suggested a possible precipitation of iron oxi-hydroxides for similar geochemical conditions.

Table 2.5 Iron sorption isotherm models for organic materials and sediment at pH 3 and pH 6 (only the model which fits the best is presented, F= Freundlich, L= Langmuir)

Isotherm models	pH 3				pH 6					
	Best fit model	R^2	k_f (mg/g)	n	Best fit model	R^2	k_f (mg/g)	n	q_{max} (mg/g)	b (L/mg)
Maple chips	F	0,95	0,30	0,35	F	0,98	2,55	0,30		
Maple sawdust	F	0,96	0,06	0,53	F	0,95	0,05	0,63		
Chicken manure	F	0,88	5,05	0,23	F	0,96	1,06	0,39		
Cow manure	F	0,95	0,03	0,24	F	0,93	1,62	0,37		
Sheep manure	F	0,98	5,05	0,21	F	0,99	1,00	0,40		
Leaf compost	F	0,84	5,04	0,26	L	0,91			0,17	0,21
Municipal sludge	F	0,75	13,33	0,19	F	0,98	6,77	0,14		
River Sediments	F	0,98	0,50	0,31	F	0,97	0,06	0,73		

2.3.3.2 Kinetic sorption test results

The kinetic data of iron sorption onto tested materials are presented in Figure 2.3. Sorption capacity at pH 3 for the materials studied (except for sediments) stabilized after approximately 8 hours at 8.7 mg/g. For sediments, the stabilization was not reached after 24 hours at pH 6. Stabilization for maple sawdust and chips was reached at 0.9 mg/g, at 1.4 for sediments, and at 2.1 for other materials. The results also showed that 24 h was sufficient to reach equilibrium conditions and confirm the choice made for batch sorption isotherm tests (see section 2.3.1). Iron uptake kinetics seemed to be similar at pH 3 and 6 for municipal sludges, compost, cow, chicken, and sheep manure. The fact that no decrease in iron

concentration was observed for maple sawdust and chips at pH 3 confirms that cellulosic wastes are weak adsorbents.

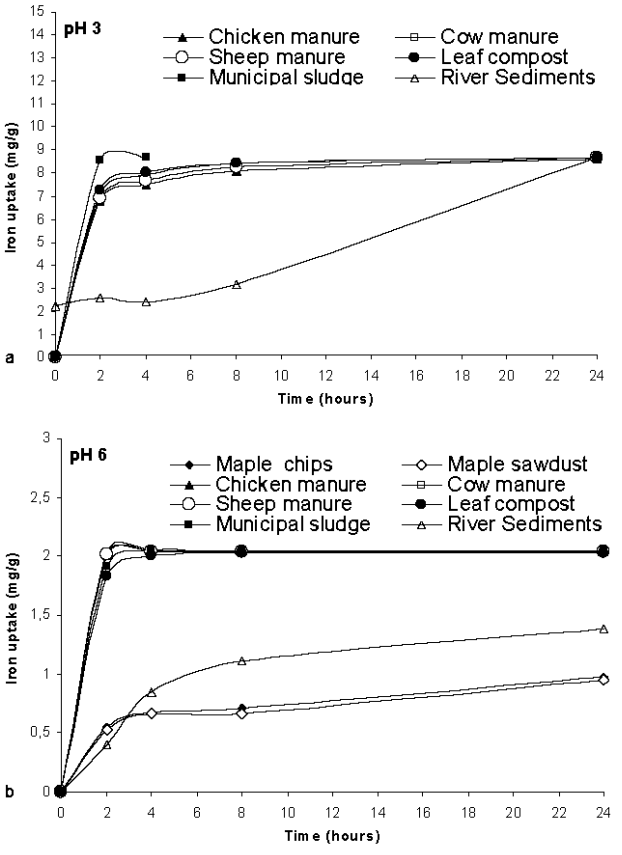

Figure 2.3 Iron kinetic uptake at pH 3 (Fig. 3a) and pH 6 (Fig. 3b) for the different materials

The kinetic iron sorption modeling results for the organic materials and sediments are presented in Table 2.6, for pH 3 and 6. The pseudo-second order reaction rate fit well with experimental data at pH 3 and 6, except for river sediments at pH 3 where a pseudo first order kinetic law better represents the results obtained; results for maple chips and sawdust at pH 3 cannot be fit by either model because iron concentration did not decrease during the test. Sorption of iron was limited by the reaction between dissolved iron and material surface according to a pseudo second order kinetic law or a pseudo first order for river sediment at pH 3. The pseudo-second order kinetics model is often used for chemisorption modelling and

has been applied successfully to biosorption systems (with living or dead biomass) and organic materials (Ho et al., 2000).

Table 2.6 Main parameters of the iron sorption kinetic models for the organic materials and sediments at pH 3 and 6

Kinetic models	pH 3					pH 6			
	Best fit model	R^2	k_2 (g.mg.h^{-1})	k_1 (h^{-1})	q_e (mg/g)	Best fit model	R^2	k_2 (g.mg.h^{-1})	q_e (mg/g)
Maple chips	No iron concentration decrease					pseudo second order	0,99	0,35	1,07
Maple sawdust	No iron concentration decrease					pseudo second order	0,98	0,35	1,04
Chicken manure	pseudo second order	0,99	0,17		8,85	pseudo second order	0,99	15,48	2,08
Cow manure	pseudo second order	0,99	0,31		7,75	pseudo second order	0,99	47,92	2,04
Sheep manure	pseudo second order	0,99	0,18		8,89	pseudo second order	0,99	240,59	2,04
Leaf compost	pseudo second order	0,99	0,03		8,82	pseudo second order	0,99	3,68	2,04
Municipal sludge	pseudo second order	0,99	5,27		8,71	pseudo second order	0,99	7,08	2,06
River Sediments	pseudo first order	0,96		0,08	1,04	pseudo second order	0,98	0,12	1,69

Thereby, chemisorption could be an important phenomenon behind the iron sorption; iron has a high affinity towards organic material (Vodyanitskii, 2010). Moreover, the kinetic constants (k_1 and k_2) were higher at pH 6 than at pH 3 for all materials. The values of kinetic constants mean that iron sorption proceeded faster at pH 6 than at pH 3, as observed by others in the literature (e.g. Ho et al., 1995, Brown et al., 2000, Ma and Tobin, 2004, Champagne et al.,

2008). The results observed are in accordance with the point of zero charge (PZC) of organic soils that are usually close to pH 3 (Asadi et al., 2009). Consequently, iron (and cations) sorption becomes impossible when the pH falls below this value. At pH 6, sorption sites are charged negatively (uptake of iron cations) and sorption is favoured (Asadi and al., 2009).

2.4 Conclusions

Batch tests were used to identify the best mixtures that could treat a high iron concentrated acid mine drainage in sulphate-reducing passive bioreactor. Results showed that different organic materials (chicken, cow, sheep manures or municipal sludge) could be used without affecting significantly the performance of a SRPB to treat the AMD tested. Furthermore, the presence of sediment as bacteria inoculums was not essential since other materials of the mixtures tested already contained sulphate reducing bacteria. The addition of 50 % weight of structural agent (calcitic sand or sand), to improve hydraulic properties, did not affect significantly the metal retention efficiency. Moreover, batch tests allowed demonstrating that sulphate reduction was not the only treatment mechanism at the beginning of biofilter operation; sorption also plays an important role during the first steps of SRPB process.

Iron sorption description was performed and showed that the relation between iron in solution and iron uptake at equilibrium was close to the Freundlich model (in other words, sorption occurred on a heterogeneous surface). Iron sorption kinetics can be described for most of materials tested by a pseudo-second order equation, which often represented a strong link between the material surface and ions (like chemisorption). Based on this test, organic material (manures and municipal sludges) and vegetal compost had the higher iron sorption capacity; and the finer the material was the higher was the sorption capacity. Cation exchange was also one of the sorption mechanisms of materials.

Since batch tests gave similar metal retention efficiency (for mixture #1 to #7), the most promising mixtures, #1, #4 and #7 (organic material mixture with or without 50% of structural agent) for AMD treatment were selected and will be used in column tests to evaluate hydraulic behaviour and metal removal in continuous-flow conditions (see companion paper).

Acknowledgements

This research was supported by the Canada Research Chair on Restoration of Abandoned Mine Sites and the Natural Sciences and Engineering Research Council of Canada (NSERC) through the Industrial NSERC Polytechnique-UQAT Chair in Environment and Mine Wastes Management. The authors gratefully acknowledge the industrial and governmental partners of the industrial Chair for the funding of this study.

References

Al-Degs, Y., El-Barghouthi, M., Issa, A., Khraisheh, M., Walker, G., 2006. Sorption of Zn(II), Pb(II), and Co(II) using natural sorbents: Equilibrium and kinetic studies. Wat. Res. 40, 45-2658.

Asadi, A., Huat, B., Hanafi, M., Mohamed, T., Shariatmadari, N., 2009. Role of organic matter on electroosmotic properties and ionic modification of organic soils. Geosci. J. 13, 175-181.

ASTM, 1995. Standard test method for pH of soils, in: Annual book of ASTM standards. (vol. 04.08, section D4972-95a), Washington, DC, pp. 27–28.

ASTM, 1990. Standard methods for sulphate reducing bacteria in water and water-formed deposit, in: Annual book of ASTM Standards (vol. 04.08., section D 4412 – 84), Washington, DC, pp. 533-535.

Aubé, B., 2005. Étude en usine pilote de la production de boues à haute densité durant le traitement des eaux de drainage minier acide, in : Proceeding of the Symposium 2005 sur l'environnement et les mines, Rouyn-Noranda, pp 1-25.

Aubertin, M., Bussière, B., Bernier, L., 2002. Environnement et gestion des rejets miniers. Edition Presses Internationales Polytechnique, Montréal.

Ayari, F., Srasra, E., Trabelsi-Ayadi, M., 2004. Application des modèles de Langmuir et Freundlich aux isothermes d'adsorption des métaux lourds par l'argile purifiée. J. Phys. IV France. 122, 229-234.

Beaulieu, S., 2001. Applications des techniques de bioactivation et de bioaugmentation pour le traitement en conditions sulfato-réductrices des eaux de drainage minier acide. Master Dissertation, École polytechnique de Montréal, Canada, pp 1-235.

Benner, S., Blowes, D., Ptacek, C., 1997. A full scale Porous reactive wall for prevention of acid mine drainage, in: Proceeding of FALL 1997 GWMR, pp 99-107.

Benzaazoua, M., Bussiere, B., Dagenais, A.M., Archambault, M., 2004. Kinetic tests comparison and interpretation for prediction of the Joutel tailings acid generation potential. Environ. Geol. 46, 1086-1101.

Blowes, D.W., Ptacek, C.J., 1994. System for treating contaminated groundwater, in: U.S. Patent 5,362,394, filed March 3, 1992, issued Nov. 8, 1994.

Brown, P., Gill, S., Allen, J., 2000. Metal removal from wastewater using peat. Wat. Res. 34, 3907-3916.

Brown, M., Barley, B., Wood, C., 2002. Minewater treatment technology, application and policy. IWA Publishing, Londres.

Champagne, P., Van Geel, P., Parker, W., 2008. Impact of Temperature and Loading on the Mitigation of AMD in Peat Biofilter Columns. Mine Wat. Environ. 27, 225-240.

Cocos, I.A., Zagury, G.J., Clement, B., Samson, R., 2002. Multiple factor design for reactive mixture selection for use in reactive walls in mine drainage treatment. Wat. Res. 32, 167-177.

Coles, C., Yong, R., 2002. Aspects of kaolinite characterization and retention of Pb and Cd. Ap. Clay Sci. 22, 39-45.

Costa, M. C., Martins, M., Jesus, C., Duarte, J. C., 2008. Treatment of acid mine drainage by sulphate-reducing bacteria using low cost matrices. Wat. Air Soil Pollut. 189, 149-162.

Cravotta, C. A., Trahan, M. K., 1999. Limestone drains to increase pH and remove dissolved metals from acidic mine drainage. Ap. Geochem. 14, 581-606.

Dann, A., Cooper, R., Bowman, J., 2009. Investigation and optimization of a passively operated compost-based system for remediation of acidic, highly iron- and sulfate-rich industrial waste water. Wat. Res. 43, 2302-2316.

Evangelou, V.P., Zhang, Y.L., 1995. A review: pyrite oxidation mechanisms and acid mine drainage prevention. Environ. Sci. Tech. 25, 141-199.

Fonseca, M., Oliveira, M., Arakaki, L. 2006. Removal of cadmium, zinc, manganese and chromium cations from aqueous solution by a clay mineral. J. Hazard. Mater. 137, 288-292.

García-Mendieta, A., Solache-Ríos, M., Olguin, M., 2009. Evaluation of the sorption properties of a Mexican clinoptilolite-rich tuff for iron, manganese and iron–manganese systems. Microporous and Mesoporous Mater.118, 489-495.

Garcıa-Sanchez, A., Alastuez, A., Querol, X., 1999. Heavy metal adsorption by different minerals: application to the remediation of polluted soils. Sci. Total Environ. 242, 179-188.

Gazea, B., Adam, K., Kontopoulos, A., 1995. A review of passive systems for the treatment of acid mine drainage. Miner. Eng. 9, 23-42.

Genty, T., Bussière, B., Potvin, R., Benzaazoua, M., Zagury, G.J., 2011. Dissolution of different limestone in highly contaminated acid mine Drainage: Application to anoxic limestone drains. Submitted to Environ. Earth Sci. in November 2010.

Genty, T., 2011. Comportement hydrogéochimique des systèmes passifs pour le traitement du drainage minier acide. PhD. Dissertation, Chaire industrielle CRSNG Polytechnique – UQAT, Rouyn-Noranda, Canada.

Germain, D., Cyr, J., 2003. Evaluation of biofilter performance to remove dissolved arsenic: Wood Cadillac, in: Proceeding of the Sudbury 2003 – Mining and the Environment, Sudbury, pp 1-9.

Gibert, O., de Pablo, J., Cortina J.L., Ayora, C., 2004. Chemical characterisation of natural organic substrates for biological mitigation of acid mine drainage. Wat. Res. 38, 4186-4196.

Gibert, O., de Pablo, J., Cortina, J.L., Ayora, C., 2005. Municipal compost-based mixture for acid mine drainage bioremediation: Metal retention mechanisms. Ap.Geochem. 20, 1648-1657.

Gupta, B., Curran, M., Hasan, S., Ghosh, T.K., 2009. Adsorption characteristics of Cu and Ni on Irish peat moss. J. Environ. Manag. 90, 954-960.

Gusek, J.J., 2001. Why do some passive treatment systems fail ? The Center for Environmental Health Sciences at Darmouth. http://www.leo.lehigh.edu/envirosci/enviroissue/amd/links/passive_fail.html. Accessed 25 February 2011.

Ho, Y.S., Wase, J., Forester, F., 1995. Batch Nickel removal from aqueous solutions by sphagnum moss peat. Wat. Res. 29, 1327-1332.

Ho, Y.S., Ng, J.C.Y., McKay, G., 2000. Kinetics of pollutant sorption by biosorbent: reviews. Clear Wat. Sep. Purif. Methods, 29, 189-232.

Jha, V., Matsuda, M., Miyake, M., 2008. Sorption properties of the activated carbon-zeolite composite prepared from coal fly ash for Ni2+, Cu2+, Cd2+ and Pb2+. J. Hazard. Mater. 160, 148-153.

Jong, D., Parry, C., 2006. Microbial sulphate reduction under sequentially acidic conditions in an upflow anaerobic packed bed bioreactor. Wat. Res. 40, 2561-2571.

Karathanasis, A.D., Edwards, J.D., Barton, C.D., 2010. Manganese and sulphate removal from a synthetic mine drainage through pilot scale bioreactor batch experiments. Mine Wat. Environ. 29, 144-153.

Kleinmann, R.L.P., Crerar, D.A., Pacelli, R.R., 1981. Biogeochemistry of acid mine drainage and a method to control acid formation. Mining Eng. 300-304.

KTH., 2010. Visual MINTEQ A free equilibrium speciation model, version 3.0, beta version. http://www.lwr.kth.se/English/OurSoftware/vminteq/index.html. Accessed 15 September 2010.

Kuyucak, N., St-Germain, P., 1994. In situ treatment of acid mine drainage by sulfate reducing bacteria in open pits: scale-up experiences, in: Proceedings of the International Land Reclamation and Mine Drainage Conference, pp 303-309.

Kuyucak, N., Chabot, F., Martschuk, J., 2006. Successful implementation and operation of a passive treatment system in an extremely cold climate, northern Quebec, Canada, in: Barnhisel, R.I. (Ed.), Proceedings of the 7th International Conference on Acid Rock Drainage (ICARD), American Society of Mining and Reclamation (ASMR), vol. 38. Lexington, KY, pp. 3131-3138.

Limousin, G., Gaudet, J.P., Charlet, L., Szenknect, S., Barthes, V., Krimissa, M., 2007. Sorption isotherms: A review on physical bases, modeling and measurement. Ap. Geochem. 22, 249-275.

Luptakova, A., Kusnierova, M., 2005. Bioremediation of acid mine drainage contaminated by SRB. Hydrometallurgy. 77, 97-102.

Ma, W., Tobin, J.M., 2004. Determination and modelling of effects of pH on peat biosorption of chromium, copper and cadmium. Biochem. Eng. J. 18, 33-40.

Macdonald, R.J.C., Kondos, P.D., Crevier, S., Rubinsky, P., Wasserlauf, M., 1989. Generation of, and Disposal Options for Canadian Mineral Industry Effluent Treatment Sludges, in: Procceeding of the Tailings and Effluent Management Symposium, Halifax.

Molson, J., Aubertin, M., Bussière, B., Benzaazoua, M., 2008. Geochemical transport modelling of drainage from experimental mine tailings cells covered by capillary barriers. Ap. Geochem. 23, 1-24.

Morin, K., Hutt, N. 1997. Prediction of mine site-drainage chemistry through closure using operational monitoring data. J.Geochem. Expl. 73, 123-130.

Neculita, C.M., Zagury, G.J., Bussiere, B., 2007. Passive treatment of AMD in bioreactors using SRB: critical review and research needs. Environ. Qual. 36, 1-16.

Neculita, C.M., Zagury, G.J., 2008. Biological treatment of highly contaminated acid mine drainage in batch reactors: Long-term treatment and reactive mixture characterization. J. Hazard. Mater. 157. 358-366.

Neculita, C.M., Zagury, G.J., Bussiere, B., 2008a. Effectiveness of sulphate-reducing passive bioreactors for treating highly contaminated acid mine drainage: I. Effect of hydraulic retention time. Ap. Geochem. 23, 3442-3451.

Neculita, C.M., Zagury, G.J., Bussiere, B., 2008b. Effectiveness of sulphate-reducing passive bioreactors for treating highly contaminated acid mine drainage: II. Metal removal mechanisms and potential mobility. Ap. Geochem. 23, 3545-3560.

Perkins, E.H., Nesbitt, H.W., Gunter, W.D., St-Armand, L.C., Mycroft, J.R., 1995. Critical review of processes and geochemical models adaptable for prediction of acidic drainage from waste rock, in: Mine Environment Neutral Drainage (MEND), Report 1.42.1. CANMET secretariat, Ottawa, Ontario.

Plante, B., Benzaazoua, M., Bussiere, B., 2010. Study of Ni sorption onto Tio mine waste rock surfaces and its effect on drainage geochemistry. Ap. Geochem. 25, 1830-1844.

Potts, P.J., 1987. A Handbook of Silicate Rock Analysis, Blakie & Son Ltd.

Potvin, R. 2009. Évaluation à différentes échelles de la performance de systèmes de traitement passif pour des effluents fortement contaminés par le drainage minier acide. PhD. Dissertation, Chaire industrielle CRSNG Polytechnique – UQAT, Rouyn-Noranda, Canada, pp 1-365.

Raudsepp, M., Pani, E., 2003. Application of Rietveld analysis to environmental mineralogy, in: Jambor J.L., Blowes D.W., Ritchie A.I.M. (Eds.), Environmental Aspects of Mine Wastes, Short Course Series, vol. 31. Mineralogical Association of Canada, pp. 163–180.

Rötting, T., Caraballo, M., Serrano, J., Ayora, C., 2008. Field application of calcite dispersed Alkaline Substrate (calcite-DAS) for passive treatment of acid mine drainage with high Al and metal concentrations. Ap. Geochem. 23, 1660-1674.

Skousen, J.G., Ziemkiewicz, P.F., 2005. Performance of 116 Passive Treatment Systems for Acid Mine Drainage, in: ASMR, 3134 Montavesta Rd. Publication, Proceeding of the National Meeting of the American Society of Mining and Reclamation, Breckenridge, Lexington.

Tassé, N., Germain, D., 2002. Évaluation de la performance de divers types de résidus forestiers pour le traitement du drainage minier acide, in : Proceeding of the Symposium 2002 sur l'environnement et les mines, Rouyn-Noranda, Canada, pp 1-11.

Villeneuve, M., 2004. Évaluation du comportement géochimique à long terme de rejets miniers à faible potentiel de génération d'acide à l'aide d'essais cinétiques. Master Dissertation, Chaire industrielle CRSNG Polytechnique – UQAT, Rouyn-Noranda, Canada, pp 1-325.

Vizier, J.F.,1987. Analyse des mécanismes d'adsorption et de désorption du fer ferreux dans les milieux saturés. Cah. ORSTOM str. P&OL, 13, 157-167.

Vodyanitskii, Y.N., 2010. The role of iron in the fixation of heavy metals and metalloids in soils. Eurasian Soil Sci. 43, 519-532.

Volesky, B., Holan, Z. R., 1995. Biosorption of heavy metals. Biotechnol. Prog. 11, 235-250.

Waybrant, K.R., Blowes, D.W., Ptacek, C.J., 1998. Selection of reactive mixtures for use in permeable reactive walls for treatment of acid mine drainage. Environ. Sci. Technol. 32, 1972-1979.

Yurtsever, M., Sengil, A., 2009. Biosorption of Pb(II) ions by modified quebracho tannin resin. J. Hazard. Mater. 163, 58–64.

Zagury, J.G., Oudjehani, K., Deschênes, L., 2004. Characterization and availability of cyanide in solid mine tailings from gold extraction plants. Sci. Total Environ. 320, 211-224.

Zagury, G.J., Kulnieks, V., Neculita, C.M., 2006. Characterization and reactivity assessment of organic substrates for sulphate-reducing bacteria in acid mine drainage treatment. Chemosphere. 64, 944-954.

Zaluski, M.H., Trudnowski, J.M., Harrington-Baker, M.A., Bless, D.R., 2003. Post-mortem findings on the performance of engineered SRB field-bioreactors for acid mine drainage control. in: Proc. of the 6th Int.Conf. on Acid Rock Drainage, Cairns, QLD. 12-18 July, 2003, pp 845-853.

CHAPITRE 3

TREATMENT OF ACID MINE DRAINAGE WITH HIGH IRON CONCENTRATION USING SULPHATE REDUCING PASSIVE BIOREACTOR: II. LONG-TERM COLUMN EXPERIMENTS

Cet article a été soumis à Applied Geochemistry, en novembre 2011.

Auteurs

Thomas Genty[1], Bruno Bussière[1], Mostafa Benzaazoua[2], Gérald J. Zagury[3]

[1]Industrial Chair CRSNG Polytechnique-UQAT: Environment and mining wastes management, University of Québec in Abitibi-Témiscamingue, Rouyn-Noranda, Québec, Canada

[2]Laboratoire de Génie Civil et d'Ingénierie Environnementale, INSA de Lyon, Villeurbanne, France

[3]Industrial Chair CRSNG Polytechnique-UQAT : Environment and mining wastes management, École Polytechnique, Québec, Canada

Abstract

This study deals with acid mine drainage (AMD) control using a biological based passive treatment. Long-term efficiency (more than 450 days) of continuous-flow column bioreactor tests (10.7 L), treating an AMD with a high concentration of iron (between 1000 and 4000 mg/L), were evaluated. Columns were filled with three different reactive mixtures (containing an organic material, vegetable compost, cellulosic wastes, a SRB inoculum, a neutralizing agent, a structural agent, and a nitrogen source). The difference between mixtures is the proportion and type of structural agent used: 20% of inert sand for mixture #1; 50% of calcitic sand and 10% of inert sand for mixture #4; and 50% of inert sand for mixture

#7. Results for the three tested mixtures showed that pH of column effluents increased up to 6, metals such as Al, Cd, Cr, Ni, Pb, Zn were usually removed at values up to 90%, but iron could not be successfully removed (32% on average for the three mixtures). Moreover, no significant differences were observed between the three mixtures tested. Post-testing characterization of biofilter mixtures showed that iron (the most problematic element to treat in the studied AMD) was mainly retained by the formation of hydroxides or oxyhydroxides and then by sulphides precipitation. Finally, a hydraulic investigation demonstrated that clogging phenomena were not problematic after one year of biofilter operation. Therefore, results suggest that sulphate reducing biofilters are in general efficient to treat most of metal present in the tested AMD, but the system needs to be combined with other water treatment approaches to improve iron removal.

Keywords: acid mine drainage, sulphate-reducing passive bioreactor, column tests, metal removal mechanisms.

3.1 Introduction

Acid mine drainage (AMD) is one of the most important environmental challenges facing the mining industry (Aubertin et al., 2002). Indeed, AMD is produced by sulphide mineral oxidation such as pyrite or pyrrhotite occurring in mine wastes after reaction with atmospheric elements (water and air). The chemical and microbiological oxidation reactions generate sulphuric acid and dissolved metals in the effluent (e.g. Kleinmann and al., 1981; Blowes and Ptacek, 1994; Evangelou and Zhang, 1995).

Solutions for acid mine drainage treatment are subdivided into two main categories: active systems, represented by conventional neutralization plants (Brown et al., 2002), and passive systems. The second category is usually preferred for closed mines because it often uses natural or waste materials, needs lower investment costs and lower energy supply (Neculita et al., 2007). Passive treatment can be divided into two types: biological systems such as bioreactors with sulphate-reducing bacteria (e.g. Neculita et al. 2007) and wetlands (e.g. Skousen and Ziemkiewicz 2005; Barley et al. 2005), and chemical treatments such as oxic and anoxic limestone drains (e.g. Cravotta and Trahan 1999, Genty et al., 2011a).

Sulphates reducing passive bioreactors (SRPBs) consist of degrading a carbon source to reduce sulphates into hydrogen sulphide by sulphate reducing bacteria (SRB). Then, metals contained in the AMD precipitate as sulphide minerals and acidity is neutralized by the production of alkalinity resulting from the carbon source degradation (Neculita et al., 2007). However, recent studies showed that metal retention mechanisms are not only due to sulphides precipitation; sorption, physical filtration, hydroxide or carbonate precipitation can also occur in SRPBs (Neculita et al., 2008b, Karathanasis et al., 2010). More information on the functioning of SRPBs can be found in a companion paper (Genty et al., 2011b).

Moreover, recent studies done by Neculita et al. (2008a) and Potvin (2009) show that AMD with a relatively high concentration of iron (approximately 500 mg/L) can be treated with a SRPB. However, related SRPB efficiency is significantly affected in the case of high iron loads in AMD, which is typical of AMD encountered in Canadian hard rock mines (Aubertin et al., 2002). This efficiency decrease is mainly due to the high acidity and the toxicity in SRPB effluent caused by iron (Neculita et al., 2008c).

In a previous study (see Genty et al., 2011b), batch tests were performed to select the three most promising carbon sources to be used in biofilters to treat high iron concentrated AMD. Even if batch tests are useful to pre-select SRPB mixtures, they are not representative of field conditions (Jong and Parry, 2006, Neculita et al., 2008a). The main objective of this paper is to further evaluate the treatment efficiency of the three selected SRPB mixtures (see Genty et al., 2011b) through long-term and continuous flow column tests. The originality of this research compared to the numerous studies on AMD treatment using SRPBs is the quality of the AMD treated that contains a high iron concentration (approximately 4000 mg/L compared to 1080 mg/L Waybrant et al., 1998, 189 mg/L for Champagne et al., 2005, 1066 mg/L for Neculita et al., 2008a, etc.). The column tests also allow evaluating the influence of hydraulic retention time (an important design parameter) on the treatment performance in order to evaluate the possible influence of a change in saturated hydraulic conductivity of the system with time (e.g. Seki et al., 2006, Neculita et al., 2008a). Finally, post-testing characterization of the mixture was undertaken to better understand metal treatment mechanisms in the tested SRPBs when a high iron concentrated AMD is treated.

3.2 Materials characterization and methods

3.2.1 Mixtures characterizations

SRPB mixtures tested in the columns contain organic materials (chicken manures), leaf compost, cellulosic wastes (maple sawdust and chips), a SRB inoculum (river sediments), a neutralizing agent (calcite, carbonates), a structural agent (sand or calcitic sand) and a nitrogen source (urea). Proportions of the different mixtures tested (see Table 3.1) were optimized using batch tests (see the companion paper for more information on materials description and characterization; Genty et al., 2011b).

Table 3.1 Composition of the three biolfilter mixtures used in the tested SRPB columns (composition given in dry mass %)

Mixture	#1	#4	#7
Celullosic wastes			
Maple chips	10	5	6
Sawdust	20	10	11
Organic wastes			
Chiken manure	10	5	8
Sheep manure			
Cow manure			
Waste water sludges			
Leaf compost	20	10	12
Inoculum			
River sediment	15	8	8
Inert structural agent			
Sand	20	10	50
Nutriment (Nitrogen)			
Urea	3	2	3
Neutralizing agent			
Calcium carbonate	2		2
Calcite		50	

3.2.2 Synthetic acid mine drainage

The tests were carried out with two AMD solutions having characteristics given in Table 3.2. The metallic salts used in the preparation of AMD were dissolved in tap water. AMD had a pH of 3.5, a high concentration in iron (approximately 4000 mg/L for AMD 1 and 1000 mg/L for AMD 2), and a sulphate concentration above 9000 mg/L.

Table 3.2Targeted concentrations of the two influent synthetic AMD solutions (in mg/L except pH). *AMD with an iron concentration of 4000 mg/L is called AMD 1 and AMD with an iron concentration of 1000 mg/L is called AMD 2.

Elements	mg/L	Salt used
Al	7	$Al_2(SO_4)_3,18H_2O$
Cd	0,5	$CdSO_4,8H_2O$
Cr	1	$CrK(SO_4)_2,12H_2O$
Fe	4000/ 1000*	$FeSO_4,7H2O$
Mg	10	$MgSO4,7H_2O$
Mn	35	$MnSO_4,H_2O$
Ni	2	$NiSO_4,6H_2O$
Pb	0,5	$Pb(NO_3)_2$
SO_4^{2-}	9000	$Na_2SO_4,10H_2O$
Zn	40	$ZnSO_4,7H_2O$
pH	3,5	HCl 1N

3.2.3 Continuous flow columns experiments

Column tests provide information on treatment efficiency for longer periods compared to batch tests and simulate conditions more representative of a full scale plant (Neculita et al., 2008a, Robinson-Lora and Brennan, 2009). This series of tests was performed in five 10.7 L bioreactors columns (14 cm in diameter and 70 cm height), filled with three different mixtures numbered #1, #4 and #7. Figure 3.1 represents the column test configuration and Table 3.3 presents the column test characteristics. Porosity in the columns was between 0.40 and 0.46 for the five columns. The porosity was estimated with the volume of Postgate B medium volume needed to fill up the entire column.

In addition to the three columns with mixture #1, #4, and #7, two columns, named #4D and #7D, were performed as duplicates of #4 and #7 for saturated hydraulic conductivity investigation. The chemical analysis of leachates from the duplicate columns were analysed using a standard statistical tool, the paired difference test (Mendelhall and Beaver, 1994; see Demers et al., 2011, for more information on the approach). The test was applied to analyse geochemical data such as pH, Eh, alkalinity, acidity, iron and sulphates content for duplicate columns during a period of 64 days. The statistical analysis proved that data (pH, Eh,

alkalinity, acidity, iron and sulphates) can be considered to come from the same population (for a confidence interval of 95%), and thus comes from identical tests. More information on the repeatability evaluation of these column tests can be found in Genty et al. (2011c)[6].

Table 3.3 Column characteristics and operational conditions

Mixture	#1	#4	#7	#4 (duplicate)	#7 (duplicate)
Column characteristics					
Column number	#1	#4	#7	#4D	#7D
Mixture mass (g)	9038	10447	9917	9970	9824
Height of mixture (cm)	60	60	60	60	60
Estimated porosity	0,46	0,41	0,40	0,41	0,42
Operational conditions (according to typical values found in literature)					
HRT 5 days and AMD 1	period 1 between 0 and 55 days			between 0 and 258 days	
HRT 5 days and AMD 2	period 2 between 55 and 173 days				
HRT 7 days and AMD 2	period 3 between 173 and 229 days				
HRT 7 days and AMD 1	period 4 between 229 and 291 days				
HRT 5 days and AMD 1	period 5 after 291 days				

Columns were fed from the bottom with AMD solution to allow constant anoxic conditions. A perforated plastic plate covered with a geotextile was placed at the bottom to uniformly feed the column. The flow was controlled by a peristaltic pump and was selected to obtain the targeted hydraulic retention time (HRT).

The bioreactors were saturated with Postgate B medium after set-up (Postgate, 1984). The Postgate B medium was prepared in distilled water and had the following composition: 3.5 g/L sodium lactate; 2.0 g/L $MgSO_4,7H_2O$; 1.0 g/L NH_4Cl; 1.27 g/L $CaSO_4,2H_2O$; 1.0 g/L yeast extract; 0.5 g/L KH_2PO_4; 0.5 g/L $FeSO_4,7H_2O$; 0.1 g/L thioglycolic acid, and 0.1 g/L ascorbic acid. After addition of the Postgate B medium, the columns were incubated at room

[6] Voir Appendice A

temperature for four weeks before starting their operation (acclimation period). The first day of AMD treatment began when Eh reached below -150mV, according to Neculita et al. (2008a).

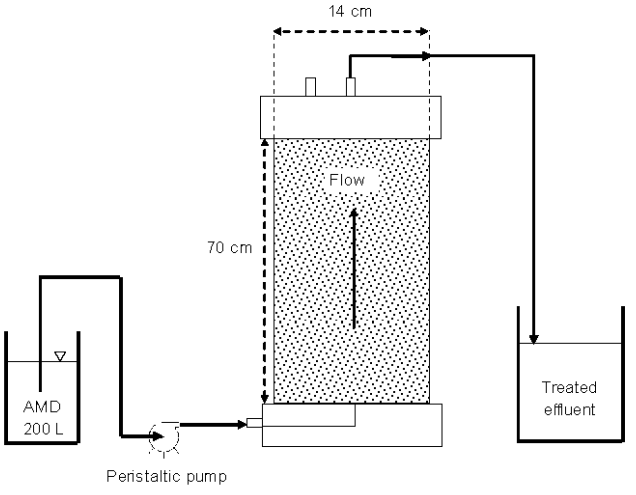

Figure 3.1 Column test configuration (picture not to scale)

During the first 173 days and after 291 days (see Table 3.3), the flow rate was set at 0.6 mL/min to obtain a hydraulic residence time (HRT) of approximately 5 days. Between 173 and 291 days, the hydraulic residence time was set at 7 days (flow rate of 0.4mL/min). After 55 days, iron concentration was decreased to 1000 mg/L (AMD 2) and after 229 days, the concentration was increased to its initial value (4000 mg/L). These HRT and iron concentration changes were done to evaluate the bioreactor performance for two AMD (with two iron concentrations) and two HRT. In fact, HRT in a field SRPB often changes with the seasons and weather. To assess the performance of the tested SRPB for these different conditions, pH, Eh, sulphate, acidity, alkalinity, and metals were measured at the influent and effluent along the experiment (parameters evaluation of column #1 were stopped after 284 days). SRB population enumeration was also performed on leachates from the two duplicates #4D and #7D using the Most Probable Number technique (ASTM, 1990, Beaulieu 2001).

3.2.4 Hydraulic parameters evaluation

Saturated hydraulic conductivity k_{sat} is a useful parameter to quantify clogging phenomena in SRPBs and may state on their life-time. A significant decrease in k_{sat} indicates that the system

is partially clogged (Neculita et al., 2008a). Saturated hydraulic conductivity k_{sat} was evaluated monthly, directly in the columns. The technique used was the falling head method, adapted from ASTM (1995) method. The saturated hydraulic conductivity k_{sat} (cm/s) for the falling head experiment is calculated with equation [3-1] (McCarthy, 1977):

[3-1] $$k_{sat} = \frac{aL}{At} \ln(\frac{h_1}{h_2})$$

Where a (cm^2) is the area of the water head column, L (cm) the length of the sample, A (cm^2) the area of the sample, t (s) the time necessary for the water head column to drop from the height h_1 (cm) to h_2 (cm).

The other important hydraulic parameter is the hydraulic retention time (HRT). A tracer test was performed during the last week of column #4 operation to estimate the HRT. The test used NaCl as tracer element and measurements of chloride concentrations at the exit of column #4 were used to obtain the breakthrough curve. Chloride concentration was determined by Metrohm 881 compact IC pro ions chromatograph (with chemical and CO_2 suppressor, column Metrosep A supp 5-150/4.0, elluent: 3.2 mmol Na_2CO_3 and 1 mmol $NaHCO_3$, flow rate: 0.7 mL/min, 25°C). NaCl concentration in AMD was set to 5 g/L. Injection was performed to reproduce a step tracer experiment (Fogler, 2006), which consists of increasing and maintaining the chloride concentration in AMD solution from close to 0 to 5 g/L during the testing period (11 days). The theory of the residence time distribution was used to analyse the tracer test.

The theory of the residence time distribution was developed to characterize the flow in reactors, based on a tracer test (Roche et al., 1994, Faure et al., 2008). The main hypotheses (considered valid here) related to this approach are (Roche et al., 1994, Faure et al., 2008):

- the studied system is an open reactor, having an input and an output;
- the flow is constant;
- the fluid is uncompressible.

To evaluate hydraulic retention time for a piston reactor and a continuous stirred reactor, the following equations were used (Fogler, 2006). These two equations present the response of these two types of reactor to a tracer injection made with a step tracer experiment.

[3-2] Piston reactor: $C(t) = 0$ if $t<\tau$ and $C(t) = 1$ if $t>\tau$

[3-3] Continuous stirred reactor: $C(t) = C_0(1-\exp(-\frac{t}{\tau}))$

where C(t) is the tracer concentration at the exit of the reactor at time t, C_0 the tracer concentration at the exit of the reactor at equilibrium, τ the hydraulic retention time.

3.2.5 Bacterial enumeration method

Sulphate reducing bacteria enumerations in organic material, sediment and in column effluents were performed using the Most Probable Number according to ASTM (1990) and Beaulieu (2001). The method consists in incubation of different dilution of SRB solution into different tubes with a medium Starkey A.

3.2.6 Analytical method for water quality evaluation

The pH of liquid samples were measured with an Orion Triode sensor coupled with a Benchtop pH/ISE Meter Orion model 920 (relative precision +/- 0.01 pH), and the redox potential (Eh), corrected relative to the standard hydrogen electrode, by a Pt/Ag/AgCl sensor link to a Benchtop pH/ISE Meter Orion 920 (relative precision +/- 0.2 mV). The alkalinity concentration was obtained by titration of non-filtered sample with sulphuric acid 0.02N (precision of 1 mg $CaCO_3$/L), and the acidity concentration by titration of non-filtered sample with sodium hydroxide 0.1N (precision of 1 mg $CaCO_3$/L) (APHA, 1995). Filtered samples (0.45 µm filter) used for metal analysis were acidified with 2% volume with nitric acid (70%) before analysis with a Inductively Coupled Plasma-Atomic Emission Spectrometry (ICP-AES) Perkin Elmer OPTIMA 3100 RL (relative precision evaluated at 5% by Villeneuve, 2004). Finally, sulphate concentration was evaluated on filtered samples using a nephelometric method based on the precipitation of barium sulphate (AFNOR, 1986) and

measurement of absorbance at 650 nm with an Ultraspec 2100 pro spectrometer (relative precision of +/- 0.5%).

3.2.7 Columns post-testing characterization

Reactive mixture samples were collected from each bioreactor at the end of the experiment. Samples were rapidly frozen to prevent sulphide oxidation, except for SRB enumeration where samples were stored at 4°C. Solids sampling was carried out in the layer at 35 cm from the bottom of reactors (which corresponds to the middle of reactors) because no visual difference was observed between the top and the bottom during dismantling. It is worth mentioning that total sulphur content was determined on samples coming from the top, the middle and the bottom of the column with a carbon sulphur determinator ELTRA CS 2000. For a given column, results showed no significant difference in sulphur content for samples taken at these different locations.

Physicochemical analyses carried out on solid samples were:

- the total organic carbon TOC (measured by adding potassium dichromate and sulphuric acid, followed by measurement of excess of potassium dichromate),

- the total Kjeldahl nitrogen TKN (carried out by mineralization of organic matter into ammonium, carbon dioxide and water, with sulphuric acid, and measurement of the ammoniaum formed),

- the dissolved organic carbon DOC on water extracts 1:10 solid:liquid ratio (by using a heated tube at 680°C with a catalyser and an infra-red detection of carbon dioxide emitted).

To determine metal content by ICP-AES of each mixture, solids were digested in HNO_3, Br_2, HCl and HF (Potts, 1987). SRB population accounting was also made using the most probable number technique (see Beaulieu, 2001, for more details on the protocol).

Stability of metal precipitates and potential mobility in reactive mixtures were estimated using numerous techniques. First, a semi-quantitative method was used: the sequential

extraction procedure (SEP, Zagury et al., 1997). Five fractions were extracted from 1 g of wet solid sample using different reagents:

- Soluble and exchangeable metals (extracted with 8 mL $MgCl_2$ 0.5 M, pH 7, 1 h at room temperature)

- Carbonate-bound (leached by 8 mL NaOAc 1 M buffered with HOAc, pH 5, 5 h at room temperature)

- Reducible or bound to Fe–Mn oxides (extracted with 20 mL NH_2OH-HCl 0.04 M in 25% (v/v) HOAc, 6 h at 96°C)

- Oxidisable or bound to organic matter (released by 3 mL HNO_3, 5 mL H_2O_2 30% pH 2, 2 h at 85°C, then 3 mL H_2O_2 30% pH 2, 3 h at 85°C, and 5 mL NH_4OAc 3.2 M in 20% (v/v) HNO_3, 0.5 h at room temperature) diluted to 20 mL.

- Residual metal fraction (dissolved by acid attack with HNO_3, HF, and HCl).

Scanning electron microscopy (SEM) coupled with X-ray microanalysis was used to analyse the samples microstructure and mineralogy using a Hitachi 3500-N scanning electron microscope (SEM) coupled with an energy dispersive spectrometry (EDS) of an X-ray probe (voltage of 20 keV, amperage of 140 A, pressure around 25 kPa and work distance of 15 mm).

Finally, liquid-solid chemical equilibriums were estimated by geochemical modeling. Saturation indices of the main minerals susceptible to precipitate were calculated using a thermodynamic chemical equilibrium model (Vminteq v 2.53) with the activity correction proposed in the SIT model (KTH, 2010). One of the limitations of the model is that it does not take into account the sulphate reducing bacteria activity. To confirm Vminteq modeling, results were presented in an redox potential versus pH diagram using a second geochemical modeling software: JCHESS version 2.0 (Van Der Lee, 1993). Results from this software also allow determining (like Vminteq) which iron phases were more likely to precipitate in the mixtures.

3.3 Results and interpretations

3.3.1 Period 1 (between 0 and 55 days), 5 days HRT and 4000 mg/L of iron

Figures 3.2a to 3.2f present results for pH, Eh, iron concentration, sulphates, alkalinity, and acidity. During this first period (0 to 55 days), the iron AMD concentration was approximately 4000 mg/L and the estimated HRT was 5 days. The pH decreased rapidly from 8.6 for column #1, 8.1 for column #4 and 7 for column #7, to a pH between 6.7 and 6.2 (see Figure 3.2a and Table 3.4). The Eh varied from -100 mV to 100 mV as showed in Figure 3.2b with an average at 31 mV for column #1, 7 mV for column #4 and 30 mV column #7. Iron concentrations (see Figure 3.2c) at the column exit started at low values during the first week of operation (13 mg/L for mixture #1, 64 mg/L for mixture #4), except for mixture #7 where iron concentration was 939 mg/L. Then, iron concentrations increased progressively to approximately an average of 2700 mg/L at the end of this first operational period. These results can also be expressed in terms of iron removal percentage (based on influent concentration). This parameter started from 99% to 75% depending on the column and decreased quickly to values close to 0%, and finally stabilized at approximately 30 to 45% at 55 days. The average iron removal percentage during this period was 36% for column #1, 49% for column #4, and 26% for column #7 (see Table 3.4). As presented in Figure 3.2d, sulphate concentrations varied from 8367 to 12612 mg/L at the influent. After treatment by the SRPBs, sulphate concentrations varied from 6816 to 10694 mg/L for column #1 (average of 8804 mg/L), from 7265 to 10000 mg/L for column #4 (average of 8693 mg/L), and from 8245 to 12245 mg/L for column #7 (average of 10023 mg/L). Alkalinity (Figure 3.2e) decreased from 10800 mg/L $CaCO_3$ to stabilize at values between 400 and 700 mg/L $CaCO_3$ at 55 days. Acidity increased for all columns from an average of 1060 mg/L $CaCO_3$ (at the beginning) up to 4000 mg/L $CaCO_3$ between the period 0 to 55 days.

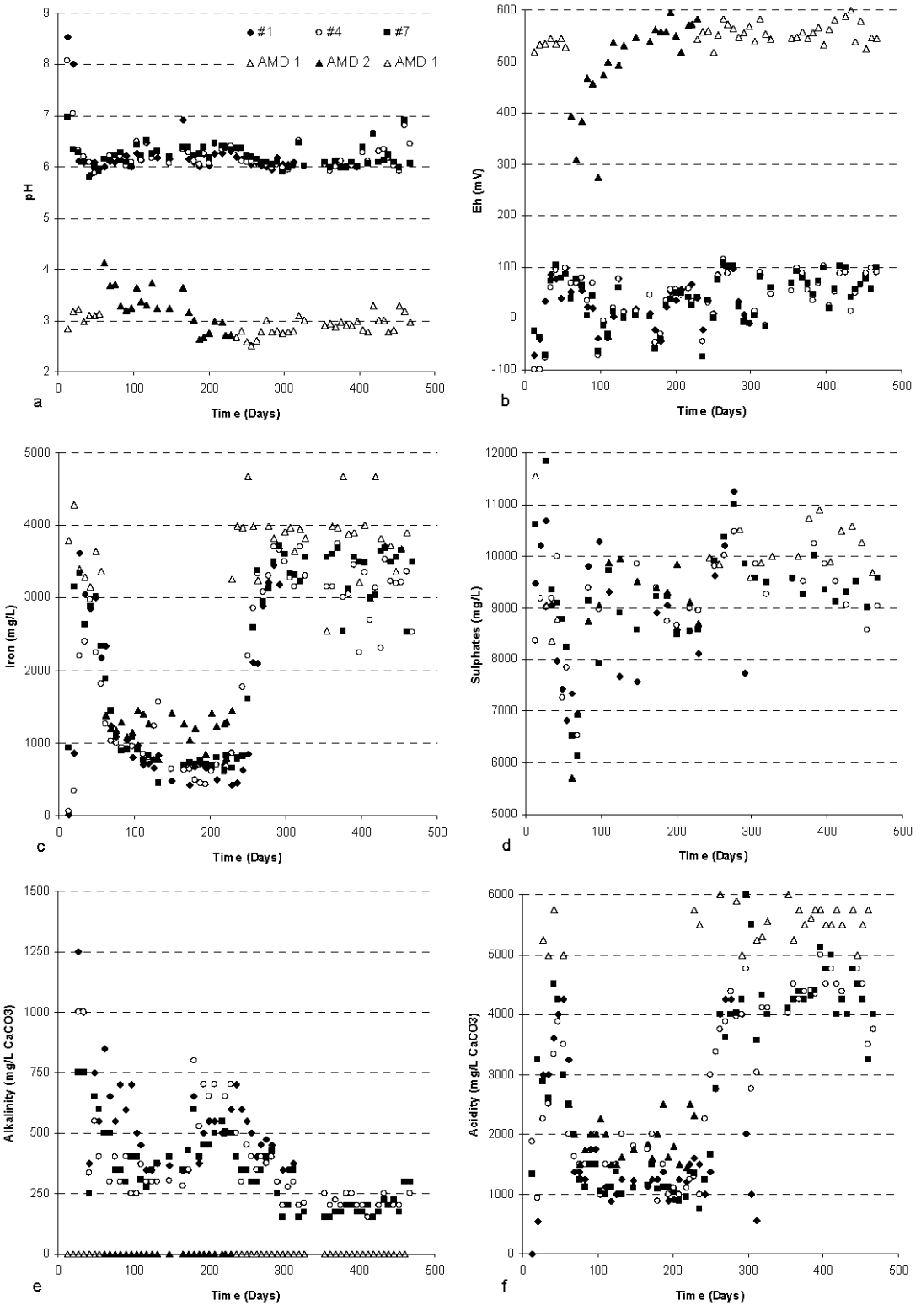

Figure 3.2 Evolution of column parameters a) pH, b) Eh (mV), c) iron (mg/L), d) sulphates (mg/L), e) alkalinity (mg/L eq. CaCO3) and f) acidity (mg/L eq. CaCO3)

3.3.2 Period 2 (between 55 and 173 days), 5 days HRT and 1000 mg/L of iron

For all columns, pH remained stable at approximately 6.2 and Eh varied between 11 and 29 mV. Iron concentrations at the column effluent decreased and stabilized at an average value of 955 mg/L for column #1, 980 mg/L for column #4 and 972 mg/L for column #7, which correspond to an iron removal percentage between 27 and 33%. Sulphate concentrations were most of the time below AMD values (retention between 8 and 11% on average), and the minimum sulphate concentration was reached in column #1 at 7347 mg/L. Acidity and alkalinity stabilized respectively at values between 1000 and 2000 mg/L $CaCO_3$ and 327 to 521 mg/L $CaCO_3$ with the highest alkalinity generation in column #1. Except for alkalinity, pH (6.2 on average), Eh (11 to 29 mV), iron (27-33%) and sulphate (8-11%) removal percentage were in the same order of magnitude for the three tested mixtures, as presented in Table 3.4.

3.3.3 Period 3 (between 173 and 229 days), 7 days HRT and 1000 mg/L of iron

There was no significant change in comparison with period 2: pH values stayed close to 6.2 for the three mixtures (Table 3.4), Eh values were between 16 and 27 mV and iron concentrations continued to decrease (reaching values between 615 and 732 mg/L depending on the mixture) to reach an iron removal between 37 and 50% at the end of the third period. Although there was no significant difference between mixtures, iron removal was higher than the previous periods (between 27 and around 33%). Sulphate concentrations at columns exit were on average close to AMD (AMD was 8847 mg/L and 8771 mg/L for column #1, 8985 mg/L for column #4, 8873 mg/L for column #7). Sulphate removal percentage was in the same range as in period 2 (between 7 and 11%). Acidity concentration stayed between 900 and 1600 mg/L $CaCO_3$. However, alkalinity concentration increased significantly for columns #4 and #7 in comparison with period 2 (respectively 571 mg/L $CaCO_3$ and 485 mg/L). For column #1, alkalinity concentration remained relatively constant (average of 496 mg/L of $CaCO_3$).

Table 3.4 Average parameters of AMD solutions (before and after treatment) for the three columns tested and the five periods. Units are mV for Eh, mg/L for iron and sulphate concentration, mg/L eq. CaCO3 for alkalinity (Alk.). Iron and sulphate removal are expressed as average (av) percent removal.

	pH	Eh	Alk.	Fe	SO_4^{2-}	Iron removal %			Sulphate removal %		
						av.	min	max	av.	min	max
Period 1 (HRT = 5 days, iron concentration = 4000 mg/L)											
AMD	2.8	555	0	3712	9930	-	-	-	-	-	-
#1	6.7	31	3824	2225	8804	36	0	99	21	9	41
#4	6.5	7	2609	1720	8693	49	6	98	24	1	42
#7	6.2	30	1738	2615	10023	26	2	75	14	1	31
Period 2 (HRT = 5 days, iron concentration = 1000 mg/L)											
AMD	3.2	498	0	1209	8847	-	-	-	-	-	-
#1	6.2	11	521	955	8416	33	5	66	8	0	21
#4	6.2	29	327	980	9303	29	8	45	9	4	24
#7	6.2	16	373	972	8127	27	1	47	11	4	22
Period 3 (HRT = 7 days, iron concentration = 1000 mg/L)											
AMD	3.2	498	0	1209	8847	-	-	-	-	-	-
#1	6.2	27	496	629	8771	47	23	66	11	10	11
#4	6.2	25	571	615	8985	50	38	45	7	6	9
#7	6.3	16	485	732	8873	37	16	47	10	8	11
Period 4 (HRT = 7 days, iron concentration = 4000 mg/L)											
AMD	2.8	555	0	3712	9930	-	-	-	-	-	-
#1	6.1	52	525	1789	9803	32	10	55	8	4	12
#4	6.1	46	430	2433	9816	22	5	45	4	2	6
#7	6.2	45	375	2155	9961	28	9	60	5	1	7
Period 5 (HRT = 5 days, iron concentration = 4000 mg/L)											
AMD	2.8	555	0	3712	9930	-	-	-	-	-	-
#1	6.1	23	343	3190	9746	-	-	-	-	-	-
#4	6.1	33	241	3363	9634	18	0	50	8	4	16
#7	6.1	57	201	3387	9471	14	2	36	7	0	14

3.3.4 Period 4 (between 229 and 291 days), 7 days HRT and 4000 mg/L of iron

Significant changes appeared in iron concentrations and acidity values: iron concentrations increased between 1789 and 2433 mg/L on average depending on the column; iron removal percentage decreased in comparison with the previous period to an average of 32% for column #1, 22% for column #4 and 28% for column #7. Acidity increased to values obtained during the first period (close to 4000 mg/L $CaCO_3$). For the other parameters (see Table 3.4), pH values stayed close to 6.1, Eh values were between 45 and 52 mV on average, while

alkalinity values were between 375 and 525 mg/L $CaCO_3$. The average sulphate concentrations at the outlet stayed between 9803 and 9961 mg/L, which correspond to an effective removal percentage of 4 to 8% (lower than for period 3).

3.3.5 Period 5 (after 291 days), 5 days HRT and 4000 mg/L of iron

Finally, the initial conditions of the first period were tested again after 291 days. Parameters such as pH and Eh stayed in the same range as those measured during period 4 (pH of 6.1, Eh between 23 and 57 mV). Alkalinity concentrations decreased to values between 201 to 343 mg/L $CaCO_3$ on average (slightly lower values than for period 4). Iron percentage removal varied for all mixtures in the range of 14 to 18% (average iron concentration was 9634 mg/L for column #4 and 9471 mg/L for column #7); these values are lower than for the previous period. Sulphate removal percentage stayed in the same rang as for the previous period (between 8 and 7%). Values of parameters at the end of the first period (similar operational conditions and after reaching an equilibrium) are similar to those measured during period 5. These observations mean that the three columns kept their treatment capacity after more than one year of operation.

3.3.6 Aeration of SRPB effluents

Figure 3.3 presents the evolution of column effluents' pH and redox potential when they are exposed to aerobic conditions in a 500 mL container. For each column effluent, pH dropped from an average of 6.4 to 4.4 after 8 hours of aerobic conditions. At the same time, redox potential increased due to aeration. This phenomenon was typical of the oxidation of ferrous iron into ferric iron and of precipitation of ferric hydroxide, which released protons that decreased pH (Ulrich, 1998, Cravotta and Trahan, 1999, Santini et al., 2010, Genty et al., 2011a[7]). Moreover, the net acidity calculated by the difference between acidity and alkalinity (Kirby and Cravotta, 2005) showed that for each column, alkalinity in the column effluent was not sufficient to neutralize acidity. A pH close to neutrality in column effluents did not ensure that pH does not decrease after a few hours when an AMD with a high concentration of iron is treated.

[7] Voir Appendice B

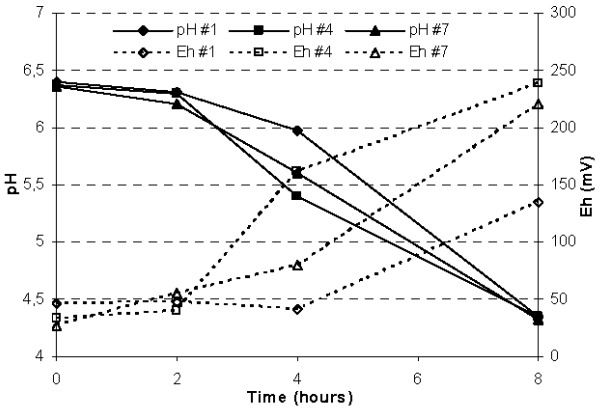

Figure 3.3 pH and Eh evolution of column effluents with a natural aeration

3.3.7 Microbial enumeration

SRB enumerations carried out on the two duplicate column effluents #4D and #7D are an indication of the SRB activity. Figure 3.4 presents the number of SRB in 100 mL of column effluent. SRB cell count in both effluents decreased from the beginning of the experiment and stabilized to approximately 200 SRB/100mL. Columns #4D and #7D were fed during the entire experiment only by the high iron AMD 1 with a HRT of 5 days. A similar behaviour in terms of SRB evolution in effluents from SRPBs was also observed by Neculita et al. (2008a) when an AMD with an iron concentration of approximately 1600 mg/L was treated (SRB cells varied between 20 and 20000 cells/100mL but increased up to 10^7 cells/100mL when iron concentration in AMD was set to 500 mg/L). Results of Costa et al. (2009) also show a similar range of SRB (between 100 and 1000 SRB cells/100 mL) with wine wastes as the carbon source. However, SRB cells can increase up to 10^8 cells/mL when the carbon source is more available, such as lactate (Elliott et al., 1998). For similar mixtures as those used in this study, but for low iron concentrated AMD, SRB cells can be between 10^6 and 10^8 cells/100 mL (Zaluski et al., 2003). Moreover, enumeration carried out directly on the mixture in the middle of the reactor after dismantling of columns #1, #4 and #7 gave a proportion of 2400 cell/100mL for mixture #1, mixture #4, and mixture #7. These results were close to other studies made on similar mixtures (Neculita et al., 2008b). To summarize, these SRB counts showed that SRBs continue to survive even when a high iron concentrated AMD is treated. However, this high iron concentration limited the growth of SRBs.

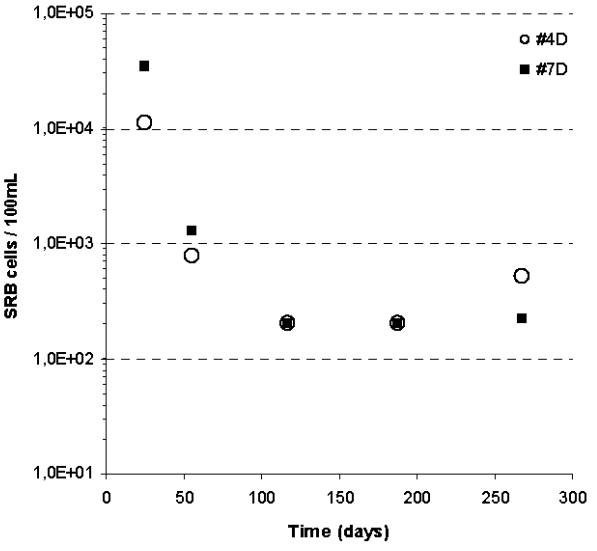

Figure 3.4 Evolution of SRB populations in effluent of duplicated columns treating AMD 1

3.3.8 Saturated hydraulic conductivity evolution

SRPB clogging can be estimated by measuring k_{sat} (Soleimani et al., 2009); a decrease of k_{sat} can be related to a reduction of the effective porosity due to pore filling. This filling of the porosity can be explained by numerous phenomena such as biofilm formation due to biomass growth, physical deposit of particles, gaz production, chemical and biological precipitation (Soleimani et al., 2009, Seki et al., 2006, Anello et al., 2005). Some studies reported that the decrease of k_{sat} can be important in a one dimensional flow column (Seki et al., 2006). Neculita et al. (2008a) reported a decrease of k_{sat} from $2x10^{-3}$ cm/s to $7x10^{-9}$ cm/s for an hydraulic retention time of 10 days, and to $2x10^{-5}$ cm/s for an hydraulic retention time of 7.3 days, for SRPB columns used to treat acid mine drainage (with a down-flow feeding). In this last example, the authors suggested that the reduction of hydraulic conductivity was due to the formation of iron oxy-hydroxide at the top of the columns.

Figure 3.5 presents results of saturated hydraulic conductivity k_{sat} measurements for column #4D and #7D. k_{sat} stayed relatively stable at a value of $2.1x10^{-3}$ cm/s for column #4D. For column #7D, the average k_{sat} value was $9.9x10^{-3}$ cm/s, but the value decreased from a maximum of $5.2x10^{-2}$ cm/s to a minimum of $4.2x10^{-3}$ cm/s. These results were comparable to

other values found in the literature for SRPBs: $5x10^{-4}$ cm/s to $1x10^{-2}$, URS report (2003); $1x10^{-3}$ to $1x10^{-4}$ cm/s, Waybrant et al. (1998). It is important to recall that the columns in this study were fed from the bottom to the top. This approach, as suggested by the URS report (2003), seems to prevent the SRPBs from clogging.

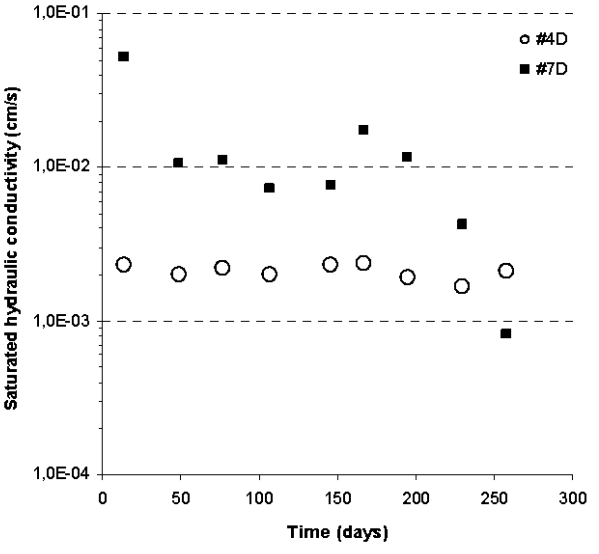

Figure 3.5 Evolution of saturated hydraulic conductivity in columns #4D and #7D

3.3.9 Characterization of the SRPB sampled from columns post-testing

Mixture analysis after columns dismantling showed an increase of TOC/NTK ratio, which corresponds to a lack of nitrogen towards carbon for bacteria development. Thereby, the bacteria environment could affect their long term viability and growing. Furthermore, water extracted for dissolved organic carbon analyses, made on column mixtures after dismantling, presented a clear decrease in comparison with the initial values (DOC values were respectively 14%, 3%, and 1% of the initial DOC value for mixtures #1, #4 and #7 after dismantling). The easily available carbon for bacteria became less present, and thus bacteria population could be affected in the long term.

Mixture digestion has been carried out to evaluate the metal retention capacity in each column. However, only an increase in iron and total sulphur appeared in the elemental

analysis of mixture #1, #4 and #7 (respectively a increased in iron content of 4%, 3%, and 2% for mixtures #1, #4 and #7). A fractionation using a sequential extraction procedure was performed on a sample collected from the middle of each column in order to understand metal removal mechanisms occurring in the SRPBs during AMD treatment. The sequential extraction procedure allows categorizing metals as soluble and exchangeable (fraction 1), coming from the carbonate-bound fraction (fraction 2), as reducible metals or bound to Fe–Mn oxide fraction (fraction 3), as oxidisable or bound to organic matter fraction (fraction 4), or as integrated into the residual fraction (fraction 5). Results of metal fractionation are summarized in Table 3.5.

Most of the aluminum was contained in the residual part whatever the mixture (86 to 93%). A small proportion was oxidisable or bound to organic matter and reducible or bound to Fe-Mn oxides-hydroxides (1 to 9%). Vminteq modelling carried out on biofilter effluent suggested also the precipitation of boehmite, diaspore and gibbsite, which are all aluminium hydroxides. The tendency for chromium was quite similar to aluminium (2-4% oxidisable or bound to organic matter, 23-55 % reducible or bound to Fe-Mn oxides-hydroxides and 40-69% in the residual fraction). Lead was retained mainly in fraction 3 (0 to 54%), 4 (3 to 40%) and 5 (0 to 96%). The formation of reducible phases or Fe-Mn oxide-hydroxides-bound phases (fraction 3) seemed to be the predominant mechanism for zinc retention (73-86%), followed by the formation of oxidisable or bound to organic matter phases (9-24%). The soluble and exchangeable fraction (fraction 1) of nickel was not negligible (6-12%) although nickel retention was mainly due to the formation of reducible phases or Fe-Mn oxide-hydroxide-bound phases (37-64%), followed by the formation of oxidisable or bound to organic matter phases (16-38%). A similar trend was observed for manganese (Vminteq results suggested also the formation of a carbonate phase as rhodochrosite). Cadmium had a different behaviour with a high portion found in fraction 1 (0-50%). The other mechanism of cadmium removal was the formation of reducible phases or Fe-Mn oxide-hydroxide-bound phases (40-60% depending on the mixture). Iron was mainly present in the reducible or bound to Fe-Mn oxides-hydroxide fraction (51-67%), but also in the oxidisable or bound to organic matter fraction (probably under the sulphur form) and in the residual fraction (8-

26%). The same observation was made by Neculita et al. (2008b) who found iron mainly under hydroxide or sulphide forms. Finally, a small portion of iron was bound to carbonate

Table 3.5 Metal fractionation in the reactive mixtures after column dismantling using a sequential extraction procedure (results are expressed in % except for the sum of metal in each fraction in mg/g).

	Fraction 1	Fraction 2	Fraction 3	Fraction 4	Fraction 5	Sum (mg/g)
			Al			
mixture #1	0	0	2	5	93	27,0
mixture #4	0	0	2	9	89	13,0
mixture #7	0	0	1	7	86	22,0
			Cd			
mixture #1	50	11	40	0	0	0,00077
mixture #4	35	12	53	0	0	0,00035
mixture #7	0	40	60	0	0	0,00011
			Cr			
mixture #1	0	0	4	55	40	0,008
mixture #4	0	0	2	23	75	0,022
mixture #7	0	0	4	27	69	0,024
			Fe			
mixture #1	1	10	67	14	8	44,0
mixture #4	3	6	61	17	14	32,0
mixture #7	4	6	51	15	26	38,0
			Mn			
mixture #1	16	28	31	8	17	0,28
mixture #4	14	11	59	4	12	0,44
mixture #7	15	13	31	7	35	0,45
			Ni			
mixture #1	6	9	64	21	0	0,11
mixture #4	12	6	37	38	7	0,047
mixture #7	10	10	59	17	4	0,083
			Pb			
mixture #1	4	0	54	40	0	0,016
mixture #4	0	0	0	3	96	1,40
mixture #7	2	0	44	13	44	0,023
			Zn			
mixture #1	1	3	76	21	0	0,54
mixture #4	1	2	73	24	0	0,20
mixture #7	1	4	86	9	0	0,24

(6-10%), or soluble and exchangeable (1-4%). The iron carbonate and oxyhydroxide precipitation as siderite, ferrihydrite, goethite and lepidocrocite was suggested by Vminteq modeling. The sum of metal holdup in mixture #1, #4 and #7 were respectively 72 mg/g, 47 mg/g and 61 mg/g (mixture #1 seemed to have the higher metal retention capacity).

Figure 3.6a to Figure 3.6c show secondary electron images and related X-mapping of the main chemical elements observed on reactive mixture #1, #4, and #7 using the EDS technique. X-mapping technique is more appropriate for polished sample sections. However in the case of this study, X-mapping was done on unpolished material. The X-mapping for the three mixtures showed a superposition of iron, oxygen, carbon, and aluminum. This observation confirms the precipitation of oxide or hydroxide phases of iron or aluminum at the surface of organic material (represented by carbon). Moreover, a superposition of iron and sulphur is observed in Figure 3.6a and 3.6b. This observation suggests a possible precipitation of iron sulphide in these two columns. However, sulphide mineral observation was difficult due to the sample preparation. Indeed, SEM analyses require dry samples, and sulphide minerals were probably oxidised and transformed into hydroxides. A similar remark could be applied for sequential extraction procedure analyses.

3.3.10 JCHESS modelling

Redox potential versus pH diagram was made using JCHESS version 2.0 to better visualize the iron behaviour in the columns. The temperature selected to construct the graph (see Figure 3.7) was 21°C (laboratory temperature), and activity of iron and sulphates were calculated using Vminteq 2.53 (average concentrations were used for each bioreactor). Magnetite and hematite were excluded from the diagram because their formation conditions are different from those observed in our columns. Based on modelling results, iron retention in each column occurred mainly because of goethite precipitation; these results are in accordance with sequential extractions that showed that most of the iron was contained in the reducible phase or in Fe-Mn oxides-hydroxides (fraction 3). Moreover, column effluents were near the area of pyrite stability, and confirmed that locally some iron sulphide could precipitate. Another treatment step would be required to promote iron sulphide precipitation.

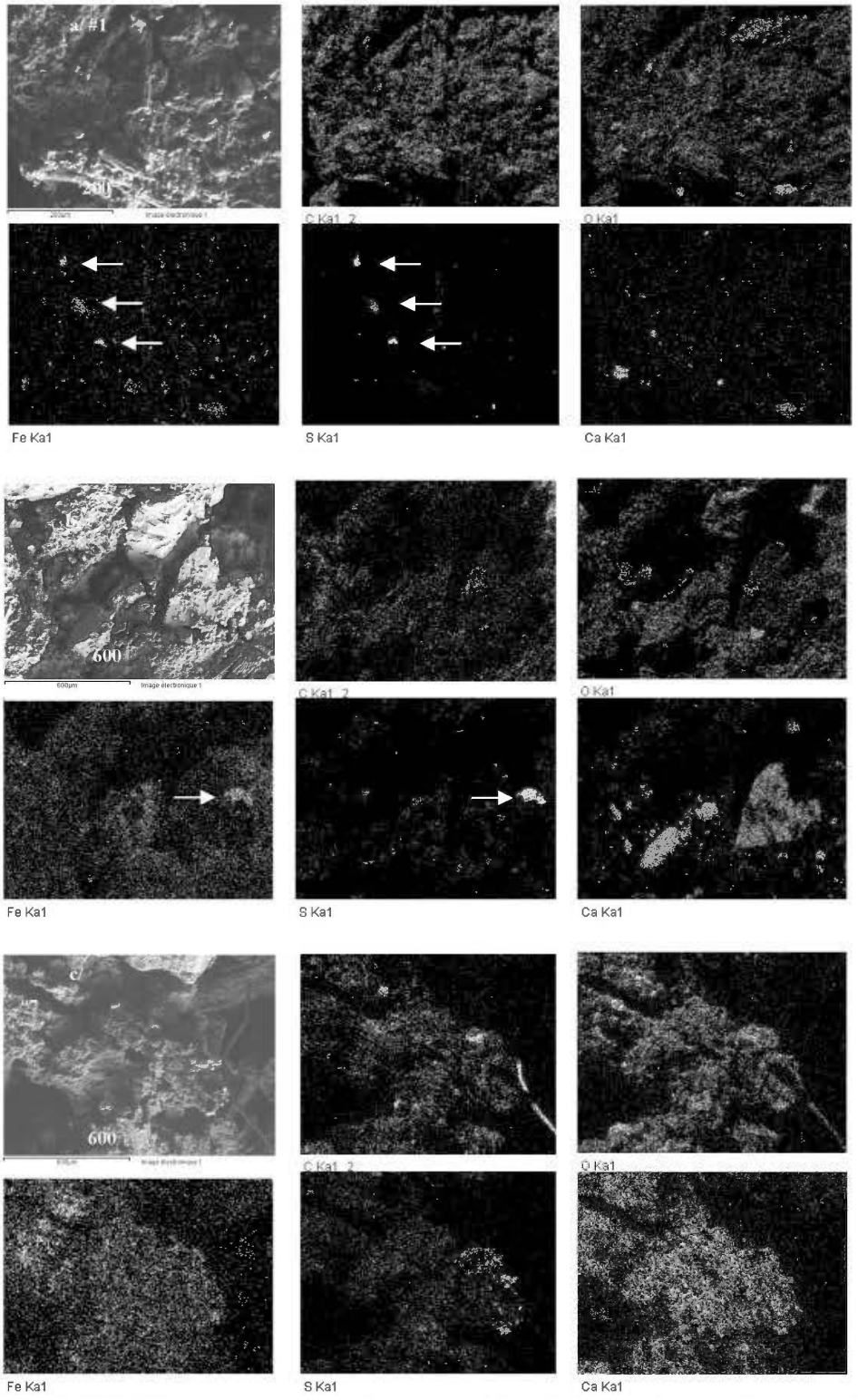

Figure 3.6 SEM images (secondary electron mode) and elemental maps: a) mixture #1, b)mixture #4 and c) mixture #7.

This step should decrease the redox potential below approximately -100 mV using another SRPB.

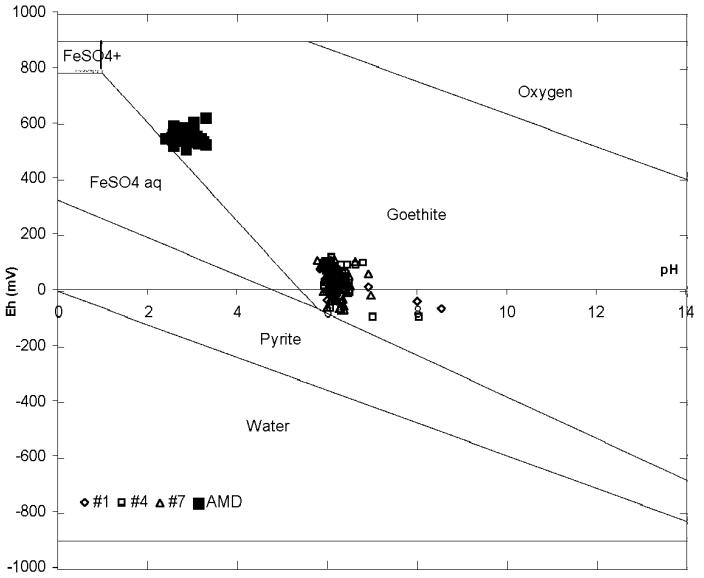

Figure 3.7 Redox potential versus pH diagram for iron in the tested SRPBs

3.4 Discussion

3.4.1 SRPB performances

Period 1 was excluded to compare biofilter performances because columns were in starting mode and not in a steady state (mainly due to the dilution of Postgate B medium). SRPB performances depend mainly on three parameters: hydraulic retention time, SRPB mixture and metal concentrations in AMD (Neculita et al., 2008a). There was no important differences between the three columns tested (#1, #4 and #7) in terms of performance for pH, Eh, alkalinity, iron and sulphate removal percentages for a given period (see Table 3.4).

Two HRT have been investigated during the treatment of the two types of AMD (AMD 1 and AMD 2): 5 and 7 days. Results presented in Table 3.4 show that a higher HRT promoted higher alkalinity generation whatever the AMD treated. A decreased of HRT from 7 to 5 days (from period 4 to 5 for example) caused a decrease of alkalinity for column effluents from an

average of 525-375 to 343-201 mg/L $CaCO_3$ depending on the mixture, and a decrease of iron removal percentage (from 32-22% on average in period 5 to 18-14% in period 5). A similar behaviour was also observed between Period 2 and 3. Average iron concentration was between 955 and 980 mg/L in period 2 (HRT of 5 days) and decreased between 732 and 615 mg/L in period 3 (HRT of 7 days). However, the small difference in performance between results of columns with 7 days or 5 days of HRT for alkalinity generation, iron removal percentage, pH, Eh and sulphate concentrations suggests that 5 days or 7 days would be acceptable options as HRT.

The third important parameter which affects SRPB performance is AMD iron concentration (Neculita et al., 2008a). Indeed, for an HRT of 5 days, iron removal was on average between 33 and 27% depending on the mixture during period 5 when AMD with 4000 mg/L of iron was treated. This removal percentage was between 14 and 18% in period 2 when AMD with 1000 mg/L of iron was treated. For an HRT of 7 days, iron removal decreased from an average of 50-37% in period 3 to 22-32% in period 4. The conclusion was that high iron concentrations decreased the performance of iron retention for any of the three tested mixtures probably because SRB were not efficient to produce sulphides, and a short HRT does not allow a significant precipitation of iron hydroxides.

The emphasis in this article is put on iron treatment. However, the performance of SRPBs was also evaluated for other metals contained in the AMD solutions tested. Removal percentages for Al, Cd, Cr, Ni, Zn for all columns were always higher than 90%, between 52 and 80% for Pb, and between 1 and 28 % for Mn. There were no real differences in this present study between the three mixtures tested for metal removal performances. Mn removal percentages are in accordance with those found in the literature for this element (Neculita et al., 2008a, Potvin, 2009). Low Mn removal could be explain by several causes (Edwards et al., 2009): precipitation is inhibited if the Fe/Mn ratio is too high (which is the case in our study), precipitates were dissolved when ferrous concentrations are too high, and most other metals preferentially complex with sulphides before Mn.

Sulphate removal never exceeded 24% (see Table 3.4) whatever the column for treatment periods after 55 days (period 1 excluded). Sulphate removal was most of the time similar for

the different columns, whatever the AMD treated and the HRT in the columns. The ratio DOC/SO_4 decreased from 0.0133 for mixture #1, 0.0156 for mixture #4, 0.0567 for mixture #7 at the beginning of the experiment to 0.004 for mixture #1, 0.0009 for mixture #4 and #7 at the end. This lack of available carbon (DOC) for bacteria explains (at least partially) the low sulphate removal percentage (Neculita and Zagury, 2008).

3.4.2 Hydraulic residence time evaluation

HRT is a critical parameter that affects the performances of SRPBs, as shown earlier and in the literature (Neculita et al., 2008a). HRT values can be estimated theoretically (using the total volume, the porosity and the flow rate) and can also be measured using tracer tests. The response of column #4 to a step injection of NaCl is presented in Figure 3.8. Chloride concentration stayed relatively stable between 201 and 280 mg/L during 96 hours. Then, chloride concentration increased to stabilize at approximately 2150 mg/L at 264 hours; the chloride concentration in AMD during the tracer test (5000 mg/L) was not completely recovered.

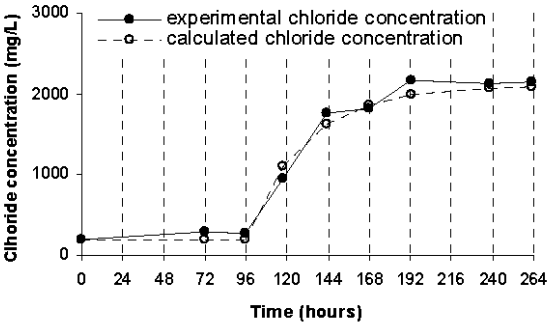

Figure 3.8 Chloride concentration evolution during the tracer test performed in column #4.

According to the chloride concentration, the system could be model as a succession of a plug flow reactor with a hydraulic retention time of 96 hours (corresponding to the latency period) and a continuous stirred reactor (corresponding to the increase of chloride concentration) with a hydraulic retention time of 34.7 hours. The total hydraulic residence time of the column #4 (sum of the plug flow reactor HRT and the continuous stirred reactor HRT) can be

estimated at 5.4 days. This hydraulic retention time corresponds to a total porosity of 0.47, a value slightly higher than the one determined initially (0.41).

Result obtained from the tracer test also showed that the HRT did not decreased with time, since the value estimated by the tracer test was close to the initial calculated HRT. The deducted porosity at the end of the experiment (0.47) was slightly higher than the initial porosity (0.41). The slight change of saturated hydraulic conductivity and porosity indicated that no major clogging appeared in the column during the experiment; this observation was also confirmed by visual observations at the dismantling stage.

3.5 Conclusions

The results presented in this study showed that treatment of high iron concentrated AMD with SRPBs was limited. Although eight different mixtures tested in batch tests provided an efficient metal removal (Genty et al., 2011b), continuous-flow column tests with three of these mixtures did not allow eliminating the entire contamination. SRPB columns increased the pH up to 6, allowing removal of metals like Al, Cd, Cr, Ni, Pb, Zn, but iron remained present at a high concentration (approximately 3190 mg/L to 3387 mg/L on average for period 5). This high iron concentration in biofilter effluents led to high acidity and caused a decrease of effluent pH after few hours, when column effluents were exposed to atmospheric conditions. The metal retention efficiency was slightly affected by hydraulic retention time; when increased from 5 to 7 days, a longer HRT favoured alkalinity generation. In this study, the difference in efficiency between the three tested mixtures was not really observable, as opposed to the batch test results. The addition of 50 % weight of structural agent (calcitic sand or sand), to improve hydraulic properties, did not affect the metal removal efficiency. Moreover, measurements of saturated hydraulic conductivity for mixtures with and without 50 % weight of sand or calcitic sand (mixtures #4, #7) showed that the structural agent did not really improve the hydraulic properties. Saturated hydraulic conductivity values stayed relatively stable (on average 2.1×10^{-3} cm/s for column #4D and 9.9×10^{-3} cm/s for column #7D) during more than one year. Tracer tests carried out at the end of the column test showed no major change in mixture porosity, and thus confirmed that the clogging phenomena were not really present in the tested SRPBs. Iron retention mechanisms were mainly hydroxide or

oxyhydroxide precipitation although sorption was an important phenomenon occurring during the first days of treatment; sulphide precipitation was also present in the three studied biofilters.

In summary, sulphate reducing biofilters were not efficient to remove adequately iron from high iron concentrated AMD. Hence, a multi-step passive treatment system would probably be a good option to treat highly contaminated AMD. SRPB could have an important contribution in this treatment combination because of its capacity to generate alkalinity and to retain most of the metals present in the AMD, but the addition of a specific step such as sorption for iron removal seems to be essential to reach typical regulation criteria at the final effluent.

Acknowledgements

This research was supported by the Canada Research Chair on Restoration of Abandoned Mine Sites and the Natural Sciences and Engineering Research Council of Canada (NSERC) through the Industrial NSERC Polytechnique-UQAT Chair in Environment and Mine Wastes Management. The authors gratefully acknowledge the industrial and governmental partners of the industrial Chair for the funding of this study.

References

AFNOR., 1986. Essais des eaux - Dosage des ions sulfates - Méthode néphélométrique, in : Norme Française NF T90-040.

Anello, G., Lamarche, P., Héroux, J.A. 2005. Reduction of hydraulic conductivity changes in an in-ground bioreactor. J. Environ. Eng. Sci. 4, 195-207.

APHA, 1995. Alkalinity titration, in: Greenberg, A., (Eds.), Standard methods for the examination of water and wastewater, 19th edn. Washington DC.

ASTM, 1990. Standard methods for sulphate reducing bacteria in water and water-formed deposit, in: Annual book of ASTM Standards (vol. 04.08., section D 4412 – 84), Washington, DC.

ASTM, 1995. Standard test method for permeability of granular soils, in: Annual book of ASTM Standards (vol. 04.08., section D 2434 – 68), Washington, DC.

Aubertin, M., Bussière, B., Bernier, L., 2002. Environnement et gestion des rejets miniers. Édition Presses Internationales Polytechnique, Montréal.

Barley, W., Hutton, T.C., Brown, M.M.E., Cusworth, J.E., Hamilton, T.J., 2005. Trends in biomass and metal sequestration associated with reeds and algae at Wheal Jane Biorem pilot passive treatment plant. Sci. Total Environ. 345, 279-286.

Beaulieu, S., 2001. Applications des techniques de bioactivation et de bioaugmentation pour le traitement en conditions sulfato-réductrices des eaux de drainage minier acide. Master Dissertation, École polytechnique de Montréal, Canada, pp 1-235.

Blowes, D.W., Ptacek, C.J., 1994. System for treating contaminated groundwater, in: U.S. Patent 5,362,394, filed March 3, 1992, issued Nov. 8, 1994.

Brown, M., Barley, B., Wood, C., 2002. Minewater treatment technology, application and policy. IWA Publishing, Londres.

Champagne, P., Van Geel, P., Parker, W. 2005. A bench-scale assessment of a combined passive system to reduce concentrations of metals and sulphate in acid mine drainage. Mine Wat. Environ. 24, 124-133.

Costa, M.C., Santos, E.S., Barros, R.J., Pires, C., Martins, M. 2009. Wine wastes as carbon source for biological treatment of acid mine drainage. Chemosphere 75, 831-836.

Cravotta, C. A., Trahan, M. K., 1999. Limestone drains to increase pH and remove dissolved metals from acidic mine drainage. Ap. Geochem. 14, 581-606.

Demers, I., Bussière, B., Aachib, M., Aubertin, M. 2011. Repeatability evaluation of instrumented column tests in cover efficiency evaluation for the prevention of acid mine drainage. Wat. Air Soil Pollut. 219, 113-128.

Edwards, J. D., Barton, C. D., Karathanasis, A. D., 2009. A small-scale sulfate-reducing bioreactor for manganese removal from a synthetic mine drainage. Wat. Air Soil Pollut. 203, 267-275.

Elliott, P., Ragusa, S., Catcheside, D., 1998. Growth of sulphate-reducing bacteria under acidic conditions in an upflow anaerobic bioreactor as treatment system for acid mine drainage. Wat. Res. 32, 3724-3730.

Evangelou, V.P., Zhang, Y.L., 1995. A review: pyrite oxidation mechanisms and acid mine drainage prevention. Environ. Sci. Tech. 25, 141-199.

Faure, M., Furman, M., Corbel, S., Carré, M.C., Gérardin, F., Zahraa, O., 2008. Caractérisation de réacteurs photocatalytiques utilisés pour le traitement de l'air, in : Séminaire 2008 de l'école doctorale RP2E Ingénierie des ressources, procédés, produits et environnement, ISBN 2-9518564-6-6, Nancy.

Fogler, H.S., 2006. Element of chemical reaction engineering, fourth ed. Prentice Hall International Series in the Physical and Chemical Engineering Sciences, Massachusetts.

Genty, T., Bussière, B., Potvin, R., Benzaazoua, M., Zagury, G.J., 2011a. Dissolution of different limestone in highly contaminated acid mine Drainage: Application to anoxic limestone drains. Submitted to Environ. Earth Sci.

Genty, T., Bussière, B., Benzaazoua, M., Zagury, G.J., 2011b. Treatment of acid mine drainage with high iron concentration using sulphate reducing passive bioreactor: I. Mixtures characterization. Submitted to Ap. Geochem.

Genty, T., Bussière, B., Neculita, C.M., Benzaazoua, M., Zagury, G.J., 2011c. Passive treatment of acid mine drainage: repeatability for sulphate reducing passive bioreactor column efficiency testing, in: Proceeding of International Mine Water Association symposium 2011, Aachen, Germany, 6 pp.

Jong, D., Parry, C., 2006. Microbial sulphate reduction under sequentially acidic conditions in an upflow anaerobic packed bed bioreactor. Wat. Res. 40, 2561-2571.

Karathanasis, A.D., Edwards, J.D., Barton, C.D., 2010. Manganese and sulphate removal from a synthetic mine drainage through pilot scale bioreactor batch experiments. Mine Wat. Environ. 29, 144-153.

Kirby, C. S., Cravotta, C. A., 2005. Net alkalinity and net acidity: Theoretical considerations. Ap. Geochem. 20, 1920-1964.

Kleinmann, R.L.P., Crerar, D.A., Pacelli, R.R., 1981. Biogeochemistry of acid mine drainage and a method to control acid formation. Mining Eng. 300-304.

KTH., 2010. Visual MINTEQ A free equilibrium speciation model, version 3.0, beta version. http://www.lwr.kth.se/English/OurSoftware/vminteq/index.html. Accessed 15 September 2010.

McCarthy, D.F., 1977. Essentials of soil mechanics and foundations. Reston Publishing, Reston.

Mendelhall, W., Beaver, R.J., 1994. Introduction to probability and statistics. Duxbury Press, Belmont.

Neculita, C.M., Zagury, G.J., Bussiere, B., 2007. Passive treatment of AMD in bioreactors using SRB: critical review and research needs. Environ. Qual. 36, 1-16.

Neculita, C.M., Zagury, G.J., 2008. Biological treatment of highly contaminated acid mine drainage in batch reactors: Long-term treatment and reactive mixture characterization. J. Hazard. Mater. 157. 358-366.

Neculita, C.M., Zagury, G.J., Bussiere, B., 2008a. Effectiveness of sulphate-reducing passive bioreactors for treating highly contaminated acid mine drainage: I. Effect of hydraulic retention time. Ap. Geochem. 23, 3442-3451.

Neculita, C.M., Zagury, G.J., Bussiere, B., 2008b. Effectiveness of sulphate-reducing passive bioreactors for treating highly contaminated acid mine drainage: II. Metal removal mechanisms and potential mobility. Ap. Geochem. 23, 3545-3560.

Neculita, C.M., Vigneault, B., Zagury, G.J., 2008c. Toxicity and metal speciation in acid mine drainage treated by passive bioreactors. Environ. Toxicol. Chem. 27, 1659-1667.

Postgate, J.R., 1984. The sulfate-reducing bacteria, second ed. Cambridge University Press, Cambridge.

Potts, P.J., 1987. A Handbook of Silicate Rock Analysis, Blakie & Son Ltd.

Potvin, R. 2009. Évaluation à différentes échelles de la performance de systèmes de traitement passif pour des effluents fortement contaminés par le drainage minier acide.

PhD. Dissertation, Chaire industrielle CRSNG Polytechnique – UQAT, Rouyn-Noranda, Canada, pp 1-365.

Robinson-Lora, M.A., Brennan, R.A., 2009. Efficient metal removal and neutralization of acid mine drainage by crab-shell chitin under batch and continuous-flow conditions. Bioressour. Technol. 100, 5063-5071.

Roche, N., Bendounan, R., Prost, C., 1994. Modélisation de l'hydrodynamique d'un décanteur primaire de station d'épuration. Rev. Sci. Eau 7, 153-167.

Santini, T., Degens, B., Rate, A., 2010. Organic substrates in bioremediation of acidic saline drainage waters by sulfate-reducing bacteria. Wat. Air Soil Pollut. 209, 251-268.

Seki, K., Thullner, M., Hanada, J., Miyazaki, T., 2006. Moderate bioclogging leading to preferential flow paths in biobarriers. Gr. Wat. Monitor. Remediat. 26, 68-76.

Skousen, J.G., Ziemkiewicz, P.F., 2005. Performance of 116 Passive Treatment Systems for Acid Mine Drainage, in: ASMR, 3134 Montavesta Rd. Publication, Proceeding of the National Meeting of the American Society of Mining and Reclamation, Breckenridge, Lexington.

Soleimani, S., Van Geel, P., Isgor, B., Mostafa, M. 2009. Modeling of biological clogging in unsaturated porous media. J. Contam. Hydrol. 106, 39-50.

Ulrich, M. 1998. Non-metallic carbonous minerals in the passive treatment of mining wastewater in Slovenia. Chem. Engin. Process. 38, 249-258.

URS, Report, 2003. Passive and semi-active treatment of acid rock drainage from metal mines-state of the practice. Prepared for U.S. Army Corps of Engineers, Concord, Massachusetts, by URS Corporation, Portland.

Van der Lee, J., 1993. JCHESS version 2.0. École des Mines de Paris, Centre d'information géologique, 2000-2001. http://chess.ensmp.fr. Accessed 15 September 2010.

Villeneuve, M., 2004. Évaluation du comportement géochimique à long terme de rejets miniers à faible potentiel de génération d'acide à l'aide d'essais cinétiques. Master Dissertation, Chaire industrielle CRSNG Polytechnique – UQAT, Rouyn-Noranda, Canada, pp 1-325.

Waybrant, K.R., Blowes, D.W., Ptacek, C.J., 1998. Selection of reactive mixtures for use in permeable reactive walls for treatment of acid mine drainage. Environ. Sci. Technol. 32, 1972-1979.

Zagury, G.J., Colombano, S. M., Narasiah, K.S., Ballivy, G., 1997. Stabilisation de résidus acides miniers par des résidus alcalins d'usines de pâtes et papier. Environ. Technol. 18, 959-973.

Zaluski, M.H., Trudnowski, J.M., Harrington-Baker, M.A., Bless, D.R., 2003. Post-mortem findings on the performance of engineered SRB field-bioreactors for acid mine drainage control, in: Proc. of the 6th Int.Conf. on Acid Rock Drainage, Cairns, QLD. 12-18 July, 2003, pp 845-853.

CHAPITRE 4

CAPACITY OF WOOD ASH FILTERS TO REMOVE IRON FROM ACID MINE DRAINAGE: ASSESSMENT OF RETENTION MECHANISM

Cet article a été soumis à Mine Water and the Environment en décembre 2011.

Auteurs

Thomas Genty[1], Bruno Bussière[1], Mostafa Benzaazoua[2], Gérald J. Zagury[3]

[1]Industrial Chair CRSNG Polytechnique-UQAT: Environment and mining wastes management, University of Québec in Abitibi-Témiscamingue, Rouyn-Noranda, Québec, Canada

[2]Laboratoire de Génie Civil et d'Ingénierie Environnementale, INSA de Lyon, Villeurbanne, France

[3]Industrial Chair CRSNG Polytechnique-UQAT : Environment and mining wastes management, École Polytechnique, Québec, Canada

Abstract

Acid mine drainage (AMD) with high iron concentration is a major challenge for passive treatment systems. Indeed, literature shows some limitations of these treatments, particularly when sulphate reducing passive bioreactors (SRPBs) are used. These systems have difficulties to remove iron, which lead to maintain a high acidity in the effluent. This study assesses the capacity of wood ash filters to act as a polishing step after a SRPB treatment of a high iron AMD (4000 mg/L of Fe). The study consisted of a material characterization and an evaluation of iron sorption properties. Five columns (1,7L) with different mixtures of fly ash and sand were investigated to remove metal from a SRPB effluent during 122 days.

Characterization results showed that materials had a high specific surface area (between 46-159 m^2/g), high organic carbon content (between 12 and 32%) and high paste pH (up to 12.2). Moreover, Freundlich isotherm model represented well the iron sorption phenomena on material surface. The five columns allowed determining that wood ashes alone decreased iron concentration during a period of more than one hundred days below 10 mg/L (99% of iron removal), mainly due to iron hydroxide precipitation and sorption. The risk of system clogging was negligible in that case since saturated hydraulic conductivity stayed stable in the range of $5.0x10^{-3}$ cm/s and $3.1x10^{-2}$ cm/s. Sulphates were also removed during the treatment by gypsum precipitation at a percentage varying between 44 and 52% depending on the column.

Keywords: acid mine drainage, wood ash filter, column tests, metal retention mechanisms, sorption.

4.1 Introduction

Mine wastes produced during mining operations can cause a significant contamination of drainage water mainly due to sulphide minerals weathering reactions (Kleinmann et al., 1981, Blowes and Ptacek, 1994, Evangelou and Zhang, 1995). These chemical reactions lead to the production of sulphuric acid, which decreases the pH if no neutralizing minerals are present in the mine wastes, and favours the leaching of metals (e.g. Akcil and Koldas, 2005). Biological processes can also catalyze this weathering process called acid mine drainage (AMD).

[4-1] $$FeS_2 + 15/4O_2 + 7/2H_2O \rightarrow Fe(OH)_3 + 2H_2SO_4$$

AMD iron concentration can be elevated in several hard rock mine effluents in Canada (higher than several thousands of mg/L Aubertin et al., 2002), and provides high acidity to the drainage. Several methods exist to treat AMD and to reach environmental regulating criteria, the most employed is lime active treatment. In the case of closed mine sites, passive treatment systems are preferred to conventional chemical treatment plants because they use natural or waste materials and imply low investment, operating and maintenance costs (Johnson and Hallberg, 2005, Skousen and Ziemkievicz, 2005, Neculita et al., 2007).

Recently, some studies on AMD passive treatment systems mainly tried to demonstrate the effectiveness of single (one step) treatment system.

Passive treatment systems such as anoxic limestone drains (ALD) and sulfate-reducing passive biofilters (SRPBs) have demonstrated their effectiveness, at least in the short term, for slightly or moderately-contaminated AMD (Hedin et al., 1994, Cravotta and Trahan, 1999). However their capacity to treat highly contaminated AMD (like with high iron concentration) still has to be demonstrated (Genty et al, 2011a). Costa et al. (2008), Neculita et al. (2008a) and Potvin (2009) showed that SRPBs could effectively treat AMD with an iron concentration of approximately 500 mg/L and less. Genty et al. (2011b) and Genty et al. (2011c) tested eight different SRPBs in batch and column tests to treat a high iron acid mine drainage (pH 3.5, $[SO_4^{2-}]$ = 9000 mg/L and [Fe] = 4000 mg/L). Results showed that the neutralization was effective for all columns and metal removal efficiency reached high values (more than 90% on average) for Al, Cd, Cr, Ni, and Zn. Nevertheless, iron removal in the tested AMD could not exceed approximately 20% for all three mixtures investigated. The high iron concentration in the columns' effluent provided high acidity (Kirby and Cravotta, 2005) which leads to a decrease in pH from 6 to below 4.5 after eight hours of contact with air. Therefore, single-step SRPBs improve water quality but cannot totally remove the contaminants from a high iron concentrated AMD.

It becomes necessary for highly concentrated AMD to combine other treatment methods to reach environmental targets (Champagne et al., 2005). Iron removal studies by Champagne et al. (2005) were performed using a sorption step in a peat filter. Then, a series of SRPB, ALD and settling pond allowed treating adequately AMD (pH of 3.2 and iron concentration of 189 mg/L).

Sorption filters containing an adsorbent material are not often used in classical AMD passive treatment systems. However, these adsorbent materials can remove metal from water (e.g. Blais et al., 1999, Polat et al., 2002, Champagne et al., 2005, Vadapalli et al., 2008). In the present study, wastes from wood combustion (by-product of energy power plant called hereinafter wood ash filters) are tested for iron removal from a highly concentrated AMD because of their local availability and their high carbon content. Wood ashes are presently

considered as a waste but have a good valorization potential. This material is mainly composed of bottom and fly ashes. Sorption properties of ashes mainly come from amorphous iron and aluminium hydroxides, carbon, oxi-hydroxides, carbonated material and silicated materials (Gonzalez et al., 2009). Biomass ashes, and particularly wood ashes containing a lot of unburned material, such as those used in the present study, are not well characterized in the literature compared to coal and petroleum coke fly ashes (Ahmaruzzaman, 2010).

The main objective of the present study is to evaluate the capacity of wood ash filters to be used in the two-step treatment of high iron concentrated AMD (approximately 4000 mg/L). Wood ash filters were tested in the polishing step after an AMD treatment by SRPB. Materials were first characterized, and sorption properties toward iron were determined; iron is selected here because it is the most problematic element of the tested AMD (see Genty et al., 2011c). Then, column tests were carried out to identify metal retention mechanisms in more realistic conditions. Moreover, a saturated hydraulic conductivity investigation was performed to evaluate the risk of clogging in wood ash filters.

4.2 Materials and methods

4.2.1 Water quality of the columns influent

Chemistry of the wood ash filters influent is given in Table 4.1. This contaminated water was in fact the effluent of a passive treatment system (SRPB) tested in a laboratory column. SRPB effluent presented low concentrations in metals except for Mn and Fe which were not treated efficiently by the tested SRPBs (Neculita et al., 2008a, Neculita et al., 2008b, Genty et al., 2011c), and a relatively acidic pH (of approximately 4) due to the precipitation of iron hydroxides following exposure of the effluent to atmospheric oxygen (Genty et al., 2011c).

Table 4.1 Average concentrations (in mg/L except pH) of the main metals in the AMD and the polishing column influent (SRPB effluent).

Elements	AMD	Column influent
Fe	4000	3200
Mg	10	30
Mn	35	33
Ni	2	0.1
Pb	0,5	0.3
SO_4^{2-}	9000	8600
Zn	40	1
pH	3.5	4

4.2.2 Materials

Wood ashes[8] used to treat the contaminated drainage from the SRPB are by-products from a cogeneration plant (located at Kirkland Lake, Canada) that uses wood wastes to produce energy. These ashes, which are a mix of bottom and fly ashes, contained a significant portion of carbon and gravel. Two other materials were obtained from wood ashes to evaluate their capacity to treat AMD. The first material, named carbon wood ashes, was obtained by processing wood ashes in water and by collecting floating particles by flotation. The second material was obtained by screening dry wood ashes in a 1.18 mm sieve. These two materials will allow evaluating the role of carbon and fine particles in the neutralization and metal removal processes.

4.2.3 Physical, mineralogical and chemical characterisation of solids

Wood ashes, carbon wood ashes and fine wood ashes (below 1.18 mm diameter) were characterized to determine their physical and chemical properties. Specific gravity (G_s) was measured by a helium pycnometer Micromeritics Accupyc 1330 and the specific surface area (S_s) by a surface analyser Micromeritics Gimini III 2375 on dry samples (nitrogen adsorption with BET method). Particle size analysis was carried out using sieves having different openings (Aitcin et al., 1983). pH was determined in deionized water using a solid to liquid

[8] Il est à noter que d'autres matériaux sorbant ont été testés en laboratoire comme la tourbe (Voir Appendice C).

ratio of 1: 10 (ASTM, 1995a). Total carbon (TC) was measured under oxygen atmosphere with an ELTRA CS2000 Carbon Sulphur Determinator PC Controlled. Total organic carbon (TOC) was measured (by adding potassium dichromate and sulphuric acid and measurement of excess of potassium dichromate) and total inorganic carbon (TIC) was calculated as the difference of TC and TOC. Solids were digested in HNO_3, Br_2, HCl and HF (Potts, 1987), and the liquid resulting from this treatment was analysed for elemental composition by Inductively Coupled Plasma-Atomic Emission Spectrometry (ICP-AES) Perkin Elmer OPTIMA 3100 RL (relative precision of 5%). X-ray diffractometer (XRD) Bruker axs D8 ADVANCE was used to identify the mineralogy of the crystalline fraction of the tested materials. The instrument is equipped with a Cu anticathode and scintillation counter. Data treatment was done using Bruker A.X.S. EVA software package. A thermogravimetric analysis (TGA) coupled with a differential scanning calorimetric analysis (DSC) was performed on each material to complement the mineralogical information. Samples were heated from ambient temperature to 1000°C at a rate of 20°C per minute under Nitrogen atmosphere. The main advantage of this technique is that crystalline and amorphous phases can be studied simultaneously. Finally, cationic exchange capacity evaluation consisted of saturating all exchange sites with sodium ions (with a sodium acetate solution 1N) and to desorb them with a solution of ammonium acetate 1N (method adapted from Zagury et al., 2004). Sodium concentration was analysed using a Metrohm 881 compact IC pro ions chromatograph (column Metrosep C415/40, elluent: 1.7 mmol HNO_3 and 0.7 mmol dipicolinic acid, flow rate: 0.9 mL/min).

4.2.4 Sorption experiments description

4.2.4.1 Sorption isotherm and sorption kinetic models

The two most common isotherm models have been investigated in this work: the Langmuir and Freundlich equilibrium isotherms (Al-Degs et al., 2006, Jha et al., 2008, Garcia-Mendieta et al., 2009). The linear form of Langmuir equation can be represented by the following equation [4-2]:

[4-2] $$\frac{C_e}{q_e} = \frac{1}{b.q_{\max}} + \frac{C_e}{q_{\max}}$$

where C_e is the equilibrium concentration of remaining metal in the solution (mg/L), q_e is the amount of a metal adsorbed per unit mass of sorbent at equilibrium (mg/g), q_{max} is the amount of adsorbate at complete monolayer coverage (mg/g), and b (L/mg) is a constant related to the heat of adsorption. Freundlich linear isotherm can be expressed by the following equation:

[4-3] $$\log q_e = \log k_f + n.\log C_e$$

k_f is the equilibrium constant (mg/g) indicative of adsorption capacity ,and n represents the sorption equilibrium constant.

Sorption kinetic models can be divided into two main types: reaction-based models and diffusion-based models (Ho et al., 2000, Al-Degs et al., 2006, Jha et al., 2008, Garcia-Mendieta et al., 2009). Equations [4-4], [4-5] and [4-6] represent three different sorption models:

[4-4] pseudo first order: $\log(q_e - q_t) = \log q_e - k_1.\frac{t}{2.303}$

[4-5] pseudo second order: $\frac{1}{q_e - q_t} = \frac{1}{q_e} + k_2.t$

[4-6] pseudo second order for chemisorption: $\frac{t}{q_t} = \frac{1}{k_3.q_e^{\,2}} + \frac{t}{q_e}$

where q_t is the amount of a metal adsorbed per mass unit of sorbent (mg/g) at time t (s), k_1 is the pseudo first order rate constant (s^{-1}), k_2 and k_3 the pseudo second order rate constant ($g.mg.s^{-1}$).

However, if the external or internal diffusion of metal cations is the rate-limiting step in metal sorption, kinetic reaction law can be represented respectively by:

[4-7] external diffusion : $\ln \frac{C_t}{C_i} = -k_f . \frac{A}{V} . t$

[4-8] internal diffusion : $q_t = k_d . t^{1/2}$

with C_i the initial concentration of metal in the solution (mg/L), C_t the concentration at the time t, k_{fe} and k_d are the external and internal diffusion coefficient (respectively in cm/s and $mg.g^{-1}.s^{-1/2}$), A the external surface of absorbent (cm^2) and V the volume of adsorbant (cm^3).

4.2.4.2 Sorption isotherm and kinetics experiments

Two grams of adsorbent (wood ashes, carbon wood ashes and wood ashes below 1.18 mm diameter) were weighted and placed into 200 mL erlenmeyers. For isotherm experiments, 100 mL AMD solutions of different concentrations (from original AMD to AMD diluted fifty times; see Figure 4.1 for AMD concentration) were prepared and then transferred into the sample bottles. Diluted AMD solution was used in batch test although only iron concentration was measured. Indeed, since ionic competition can occur on sorption sites, it was considered more representative to use AMD solutions with numerous metal salts (Limousin et al., 2007) instead of deionised water with a known iron concentration. The selected ratio solid material / solution ensure that equilibrium conditions are reached (all the metal ions are not adsorbed which allows determining the equilibrium point, Gupta et al., 2009). For kinetics experiments, 100 mL of aqueous AMD solutions were transferred into the sample bottles. The sample erlenmeyer flasks were placed on a shaking table (200 rpm) at 21°C. Experiments were conducted at pH 3 and 6; pH adjustment was performed by adding NaOH 1N or HCl 1N solutions. Samples for isotherm experiments were filtered (0.45 µm) for metal analysis by ICP-AES after reaching equilibrium (24 h). Sorption capacity q_e (mg/g) of the sorbent was calculated by the mass balance equation [4-9] (Al-Degs et al., 2006):

[4-9] $$q_e = [C_i - C_e] . \frac{V}{m}$$

where C_i, C_e, V, and m are respectively initial metal concentration (mg/L), metal concentration at equilibrium (mg/L), total volume (L) and weight (g) of sorbent. Water

sample for kinetic experiments were taken and filtered (0.45 µm) for metal concentration determination at 0h, 0.5h, 3h, 7h and 28h.

4.2.4.3 Analysis of material surface by FTIR

Fourier Transform Infrared spectroscopy (FTIR) is one of the most widely tool for organic coumpound identification (Griffiths, 1975). FTIR allows mainly determinating organic functional groups at the surface of samples but quantification is often not easy (Skoog et al., 1997). Materials surfaces before and after iron sorption were analyzed with a FTIR spectrometer Tensor 27 Bruker AXS under ambient conditions after 24 h of contact with AMD according to isotherm experiments. Dry samples were placed on a ZnSe mirror and analysed using reflection mode HATR (Horizontal Attenuated Total Reflection) from PIKE (MIRacle Single Reflection ATR) in the wave number range of 500–4000 cm^{-1}. The shift of some organic function peaks in FTIR spectrum or modification of intensity of the peaks after contact with a metal solution (AMD) indicate that these functional groups interfere with metals (Deng and Ting, 2005, Nurchi et al., 2010).

4.2.5 Column experiment description

Five 1.6 L columns (20 cm in height and 10.5 cm in diameter; see Figure 4.1 for a schematic representation) were made to determine the capacity of wood ashes to improve water quality (particularly to remove iron) after a sulphate reducing passive biofilter. Polishing columns filled with five different mixtures were investigated (Table 4.2). These mixtures were chosen to determine the influence of the type of fly ashes (carbon and fraction below 1.18 mm diameter) and sand proportion on iron removal and on column clogging. Sand used in some mixtures was 97% silica and had the following particle size characteristics: D_{10} (D_x is the effective diameter, corresponding to x% passing on the cumulative grain-size distribution curve) of 0.22 mm, a D_{50} of 0.32 mm and a uniformity coefficient ($C_U=D_{60}/D_{10}$) of 1.7.

Table 4.2 Polishing column mixture composition (% w/w dry) and characteristics

Mixture	#1	#2	#3	#4	#5
Mixture composition					
Wood ashes	100%			40%	70%
Carbon wood ashes		100%			
Wood ashes (below 1.18 mm diameter)			100%		
Sand				60%	30%
Column characteristics					
Column number	#1	#2	#3	#4	#5
Mixture mass (dry g)	1089	471	1027	1537	1408
Height (cm)	20	20	20	20	20
Estimated porosity	0.47	0.68	0.57	0.44	0.44
Estimated HRT (days)	5.3	7.8	6.6	5.0	5.1

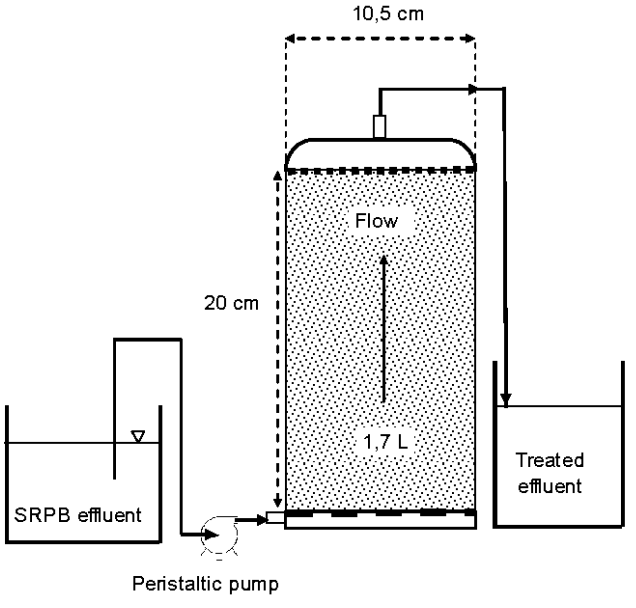

Figure 4.1 Polishing column test configuration (figure not to scale)

Polishing columns were fed with the SRPB effluent by a peristaltic pump (from bottom to top at a flow rate of 0.1 mL/min). SRPB column tests are presented in Genty et al. (2011c).The base of the columns was made of a perforated plastic plate covered by a geotextile. Porosity was estimated with the water volume needed to fill up the column; porosity values varied from 0.68 to 0.44, as showed in Table 4.2. Considering a flow rate of 0.1 mL/min, the HRT were 5.0 days for column #4, 5.1 days for column #5, 5.3 days for column #1, 6.6 days for column #3, and 7.8 days for column #2.

4.2.6 Analytical method for water quality evaluation

pH, Eh, sulphate, acidity, alkalinity, and metal concentrations of both influents and effluents, were determined during the experiment. pH was determined with an Orion Triode sensor coupled with a Benchtop pH/ISE Meter Orion model 920 (relative precision +/- 0.01 pH) and Eh (redox potential, values were corrected relative to the standard hydrogen electrode) was measured by a Pt/Ag/AgCl sensor linked to a Benchtop pH/ISE Meter Orion 920. The alkalinity concentration was obtained by titration on non-filtered sample with sulphuric acid 0.02N (precision of 1 mg $CaCO_3$/L) and the acidity concentration by titration on non-filtered sample with sodium hydroxide 0.1N (precision of 1 mg $CaCO_3$/L). Filtered samples (0.45 µm filter) used to quantify metal content were acidified with 2% volume with nitric acid (70%) before analysis by ICP-AES. Sulphate determination assumed that all sulphur was under a sulphate form (sulphate concentration was obtained by multiplying sulphur concentration by the ratio of sulphate molar mass on the sulphur molar mass, Potvin, 2009). This hypothesis was confirmed by thermodynamic modeling (sulphur was mainly under sulphates form).

4.2.7 Saturated hydraulic conductivity evaluation

To quantify a possible clogging of the tested systems, saturated hydraulic conductivity k_{sat} was evaluated monthly on the columns during the operation using the falling head method (adapted from ASTM, 1995b). Values of k_{sat} (cm/s) were calculated with the following equation (McCarthy, 1977):

[4-10] $$k_{sat} = \frac{aL}{At}\ln(\frac{h_1}{h_2})$$

where a (cm^2) is the area of the water head column, L (cm) the length of the sample, A (cm^2) the area of the sample, t (s) the time necessary for the water head column to drop from the head h_1 (cm) to h_2 (cm).

4.2.8 Columns post-testing characterisation

At the end of the experiment, samples were collected at 10 cm from the top for each column. Metal fractionation in the five tested mixtures was estimated with a semi-quantitative sequential extraction procedure (SEP) (Zagury et al., 1997, Neculita et al., 2008b). The five fractions were extracted from 1 g of wet solid sample using different reagents:

- Soluble and exchangeable metals (extracted with 8 mL $MgCl_2$ 0.5 M, pH 7, 1 h at room temperature)

- Carbonate bound (leached by 8 mL NaOAc 1 M buffered with HOAc, pH 5, 5 h at room temperature)

- Reducible or bound to Fe–Mn oxides (extracted with 20 mL NH_2OH-HCl 0.04 M in 25% (v/v) HOAc, 6 h at 96°C)

- Oxidisable or bound to organic matter (released by 3 mL HNO_3, 5 mL H_2O_2 30% pH 2, 2 h at 85°C, then 3 mL H_2O_2 30% pH 2, 3 h at 85°C, and 5 mL NH_4OAc 3.2 M in 20% (v/v) HNO_3, 0.5 h at room temperature). Solution was diluted to 20 mL.

- Residual metal fraction (dissolved by acid attack with HNO_3, HF, and HCl).

To evaluate the mineralogy of solid crystalline phases produced in the columns, XRD analyses were carried out on samples coming from each column. Then, a Hitachi 3500-N scanning electron microscope (SEM) with the secondary electron mode coupled with an energy dispersive spectrometry (EDS) of an X-ray probe (voltage of 20 keV, amperage of 140 A, pressure around 25 kPa and work distance of 15 mm) was used to characterize the microstructure, texture and chemistry of samples. Chemical analyses of samples from the tested columns were performed according to the methodology presented in section 2.3.

Finally, chemical speciation at equilibrium was estimated using the composition of column effluents. Saturation index of the main minerals susceptible to precipitate were calculated using a thermodynamic chemical equilibrium model (Vminteq v 2.53) with the activity correction proposed in the SIT model (KTH, 2010).

4.3 Characterization results

4.3.1 Materials characterisation

Physical and chemical characteristics of the reactive materials are showed in Table 4.3. As expected, fine fraction wood ashes (below 1.18 mm diameter) had the smallest particle size distribution (D_{10} of 0.09 mm and D_{50} of 0.45 mm) and the highest specific gravity (G_s = 2.70). Carbon wood ashes had a G_s of 2.55 and had the coarsest particle size distribution (D_{10} of 0.66 mm and D_{50} of 1.15 mm). Woods ashes specific gravity was 1.74. Each material contained a non-negligible part of organic carbon (between 12% for wood ashes below 1.18 mm diameter and 32% for carbon wood ashes). These high total organic carbon (TOC) contents indicate that the three materials contained a lot of unburned wood (unburned wood was directly linked to the TOC content). Thus, carbon wood ashes had the highest TOC content (64%) because of the preparation method (wood ashes concentration by collectorless flotation). Wood ashes and wood ashes below 1.18 mm diameter had a total carbon content of respectively 36% and 31%. S_s values were approximately 46 m^2/g for wood ashes, 159 m^2/g for carbon wood ashes, and 52 m^2/g for wood ashes below 1.18 mm diameter. These relatively high specific surface areas should provide good sorption ability.

Table 4.3 Reactive material characteristics

	Wood ashes	Carbon wood ashes	Wood ashes below 1.18 mm diameter
Physical characteristics			
D_{50} (mm)	0.60	1.15	0.45
D_{10} (mm)	0.11	0.66	0.09
Specific gravity	1.74	2.55	2.70
Specific surface area (m^2/g)	46.03	158.77	51.60
Chemical characteristics			
Total carbon (% dry)	36	64	31
Total organic carbon (% dry)	19	32	12
Total inorganic carbon (% dry)	17	32	19
pH	12.2	9.9	10.3
Element abundance by ICP-AES			
Al (wt%)	2.3	2.1	0.5
Ca (wt%)	12.3	14.0	7.2
Fe (wt%)	1.5	1.4	0.4
Mg (wt%)	1.4	1.3	0.6
Mn (wt%)	0.2	0.3	0.1
S (wt%)	0.2	0.2	0.1

Wood ashes were more alkaline than the other wood ash materials studied. Indeed their pH was 12.2 compared to 9.9 for carbon wood ashes and 10.3 for wood ashes below 1.18 mm diameter. Digestion of materials and analysis of metal content showed that calcium was an important element (12.3% for wood ashes, 14.0% for carbon wood ashes and 7.2% for wood ashes below 1.18 mm diameter). However, digestion was not complete because some particles were not totally dissolved at the end of the preparation. Mineralogical quantification by XRD on initial material could not be done because the studied materials contained a large part of amorphous phases. Nevertheless, XRD showed that quartz and calcite were mainly present in crystalline fraction of the three materials; presence of calcite was in accordance with the relatively high calcium concentration (between 7.23 and 14%) determined by ICP-AES on solid samples. Other minerals were identified in the materials: silicates (muscovite, albite, anorthite, actinolite, chlorite, and microcline), sulphates (gypsum), oxides (rutile), carbonates (siderite), and sulphur. Silicates, oxides, sulphates, silica and carbonates have been identified in fly ashes from different sources (Gonzalez et al., 2009). The thermal analysis TGA-DSC (see Figure 4.2) performed on the three initial wood ash materials allowed determining which material contained the highest calcite content. The differential

weight loss curve and the DSC signal showed two main endothermic weight losses occurring at 82-88°C and 753-767°C. The first loss at 82-88°C is probably due to the uptake water release because sample were dried at only 40°C before analysis. Between this temperature and 700°C, a regular loss of weight appeared for each material, corresponding to the decomposition of organic unburned materials present initially. The last reaction at 753-767°C is due to calcite decarbonatation (CO_2 release, Ouellet et al., 2006). Results showed a weight loss of 6.9% for wood ashes, 6.8% for carbon wood ashes and 10.1% for wood ashes below 1.18 mm diameter. These last results showed that wood ashes below 1.18 mm diameter have probably the highest carbonate content and contradicted the result of metal quantification by ICP (probably because of the partial chemical digestion mentioned earlier).

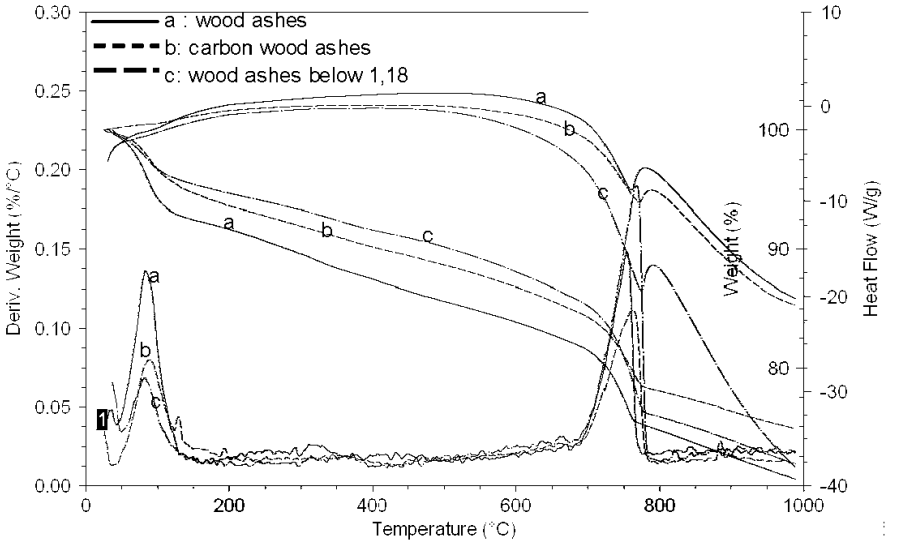

Figure 4.2 TGA and DSC profiles (weight percentage and heat flow in W/g versus temperature in degree Celsius).

4.3.2 Sorption batch test results and iron retention

Table 4.4 presents the fitting of Langmuir and Freundlich models with experimental isotherm data[9]. Freundlich model was more appropriate to represent the isotherms obtained for both pH 3 and 6, and for the three wood ash materials tested. The Freundlich model indicated that

[9] Data used to built sorption test graphs are available in Appendice G.

sorption was done on a heterogeneous surface (Jha et al., 2008). Furthermore, isotherm results showed that iron removal was more important at pH 3 than at pH 6 with higher k_f values (k_f represents the adsorbed quantity of iron in mg per gram of material for an iron equilibrium concentration of 1 mg/L), and that wood ashes below 1.18 mm diameter had the highest iron retention capacity.

Table 4.4 Iron sorption isotherm models for pH 3 and 6 on the three wood ash materials studied (F=Freundlich)

Isotherm models	pH 3					pH 6				
	Best model fit	R^2	k_f (mg/g)	n	$q_{e,Freundlich}$ (mg/g)	Best model fit	R^2	k_f (mg/g)	n	$q_{e,Freundlich}$ (mg/g)
Wood ashes	F	0,81	16.62	0.14	49.37	F	0,97	8.41	0.21	38.96
Carbon wood ashes	F	0,78	14.87	0.28	108.23	F	0,99	4.36	0.43	75.30
Wood ashes below 1.18 mm diameter	F	0,68	81.65	0.64	168.30	F	0,99	23.68	0.60	112.35

q_e (mg/g) values calculated with equation [4-13] are noted in the paper as $q_{e,Freundlich}$. At pH 3, C_0 was 3370 mg/L and at pH 7 2260 mg/L. m value was 20.

Sorption phenomena can also be described by kinetic sorption tests. The equilibrium capacity (q_e) has been determined in order to use kinetic models presented in [4-4] and [4-5]. The values of q_e were calculated from the Freundlich equation. The equilibrium concentration C_e can be represented by the following equation (Al-Degs et al., 2006):

[4-11] $$C_e = C_0 - C_{surface}$$

where, C_0 and $C_{surface}$ are, respectively, the initial concentration of iron (mg/L) and the surface concentration at equilibrium (mg/L). The ratio of the sorbent mass (g) to the volume of the solution (L) can be presented as the parameter m_r:

[4-12] $$m_r = \frac{mass}{volume}$$

The surface concentration ($C_{surface}$) is equal to $m_r . q_e$

By combining equations [4-3], [4-11] and [4-12], q_e (mg/g) values were calculated using the following equation:

[4-13] $$\log(q_e) - \log(k_f) - n.\log(C_0 - m_r.q_e) = 0$$

Values of q_e which solved equation [4-13] are called $q_{e,Freundlich}$ and are presented in Table 4.4. These values were then used to model experimental kinetic data according to equation [4-4] to [4-8]. Table 4.5 shows that several kinetic models can fit to experimental data with a high correlation coefficient for most materials at the two tested pH.

The selection of the most appropriated kinetic model was made by calculating the sum of square of the errors (SSE) according to Cheung et al. (2000) and Al-Degs et al. (2006).

[4-14] $$SSE = \sum (q_{t,\exp} - q_{t,theo})^2$$

where $q_{t,\exp}$ and $q_{t,theo}$ are the experimental sorption capacity of iron (mg/g) at time t and the corresponding value obtained with the kinetic models. $q_{t,theo}$ was determined using kinetic models according to parameter of Table 4.5 and equation [4-4] to [4-8]. The model with the lower SSE value can give an indication of the sorption limiting step (Cheung et al., 2000, Al-Degs et al., 2006). According to the SSE values, the model that best represents the sorption kinetic for wood ashes and carbon wood ashes at pH 3 and wood ashes below 1.18 cm at pH 6 was a pseudo second order reaction (equation [4-6]). This reaction is typical of chemisorption reaction (Ho et al., 2000). For wood ashes and carbon wood ashes at pH 6 and fine wood ashes (below 1.18 mm) at pH 3, the kinetic limiting step seemed to be the diffusion of iron to the sorption site. This diffusion could be external (equation [4-7], wood ashes, pH 6) i.e. the surface process occurred on the exterior of the sorbent particle, (equation [4-8], carbon wood ashes, pH 6 and wood ashes below 1.18 mm, pH 3) or internal i.e. the process of sorption is controlled by a migration of iron ions inside the sorbent particle (Al-Degs et al., 2006).

Table 4.5 Iron sorption kinetic models for pH 3 and 6 on the three wood ash materials studied

Material :	pH 3		Kinetic reaction models				Diffusion reaction models	
	Kinetic model	R^2	k_1 (h^{-1})	k_2 ($g.mg.h^{-1}$)	k_3 ($g.mg.h^{-1}$)	q_e (mg/g)	$k_{fe}.A/V$ ($cm.h^{-1}$.$cm^2.cm^{-3}$)	k_d ($mg.g^{-1}.h^{-1/2}$)
Wood ashes	pseudo second order [4-6]	0.99	-	-	0.0032	126.58	-	-
Carbon wood ashes	pseudo second order [4-6]	0.99	-	-	0.0029	133.33	-	-
Wood ashes below 1.18 mm diameter	pseudo first order [4-4]	0.99	0,093	-	-	8.60	-	-
	pseudo second order [4-6]	0.97	-	-	0.012	181.82	-	-
	external diffusion [4-7]	0.98	-	-	-	-	0,10	-
	internal diffusion [4-8]	0.98	-	-	-	-	-	30.18
Material :	pH 6		Kinetic reaction models				Diffusion reaction models	
	Kinetic model	R^2	k_1 (h^{-1})	k_2 ($g.mg.h^{-1}$)	k_3 ($g.mg.h^{-1}$)	q_e (mg/g)	$k_{fe}.A/V$ ($cm.h^{-1}$.$cm^2.cm^{-3}$)	k_d ($mg.g^{-1}.h^{-1/2}$)
Wood ashes	pseudo second order [4-6]	0.99	-	-	0.023	123,46	-	-
	external diffusion [4-7]	0.99	-	-	-	-	0,148	-
	internal diffusion [4-8]	0.91	-	-	-	-	-	21.66
Carbon wood ashes	pseudo first order [4-4]	0.99	0.092	-	-	6.39	-	-
	pseudo second order [4-5]	0.97	-	0.0062	-	294,12	-	-
	external diffusion [4-7]	0.91	-	-	-	-	0,036	-
	internal diffusion [4-8]	0.99	-	-	-	-	-	13.29
Wood ashes below 1.18 mm diameter	pseudo second order [4-6]	0.99	-	-	0.0035	123.46	-	-
	external diffusion [4-7]	0.93	-	-	-	-	0,360	-

Only best fit model (with R^2>0.90), are presented.

Sorption of metal onto a material surface is complex and numerous mechanisms can occur such as adsorption (physisorption or chemisorption), cationic exchange, and surface precipitation. Isotherms and kinetic tests characterization allow respectively describing the sorption mode (sorption onto a homogeneous surface or a heterogeneous surface) and to determine if the diffusion of metal or the reaction at the surface is the limiting step during the

sorption mechanism. However, the mechanisms of sorption cannot be specifically identified. The measured CEC values for the reactive materials showed that ion exchange is one of main sorption phenomena that explain iron retention in the three tested wood ash materials. Values of CEC were 24.9 meq/100g (dry) for wood ashes, 49.8 meq/100g (dry) for carbon wood ashes and 12.8 meq/100g (dry) for wood ashes below 1.18 mm diameter. These values are in the same range as those observed for organic material like compost (53.2 meq/100g, Karathanasis et al., 2010), but lower than that of peat (119.5 meq/100g,, Twardowska and Kyziol, 2008), which is recognized has having a high CEC (Twardowska and Kyziol, 2008). Indeed, activated carbons, which are close to the tested material of this study, are usually not considered to have a high exchange capacity (Johnson et al., 1986).

FTIR analyses of the material surface after iron sorption can help to understand the surface reaction mechanism responsible of metal retention (Deng and Ting, 2005, Nurchi et al., 2010). Indeed, the formation of hydroxide phases on the surface during iron sorption was suggested by the FTIR analysis. A difference appeared in FTIR spectrum (see Figure 4.3) between samples before and after sorption with iron (3370 mg/L, pH 3). These changes appeared mainly at wavelengths of approximately 2800 to 3600 cm^{-1}. The main peaks were at 3242 and 3395-3547 cm^{-1}. This range in the FTIR spectrum is typical of hydroxide lattice water or hydroxo-group (Deng and Ting, 2005, Prasad et al., 2006, Twardowska and Kyziol, 2008). Formation of iron hydroxides at the materials surface is plausible because materials had high paste pH (between 9.9 and 12.2 depending on the material) and iron precipitation at these pH values is probable.

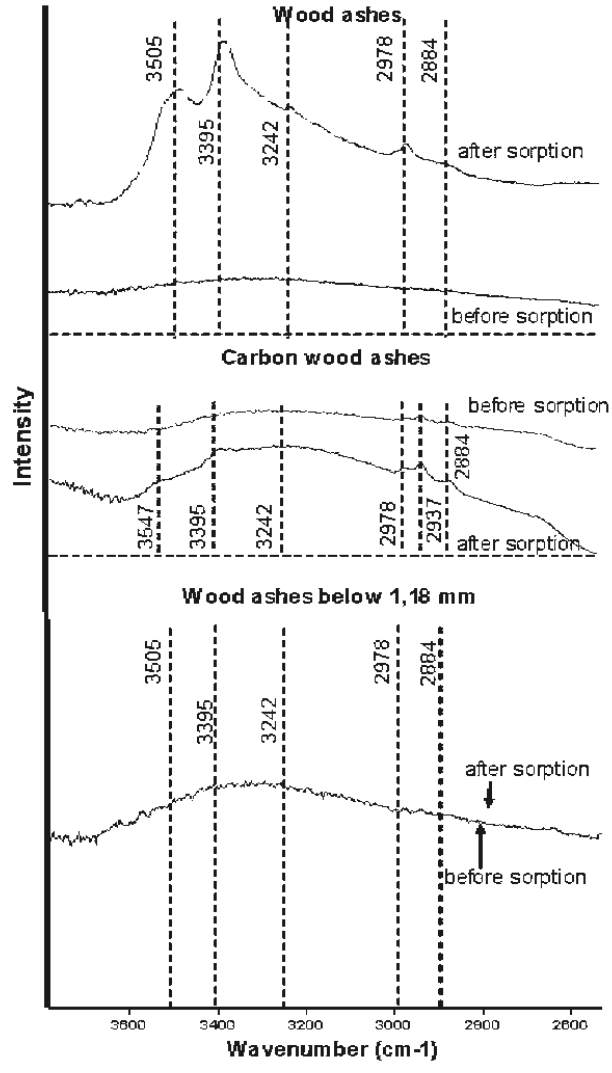

Figure 4.3 FTIR profiles before and after iron sorption tests on the three wood ash materials studied

4.4 Column treatment performances

4.4.1 Treatment with wood ashes after a sulphate reducing biofilter

Values of pH in the polishing column effluents rose up initially to approximately 11 for columns containing 100% (column #1), 70% (column #5) and 40% (column #4) of wood ashes. For wood ashes below 1.18 mm diameter (column #3) and carbon wood ashes (column #2), pH increased initially up to respectively 8-10 and 7-8 (Figure 4.4a). Then pH decreased

progressively with time to a value of approximately 6 for all columns except for column #2 which maintained a pH close to the one of the SRPB effluent (average pH of 3.5) at the end of the experimental period. The redox potential (Eh) value decreased between -100 mV and 100 mV for each column (Figure 4.4b). However, the values tended to increase with time; for column #2, Eh increased rapidly after 80 days to reach the value observed at the SRPB effluent column (approximately 526 mV).

Iron concentration decreased from approximately 2972 mg/L for the SRPB effluent to below 7 mg/L during the first 108 days for column #1 (see Figure 4.4c). Then, iron concentration increased rapidly to reach the initial SRPB effluent iron concentration. A similar trend was observed for the other columns but the time (called the breakthrough time) to reach the SRPB effluent value was different: 20, 53, 60 and 67 days (before this date, iron concentration was below 1 mg/L) for column #2, column #3, column #4, and column #5, respectively. The number of pore volume (see Figure 4.5) necessary to saturate sorption sites with iron for each column were estimated to 20, 14, 13, 9 and 6 days for column #1, column #5, column #4, column #3, and column #2, respectively. This result means that the treatment life of a polishing treatment step is affected by the type of material used.

Sulphate retention was effective before the breakthrough time with a decrease from values higher than 8640 mg/L on average for SRPB effluent to below 4869, 4200, 4422, 4920, 4416 mg/L for columns #1, #2, #3, #4 and #5 exit, respectively (see Figure 4.4d). The breakthrough time was approximately 108, 81, 74, 60, 53 days for column #1, column #5, column #3, column #4, and column #2 respectively. After this period, sulphate concentration increased to values similar to those observed at the SRPB effluent. A release of sulphates was also observed at the end of the experimental period since concentrations at the effluent of all polishing columns exceeded influent concentration.

Alkalinity (Figure 4.4e) was generated in each column with higher values for column containing carbon wood ashes (average value of 227 mg/L $CaCO_3$ for column #2, and between 53 and 80 for the four other columns). Acidity evolution (see Figure 4.4f) was related to iron concentration at the exit of the polishing columns. Indeed, acidity increased from low values (close to 0 mg/L $CaCO_3$) before the breakthrough time for iron to values

similar to SRPB effluent and even higher at the end of experiment (approximately 4000 mg/L $CaCO_3$).

A breakthrough can also be observed for the other metals present in the SRPB effluent (Mn, Ni, Pb and Zn). Metal retention was relatively effective before this breakthrough time in each column with concentrations below 10 mg/L for Mn, 0.1 mg/L for Ni, 0.3 mg/L for Pb, and 1 mg/L for Zn. The breakthrough for Ni, Pb and Zn was observed at 108 days for columns #1, 47 days for columns #2, 74 days for columns #3, between 67 and 74 days columns #4, and between 74 and 81 days for columns #5. The breakthrough happened for Mn at the same time as for Ni, Pb and Zn for columns #1, #2 and #5 (respectively 108, 47 and between 74 and 81 days). The breakthroughs for Mn in columns #3 and #4 were after 40 days and 47 days respectively. After the breakthrough, effluent metal concentrations of polishing columns reached the concentrations of the initial SRPB effluent.

Saturated hydraulic conductivity (k_{sat}) is a useful parameter to evaluate the long term performance of a filter and particularly to quantify the clogging phenomenon (Seki et al., 2006, Soleimani et al., 2009). Saturated hydraulic conductivity k_{sat} stayed relatively stable for each column at values between $5.0x10^{-3}$ cm/s and $3.1x10^{-2}$ cm/s. These values seemed to indicate that columns did not clog during the treatment. Moreover, high values of k_{sat} measured during the test showed that materials were relatively permeable (values similar to sandy materials, Chapuis, 2004).

Globally, the polishing column containing only wood ashes had the best treatment performance. Indeed, metal retention was effective during the longest period (compared to the other materials) while keeping a saturated hydraulic conductivity similar to those of wood ashes containing sand (said differently, adding sand to the studied wood ashes was not necessary to avoid clogging of the system). According to the literature (e.g. Benner et al., 1997), adding sand should prevent clogging and improve the saturated hydraulic conductivity. Moreover, adding sand did not affect the HRT (columns #1, #4 and #5 had similar HRT). However, sand affected the treatment performance, since column #1 was more efficient to remove iron than columns #4 and #5.

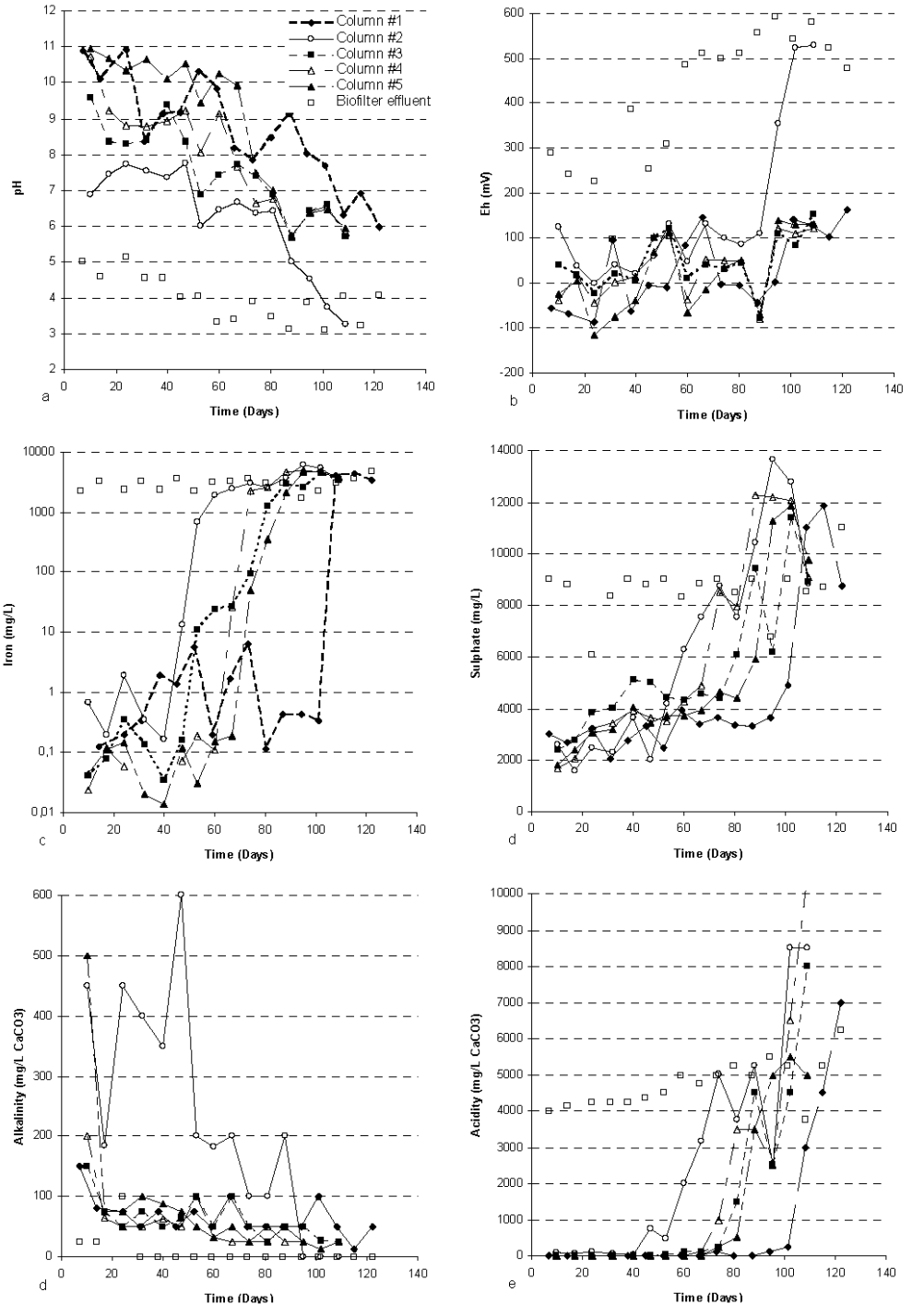

Figure 4.4 Polishing column chemical parameters (a) pH, b) Eh (mV), c) iron concentration (mg/L), d) sulphate concentration (mg/L), e) alkalinity (mg/L eq. CaCO3) and f) acidity (mg/L eq. CaCO3)) for all column tests studied

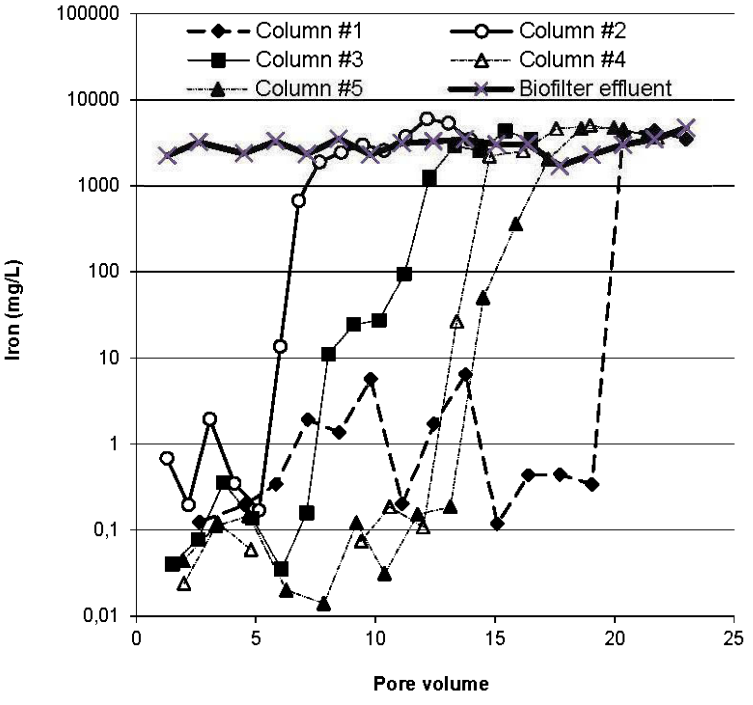

Figure 4.5 Iron concentration versus pore volume for all column tests

4.4.2 Metal retention mechanisms

According to the literature, metal retention in wood ash materials occurs in different ways. Aluminium removal mainly comes from the precipitation of amorphous hydroxides at pH higher than 5 (Vadapalli et al., 2008). Other metal removal, like Ni, Zn, Pb, Cr, Cd, could be attributed to precipitation, co-precipitation, sorption onto the surface of fly ashes and sorption onto amorphous Fe, Al hydroxides and oxohydroxide (Polat et al., 2002, Gitari et al., 2006, Gitari et al., 2008, Vadapalli et al., 2008, Gonzalez et al., 2009, Ahmaruzzaman, 2010). XRD analyses of samples taken from the five columns post-testing confirmed the precipitation of magnesite (magnesium carbonate) for column #3, goethite (iron oxyhydroxide) and diasopre (aluminum oxyhydroxide) for column #1.

In all columns, precipitation of a calcium sulphate occurred under the form of anhydrite. Indeed, literature shows that sulphates can be removed by formation of calcium sulphate like gypsum or ettringite in fly ash materials (Reynolds and Petrik, 2005, Vadapalli et al., 2008,

Madzivire et al., 2010), but also by sorption onto iron hydroxide and oxi-hydroxi-sulphates (Gitari et al., 2006, Vadapalli et al., 2008). Moreover, the XRD calcite line intensity was lower than initially, which is probably due to calcite dissolution during treatment. This observation is confirmed by the total calcium content in the post-testing samples, which decreased between 0.7 and 12.2% after treatment depending on the column (see Table 4.6). Iron content increased between 0.6 and 6.4%, and sulphide between 0.9 and 2.7% depending on the column (see Table 4.6). In addition, modelling using Vminteq at 10 days suggested a precipitation of carbonate (calcite, magnesite, dolomite, rhodochrosite) and hydroxides (geothite, lepidochrocite, ferrihydrite) in the five polishing columns. However, at the end of the experiment (109 days), only the precipitation of geothite, lepidochrocite, ferrihydrite, and siderite was possible according to the thermodynamic modeling (see Table 4.6).

Results about metal fractionation are summarized in Table 4.7. Iron, which was the most problematic metal to be treated in the tested AMD, was stabilized mainly in the reducible or bound to Fe-Mn oxides-hydroxides fractions (73.4-51.1%) confirming the possible precipitation of goethite observed in XRD analyses and predicted by geochemical modelling. The same observation is true for Mn, Pb and Zn. Oxides or hydroxides forms represented a relatively stable phase for these metals. The second iron retention mechanism in term of percentage was association with organic matter (15-28%).

The second observation pointed out by the sequential extraction procedure was that the soluble or exchangeable fraction (fraction 1) was not negligible for Mn (between 2.9 and 33.3%) and for Ni (8.3 to 71.8%). The consequence is that precaution should be taken to prevent remobilization of Ni and Mn. Moreover, the quantity of soluble or exchangeable phase was always higher for each metal when carbon wood ashes were used as treating material. Thus, use of carbon wood ash filter is not recommended because of the high mobility of most metals retained on this material, and because this material had the shortest metal retention efficiency period (see section 4.1.). Finally, SEM observations confirmed the retention of sulphate under the form of gypsum (superposition of Ca, S and O in Figure 4.6b for carbon wood ashes under the form of gypsum flakes). Iron was probably precipitated under hydroxides or oxyhydroxides since Fe and O were superimposed for wood ashes and carbon wood ashes (see Figure 4.6a and Figure 4.6b).

Table 4.6 Metal retention mechanisms

Characterization techniques	Observation in all columns	Metal retention and neutralization mechanisms
XRD	- magnesite in column #3 - geathite, diaspore in column #1 - anhydrite in all columns - decrease of calcite ray intensity	- formation of Mg carbonates - formation of Fe et Al oxy/hydroxides - formation of calcium sulphate - dissolution of Ca carbonate during column test
Digestion and metal content analysis by ICP-AES	- decrease of Ca content : between 0.7 to 12.2% - increased of Fe content: between 0.6 to 6.4% - increased of S content: between 0.9 to 2.7%	- dissolution of Ca mineral - retention of Fe - retention of S
Vminteq modeling	- at 10 days: precipitation of magnesite, calcite, dolomite, rodochrocite, geothite, lepidochrocite, ferrihydrite - at 109 days: precipitation of geothite, lepidochrocite, ferrihydrite, siderite	- formation of Fe oxy/hydroxides and carbonates (Mg, Mn, Fe, Ca) - formation of Fe oxy/hydroxides and Fe carbonates
Metal fractionation	- fraction 3 had for most of metals the highest content - non negligible fraction 1 for Ni and Mn - non negligible fraction 1 for carbon wood ashes for every metal	- formation of reducible or bound to Fe-Mn oxide-hydroxide phases - Ni and Mn were in part soluble or exchangeable - Every metal was soluble or exchangeable in high quantity for carbon wood ashes
SEM-EDS	- Fe and O were superimposed - Ca, S and O were superimposed	- formation of Fe oxy/hydroxides - formation of calcium sulphate (gypsum)

Table 4.7 Metal fractionation in the five polishing columns after dismantling using sequential extraction procedure (results are expressed in % except for the sum of metal in each fraction expressed in mg/g).

	Fraction 1	Fraction 2	Fraction 3	Fraction 4	Fraction 5	Sum (mg/g)
			Fe			
wood ashes	0,5	8,0	51,1	28,0	12,5	8,83E+01
carbon wood ashes	5,1	0,5	76,1	16,8	1,6	8,19E+01
wood ashes below 1,18 mm	0,0	2,5	58,7	23,4	15,2	6,38E+01
40% wood ashes + 60% sand	0,0	3,7	73,4	15,0	8,0	2,92E+01
70% wood ashes + 30% sand	0,0	5,5	61,5	21,6	11,4	5,60E+01
			Mn			
wood ashes	5,9	15,0	50,4	18,8	9,9	3,13E+00
carbon wood ashes	33,3	3,5	18,4	17,5	27,3	5,13E-01
wood ashes below 1,18 mm	2,9	18,3	58,8	12,2	7,8	3,52E+00
40% wood ashes + 60% sand	5,7	28,9	49,8	10,2	5,4	1,11E+00
70% wood ashes + 30% sand	4,5	18,9	51,0	14,1	11,5	2,30E+00
			Ni			
wood ashes	13,5	7,9	23,8	21,9	32,9	7,60E-02
carbon wood ashes	71,8	2,6	7,8	4,5	13,2	3,78E-02
wood ashes below 1,18 mm	20,4	8,1	33,1	17,9	20,5	4,89E-02
40% wood ashes + 60% sand	31,6	14,8	41,8	11,8	0,0	2,39E-02
70% wood ashes + 30% sand	8,3	5,2	45,8	11,3	29,3	8,53E-02
			Pb			
wood ashes	0,0	1,2	61,0	33,5	4,2	2,35E-01
carbon wood ashes	26,5	4,3	50,2	19,0	0,0	1,27E-01
wood ashes below 1,18 mm	0,0	1,3	65,0	29,6	4,1	2,45E-01
40% wood ashes + 60% sand	0,0	4,4	79,1	16,6	0,0	1,48E-01
70% wood ashes + 30% sand	0,0	1,8	65,3	33,0	0,0	1,12E-01
			Zn			
wood ashes	0,7	8,5	67,8	13,1	9,9	7,54E-01
carbon wood ashes	16,8	7,9	58,2	17,0	0,0	1,85E-01
wood ashes below 1,18 mm	0,7	10,0	65,3	14,6	9,4	6,89E-01
40% wood ashes + 60% sand	1,5	20,9	68,2	9,4	0,0	2,13E-01
70% wood ashes + 30% sand	0,6	13,0	73,0	10,7	2,7	5,46E-01

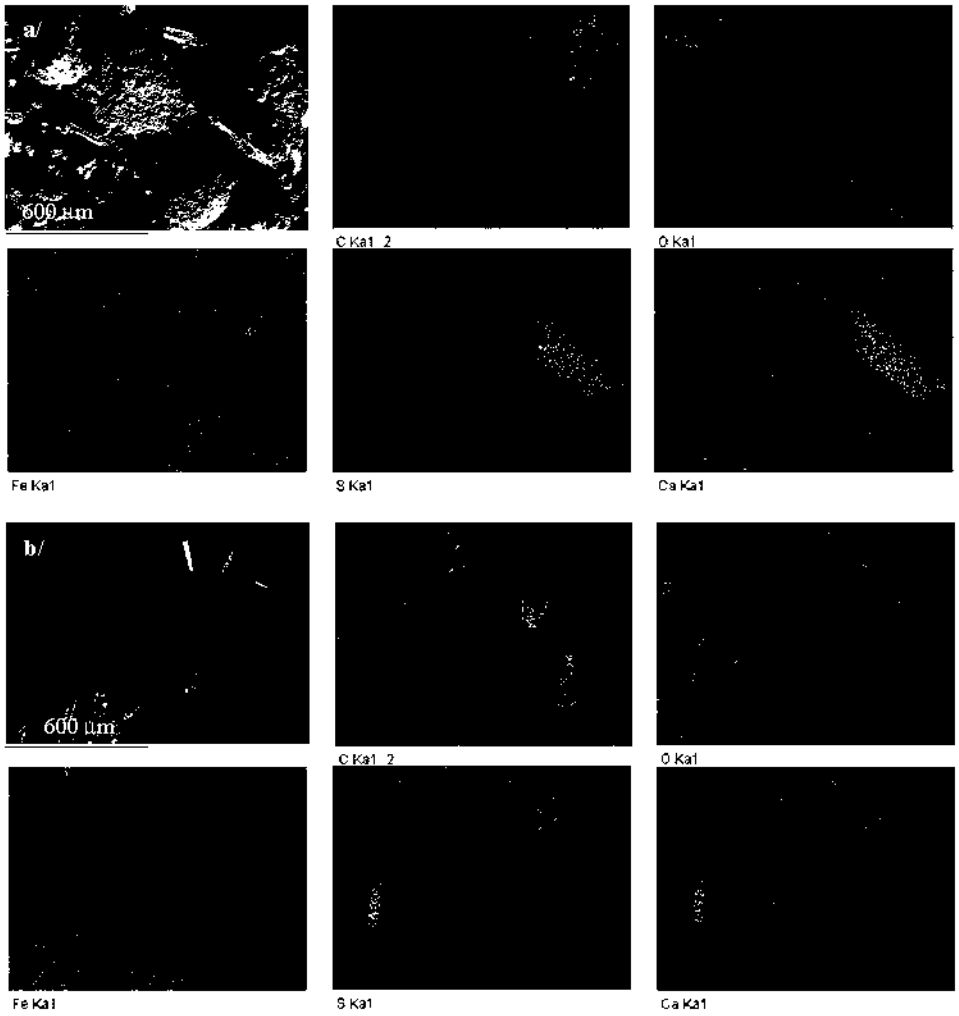

Figure 4.6 SEM images and elemental maps: a) wood ashes and b) carbon wood ashes.

4.5 Conclusion

Treatment of high iron concentrated AMD (4000 mg/L of iron) by sulphate reducing passive biofilter (SRPB) is generally limited (Genty et al., 2011c). Wood ash from cogeneration plant is a low cost available material and is known for its metal retention properties and neutralization capacity. Iron sorption isotherm corresponds to the Freundlich model for wood ashes, carbon wood ashes and fine wood ashes (below 1.18 mm diameter) at pH 3 and 6. However, the limiting steps of iron sorption depended on material and pH. A pseudo-second

order reaction at the surface of material, or an internal and external diffusion of iron at the surface of the grain could explain the sorption kinetic.

In this study, polishing treatment systems containing different wood ashes mixtures (wood ashes, 70% wood ashes + 30% sand, 40% wood ashes + 60% sand, wood ashes below 1.18 mm and carbon wood ashes) were evaluated for a contaminated drainage effluent coming from a SRPB, using five columns. Results showed that acidity can be neutralized and the column which contained only wood ashes had the longest life time. This lifetime was estimated at more than 100 days (corresponding to 20 pore volume). During this period, iron concentration decreased form an average of 3200 mg/L and did not exceed 10 mg/L.

Iron (the most problematic element to be treated in the studied AMD) removal occurred mainly due to hydroxides or oxi-hydroxides precipitation. Indeed, SEM analyses showed a correlation between Fe and O elements on material surface and XRD analyses of post testing material indicated the formation of goethite precipitates in the material. Finally, sequential fractionation of metal highlighted that iron was mainly contained (73.4-51.1%) in a reducible or bound to Fe-Mn oxides-hydroxides fraction. Sorption could also play an important treatment role since fraction 4 of sequential fractionation (bound to organic matter phase) was not negligible for each material. The second important contaminant retained in columns was sulphate. Indeed, concentration of AMD sulphate was decreased (removal percentage between 43 and 51% depending on the column) mainly by precipitation of calcium sulphate phases (gypsum or anhydrite). Because the wood ash filter system was efficient only for approximately 20 pore volume to treat an effluent with 3200 mg/L of iron on average, the system would have to be changed periodically to maintain an acceptable water quality at the exit of the system. Finally, this study showed that wood ashes could be a serious option to substitute traditional materials (like limestone, peat) in passive systems because of their neutralizing potential and metal removal properties.

Acknowledgements

This research was supported by the Canada Research Chair on Restoration of Abandoned Mine Sites and the Natural Sciences and Engineering Research Council of Canada (NSERC) through the Industrial NSERC École Polytechnique - UQAT Chair in Environment and Mine

Wastes Management. The authors acknowledge gratefully the industrial and governmental partners of the industrial Chair for the funding of this study and Brian Coghlan from Wood Ash Industries Inc for graciously supplying wood ashes.

References

Ahmaruzzaman, M., 2010. A review on the utilization of fly ash. Prog. Eng. Combust. Sci. 36, 327-363.

Aitcin, J.C., Jolicoeur, G., Mercier, M., 1983. Technologie des granulats, Les éditions Le Griffon d'Argile inc., Sainte-Foy.

Akcil, A., Koldas, S., 2005. Acid mine drainage: causes, treatment and case studies, J. Clean. Prod. 14, 1139-1145.

Al-Degs, Y., El-Barghouthi, M., Issa, A., Khraisheh, M., Walker, G., 2006. Sorption of Zn(II), Pb(II), and Co(II) using natural sorbents: Equilibrium and kinetic studies. Wat. Res. 40, 45-2658.

ASTM, 1995a. Standard test method for pH of soils, in: Annual book of ASTM standards. (vol. 04.08, section D4972-95a), Washington, DC, pp. 27–28.

ASTM, 1995b. Standard test method for permeability of granular soils, in: Annual book of ASTM Standards (vol. 04.08., section D 2434 – 68), Washington, DC.

Aubertin, M., Bussière, B., Bernier, L., 2002. Environnement et gestion des rejets miniers. Edition Presses Internationales Polytechnique, Montréal.

Benner, S., Blowes, D., Ptacek, C., 1997. A full scale Porous reactive wall for prevention of acid mine drainage, in: Proceeding of FALL 1997 GWMR, pp 99-107.

Blais, J.F., Dufresne, S., Mercier, G., 1999. État du développement technologique en matière d'enlèvement des métaux des effluents industriels. Revue des sciences de l'eau 12, 687-711.

Blowes, D.W., Ptacek, C.J., 1994. System for treating contaminated groundwater, in: U.S. Patent 5,362,394, filed March 3, 1992, issued Nov. 8, 1994.

Champagne, P., Van Geel, P., Parker, W. 2005. A bench-scale assessment of a combined passive system to reduce concentrations of metals and sulphate in acid mine drainage. Mine Wat. Environ. 24, 124-133.

Chapuis, R.P., 2004. Predicting the saturated hydraulic conductivity of sand and gravel using effective diameter and void ratio. Can. Geotech. J. 41, 787-795.

Cheung, C.W., Porler, J.F., McKay, G., 2000. Elovich equation and modified second-order equations for sorption of cadmium ions onto bone char. J. Chem. Technol. Biotechnol. 75, 963-970.

Costa, M. C., Martins, M., Jesus, C., Duarte, J. C., 2008. Treatment of acid mine drainage by sulphate-reducing bacteria using low cost matrices. Wat. Air Soil Pollut. 189, 149-162.

Cravotta, C. A., Trahan, M. K., 1999. Limestone drains to increase pH and remove dissolved metals from acidic mine drainage. Ap. Geochem. 14, 581-606

Evangelou, V.P., Zhang, Y.L., 1995. A review: pyrite oxidation mechanisms and acid mine drainage prevention. Environ. Sci. Tech. 25, 141-199.

Deng, S., Ting, Y.P., 2005. Characterization of PEI-modified biomass and biosorption of Cu(II), Pb(II) and Ni(II). Wat. Res. 39, 2167-2177.

García-Mendieta, A., Solache-Ríos, M., Olguin, M., 2009. Evaluation of the sorption properties of a Mexican clinoptilolite-rich tuff for iron, manganese and iron–manganese systems. Microporous and Mesoporous Mater.118, 489-495.

Genty, T., Bussière, B., Potvin, R., Benzaazoua, M., Zagury, G.J., 2011a. Dissolution of different limestone in highly contaminated acid mine Drainage: Application to anoxic limestone drains. Submitted to Environ. Earth Sci. in November 2010.

Genty, T., Bussière, B., Benzaazoua, M., Zagury, G.J., 2011b. Treatment of acid mine drainage with high iron concentration using sulphate reducing passive bioreactor: I. Mixtures characterization. Submitted to Ap. Geochem.

Genty, T., Bussière, B., Benzaazoua, M., Zagury, G.J., 2011c. Treatment of acid mine drainage with high iron concentration using sulphate reducing passive bioreactor: II. Column tests. Submitted to Ap. Geochem.

Gitari, W., Petrik, L., Etchebers, O., Key, D., Iwuoha, E., Okujeni, C., 2006. Treatment of acid mine drainage with fly ash: removal of major contaminants and trace elements. J. Envir. Sci. 41, 1729-1747.

Gitari, W., Petrik, L., Etchebers, O., Key, D., Iwuoha, E., Okujeni, C., 2008. Passive neutralisation of acid mine drainage by fly ash and its derivatives: A column leaching study. Fuel 87, 1637-1650.

Gonzalez, A., Navia, R., Moreno, N., 2009. Fly ashes from coal and petroleum coke combustion: current and innovative potential applications. Waste Manag. Res. 27, 976-987.

Gupta, B., Curran, M., Hasan, S., Ghosh, T.K., 2009. Adsorption characteristics of Cu and Ni on Irish peat moss. J. Environ. Manag. 90, 954-960.

Hedin, R.S., Nairn, R.W., Kleinmann, R.L.P., 1994. Passive treatment of coal mine drainage, US Bureau of Mines, Pittsburgh, PA, 35 pp.

Ho, Y.S., Ng, J.C.Y., McKay, G., 2000. Kinetics of pollutant sorption by biosorbent: reviews. Clear Wat. Sep. Purif. Methods, 29, 189-232.

Jha, V., Matsuda, M., Miyake, M., 2008. Sorption properties of the activated carbon-zeolite composite prepared from coal fly ash for Ni2+, Cu2+, Cd2+ and Pb2+. J. Hazard. Mater. 160, 148-153.

Johnson, J.S., Westmoreland, C.G., Sweeton, F.H., Kraus, K.A., Hagaman, E.W., 1986. Modification of cation exchange properties of activated carbon by treatment with nitric acid, J. Chromatography. 345, 231-248.

Johnson, D.B., Hallberg, K.B., 2005. Acid mine drainage remediation options: a review, Sci. Total Environ. 338, 3-14.

Karathanasis, A.D., Edwards, J.D., Barton, C.D., 2010. Manganese and sulphate removal from a synthetic mine drainage through pilot scale bioreactor batch experiments. Mine Wat. Environ. 29, 144-153.

Kirby, C.S., Cravotta, C.A., 2005. Net alkalinity and net acidity: Theoretical considerations. Ap. Geochem. 20, 1920-1964.

Kleinmann, R.L.P., Crerar, D.A., Pacelli, R.R., 1981. Biogeochemistry of acid mine drainage and a method to control acid formation. Mining Eng. 300-304.

KTH., 2010. Visual MINTEQ A free equilibrium speciation model, version 3.0, beta version. http://www.lwr.kth.se/English/OurSoftware/vminteq/index.html. Accessed 15 September 2010

Limousin, G., Gaudet, J.P., Charlet, L., Szenknect, S., Barthes, V., Krimissa, M., 2007. Sorption isotherms: A review on physical bases, modeling and measurement. Ap. Geochem. 22, 249-275.

Madzivire, G., Petrik, L., Gitari, W., Ojumu, T., Balfour, G., 2010 Application of coal fly ash to circum-neutral mine waters for the removal of sulphates as gypsum and ettringite, Miner. Eng. 23, 252-257.

McCarthy, D. F., 1977. Essentials of soil mechanics and foundations. Reston Publishing, Reston.

Neculita, C.M., Zagury, G.J., Bussiere, B., 2007. Passive treatment of AMD in bioreactors using SRB: critical review and research needs. Environ. Qual. 36, 1-16.

Neculita, C.M., Zagury, G.J., Bussiere, B., 2008a. Effectiveness of sulphate-reducing passive bioreactors for treating highly contaminated acid mine drainage: I. Effect of hydraulic retention time. Ap. Geochem. 23, 3442-3451.

Neculita, C.M., Zagury, G.J., Bussiere, B., 2008b. Effectiveness of sulphate-reducing passive bioreactors for treating highly contaminated acid mine drainage: II. Metal removal mechanisms and potential mobility. Ap. Geochem. 23, 3545-3560.

Nurchi, V.M., Crisponi, G., Villaesca, I., 2010. Chemical equilibria in wastewaters during toxic metal ion removal by agricultural biomass. Coord. Chem. Rev. 254, 2181-2192.

Ouellet, S., Bussière, B., Mbonimpa, M., Benzaazoua, M., Aubertin, M., 2006. Reactivity and mineralogical evolution of an underground mine sulphidic cemented paste backfill. Miner. Eng.19, 407-419.

Polat, M., Guler, E., Akar, G., Mordogan, H., Ipekoglu, U., Cohen, H., 2002. Neutralization of acid mine drainage by Turkish lignitic fly ashes; role of organic

additives in the fixation of toxic elements. J. Chem Technol. Biotechnol. 77, 372-376.

Potts, P.J., 1987. A Handbook of Silicate Rock Analysis, Blakie & Son Ltd.

Potvin, R. 2009. Évaluation à différentes échelles de la performance de systèmes de traitement passif pour des effluents fortement contaminés par le drainage minier acide. PhD. Dissertation, Chaire industrielle CRSNG Polytechnique – UQAT, Rouyn-Noranda, Canada, pp 1-365.

Prasad, P.S.R., Prasad, S., Krishna, V., Babu, E.V.S.S.K., Sreedhar, B., Ramana, S., 2006. In situ FTIR study on the dehydration of natural goethite, J. Asian. Earth. Sci. 27, 503-511.

Reynolds, K., Petrik, L., 2005 The use of fly ash for the control and treatment of acid mine drainage, in: Proceedings of world of coal ash symposium 2005, Lexington, USA.

Seki, K., Thullner, M., Hanada, J., Miyazaki, T., 2006. Moderate bioclogging leading to preferential flow paths in biobarriers. Gr. Wat. Monitor. Remediat. 26, 68-76.

Skousen, J.G., Ziemkiewicz, P.F., 2005. Performance of 116 Passive Treatment Systems for Acid Mine Drainage, in: ASMR, 3134 Montavesta Rd. Publication, Proceeding of the National Meeting of the American Society of Mining and Reclamation, Breckenridge, Lexington.

Soleimani, S., Van Geel, P., Isgor, B., Mostafa, M., 2009. Modeling of biological clogging in unsaturated porous media. J. Contam. Hydrol. 106, 39-50.

Twardowska, I., Kyziol, J., 2008. Sorption of metals onto natural organic matter as a function of complexation and adsorbent–adsorbate contact mode. Environ. Int. 28, 783-791.

Vadapalli, K., Klink, M., Etchebers, O., Petrik, L., Gitari, W., White, R., Key, D., Iwuoha E., 2008. Neutralization of acid mine drainage using fly ash, and strength development of the resulting solid residues. South African J. Sci. 104, 317-322.

Zagury, G.J., Colombano, S. M., Narasiah, K.S., Ballivy, G., 1997. Stabilisation de résidus acides miniers par des résidus alcalins d'usines de pâtes et papier. Environ. Technol. 18, 959-973.

Zagury, J.G., Oudjehani, K., Deschênes, L., 2004. Characterization and availability of cyanide in solid mine tailings from gold extraction plants. Sci. Total Environ. 320, 211-224.

CHAPITRE 5

LABORATORY MULTI-STEP TREATMENT OF ACID MINE DRAINAGE WITH HIGH IRON CONCENTRATION: COLUMN AND MEDIUM SIZE REACTOR TESTS

Ce chapitre ce présente sous la forme d'un article. Toutefois, ce dermier n'a pas encore été soumis lors du dépôt de la thèse.

Auteurs

Thomas Genty[1], Bruno Bussière[1], Mostafa Benzaazoua[2], Gérald J. Zagury[3]

[1]Industrial Chair CRSNG Polytechnique-UQAT: Environment and mining wastes management, University of Québec in Abitibi-Témiscamingue, Rouyn-Noranda, Québec, Canada

[2]Laboratoire de Génie Civil et d'Ingénierie Environnementale, INSA de Lyon, Villeurbanne, France

[3]Industrial Chair CRSNG Polytechnique-UQAT : Environment and mining wastes management, École Polytechnique, Québec, Canada

Abstract

A multi-step treatment of an acid mine drainage with an elevated iron concentration (pH = 3; between 4000 and 2000 mg/L) was tested during one year in 3 columns in series (total of 33 L) and in a medium size reactor (2640 L). The two multi-step systems include three separate treatment sections. The first one consisted in a sulphate reducing passive bioreactor (SRPB) with 50% of a SRPB reactive mixture (manure, sawdust, maple chips, compost, urea, sediment, sand) and 50% of calcite. Its aim was to neutralize acidity and to remove a portion of the metals. The second section contained wood ashes and acted as a neutralizer and an iron

filter (iron retention by sorption and precipitation). The last section was a polishing SRPB intended to remove the residual metals. The results showed that pH was increased to 6 on average in both columns and medium size reactor, and that redox potential (Eh) decreased from 550 mV to -100 mV in the second SRPB of the reactor and to 135 mV at the exit of columns. Iron, which was the most problematic element in the tested AMD, was reduced to approximately 100 mg/L in the medium size reactor, while it decreased to an average of 712 mg/L in the multi-step column treatment. The key element of the multi-step treatment system is the capacity of the wood ash filter to retain iron. Once the filter is saturated, the performance of the second SRPB can be affected. The water quality of the system reached the Canadian mining effluent standards for other metals (such as Al, Cd, Cr, Ni, Pb, and Zn).

Keywords: acid mine drainage, sulphate-reducing passive bioreactor (SRPB), wood ashes, column tests, medium size reactor, multi-step treatment.

5.1 Introduction

Acid mine drainage (AMD) is a major water pollution problem for the mining industry (Aubertin and al., 2002, El-Gharmali et al., 2004, Gomes and Favas, 2006). AMD results from the oxidation of sulphide minerals, which produces acidity and releases high concentrations of dissolved metals (e.g. Kleinmann and al., 1981; Blowes and Ptacek, 1994; Evangelou and Zhang, 1995; Perkins and al., 1995; Morin and Hutt, 1997). Passive treatment of AMD for closed mines is a more adapted solution than active treatment because of the low investment and maintenance costs (Gazea and al., 1995, Morin and Hutt, 1997, Skousen and Ziemkiewicz, 2005). However, passive treatment systems are often performance and time-limited for highly contaminated AMDs (e.g. Hedin et al., 1994, Trumm, 2006, Potvin, 2009). Recent studies showed the limits of sulphate reducing passive bioreactors (SRPBs) for AMDs with high iron concentrations (Neculita et al., 2008a, Potvin, 2009, Genty et al., 2011a, Genty et al., 2011c). Indeed, metal hydroxides can be formed within the SRPB leading to a reduction of sulphate reducing bacteria (SRB) activity and a modification of the hydraulic behavior of the system (Neculita et al., 2008a). In addition, remaining iron at the output of SRPB can cause effluent toxicity (Neculita et al., 2008c) and re-acidifcation of the effluent due to iron hydroxides precipitation (Genty et al., 2011c). Hence, it may be necessary to

combine several methods to treat highly contaminated AMD in order to reach environmental regulation criteria at the effluent.

The use of combined treatment processes, also called multi-step treatment, showed very good efficiency for AMD containing relatively low iron concentrations. Champagne et al. (2005) used a series of passive systems to treat an AMD with an iron concentration of 189 mg/L, a pH of 3.2 and sulphate concentration of 3140 mg/L. The treatment consisted of an aeration stage and settling pond for iron pre-treatment (oxidation of ferrous iron into ferric iron followed by precipitation of ferric hydroxides), a filtration step on peat (sorption of metals and reduction of the redox potential in order to provide anoxic conditions), a biofiltration step with a SRPB (to increase alkalinity, decrease metals), and finally a polishing step using an anoxic limestone drain that increases the alkalinity (Rouhani et al., 2003, Champagne et al., 2005). The performance of metal retention in the system reached 99% for most of metals except Cd (Champagne et al., 2005). A second study by Figueroa et al. (2007) presents a system composed of an oxic limestone drain followed by a SRPB to treat an AMD with an iron concentration of 40 mg/L. The oxic limestone drain allows a good treatment of iron by precipitation and increases the pH of the effluent to ensure optimal conditions for SRPB. The SRPB can retain adequately metals by sulphate reduction and sulphide metal precipitation. The use of multi-step treatment should be one of the solutions to treat highly contaminated AMD since one characteristic of AMD (one metal or pH, for example) of the pollution could be treated in each section.

Preliminary works on iron-concentrated AMD (approximately 4000 mg/L) showed that multistep treatment with SRPB and wood ash filters were a promising solution (e.g. Genty et al., 2011d). Before designing a field size treatment system, it was decided to evaluate the treatment performance at the bench-scale and the laboratory pilot-scale.

To sum up, literature showed that the treatment of AMD with high iron concentration is a challenge and that the multi-step treatment is probably the most appropriate option for this type of AMD. The main objective of this study is to test in columns and in medium size reactor (approximately 2000L) a multi-step treatment composed of an SRPB, followed by a wood ash filter and another SRPB, for an AMD with an iron concentration between 2000 and

4000 mg/L. Specific objectives are to evaluate the scale effect on the treatment efficiency and metal retention mechanisms in the medium size test.

5.2 Materials and methods

5.2.1 Synthetic acid mine drainage quality

A synthetic acid mine drainage was produced with different salts dissolved in tap water (see Table 5.1) to feed the columns and medium size test. AMD was characterized by a high iron and sulphate concentrations (respectively 4000 and 9000 mg/L, iron precipitation was negligible because its concentration stayed relatively stable), typical of base metal mine sites AMD (Aubertin et al., 2002). However[10], to take into consideration the variability of AMD concentration, a second AMD (called AMD light) was prepared (Potvin, 2009). This AMD light was characterized by lower iron and sulphate concentrations in comparison with the first AMD (respectively 2000 and 5000 mg/L).

Table 5.1 Targeted concentrations (in mg/L, except pH) of highly contaminated synthetic AMDs

Elements	Salt used	AMD	AMD light
Al	$Al_2(SO_4)_3,18H_2O$	7	0.5
Cd	$CdSO_4,8H_2O$	0,5	0
Cr	$CrK(SO_4)_2,12H_2O$	1	0
Fe	$FeSO_4,7H2O$	4000	2000
Mg	$MgSO4,7H_2O$	10	9.5
Mn	$MnSO_4,H_2O$	33	6
Ni	$NiSO_4,6H_2O$	2	0.5
Pb	$Pb(NO_3)_2$	0,5	0,1
SO_4^{2-}	$Na_2SO_4,10H_2O$	9000	5000
Zn	$ZnSO_4,7H_2O$	40	40
pH	HCl 1N	3	3

[10] Entre 2008 et 2010, les concentrations en métaux du DMA du site Lorraine, sur lequel est basé cette étude, ont changé. En effet, les concentrations en métaux ont diminué grâce au système de prévention de la formation du DMA installé sur le site Lorriane. Il s'agit d'une couverture multicouhe limitant la diffusion de l'oxygène vers les résidus. De façon à mieux représenter l'évolution des concentrations du terrain, deux DMA ont alors été traités en laboratoire.

5.2.2 Column experiments description

5.2.2.1 Column test description

After preliminary laboratory tests[11] (data not shown), it was decided that the AMD multi-step treatment would be performed into three columns connected in series. The first column (SRPB 1; 14 cm diameter, 70 cm height, 10.7 L), contained the SRPB mixture #1 as described in Table 5.2. The second column (wood ash filter; 30 cm diameter, 25 cm height, 12.8 L), contained only wood ashes. The 3rd column (SRPB 2; 14 cm diameter, 70 cm height, 10.7 L) contained the SRPB mixture #2 as described in Table 5.2. More details on sulphate reducing SRPB reactive mixture and wood ash characterization and selection were detailed elsewhere in Genty et al. (2011a), Genty et al. (2011b) and Genty et al. (2011c). Briefly, SRPB mixture #1 contained 50% of calcite to ensure good pH neutralization; the other components are sawdust, wood chips, chicken manure, compost, sediments and urea. SRPB mixture #2 contained mainly organic materials (sawdust, wood chips, manure and compost) to support an optimum bacterial activity. Sand (20%) is used in mixture #2 as a structural agent for bacterial attachment. Finally, the high carbon content (36%) in wood ashes and its high specific surface area (46 m^2/g using the BET method) give to the material good sorption capacities (Genty et al., 2011c).

[11] Différents matériaux et procédés ont été testés pour retenir du fer : des carbonates suivis d'une aération (Appendice B), de la tourbe (Appendice C), des cendres de bois. Finalement, seuls les BPSR et les cendres ont été retenus pour être utilisés dans un traitement en plusieurs étapes d'un DMA fortement chargé en fer.

Table 5.2 Composition of each column (composition given in dry mass %)

Mixture	SRPB 1	Wood ash filter	SRPB 2
Celullosic wastes			
Maple chips	5		10
Sawdust	10		20
Organic wastes			
Chicken manure	5		10
Compost	10		20
Inoculum			
Sediment	8		15
Inert structural agent			
Sand	10		20
Nutriment (Nitrogen) Urea	2		3
Neutralizing agent			
Calcium carbonate			2
Calcite fine	50		
Wood ashes		100	

5.2.2.1 Column test operating conditions

After materials placement, the SRPB columns were saturated with Postgate B nutrient medium (Postgate, 1984). The Postgate B medium was prepared in distilled water and had the following composition: 3.5 g/L sodium lactate; 2.0 g/L $MgSO_4,7H_2O$; 1.0 g/L NH_4Cl; 1.27 g/L $CaSO_4,2H_2O$; 1.0 g/L yeast extract; 0.5 g/L KH_2PO_4; 0.5 g/L $FeSO_4,7H_2O$; 0.1 g/L thioglycolic acid, and 0.1 g/L ascorbic acid. After addition of the Postgate B medium, the columns were incubated at room temperature (approximately 22°C on average) for four weeks before starting their operation (acclimation period). The AMD treatment began when the Eh decreased below -150mV (Neculita and al., 2008b). Columns were fed from the bottom with AMD (see Figure 5.1) to allow constant anoxic conditions. A perforated plastic plate covered with a geotextile was placed at the bottom to uniformly feed the column. The flow was controlled by a peristaltic pump (0.6 mL/min). Considering an estimated porosity of 0.41, 0.60, and 0.45 for SRPB 1, wood ash filter, and SRPB 2, respectively, the estimated hydraulic retention times (HRT) were respectively 5.1 days, 8.9 days, and 5.6 days in the three columns. Reactors were covered with cardboard to simulate field conditions and to prevent the growth of phototrophic bacteria.

Columns were not duplicated since a recent study showed that if columns were set-up and operated with a similar protocol as in this study, the test is repeatable (Genty et al., 2011e). Measurements of pH, Eh, sulphate, acidity, alkalinity, metals concentrations and saturated hydraulic conductivity were performed during the experiment. Sulphate reducing bacteria (SRB) enumeration was made regularly on the liquid at the exit of the columns using the Most Probable Number technique (ASTM, 1990, Beaulieu, 2001) to evaluate treatment performance (Neculita et al., 2008a). Saturated hydraulic conductivity (k_{sat}) was evaluated monthly on the two biofilter columns during the operation using the falling head method (adapted from ASTM, 1995).

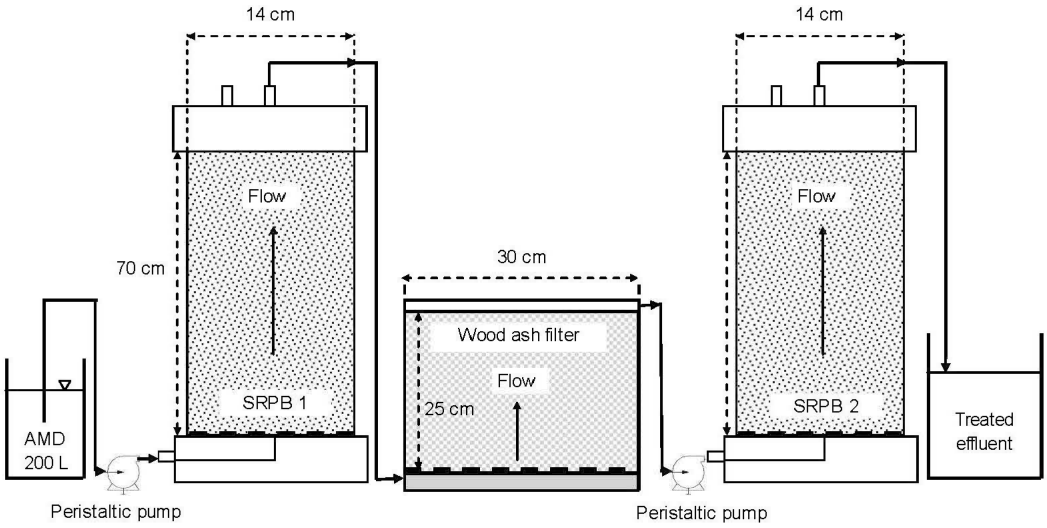

Figure 5.1 Multi-step column test configuration (not to scale)

5.2.3 Medium size test experiment description

5.2.3.1 Medium size test description

AMD multi-step treatment performance was also evaluated in a 2640 L reactor (2.46 m length and 1.6 m width) with a trapezoidal section (0.5 m at the bottom and 1 m height) covered by a lid with the same dimensions. A schematic representation of the reactor is given in Figure 5.2 (see Potvin, 2009 for more details on the reactor design). The reactor was divided into five sections (with perforated plates). The first one, with a capacity of 368 L (35

cm length), receives the AMD to treat and acts as a settling pond to remove precipitated particles. The second section is 60 cm in length (660 L) and was filled with 440 kg of SRPB mixture #1. The role of this section is to neutralize acidity and to remove metal and part of the sulphates. The next portion of the reactor is 60 cm in length (660 L), contained 360 kg of wood ashes and acts as an iron filter (iron retention by sorption and precipitation). Finally, the last treating section (814 L and 74 cm length) was filled with 380 kg of SRPB mixture #2, and acts as a polishing treatment to remove the remaining metals and sulphates. After this second SRPB, the water flows through an empty 154 L section (14 cm length) used to ensure that the exit of the model does not clogged.

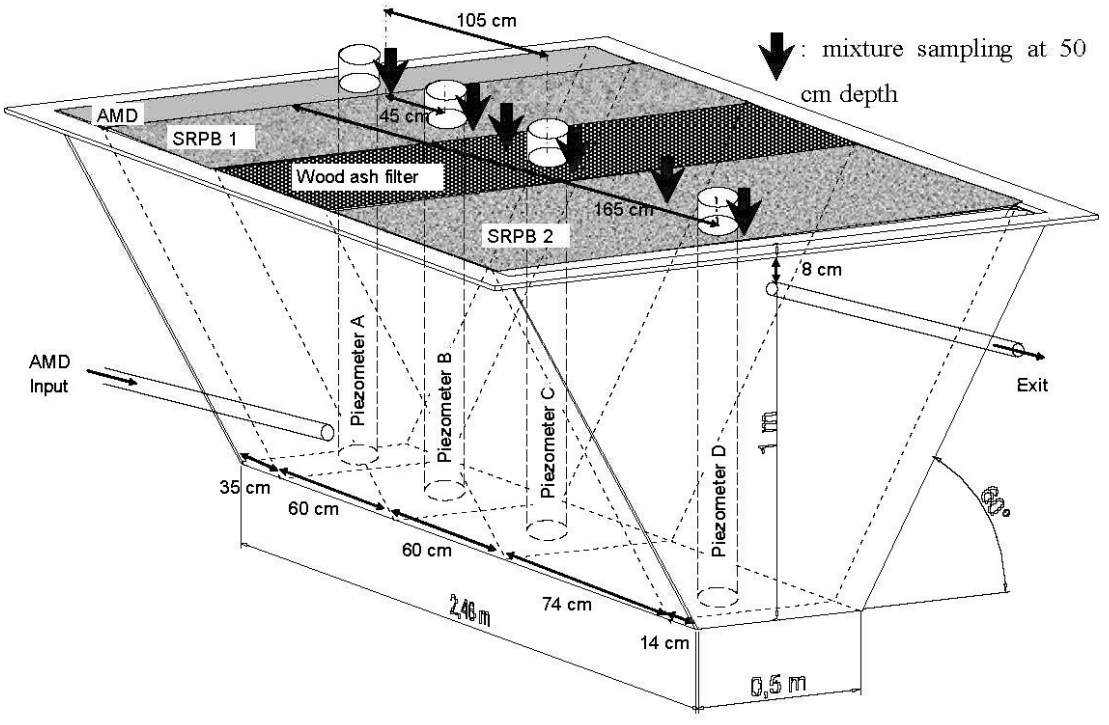

Figure 5.2 Medium size multi-step treatment set-up

5.2.3.2 Medium size test operating conditions

The reactor was fed by a peristaltic pump at 50 mL/min. The reactor was incubated before starting the AMD treatment with Postgate B medium (same manner as the one described in section 2.2.) to provide reducing conditions. The Postgate B volume used to saturate the model was also used to calculate the porosity of the three treatment sections, and the porosity

was estimated to be 0.41 on average for the three treatment sections. Considering this porosity value, the flow and the volume of each section, HRT can be estimated for each section. The HRT was 19 days in the reactor, which corresponds to an operational HRT in the three treatment sections of 12 days (which is high but still in agreement with typical values for passive systems, Neculita et al., 2008a). Considering the section volume, the flow rate and the porosity of 0.41, HRTs of each section were 5.1, 3.7, 3.7, 4.6, and 2.1 days respectively for the first section containing AMD, the first SRPB with SRPB mixture #1, the wood ash filter, the SRPB with SRPB mixture #2, and the last section at the exit.

As mentioned earlier, two AMD were used to take into account the variability of in situ AMD quality. AMD was treated during the first 150 days (see Table 5.1), and AMD light for the rest of the experiment.

The system was instrumented to evaluate the treatment performance. First, an electromagnetic Promag 33A flow meter (from Endress & Hauser) was used to control the flow. The system was equipped with four piezometers allowing water sampling for chemical analysis. Piezometer A was installed 15 cm from the input of the reactor and its samples were representative of the initial AMD quality. The second piezometer B was placed 45 cm from the beginning of the treatment section and allowed analysing water at the end of the first SRPB treatment. The third piezometer C (105 cm from the beginning of the treatment section) allowed analysing pore water quality after the wood ash treatment. Finally, piezometer D, located 165 cm from the beginning of the treatment section, allowed sampling and analysing pore water at the end of the SRPB treatment (with SRPB mixture #2). Each piezometer was equipped with a pH sensor (GLI PC1R1A with temperature compensation, precision of +/-0.1) and a redox potential sensor (GLIRC1R5N, precision of +/-20 mV) to measure these parameters online. Water sampling was performed in the initial AMD and at the exit of the reactor every week, and in the four piezometers every two weeks. Measurements of pH, redox potential (Eh), acidity, alkalinity, metal concentrations, and sulphates were performed on these samples. Sulphate reducing bacteria were measured every two months and dissolved organic carbon was measured every five weeks. The ratio DOC/SO_4 was also determined to help to understand SRPB treatment performance. Analyses

were performed immediately after sampling to prevent change of pH-redox parameters, because sampling was carried out in an aerobic environment.

5.2.3.3 Medium size test hydraulic investigation

To evaluate the hydraulic properties of the reactor, saturated hydraulic conductivity was determined using Darcy's law as presented in equation [5-1].

[5-1] $$k_{sat} = \frac{Q}{A.\frac{dH}{dL}}$$

where k_{sat} is the saturated hydraulic conductivity (m/s), Q is the flow rate (m^3/s), A is the cross section of the reactor (m^2), and $\frac{dH}{dL}$ is the hydraulic gradient (measured between the first and the fourth piezometer, in m/m).

A tracer test was also carried out to evaluate flow properties in the reactor (at 200 days of operation). The test was performed with NaCl and by measuring chloride concentration. Other sodium halide (NaBr for exemple) had been already used for tracer tests in passive system (e.g. Kruse et al., 2009).

Chloride concentration was determined by a Metrohm 881 compact IC pro ions chromatograph (with chemical and CO_2 suppressor, column Metrosep A supp 5-150/4.0, elluent: 3.2 mmol Na_2CO_3 and 1 mmol $NaHCO_3$, flow rate: 0.7 mL/min, 25°C). The test was a step injection, and consisted in increasing and maintaining the chloride concentration in AMD near 0.6 g/L during the tested period (3 weeks). Then, the results were analysed using the theory of residence time distribution (e.g. Genty et al., 2011c).

5.2.4 Chemical and biological method for water quality evaluation

The pH of sampled solutions was determined with an Orion Triode sensor coupled with a Benchtop pH/ISE Meter Orion model 920 (relative precision +/- 0.01 pH), and the Eh (redox potential, values were corrected relative to the standard hydrogen electrode) was measured by

a Pt/Ag/AgCl sensor link to a Benchtop pH/ISE Meter Orion 920 (relative precision +/- 0.1 mV). The alkalinity was obtained by titration on non-filtered aliquot with sulphuric acid 0.02N (relative precision of 1 mg $CaCO_3$/L) and the acidity by titration on non-filtered aliquot with sodium hydroxide 0.1N (precision of 1 mg $CaCO_3$/L) (APHA, 1995). Filtered aliquots (with a 0.45 µm filter) used to quantify metal content were acidified with 2% volume of nitric acid (70%) before analysis. The technique used to evaluate metal concentration was the Inductively Coupled Plasma-Atomic Emission Spectrometry (ICP-AES) using a Perkin Elmer OPTIMA 3100 RL (relative precision of 5%). Sulphate concentration was evaluated on filtered aliquot using a nephelometric method based on the precipitation of barium sulphate (AFNOR, 1986). The absorbance of the solution was measured at 650 nm with an Ultraspec 2100 pro spectrometer. Dissolved organic carbon in liquid effluent was determined using a Hach reagent set with method 10173 and a Hach DR 890 colorimeter. Finally, sulphate reducing bacteria enumerations were performed using the Most Probable Number according to ASTM (1990) and Beaulieu (2001).

5.2.5 Columns and medium size test initial and post-testing characterization

5.2.5.1 Initial material characterization

Each material and mixtures used in this study were initially characterized for their main chemical, physical, and microbiological properties. The main results are summarized in Table 5.3. Materials and mixtures were characterized for their pH, specific surface area (Ss), their total organic carbon (TOC) content, total carbon (TC) content, total Kjeldahl nitrogen (TKN) content, dissolved organic carbon (DOC) in water extract (1:10), and SRB count. More details on characterization and methods used can be found elsewhere (see Genty et al., 2011a, Genty et al., 2011b and Genty et al., 2011c). The pH of materials used in SRPB mixtures was close to neutrality. However, wood ash pH was clearly alkaline (pH of 12.2). Moreover, wood ash specific surface area and carbon content were relatively high (46.03 m^2/g and 36%, respectively). These two properties gave wood ashes a good sorption potential. TOC/TKN ratio for SRPB 2 mixture was close to an optimal value of 10 (13); providing sufficient nutriments for good SRB growth (Neculita and Zagury, 2008). Enumeration of SRB in

mixture 1 and 2 was carried out for chicken manure (450 SRB cell/100mL), compost (780 SRB cell/100mL) and sediments (1300 SRB cell/100mL).

Table 5.3 Initial materials and mixtures characterization

Material	Maple chips	Maple sawdust	Chicken manure	Leaf compost	River Sediments	SRPB 1	SRPB 2	Wood Ashes
pH	6.2	5.6	6.0	6.7	7.1			12.2
Ss (m^2/g)	0.58	0.86	1.15	1.67	13.02			46.03
TOC (%w/w dry weight)	51	49	26	24	1.5	11	13	19
TC (%w/w dry weight)								36
TKN (%w/w dry Weight)	0.1	0.2	2.6	1.3	0.04	0.4	1	
DOC (mg/L)	280	450	57	48	6.4	140	110	
TOC/TKN						28	13	
SRB (cells/100 mL)	<2	<2	450	780	1300			

5.2.5.2 Column post-testing characterization

Material samples were taken in the middle height (35 cm) of each column during dismantling to characterize metal retention phenomena that occurred in the multi-step column test system. Elemental abundance in solids was estimated by digestion in HNO_3, Br_2, HCl and HF (Potts, 1987) followed by metal analyses by Inductively Coupled Plasma-Atomic Emission Spectrometry (relative precision of 5%). Stability of metal retention in the five tested mixtures was estimated with a semi-quantitative sequential extraction procedure (SEP) according to Zagury et al. (1997). Five fractions were extracted from 1 g of wet solid sample using different reagents, and metal species are divided into: i) fraction 1: soluble and exchangeable metals, ii) fraction 2: carbonate bound, iii) fraction 3: reducible or bound to Fe–Mn oxides, iv) fraction 4: oxidisable or bound to organic matter, and v) fraction 5: the residual metal fraction. SRB count was also performed with the Most Probable Number technique according to ASTM (1990) and Beaulieu (2001). More information about post testing characterization of SRPBs and wood ash filters can be found in Genty et al., 2011c and Genty et al., 2011d.

5.2.5.3 Medium size test post-testing characterization

Samples at a depth of 50 cm on the center line of the reactor were taken. Results for six samples are presented: two in the first BPSR section at 50 and 100 cm from the AMD input, two in the first wood ash section at 115 and 150 cm from the AMD input, and two in the second SRPB section at 180 and 220 cm from the AMD input. These six samples were characterized for metal content by digestion, total organic carbon TOC (measured by adding potassium dichromate and sulphuric acid and measurement of excess of potassium dichromate), total Kjeldahl nitrogen TKN (by mineralization with sulphuric of organic matter acid into ammonium, carbon dioxide and water, and measurement of the ammonium formed), and dissolved organic carbon DOC (water extracts at 1:10 solid-liquid ratio, digestion and infra-red detection of carbon dioxide emitted). Samples at 100, 115, and 220 cm from AMD input were also analysed for metal stability by sequential extraction procedure according to Zagury et al. (1997), for SRB count using the Most probable number technique, and for their mineralogy using a Hitachi 3500-N scanning electron microscope (SEM) coupled with an energy dispersive spectrometry (EDS) with an X-ray probe (conditions: voltage of 20 keV, amperage of 140 A, pressure around 25 kPa and work distance of 15 mm). Finally, saturation indices of minerals which could be potentially present, were estimated by Vminteq v 2.53 (KTH, 2010) using the water quality at the 104^{th} and 300^{th} days. These two dates represent a steady state for the treatment of AMD and AMD light.

5.3 Results and interpretation

5.3.1 Columns treatment results

Figure 5.3 presents the pH, Eh, acidity, alkalinity, iron and sulphates evolution of the pore water for the three parts of the multi-step column system. pH (Figure 5.3a) increased from an average of 2.9 in initial AMD to 6.1 in the first SRPB. pH was relatively stable in the wood ash filter (6.2 on average) and in the last SRPB (6.6 on average). Eh (Figure 5.3b) decreased from an average 566 mV in AMD to approximately 76 mV in the first SRPB, and to 77 mV in the wood ash filter. However, Eh was negative (-65 mV on average) in the first 224 days of the second SRPB operation life. These low values provided favourable reducing conditions for sulphate reducing bacteria (SRB). Indeed, SRB count performed on the last SRPB column

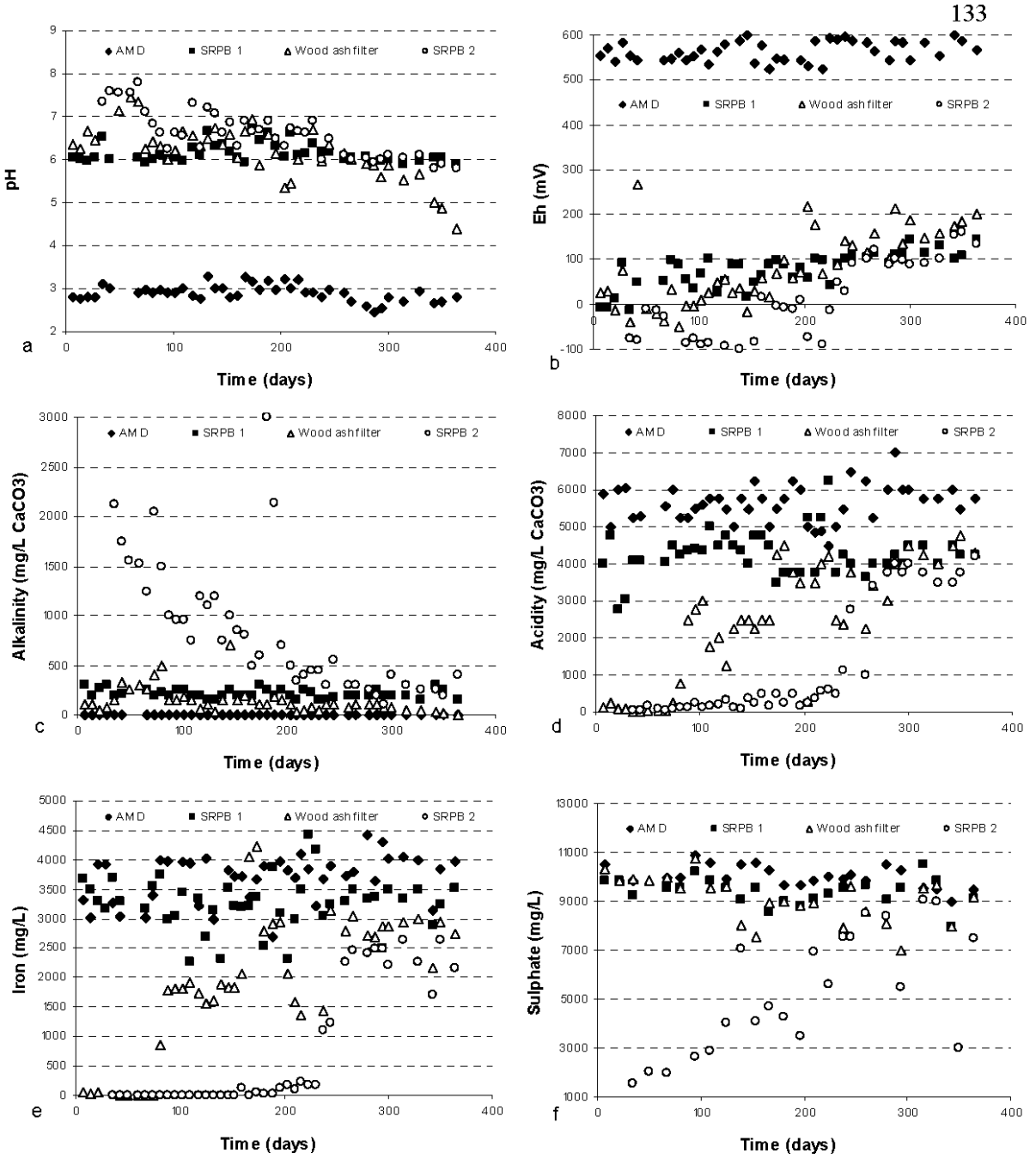

Figure 5.3 Evolution of geochemical parameters: a) pH, b) Eh (mV), c) alkalinity (mg/L CaCO3), d) acidity (mg/L CaCO3), e) iron concentration (mg/L) and f) sulphate concentration (mg/L), for the column test.

effluent at 74 days showed a value of approximately 35 000 SRB cell/100mL. For the first SRPB, the value never exceeded 200 SRB cell/100 mL. After 224 days, Eh value of the second SRPB reached around 104 mV and the reducing conditions for SRB were less favourable. In fact, SRB count performed on the last SRPB columns effluent at 253 days showed a decreased of SRB cells from 35 000 to 2400 SRB cell /100 mL. Moreover, SRB count performed on solid mixture after dismantling also confirmed a greater number of SRB in the second SRPB (204 cell/g for SRPB #1 mixture and 1253 cell/g for SRPB #2 mixture). This observation confirmed the highest sulphate reduction efficiency of the second SRPB.

Figure 5.3c showed that the first SRPB produced about 214 mg/L of $CaCO_3$ of alkalinity. Alkalinity was on average 141 mg/L of $CaCO_3$ in the wood ash filter, but the global tendency was a decrease with time. In the last SRPB, alkalinity was relatively high at the beginning of experiment (maximum of 2150 mg/L of $CaCO_3$) due to favourable condition during the first 81 operating days. Then, alkalinity values decreased with time until they reached around 200 mg/L of $CaCO_3$ at the end of the experiment.

Acidity (see Figure 5.3d) was mainly linked with pH and iron concentration (as also observed by Kirby and Cravotta, 2005). AMD acidity rose up to an average of 5625 mg/L of $CaCO_3$ while its iron concentration stayed around 3730 mg/L (see Figure 5.3e). At the exit of the first SRPB, acidity decreased to approximately 4252 mg/L of $CaCO_3$ and iron concentration to an average of 3256 mg/L. This decrease corresponds to an iron removal percentage of approximately 13% in the first SRPB. Acidity continued to decrease between 0 and 750 mg/L of $CaCO_3$ in the wood ash filter during the first 84 days. Acidity increased continually to 4500 mg/L of $CaCO_3$ on average. This increase of acidity was linked to the increase in iron concentration. Iron concentration at the exit of the wood ash column was on average 31 mg/L before 84 days (approximately 99% of iron retention). Day 84 corresponds to a first breakthrough time for iron retention in the wood ash filter. Iron concentration stayed at 2158 mg/L on average between 84 and 238 days (which corresponds to an iron removal percentage of approximately 33%). Then, iron increased on average up to 2926 mg/L, which is very close to iron concentration in the first SRPB (approximately 10% of iron retention). Day 238 seemed to be the second breakthrough time when wood ashes were totally saturated with iron. For the second SRPB, acidity and iron concentration at the exit were low during the first

224 days (respectively 250 mg/L of $CaCO_3$ and 38 mg/L on average). This period of efficiency correspond to the period before the total saturation of wood ashes. After wood ash saturation (224 to 238 days), iron concentration in the second SRPB increased gradually to stabilize after three weeks to 2156 mg/L on average (approximately 26% of iron retention). Acidity increased at the same time to stabilize near 4200 mg/L of $CaCO_3$ on average. The effective period during which the treatment was efficient was 238 days. In the tested columns, the wood ash filter is an essential step to remove iron because SRPBs were not able to treat efficiently an AMD with this level of iron concentration.

Sulphate removal was more efficient in the second SRPB (see Figure 5.3f). Indeed, sulphate concentration decreased from an average of 10116 mg/L in AMD to 9495 mg/L in the first SRPB. Then, sulphates concentration continued to decrease to approximately 9088 mg/L in the wood ash filter. In the second SRPB, sulphate concentration at the exit of the column was around 5107 mg/L (50% of sulphates were removed). However, the sulphate concentration increased to an average of 7050 mg/L in the second SRPB after 224 days, which correspond to the iron saturation of wood ash filter.

Although iron removal was the main purpose of the multi-step column system, other metals were removed. Al, Cd, Cr were removed by up to 99% in the first SRPB step, and had a concentration at the exit of the multi-step system of 0.04 mg/L Al, 0.01 mg/L Cd, and 0.006 mg/L Cr. The removal of Ni and Zn increased from 95% in the first SRPB to 98% in the last SRPB and remained at a constant residual concentration of approximately 0.06 mg/L Ni and 0.56 mg/L Zn at the system exit. A increase in removal percentage was observed for Pb (59% in the first SRPB, 82% in the wood ash filter and 95% in the second SRPB) and its residual concentration was stable at approximately 0.03 mg/L. However, Mn removal was less effective with a removal percentage of 16% at the exit of the system. Non efficient Mn removal was mainly due to the high iron concentration in effluent. Indeed, a high Fe/Mn ratio and the thermodynamic advantage for Fe precipitate formation could partially explain this low Mn retention (Edwards et al., 2009).

Saturated hydraulic conductivity (k_{sat}) stayed relatively stable for each SRPB column, with values between $3.6x10^{-4}$ and $1.7x10^{-3}$ cm/s for the first SRPB and between $7.1x10^{-4}$ and

$2.9x10^{-3}$ cm/s for the second SRPB. These values indicated that clogging phenomena did not affect the two columns.

In summary, column tests gave promising results. However, they did not provide real flow conditions. Therefore, the multi-step treatment was tested in a medium size test with horizontal flow conditions.

5.3.2 Medium size treatment test results

Performances of each treatment section are described using the water quality in each piezometer. pH of AMD (in piezometer A) was stable at a value of 2.8 on average (Figure 5.4a and Table 5.4). pH increased up to 5.6 in the first SRPB (piezometer B), was relatively stable in wood ash filter (piezometer C), and was at 6.1 on average in the last SRPB (piezometer D). Eh values were on average at 443 mV in AMD (Figure 5.4b). However, an increased in Eh was observed during the first two months due mainly to the Postgate B dilution and back mixing. After this transient period, water in the piezometer was representative of AMD. Eh decreased to 55 mV on average in the first SRPB and to -16 mV in the wood ash filter. In the second SRPB, Eh decreased to values of approximately -115 mV. Some Eh peaks are present in Figures 5.4a and 5.4b; they are mainly due to the calibration procedure. Moreover, pH and Eh values between 34 and 100 days in piezometer B were removed due to monitoring problems. A by-passing zone was observed between the first AMD compartment and piezometer B resulting from a restriction at the system exit pipe which imposed an increased of water level in the reactor. The problem was solved by pumping water from the exit at the same flow rate as in the system input.

Table 5.4 Average parameters for piezometers A, B, C and D of the medium size test reactor. Units are mV for Eh, mg/L for iron and sulphate concentration, mg/L eq. CaCO3 for alkalinity and acidity. Iron and sulphate removal are expressed using the average (av) %.

Piezometer	A	B	C	D
Material	AMD	SRPB #1	Wood ashes	SRPB #2
pH	2.8	5.6	6.1	6.1
Eh	443	55	-16	-115
Iron				
Before 150 days	4111	3804	1021	152
After 150 days	1839	1390	1022	38
Iron removal				
Before 150 days	-	21	73	96
After 150 days	-	24	45	98
Sulphates				
Before 150 days	9652	9227	6411	4084
After 150 days	4885	3892	3600	1093
Sulphates removal				
Before 150 days	-	5	34	58
After 150 days	-	20	26	78
Acidity				
Before 150 days	8628	3217	1464	651
After 150 days	4901	2053	1400	381
Alkalinity				
Before 150 days	0	296	780	1120
After 150 days	0	173	284	1515

Alkalinity was relatively stable in each compartment (Figure 5.4c) after the first two months. The first two months correspond to the dilution of Postage B solution, to the lixiviation of a large quantity of dissolved organic carbon, and the establishment of permanent hydrogeochemical conditions. Before 150 days (system fed with an AMD of 4000 mg/L of iron), alkalinity (Table 5.4) increased on average from 0 mg/L of $CaCO_3$ in AMD to 296 mg/L of $CaCO_3$ in the first SRPB, 780 mg/L of $CaCO_3$ in wood ash filter and 1120 mg/L of $CaCO_3$ in the second SRPB (the first four alkalinity values were removed from the calculation of average alkalinity because they were not representative of the treatment). After a 150-day period (treatment of AMD with 2000 mg/L of iron), alkalinity of water samples was 173 mg/L of $CaCO_3$ for the first SRPB, 284 mg/L of $CaCO_3$ for the wood ash filter, and 1515 mg/L of $CaCO_3$ for the second SRPB respectively.

Acidity (Figure 5.4d) was mainly linked to the iron content (Kirby and Cravotta, 2005). Indeed, acidity of AMD decreased from 8628 mg/L of $CaCO_3$ in AMD with 4000 mg/L of

iron to 4901 mg/L of $CaCO_3$ when iron concentration was 2000 mg/L (Table 5.4). Acidity was mainly metallic in the treatment piezometer since pH was close to neutrality. For both AMD with 4000 mg/L and with 2000 mg/L of iron, the system decreased acidity concentration (651 mg/L of $CaCO_3$ before 150 days and 381 mg/L of $CaCO_3$ after 150 days in piezometer D).

AMD iron concentration during the first 150 days was on average 4111 mg/L (Table 5.4). Iron decreased in the first SRPB to 3804 mg/L after approximately 3 weeks of variation (see Figure 5.4e) due to the dilution of Postgate B solution. The average iron retention in the first treatment step was approximately 21%. In the wood ash filter, iron concentration was 1021 mg/L, on average, which corresponds to 73% of iron retention. In the last stage of SRPB treatment (piezometer D), iron retention reached 96% (152 mg/L on average). During the next 214 days, AMD iron concentration was set to 1839 mg/L on average. Iron retention in the first SRPB stayed similar to the first period (24%), but decreased in the wood ash filter treatment step to 45% (1022 mg/L of iron in piezomenter C). Iron concentration decreased on average to 38 mg/L in the second SRPB (98% of removal).

Sulphate concentration (Figure 5.4f) was relatively variable during the first two months due to Postgate dilution. Sulphate concentrations were relatively stable at the end of the first and the second period of the treatment. Sulphate concentration in AMD was maintained at an average of 9652 mg/L before 150 days (see Table 5.4). Sulphate concentration was removed after treatment on the first SRPB at an average of 5% (corresponding to a concentration of 9227 mg/L in the piezometer A). The percentage of removal rose up to 34% in wood ash filter and 58% in the second SRPB. Sulphate concentration in AMD was set at approximately 4885 mg/L on average after 150 days. The removal percentage increased up to 20% in the first SRPB, 78% in the second SRPB, and decreased at 26% in the wood ash filter. In piezometer D, sulphate concentrations decreased to 4084 mg/L before 150 days and to 1093 mg/L in piezometer D after 150 days.

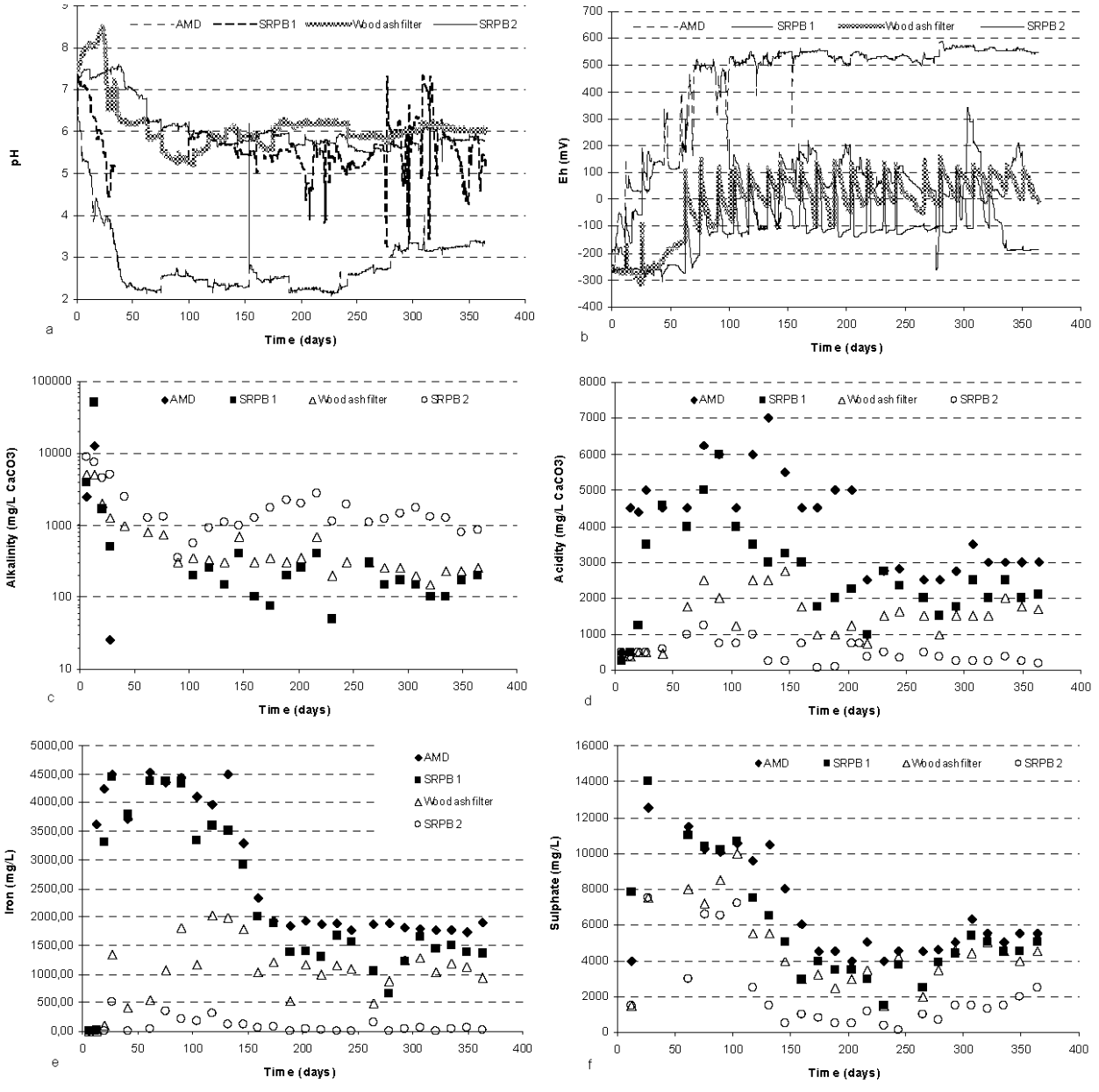

Figure 5.4 Evolution of parameters: a) pH, b) Eh (mV), c) alkalinity (mg/L CaCO3), d) acidity (mg/L CaCO3), e) iron concentration (mg/L) and f) sulphates concentration (mg/L), for the medium size test.

The removal percentage of other metallic contaminants was relatively high in the multi-step system. Indeed, Al removal increased from 72% in the first SRPB to 99% in wood ash filter.

Cd, Cr, Ni and Zn removal percentages were respectively 58%, 77%, 37% and 57% in the first SRPB, and rose up to 99% in wood ash filter. Lead removal increased continuously through the different compartment (49% in the first SRPB, 82% in the wood ash filter, and 99% in the second SRPB). All metals in the second SRPB had average concentrations below 0.01 mg/L. Mn removal varied on average from 14% in the first SRPB, 27% in the wood ash filter, and 71% in the second SRPB compartment. A significant competition occurred in SRPB between Fe and Mn (Edwards et al., 2009, Karathanasis et al., 2010). The increased of Mn removal (compared to the column tests) was mainly due to the decrease of the Fe/Mn ratio in the three parts of the treatment. Indeed, a high Fe/Mn ratio induces a serious Mn treatment inhibition (Edwards et al., 2009). The ratio Fe/Mn decreased on average from 90 in the first SRPB to 56 in the wood ash filter and to 10 in the second SRPB. Therefore, competition between Fe and Mn was less important in the second SRPB, and the Mn removal was higher.

SRB count in the water samples was performed to evaluate sulphate-reducing performance. The SRB number (Figure 5.5) decreased during the first 150 days (which correspond to the treatment of AMD with 4000 mg/L of iron and 9000 mg/L of sulphates) for the first SRPB and wood ash filter. Values decreased to approximately 0 SRB cell/100mL. However, the SRB cell number stayed stable at 2400 cells/100 mL for the second SRPB. DOC concentration and the ratio DOC/SO_4 were determined in parallel to the SRB count (Figure 5.5). The ratio decreased in each part of the system during the first 150 days. Nevertheless, the ratio in piezometer D was significantly higher (0.4 on average for the 150 first days), which maintained the SRB cell number observed; this ratio value is close the optimum ratio of approximately 0.4 proposed in the literature for sulphate-reduction (Neculita and Zagury, 2008). After the first 150 days (which correspond to the beginning of the treatment period of AMD with 2000 mg/L of iron and 5000 mg/L of sulphates), the number of SRB cells in the first SRPB and the wood ash filter stayed at 0 SRB cell/100mL and at 2400 cells/100 mL for the second SRPB. The ratio DOC/SO_4 increased mainly because of the decrease in sulphate concentration in AMD. The ratio (0.69 on average) stayed close to the optimum value in the second SRPB.

To summarize, the change of AMD iron and sulphate concentration did not affect the performance of the system since metal removal, and particularly iron, stayed high (more than 99%).

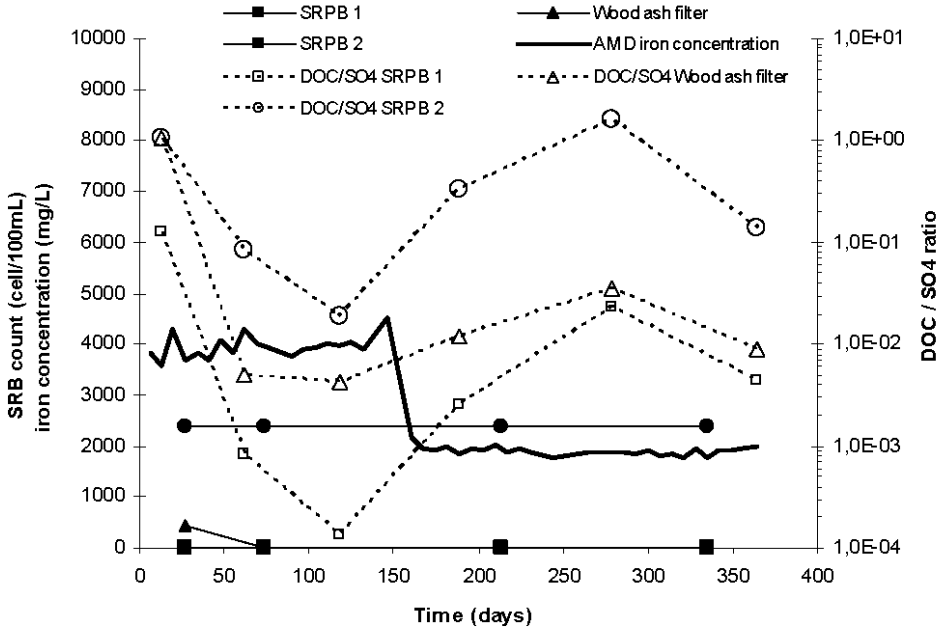

Figure 5.5 Evolution of SRB count and DOC/SO4 ratio in medium size test reactor (in the first SRPB, wood ash filter, second SRPB, and at the exit of the reactor).

5.3.3 Hydraulic investigation of medium size test reactor

Clogging phenomena can seriously decrease the life time of a passive treatment system. A decrease of saturated hydraulic conductivity (k_{sat}) value is a good indicator of clogging (e.g. Neculita et al., 2008a, Genty et al., 2011c, Genty et al., 2011d). During the medium size reactor test, k_{sat} was measured using the Darcy law as presented in equation [5-1]. Values did not vary during the test ($1.8x10^{-3}$ cm/s at 100 days, $1.5x10^{-3}$ cm/s at 286 days, $1.4x10^{-3}$ cm/s at 363 days). These values are close to those found by Genty et al. (2011c) for similar SRPB mixtures (between $2.1x10^{-3}$ and $9.98x10^{-3}$ cm/s). These results confirmed that the composition of the SRPB mixture and wood ashes prevented the system from clogging since k_{sat} values stayed almost stable during the test.

Iron concentration at the exit of the system (1072 mg/L on average; not shown in Figure 5.4) was higher than in the previous treating compartment (piezometer D). Similar observation could be made mainly for acidity and sulphate concentration. This observation could result from by-passing phenomenon (or preferential flow). Hence, the exit water quality resulted from a mix of the second SRPB effluent and water with incomplete treatment.

One of the main usefulness of a tracer test is to diagnose flow problems in reactors operation (Fogler, 2006). A tracer test with NaCl was performed to evaluate the real retention time of the system and to validate the hypothesis that there is some preferential flow that affects the water quality at the exit of the model. Figure 5.6 shows the evolution of chloride concentration at the exit of the system. During the four first days, chloride concentration stayed relatively sable at 6 mg/L (which corresponds to the background chloride concentration). After 4 days, a slight increase was observed but the major increase started after 8 days to stabilize after 20 days at 160 mg/L. The initial chloride concentration of 0.6 g/L was not recovered at the end of the test due to retention in the medium size reactor. NaCl was not a conservative tracer (only approximatelly 20% of Cl^- was recovered).

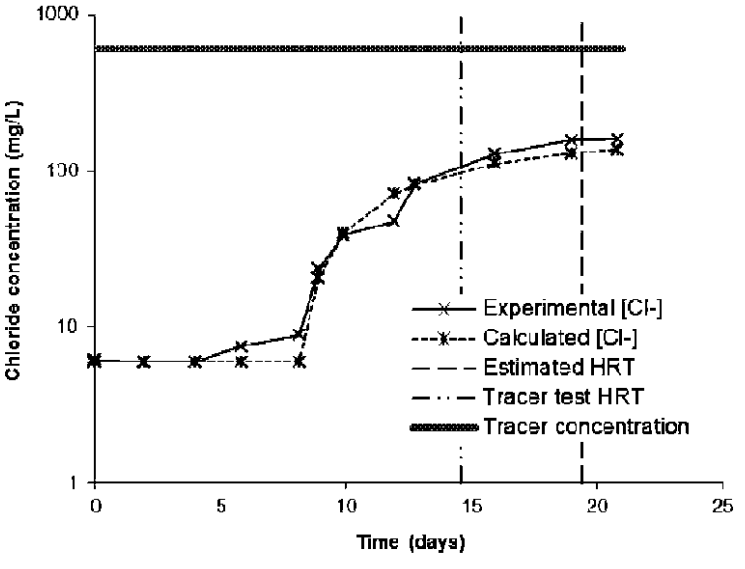

Figure 5.6 Evolution of chloride concentration (mg/L) during the tracer test at the exit of the medium size reactor.

The residence time distribution theory was used to analyse the tracer test results (e.g. Roche et al., 1994, Faure et al., 2008, Genty et al., 2011c). According to the chloride concentration, the system could be modeled as a succession of a plug flow reactor with a hydraulic retention time of 8 days (corresponding to the latency period) and a continuous stirred reactor (corresponding to the increase of chloride concentration) with a hydraulic retention time of 6.6 days. The total hydraulic residence time of the system (sum of the plug flow reactor HRT and the continuous stirred reactor HRT) is estimated at 14.6 days. A difference exists between the HRT estimated with the tracer test and the estimated HRT of 19 days calculated with the porosity and the flow rate. This difference could be explained (at least in part) by the presence of preferential flow zones in the reactor and thus potentially explain the higher metal concentration at the exit of the system (see Genty, 2011, for details).

5.3.4 Column and medium size test post-testing characterization

5.3.4.1 Medium size test analysis

Analysis of TOC and TKN showed that the ratio (TOC/TKN) increased from 18 initially to 28 after dismantling in the first SRPB, and thus suggests a decrease of available nitrogen compared to TOC. However, this ratio decreased from 16 to 13 in the second SRPB (a ratio close to 10 is known as a favourable ratio for SRB; Neculita and Zagury, 2008). SRB enumeration on post-testing materials also showed the presence 1054 cells/g and 966 cells/g in the first and second SRPB respectively. SRB count was estimated at only 386 cells/g in wood ash filter. Indeed, the DOC value was low in the wood ash filter (2.6 mg/L on average) compared with the ones in the first and second SRPB (10.5 and 12 mg/L on average), both providing better nutriments availability conditions for SRBs.

Metal content was evaluated on samples collected 50 cm deep in each of three parts of the system. The main observation was that the iron content increase was approximately 1.3% in the first SRPB, 7.8% in wood ash filter, and 4.3% in the second SRPB. These results underlined the role played by the wood ash filter to remove iron from AMD. Moreover, the sulphur content increased to 1.8% on average in the second SRPB (compared to 0.7% in the first SRPB and 1.4% in the wood ash filter). Indeed, sulphate reduction was higher in the second SRPB because sulphate reducing conditions (negative Eh values) were reached in this

compartment. To better understand the metal retention mechanisms, Vminteq modelling, SEP and SEM-EDS analyses were performed.

Thermodynamical modelling with Vminteq allowed determining that different metal retention mechanisms could occur in the three different treatment compartments. Al was probably removed in the first SRPB by the formation of hydroxides or oxihydroxides such as boehmite, diaspore and gibbsite. Iron would be retained under oxihydroxide (goethite, lepidocrocite) and carbonate forms (siderite). The formation of rhodochrosite for Mn retention is plausible. In the wood ash filter, iron would be removed by oxihydroxide (goethite, ferrihydrite, lepidocrocite), carbonate (siderite), and sulphide (pyrite) precipitation. Nickel sulphur precipitation is a possible mechanism for Ni removal. Sulphate could also be removed by gypsum formation. In the second SRPB, sulphate reduction conditions were more favourable for the formation of metal sulphides such as greigite, mackinawite, pyrite, and millerite. Carbonates (siderite and rhodochrocite) and sulphates (gypsum) could also be formed in this component of the treatment.

Figures 5.7a to 5.7d show X-mapping of the main chemical elements observed on wood ash filter (Figure 5.7a) and on reactive mixture of SRPB 2 (Figure 5.7b to 5.7d) using the EDS technique. Iron was found at the surface of the wood ash sample and associated with oxygen probably under the hydroxide form (see Genty et al., 2011d). Gypsum crystals were also observed. The X-mapping of SRPB 2 mixture showed a superposition of calcium, oxygen and sulphur, which may correspond to the precipitation of gypsum crystals (mainly in Figure 5.7c). Moreover, iron was distributed relatively homogenously at the surface of the material. However, it was not easy to assess under which form iron was retained; iron could be associated with oxygen or sulphur and thus retained under hydroxide or sulphide forms. Similar observations can also be made with the SRPB 1 mixture (not presented on Figure 5.7). However, elemental sulphur grains can be seen in Figure 5.7b. EDX microanalysis allowed determining that elemental sulphur was formed in SRPB 2 mixture. Indeed, elemental sulphur could be formed through the oxidation of hydrogen sulphide (Beaulieu, 2001) by different types of bacteria.

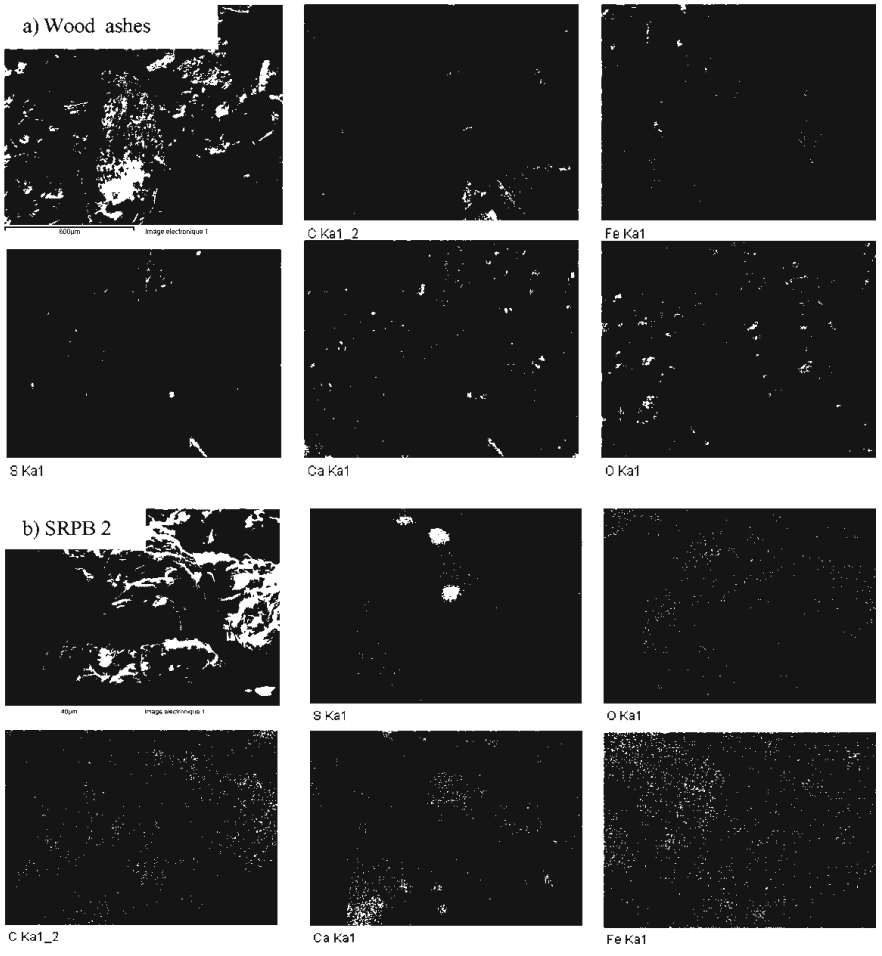

Figure 5.7 SEM images and elemental maps (voltage of 20 keV, amperage of 140 A, pressure around 25 kPa, and working distance of 15 mm): a) wood ash filter, b) c) and d) SRPB2.

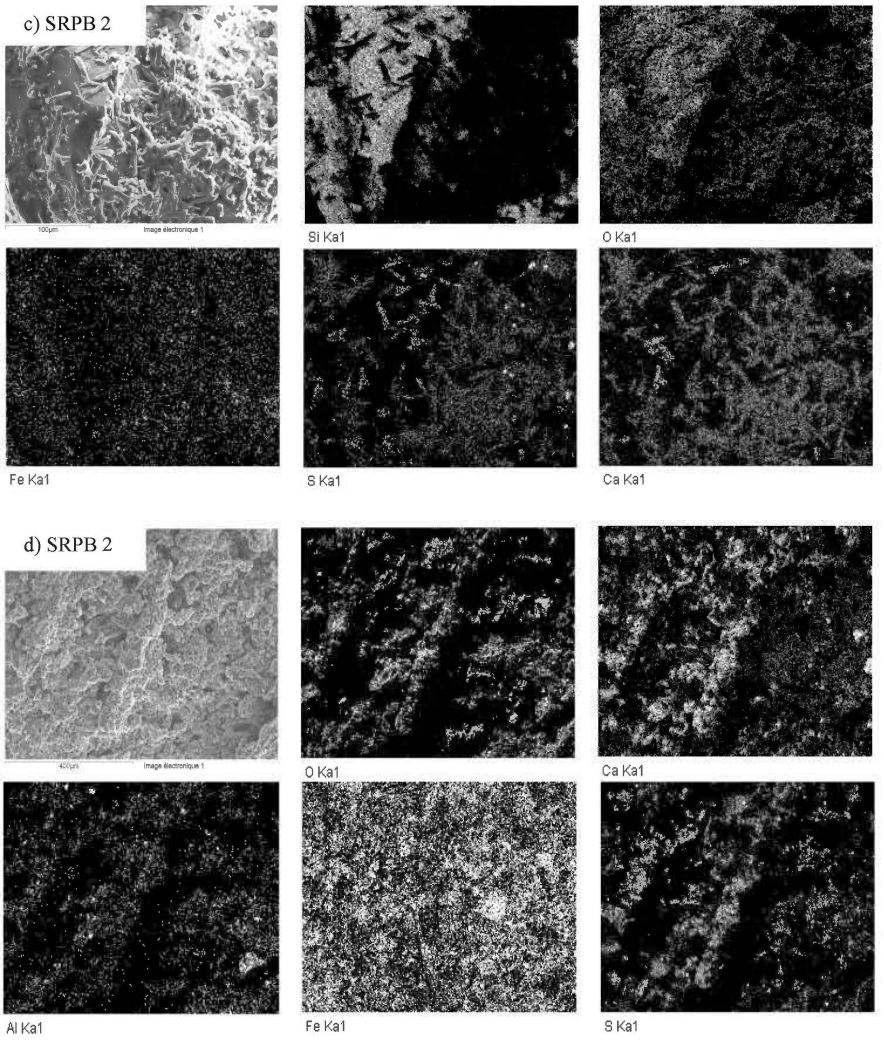

Figure 5.7 (suite) SEM images and elemental maps (voltage of 20 keV, amperage of 140 A, pressure around 25 kPa, and working distance of 15 mm): a) wood ash filter, b) c) and d) SRPB2.

5.3.4.2 Column and medium size reactor metal fractionation

Figure 5.8 presents the metal fractionation on samples from the three sections of the medium size and column experiment.

Metal distribution in the two medium size reactor SRPB sections was relatively similar. Indeed, Al, Cr and Pb were mainly retained in the residual fraction 5, Cd in fractions 2 and 3. Ni and Zn had also similar metal retention mechanisms since they were mainly contained in fraction 3, and occurred in fractions 2 and 4 in similar proportion. However, a non negligible part of Ni was soluble and exchangeable (21% and 27%). Fe and Mn fractionation was not similar in the two SRPB. Fe was found in relatively similar proportion in fraction 3, 4 and 5 in SRPB 1. In SRPB 2, Fe was mainly contained in fraction 3 (64%). Mn proportions in fraction 1 and 2 of SRPB 2 were higher in comparison with SRPB 1 (respectively from 16 to 28% and 12 to 20%) and fraction 5 had lower Mn contents (from 36 to 7%). Differences in metal retention mechanisms can be observed in the wood ash section of the medium size reactor, mainly for Cr, Fe, Ni, Pb and Zn. The distribution of Al, Cd, and Mn was similar in the two SRPBs. Although fraction 5 contained 46% of Cr, this element was present in non negligible proportions in fraction 3 and 4 (respectively 23 and 26%). Fe was mainly retained in fraction 3. Pb was separated relatively equally between fractions 3, 4 and 5 (respectively 40, 35 and 25%). Ni and Zn contents increased up to 21% and 12% in fraction 5, respectively. Ni was present in similar proportions in fractions 2, 3 and 4, and a non negligible part was soluble and exchangeable (29%). Finally, Zn was mainly contained in fractions 2 and 3.

Results of metal fractionation with samples taken in the medium size reactor were similar to the metal fractionation of samples provided by column tests for Al, Cr, Fe, Mn, Ni, Zn, Pb (except in the second SRPB). However, major difference could be observed for Cd between columns and medium size reactor. Indeed, Cd in the three treating section of the medium size reactor was mainly contained in fraction 2 while Cd was mainly in fraction 3 in column sample. Moreover, Pb in the second SRPB was mainly in the residual fraction in the medium size test while it was in fraction 3 and 4 in column test.

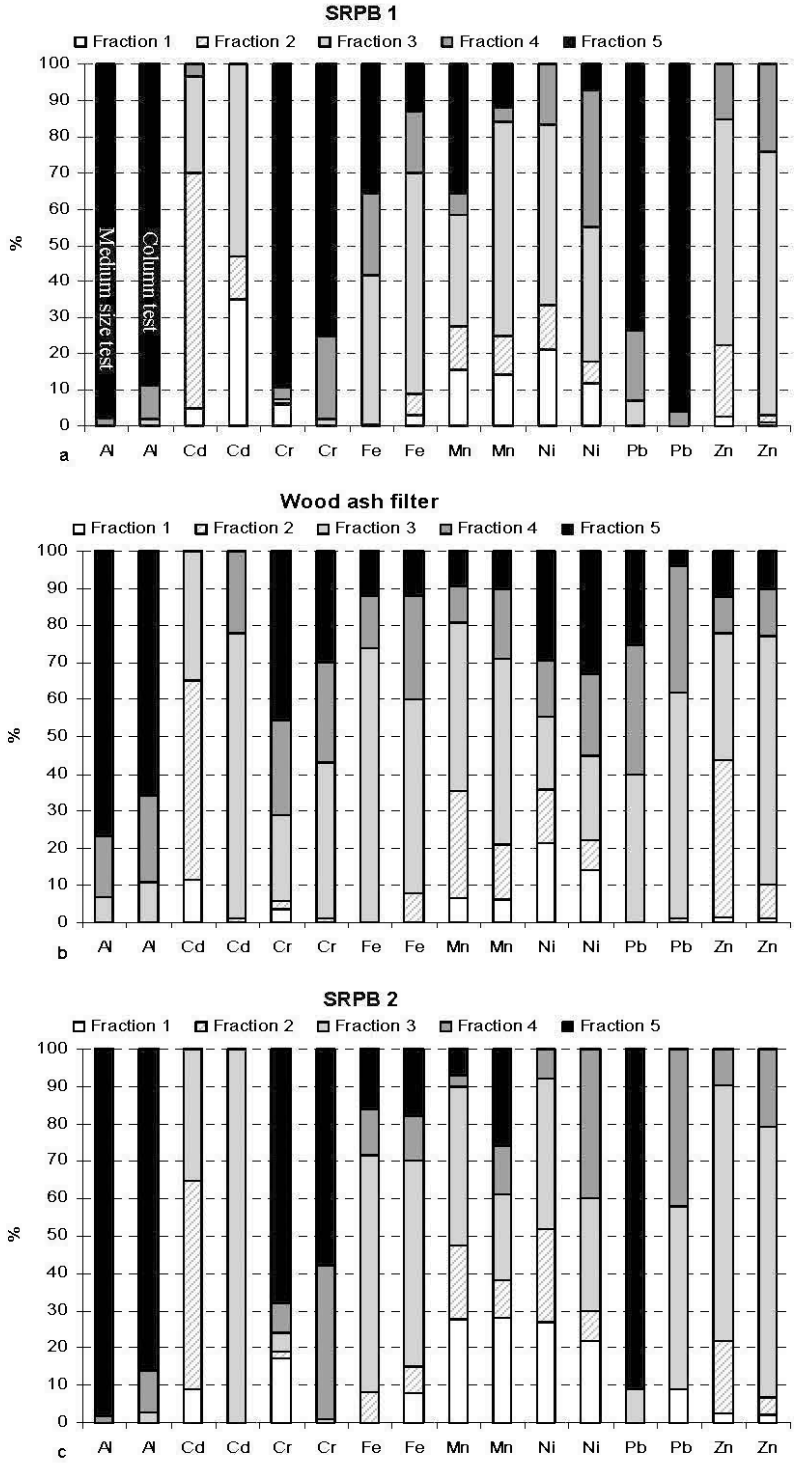

Figure 5.8 Metal fractionation in each part of medium size reactor (left column) and column (right column) tests after dismantling using sequential extraction procedure: a) SRPB 1, b) Wood ash filter, c) SRPB 2.

Overall in medium size test, Al, Cr and Pb (expect in wood ash filter) were mainly present under the most stable forms in the residual fraction. On the contrary, a non-negligible part of Cd, Mn and Ni was in a soluble or exchangeable form. In addition, Cd could be also remobilized in acidic conditions since it was mainly contained in carbonate bound fraction in the three part of the system. As a trend, Fe, Mn, Ni and Zn showed similar behavior, with the main proportions in the reducible or bound to Fe-Mn oxides-hydroxides fraction and in the oxidisable or bound to organic matter. Therefore, these metals were relatively stable under oxidizing conditions, even at low pH.

To summarize, iron, which is the most problematic metal in the treated AMD, was mainly removed by the wood ash filter (at 80 mg/g of dry material) and then by the second SRPB (at 30 mg/g of dry material). Iron was removed by the first SRPB only at 17 mg/g of dry material. These results were coherent with the decrease of metal concentration determined for each piezometer. Therefore, the role of the wood ash step as an iron filter was confirmed as useful.

5.3.5 Comparison between columns and medium size test

Two different sizes of laboratory experiments were tested. First, three columns (10.7 L each) were connected in series to mimic a multi-step passive treatment system. Secondly, a medium size experimental set up (approximately 2000 L) characterized by a more representative geometry of typical full size systems was used. In addition to the difference in volume, medium size test provided horizontal flow compared to columns which allow only vertical flow (2D vs 1D).

The comparison between results from both experiments shows that the medium size test performances are greater than the ones of the column experiment. Iron retention was efficient (97% of removal) in the column test during approximately 250 days (equivalent to 12.8 pore volume) for an iron load of 3.5 g/day, as presented in Table 5.5. Between 238 days and the end of the experiment, iron removal decreased to 39% on average due mainly to wood ash filter saturation. In the medium size test, iron retention was as efficient (96%) but for a period of more than 364 days (24.2 pore volume) for a treated iron load of around 207 g/day. Although pH stayed at similar values in both tests (between 6.5 and 6.7 on average), reducing

conditions were better maintained in the medium size test (with an average of -115 mV compared to -8mV on average in column tests) and for a longer period of time (during one year). As a result of these favourable sulphate reducing conditions, sulphates were removed at values up to 72% in the medium size test compared to values around 50% in the column test.

Table 5.5 Comparison between column and medium size tests

	Column tests	Medium size test
Operational conditions		
Total volume (L)	34.2	2134
Flow	Up-flow	Horizontal
Total HRT (days)	19.6	14.6 (19 theoretical)
Number of pore volume during the test	12.8	24.2
Exit water quality		
Average pH	6.5	6.7
Average Eh (mV)	-8	-115
Average iron (mg/L)	42 before 238 days 2444 after 238 days	89.5
Average iron % removal	97% before 238 days 39% after 238 days	96%
Average sulphate % removal	50%	72%
Wood ash saturation (days)	238	Not observed
Post-characterization procedures		
Iron content increase (ICP)	3.7% in the first SRPB 1.5% in the wood ash filter 2.1% in the second SRPB	1.3% in the first SRPB 7.8% in the wood ash filter 4.3% in the second SRPB
Iron fractionation (SEP)	Fe mainly in the reducible phase 32 mg/g in the first SRPB 88 mg/g in the wood ashes 34 mg/g in the second SRPB	Fe mainly in the reducible phase 17 mg/g in the first SRPB 80 mg/g in the wood ashes 30 mg/g in the second SRPB
SEM observations	Gypsum Iron associated to O and S (Genty et al.,2011c, Genty et al., 2011d)	Gypsum Iron associated to O and S

In terms of metal retention mechanisms, observations in columns and in the medium size test were relatively similar. The SEP also showed that iron was retained mainly in fractions 3 and 4 in each treatment section in both columns and medium size test reactor. Moreover, metal content determination by ICP and SEP showed that the wood ash filter, in both experiments,

acted mainly as an iron filter; 88 mg/g and 80 mg/g of iron were contained in wood ashes after the experiments. Finally, SEM analyses showed precipitation of gypsum and the presence of iron associated with oxygen and sulphur in both experiments.

To summarize, the medium size test geometry offered better treatment performances compared to columns tests. However, metal retention mechanisms seemed to be similar in both configurations.

5.4 Conclusion

Laboratory multi-step treatment of a high iron concentrated AMD (between 2000 and 4000 mg/L) using two SRPB stages separated by a wood ash filter showed a good efficiency. Indeed, column multi-step treatment test allows neutralizing AMD acidity during more than 250 days. Iron concentration at the exit of the treatment columns increased mainly due to the wood ash filter saturation. As a result, metallic acidity of the effluent increased considerably. However, the multi-step medium size reactor performance was higher than the series of columns in terms of iron concentrations. Indeed, iron concentrations were reduced by approximately 95% (decreased from 2750 to 90 mg/L) during over one year. Hydraulic investigation on both columns and medium size reactor showed that clogging phenomenon does not seem to affect the hydraulic properties of the materials used. Nevertheless, a tracer test performed in the medium size reactor indicated the presence of preferential flow zones which affected the water quality of the last compartment of the system. Finally, iron retention mechanisms in both columns and medium size reactor were identified as the formation of hydroxides and biogenic sulphides phases.

The methodology adopted in this article showed that the size of the experiment had an effect on metal retention efficiency in the long term. Indeed, the medium size reactor (approximately 2000L) was more efficient to remove metals than columns (33L) in a long term period. Design of full scale treatment systems for high iron contaminated AMD should be evaluated preferentially in a medium size reactor because of its more realistic operation conditions.

Acknowledgements

This research was supported by the Canada Research Chair on Restoration of Abandoned Mine Sites and the Natural Sciences and Engineering Research Council of Canada (NSERC) through the Industrial NSERC Polytechnique-UQAT Chair in Environment and Mine Wastes Management. The authors gratefully acknowledge the industrial and governmental partners of the industrial Chair for the funding of this study and Brian Coghlan from Wood Ash Industries Inc for supplying graciously wood ashes.

References

AFNOR, 1986. Essais des eaux - Dosage des ions sulfates - Méthode néphélométrique, in : Norme Française NF T90-040.

APHA, 1995. Alkalinity titration. In: Greenberg A (ed) Standard methods for the examination of water and wastewater, 19th edn. Washington DC.

ASTM, 1990. Standard methods for sulphate reducing bacteria in water and water-formed deposit, in: Annual book of ASTM Standards (vol. 04.08., section D 4412 – 84), Washington, DC, pp. 533-535.

ASTM, 1995. Standard test method for permeability of granular soils. Annual book of ASTM Standards, Vol. 04.08. D 2434 – 68, Philadelphia, PA, USA.

Aubertin, M., Bussière, B., Bernier, L., 2002. Environnement et gestion des rejets miniers. Edition Presses internationales Polytechnique, Montréal.

Beaulieu, S., 2001. Applications des techniques de bioactivation et de bioaugmentation pour le traitement en conditions sulfato-réductrices des eaux de drainage minier acide. Master Dissertation, École polytechnique de Montréal, Canada, 235 p.

Blowes, D.W., Ptacek, C.J., 1994. System for treating contaminated groundwater, in: U.S. Patent 5,362,394, filed March 3, 1992, issued Nov. 8, 1994.

Champagne, P., Van Geel, P., Parker, W., 2005. A Bench-scale Assessment of a Combined Passive System to Reduce Concentrations of Metals and Sulphate in Acid Mine Drainage. Mine Wat. Environ. 24, 124-133.

Edwards, J. D., Barton, C. D., Karathanasis, A. D., 2009. A small-scale sulfate-reducing bioreactor for manganese removal from a synthetic mine drainage. Wat. Air Soil Pollut. 203, 267-275.

El-Gharmali, A., Rada, A., El-Adnani, M., Tahlil, N., El-Meray, M., Nejmeddine, A., 2004. Impact of acid mining drainage on the quality of superficial waters and sediments in the Marrakesh Region, Morocco. Environ. Tech. 25, 1431-1442.

Evangelou, V.P., Zhang, Y.L., 1995. A review: pyrite oxidation mechanisms and acid mine drainage prevention. Environ. Sci. Tech. 25, 141-199.

Faure, M., Furman, M., Corbel, S., Carré, M.C., Gérardin, F., Zahraa, O., 2008. Caractérisation de réacteurs photocatalytiques utilisés pour le traitement de l'air, in : Séminaire 2008 de l'école doctorale RP2E Ingénierie des ressources, procédés, produits et environnement, ISBN 2-9518564-6-6, Nancy.

Fogler, H.S., 2006. Element of chemical reaction engineering, fourth ed. Prentice Hall International Series in the Physical and Chemical Engineering Sciences, Massachusetts.

Figueroa, L., Miller, A., Zaluski, M., Bless, D., 2007. Evaluation of a two-stage passive treatment approach for mining influenced waters. National Meeting of the American Society of Mining and Reclamation, Gillette, WY, 30 Years of SMCRA and Beyond June (pp. 238-247). Barnishel, R.I., Lexington, KY.

Gazea, B., Adam, K., Kontopuolos, A., 1995. A review of passive systems for the treatment of acid mine drainage. Miner. Eng. 9, 23-42.

Genty, T., Bussière, B., Potvin, R., Benzaazoua, M., Zagury, G.J., 2011a. Dissolution of different limestone in highly contaminated acid mine Drainage: Application to anoxic limestone drains. Submitted to Environ. Earth Sci. in November 2010.

Genty T., Bussière B., Benzaazoua M., Zagury G. J., 2011b. Treatment of acid mine drainage with high iron concentration using sulphate reducing passive bioreactor: I. Mixtures characterization and batch test results. Submitted to Ap. Geochem. in November 2011

Genty T., Bussière B., Benzaazoua M., Zagury G. J., 2011c. Treatment of acid mine drainage with high iron concentration using sulphate reducing passive bioreactor: II. Columns tests. Submitted to Ap. Geochem. in November 2011.

Genty T., Bussière B., Benzaazoua M., Zagury G. J., 2011d. Iron retention on wood ashes filter after sulphate reducing biofilter treating high-iron acid mine drainage. Submitted to J. Hazard. Mater. in November 2011

Genty, T., Bussière, B., Neculita, C.M., Benzaazoua, M., Zagury, G.J., 2011e. Passive treatment of acid mine drainage: repeatability for sulphate reducing passive bioreactor column efficiency testing, in: Proceeding of International Mine Water Association symposium 2011, Aachen, Germany, 6 pp.

Gomes, M.E.P., Favas, P.J.C., 2006. Mineralogical controls on mine drainage of the abandoned Ervedosa tin mine in north-eastern Portugal. Ap. Geochem. 21, 1322–1334.

Griffiths P., 1975. Chemical infrared fourier transform spectroscopy. J Wiley and Sons Inc. USA.

Gusek, J.J., 2001. Why do some passive treatment systems fail? The Center for Environmental Health Sciences at Darmouth. http://www.leo.lehigh.edu/envirosci/enviroissue/amd/links/passive_fail.html. Accessed 25 February 2011.

Hedin, R.S., Watzlaf, G.R., Nairn, R.W., 1994. Passive treatment of acid mine drainage with limestone. J. Environ. Qual., 23: 1338-1345.

Karathanasis, A.D., Edwards, J.D., Barton, C.D., 2010. Manganese and sulphate removal from a synthetic mine drainage through pilot scale bioreactor batch experiments. Mine Wat. Environ. 29, 144-153.

Kleinmann, R.L.P., Crerar, D.A., Pacelli, R.R., 1981. Biogeochemistry of acid mine drainage and a method to control acid formation. Mining Eng. 300-304.

Kirby, C.S., Cravotta, C.A., 2005. Net alkalinity and net acidity: Theoretical considerations. Ap. Geochem. 20, 1920-1964.

KTH, 2010. Visual MINTEQ A free equilibrium speciation model, version 3.0, beta version. http://www.lwr.kth.se/English/OurSoftware/vminteq/index.html. Accessed 15 September 2010.

Kruse, A.S.N, Gozzard, E., Jarvis, A.P., 2009. Determination of hydraulic residence times in several UK mine water treatment systems and their relationship to iron removal. Mine Wat. Environ. 28, 115-123.

Kuyucak, N., St-Germain, P., 1994. In situ treatment of acid mine drainage by sulfate reducing bacteria in open pits: scale-up experiences, in: Proceedings of the International Land Reclamation and Mine Drainage Conference, pp 303-309.

Morin, K., Hutt, N., 1997. Prediction of mine site-drainage chemistry through closure using operational monitoring data. J.Geochem. Expl. 73, 123-130.

Neculita, C.M., Zagury, G.J., 2008. Biological treatment of highly contaminated acid mine drainage in batch reactors: Long-term treatment and reactive mixture characterization. J. Hazard. Mater. 157. 358-366.

Neculita, C.M., Zagury, G.J., Bussiere, B., 2008a. Effectiveness of sulphate-reducing passive bioreactors for treating highly contaminated acid mine drainage: I. Effect of hydraulic retention time. Ap. Geochem. 23, 3442-3451.

Neculita, C.M., Zagury, G.J., Bussiere, B., 2008b. Effectiveness of sulphate-reducing passive bioreactors for treating highly contaminated acid mine drainage: II. Metal removal mechanisms and potential mobility. Ap. Geochem. 23, 3545-3560.

Neculita, C.M., Vigneault, B., Zagury, G.J. 2008c. Toxicity and metal speciation in acid mine drainage treated by passive bioreactors. Environ. Toxicol. Chem. 27, 1659–1667.

Perkins, E.H., Nesbitt, H.W., Gunter, W.D., St-Armand, L.C., Mycroft, J.R., 1995. Critical review of processes and geochemical models adaptable for prediction of acidic drainage from waste rock, in: Mine Environment Neutral Drainage (MEND), Report 1.42.1. CANMET secretariat, Ottawa, Ontario.

Postgate, J.R., 1984. The sulfate-reducing bacteria (2end edition). Cambridge University Press: Cambridge.

Potts, P.J., 1987. A Handbook of Silicate Rock Analysis, Blakie & Son Ltd.

Potvin, R., 2009. Évaluation à différentes échelles de la performance de systèmes de traitement passif pour des effluents fortement contaminés par le drainage minier acide. PhD. Dissertation, Chaire industrielle CRSNG Polytechnique – UQAT, Rouyn-Noranda, Canada, pp 1-365.

Roche, N., Bendounan, R., Prost, C., 1994. Modélisation de l'hydrodynamique d'un décanteur primaire de station d'épuration. Rev. Sci. Eau 7, 153-167.

Rouhani, P., Champagne, P., Van Geel, P., 2003. Impacts of hydraulic and constituent loading on a combined passive system for the treatment of acid mine drainage. 8ième conférence spécialisée sur le génie de l'environnement et durable de la société canadienne de génie civil. Moncton, New-Brunswick, Canada, 4-7 juin 2003, 10 pp.

Skoog D., West D., Holler J., 1997. Fundamentals of analytical chemistry, 7th edition. De Boek Uniuversité, Paris, Bruxelle.

Skousen, J.G., Ziemkiewicz, P.F., 2005. Performance of 116 Passive Treatment Systems for Acid Mine Drainage, in: ASMR, 3134 Montavesta Rd. Publication, Proceeding of the National Meeting of the American Society of Mining and Reclamation, Breckenridge, Lexington.

Trumm, D., 2006. Methodology to Determine Management Strategies. document CRL Energy Ltd, 14 pp.

Waybrant, K.R., Blowes, D.W., Ptacek, C.J., 1998. Selection of reactive mixtures for use in permeable reactive walls for treatment of acid mine drainage. Environ. Sci. Technol. 32, 1972-1979.

Zagury, G.J., Colombano, S. M., Narasiah, K.S., Ballivy, G., 1997. Stabilisation de résidus acides miniers par des résidus alcalins d'usines de pâtes et papier. Environ. Technol. 18, 959-973.

CHAPITRE 6

APPLICATION DES TRAVAUX DE RECHERCHE AU CAS DU SITE LORRAINE

Cette partie décrit la construction de la filière de traitement multi-étape d'un DMA fortement contaminé au fer sur le site minier abandonné Lorraine au Témiscamingue (Québec). Les travaux ont été financés par le ministère des ressources naturelles et fauniques du Québec.

6.1 Mise en contexte

Le site minier Lorraine à Latulipe, au Témiscamingue, est un site minier abandonné depuis 1968. La mine a exploitée plus de 600 000 tonnes de minerai contenant du cuivre, du nickel, de l'or et de l'argent, et entreposées les rejets de concentrateur générés par l'opération sur une superficie d'environ dix hectares (Potvin, 2009). Les minéraux sulfureux présents dans les rejets sont principalement la chalcopyrite, la pyrite, la pyrrhotite et la pentlandite.

Le site est générateur de DMA et a été restauré à partir de 1998 avec une couverture avec effets de barrière capillaire (CEBC). Celle-ci, placée sur les résidus générateurs d'acide, vise à contrôler la migration de l'oxygène (ce qui permet de limiter la production de DMA). La performance du système de recouvrement a été évaluée et présentée dans différentes publications au cours des dernières années (e.g. Dagenais 2005; Dagenais et al. 2005; Bussière et al. 2009). Même si le système de recouvrement est efficace pour limiter la migration de l'oxygène de l'atmosphère jusqu'aux résidus générateurs de DMA, l'eau contaminée contenue dans les pores va prendre un certain nombre d'années avant d'être évacuée. C'est pourquoi elle est récupérée et amenée vers trois drains dolomitiques anoxiques (DOL-1 à DOL-3) visant à traiter l'eau contaminée. La Figure 6.1 montre la qualité des eaux sortant des trois drains dolomitiques au cours des trois dernières années.

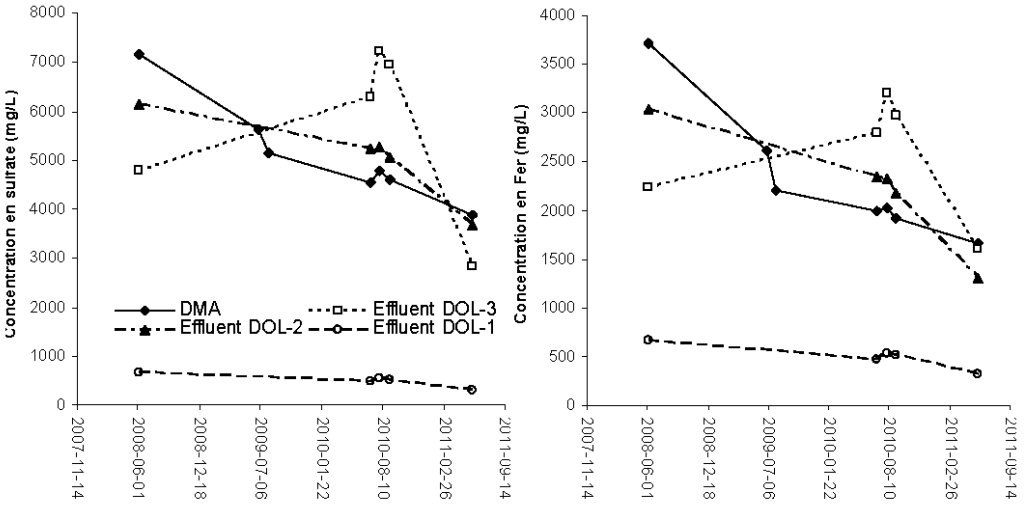

Figure 6.1 Analyses de la concentration en fer et sulfate en sortie des drains DOL-1 à 3

La concentration en fer à la sortie du drain DOL-3 est élevée (2803 mg/L en moyenne de 2008 à 2010) et souvent même plus grande que la concentration dans le DMA (2301 mg/L en moyenne). Des trois drains dolomitiques en place, la concentration en fer sortant du drain DOL-3 est la plus élevée en moyenne. On peut également noter que l'efficacité du drain DOL-1 est supérieure avec des concentrations en fer qui ont diminuées jusqu'à 500 mg/L en moyenne. En ce qui concerne le drain DOL-2, la performance de rétention du fer est faible mais légèrement supérieure à celle du drain DOL-3. Il en va de même pour la concentration en sulfates qui suit la même tendance que le fer à des concentrations de 5395 mg/L en moyenne à la sortie du DOL-3 et 5095 mg/L en moyenne dans le DMA. Le pH moyen à la sortie du drain DOL-3 est autour de 5 durant l'année 2010 par rapport à 4,4 pour le DMA (voir Potvin, 2009, pour les détails sur l'évolution des pH depuis la construction des drains).

La Figure 6.2 présente quant à elle l'évolution des débits à la sortie des drains. On remarque que le débit chute dans le drain DOL-3 au cours du temps. En parallèle, du DMA commence à s'accumuler sur le dessus du drain (voir Figure 6.3). Tout ceci tant à supposer que le drain DOL-3 se serait colmaté au cours du temps.

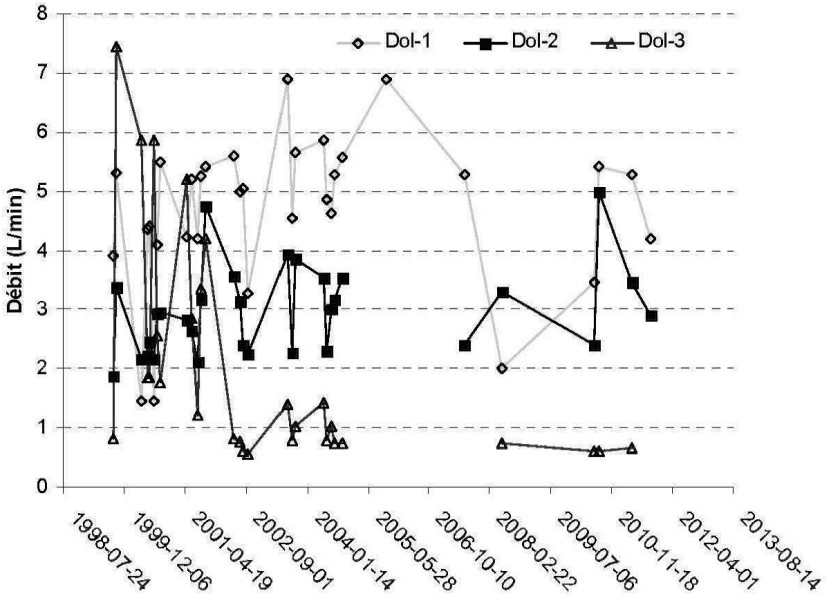

Figure 6.2 Évolution des débits en sortie des drains (adapté et modifié de Potvin, 2009)

Figure 6.3 Accumulation de DMA sur le dessus du drain DOL-3 en 2007

Étant donné que le drain DOL-3, en place actuellement sur le site Lorraine, ne permet pas de traiter les fortes concentrations en fer et qu'il semble bouché, une filière de traitement est proposée dans ce qui suit afin de remplacer le DOL-3. La conception proposée ici se base principalement sur les essais en laboratoire présentés dans les chapitres 2 à 5. La filière de traitement proposée est celle présentée au chapitre 5. Une première section du traitement contiendra un BPSR dont le rôle est de diminuer le Eh, de diminuer un peu la concentration en métaux et de neutraliser le DMA. Par la suite, l'effluent entre dans un filtre contenant des cendres de bois, qui aura pour rôle de diminuer la concentration de fer par sorption et précipitation. Enfin, l'effluent est traité dans un dernier BPSR qui précipitera et adsorbera le reste des métaux.

6.2 Conception du système de traitement

La section suivante présente plus en détails le design de la filière de traitement du DMA riche en fer proposée pour traiter les eaux du site Lorraine.

6.2.1 Dimensionnement de la filière de traitement

Le système sur le terrain est composé de trois zones distinctes, dimensionnées selon le débit d'alimentation de 5 L/min (correspondant au débit moyen de la première année après la construction du drain). Les quantités de matériaux sont estimées selon les masses utilisées dans le modèle présenté au chapitre 5.

- **Zone 1** : Traitement sur biofiltre sulfato-réducteur avec le mélange de biofiltre #4
  - Temps de rétention hydraulique : 3,4 jours
  - Débit de traitement maximal : 5 L/min
  - Pourcentage de vide estimé (porosité) : 50%
  - Volume de la zone : 49 m^3
  - Masse de mélange n° 4 : 36 000 kg

- **Zone 2** : Traitement sur filtre avec de la cendre de cogénération du bois

- Temps de rétention hydraulique : 3,4 jours. Ce temps de rétention est plus long que celui nécessaire à la sorption (voir chapitre 4, Table 4.5). Toutefois, la surdimension de cette section assure une durée de vie plus importante au système. Basé sur les résultats de détermination de la capacité maximale de rétention du fer (chapitre 4, 35 mg Fer/g de cendre à pH 6), on estime la durée de vie avant saturation de la section à environs 3 ans (sans tenir compte de la période hivernal de réduction du débit).

- Débit de traitement maximal : 5 L/min

- Pourcentage de vide estimé (porosité) : 50%

- Volume de la zone : 49 m^3

- Masse de cendre : 30 000 kg

- **Zone 3** : Traitement sur biofiltre sulfato-réducteur avec le mélange de biofiltre #1

- Temps de rétention hydraulique : 4,2 jours

- Débit de traitement maximal : 5 L/min

- Pourcentage de vide estimé (porosité) : 50%

- Volume de la zone : 60 m^3

- Masse de mélange n^o 1 : 29 000 kg

Le choix de trois sections distinctes plutôt qu'une comprenant un mélange de tout les matériaux a été fait de façon à assurer : i) des ratios carbone / azote satisfaisants pour les BPSR; ii) la possibilité de changer les matériaux d'un compartiment facilement sans avoir à refaire tout le système; iii) un traitement optimal d'après les essais préliminaires en laboratoire.

Le volume total du système est alors de 158 m^3. En considérant que l'espace disponible est de 45 m de long sur 10 m de large environ, un système de 45 mètres de long et de section de 3,5 m^2 (3.5m de large x 1m de hauteur approximativement) est creusé après avoir retiré les matériaux du drain DOL-3. La Figure 6.4 montre l'excavation du drain

Figure 6.4 Excavation du drain DOL-3

Une pente de 1% est suggérée afin de favoriser l'écoulement dans le système. Les relevés topographiques faits en aout 2011 montrent que la pente actuelle du DOL-3 est déjà très proche de 1%.

Le plan en coupe du système est présenté à la Figure 6.5.

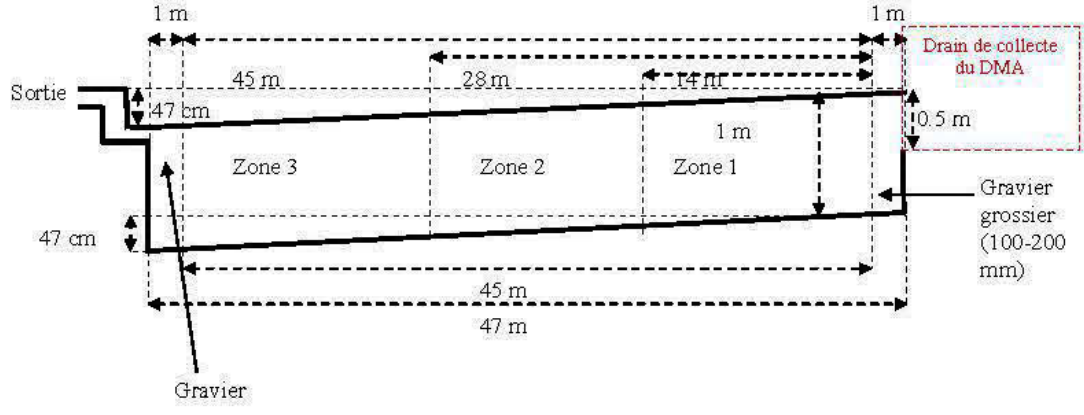

Figure 6.5 Plan en coupe du système proposé

Les compartiments à l'entrée et à la sortie contiennent du gravier régulier et du gravier grossier, ce qui permet de filtrer l'effluent à la sortie et de bien distribuer le DMA à l'entrée. Le volume de ces compartiments est d'environ 3,5 m^3 chacun. La sortie du système consiste en un tuyau en PVC de 10 cm de diamètre. La sortie sera à 45 cm au-dessus de la hauteur du système afin de s'assurer que tous les matériaux se trouvent en condition anoxique. Ce tuyau sortira de la partie contenant du gravier, en fin de système de traitement. De la pierre (100-200 mm) et de la terre sont déposées pour permettre de faire une digue à la sortie.

De la géomembrane en HDPE (type Solmax 460T-2000) a été utilisée pour créer une tranchée étanche. La profondeur de creusage respecte celle du DOL–3 déjà mis en place et longe en grande partie le socle rocheux. Les géomembranes sont toujours déposées sur une couche de géotextile afin de les protéger d'éventuels bris lors du dépôt des matériaux. La mise en place de la géomembrane et du géotextile en fond de système est présentée aux Figures 6.6 et 6.7. Afin d'assurer les conditions anoxiques dans le système, un recouvrement également constitué d'une géomembrane en HDPE et d'un sol d'une épaisseur de 0,5 m à 1 m est mis en place par-dessus le système (Zaluski et al., 2003).

Figure 6.6 Mise en place du géotextile

Figure 6.7 Mise en place de la géomembrane

6.2.2 Dimensionnement du drain d'alimentation du système de traitement

À l'entrée de la filière de traitement, il est nécessaire de collecter toutes les eaux qui s'écoulent de la digue. Pour cela, un système de drain collecte cette eau et l'amène vers la partie traitante. Un schéma de la configuration du drain est présenté à la Figure 6.8. Le drain est à cheval dans la digue et hors de celle-ci. Le volume de ce drain est d'environ 50 m^3. Cette partie sera remplie de gravier grossier (100 à 200 mm), tout comme le premier compartiment de 3,5 m^3 de la partie traitante du système (voir Figure 6.9). Une géomembrane permet d'assurer l'imperméabilité du système sur le dessus afin d'empêcher les infiltrations d'eau (Figure 6.10).

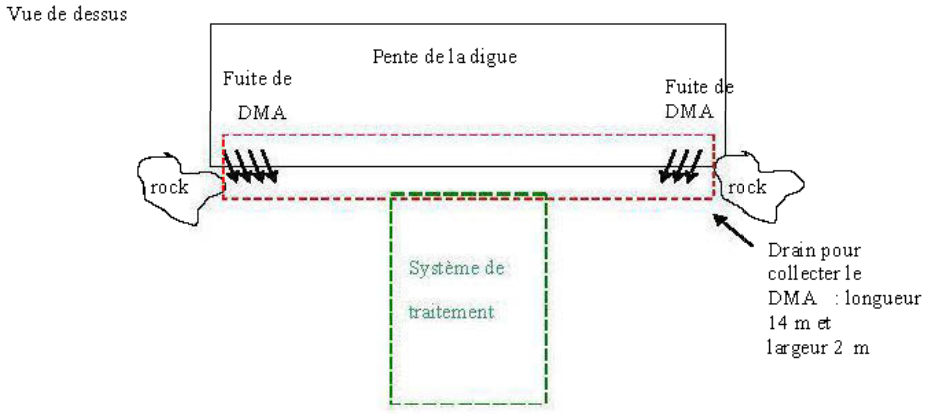

Figure 6.8 Schéma du système de collecte du DMA

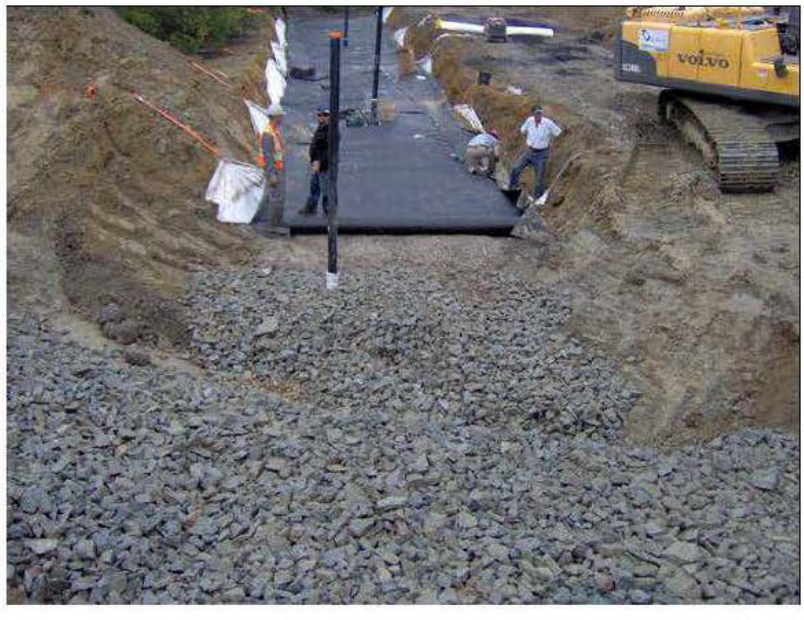

Figure 6.9 Remplissage du drain de collecte du DMA par de la pierre grossière

Figure 6.10 Mise en place de la géomembrane supérieure sur le système de traitement et le drain de collecte du DMA

6.2.3 Quantité et propriétés de matériaux utilisés dans la filière de traitement

Une légère variation est apportée aux mélanges des biofiltres par rapport aux essais dans le modèle et dans les colonnes des chapitres 2 à 5. En raison du coût élevé du carbonate de calcium de grade industriel, de la calcite concassée d'origine locale (pureté de l'ordre de 94%, pourcentage passant à 2 mm : 96%, à 0,149 mm : 58,5%, à 0,074 mm : 39%) seront utilisés à la place. Toujours pour des raisons économiques, l'ajout d'urée (nutriment azoté) n'est pas effectué, d'autant plus que le fumier de volaille utilisé est riche en azote (2.6%). La sciure et les copeaux de bois d'érable ont été remplacés par des copeaux de trembles disponibles localement. La granulométrie des copeaux est toutefois supérieure (très variable, de l'ordre d'un cm à plusieurs cm). Aucnn ajout de sédiments dans les mélanges (comme source de bactéries sulfato-réductrices) est effectué étant donné que le fumier et le compost contiennent déjà ce type de bactéries (Tableau 6.1). Le second compartiment utilisé pour la rétention du fer contient uniquement de la cendre de bois, riche en carbone organique et dont la capacité de sorption a été démontrée dans le chapitre 4. Finalement, l'utilisation de

matériaux régionaux a été privilégiée afin de limiter les coûts de transport. La composition des mélanges pour BPSR de type #1 et #4 est présentée au Tableau 6.2.

Tableau 6.1 Propriétés des matériaux utilisés dans le système (COT=carbone organique total, CT=carbone total, NTK azote totale Kjeldahl, COD=carbone organique dissous à partir d'un extrait solide liquide 1 :10, BSR=bactérie sulfato-réductrice)

Materiaux	Copeaux de tremble	Fumier de volaille	Compost de feuilles	Carbonates concassés	Cendres de bois
Provenance	Ville-Marie	Rivière-Héva	Québec	New-Liskard	Kirkland-Lake
pH	5.8	6.0	6.7	-	12.2
COT (%w/w dry weight)	44	26	24	-	19
CT (%w/w dry weight)	-	-	-	11.4	36
NTK (%w/w dry Weight)	0.063	2.6	1.3	-	-
COD (mg/L)	35	57	48	-	-
BSR (cellules/100 mL)	<2	450	780	-	-
% Carbonate de calcium basé sur le CT	-	-	-	94%	-

Tableau 6.2 Composition des BPSR sur le terrain (% massique en matériaux secs)

Composants	#1	#4
Copeaux de trembles	36	18
Fumier de volaille	17	10
Compost de feuilles	24	12
Sable	21	10
Carbonate concassé	2	50

Compte tenu de l'humidité des matériaux, de la perte de matériaux lors du transport, de la manutention et des mélanges, les masses totales de matériaux acheminés sur le site sont les suivantes (Tableau 6.3).

Tableau 6.3 Masse de matériaux pour le système complet (avec un facteur de sécurité de 10%)

Composants	Masse (tonnes)
Copeaux de trembles	20 t
Fumier de volaille	10 t
Compost de feuilles	28 t
Sable	10 t
Carbonate concassé	20 t
Cendre de cogénération	36 t

Le mélange des matériaux est réalisé par une chargeuse et le dépôt dans le système par une pelle mécanique (voir Figures 6.11 et 6.12).

Figure 6.11 Mélange des matériaux avec une chargeuse

Figure 6.12 Dépôt des matériaux dans la filière de traitement

6.2.4 Devenir de la dolomite remplissant le DOL-3

La dolomite se trouvant actuellement dans le drain a été enlevée puis déposée directement sur le recouvrement multicouche du site (Figure 6.13). En effet, une étude récente montre que les éléments constituant l'eurobage de la dolomite ne seraient pas facilement remobilisables au contact de l'eau (Potvin, 2009). Cette étude a en effet montré que l'enrobage de la dolomite du drain DOL-3 est constitué principalement de gypse et de goethite (qui sont déjà sous une forme assez stable en conditions aérobies). De plus, le fer est presque le seul métal à avoir été retenu dans le drain DOL-3. Enfin, si cet enrobage venait à relarguer des polluants, ces derniers seraient alors contenus sur le parc à rejet puis retraités par le nouveau système de traitement.

Figure 6.13 Dolomite sur le parc à résidu restauré

6.2.5 Instrumentation de la filière de traitement

La filière de traitement est instrumentée de façon à suivre les performances de chaque partie du traitement. Pour cela, les paramètres suivants sont suivis, grâce à des sondes autonomes, à l'entrée et sortie de chaque compartiment :

- Le pH : Il permet de suivre la neutralisation;
- Le Eh : Il permet de vérifier si l'eau se trouve dans des conditions réductrices;
- La température : elle permet le suivi des performances en fonction de la température;
- Des piézomètres dans chaque section de traitement : pour un prélèvement ponctuel d'échantillons afin d'analyser les métaux, l'acidité et l'alcalinité.

La figue 6.14 montre le concept de l'instrumentation.

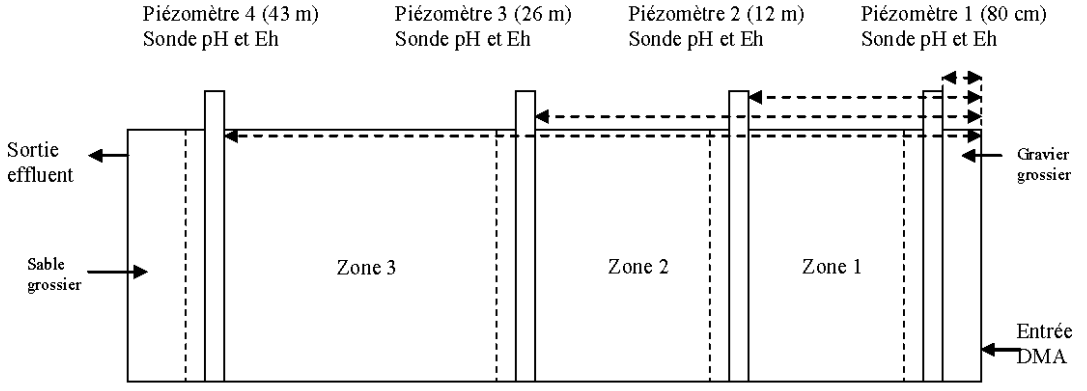

Figure 6.14 Instrumentation de la filière

6.3 Conclusion

La conception de la filière de traitement présentée dans ce chapitre résulte des conclusions des essais en laboratoire déterminés au cours de ce doctorat et de plusieurs autres études (e.g. Neculita, 2008, Potvin, 2009). De plus, le remplacement du drain DOL-3 qui ne fonctionnait pratiquement plus est l'occasion de réhabiliter un site affecté par un DMA fortement contaminé (Figure 6.15 présentant le site après les travaux) d'autant plus que le coût associé à la construction du système de traitement passif est relativement faible. Cet essai grandeur nature est très important dans la compréhension des mécanismes de traitement des DMA fortement contaminés en fer. En effet, il permettra principalement de déterminer l'effet d'échelle sur les performances de traitement ainsi que d'évaluer l'effet des conditions climatiques sur la performance de neutralisation et de rétention des métaux du système de traitement proposé.

Figure 6.15 État du site après la mise en place de la filière de traitement du DMA

CHAPITRE 7

CONCLUSIONS ET RECOMMANDATIONS

7.1 Sommaire

L'utilisation de filières de traitement est l'une des solutions les plus prometteuses pour traiter les drainages miniers acides (DMA) fortement contaminés en fer. Ainsi, la rétention des métaux et la neutralisation de l'acidité peuvent être effectuées par différents mécanismes et en plusieurs étapes.

Cette thèse est la suite logique des travaux de doctorat de C. Neculita (2008) et R. Potvin (2009) qui ont travaillé sur les systèmes passifs biologiques (biofiltres passifs sulfato-réducteurs, BPSR) et abiotiques (drains calcaires anoxiques et oxiques) pour traiter des DMA fortement contaminés en fer (plus de 500 mg/L). Toutefois, ces études (ainsi que les chapitres 2 et 3 de cette thèse) ont montré que de tels systèmes, utilisés seuls pour traiter un DMA fortement contaminé en fer, ne sont pas efficaces (peu de réduction du fer, problèmes de colmatage par des hydroxydes de fer, toxicité de l'effluent causée par le fer). Dans cette thèse, l'emphase a donc été mise sur les différentes options de traitement pour le DMA fortement chargé en fer.

L'approche adoptée dans cette étude pour rechercher une solution au traitement de tels DMA peut être divisée en cinq étapes :

1. Caractérisation physique et chimique des matériaux locaux potentiellement utilisables dans un système passif. Ces analyses permettent de mettre en lumière la capacité de certains matériaux, telle la matière organique, à soutenir l'activité des bactéries sulfato-réductrices (BSR), de démontrer une capacité de neutralisation et/ou une prédisposition favorable aux phénomènes de sorption.
2. Tests en batch (≈500 mL). Cette étape permet de pré-sélectionner les matériaux et les mélanges réactifs les plus prometteurs pour les BPSR. De plus, elle permet de

caractériser les propriétés de sorption des métaux de certains matériaux (matière organique et cendres par exemple).

3. Tests en colonne (≈10 L). Cette étape est capitale afin de déterminer l'efficacité dans le temps des systèmes en conditions plus réalistes et d'évaluer les performances hydrauliques. De plus, les paramètres d'opération, tels le temps de rétention hydraulique (TRH) et l'ordre dans lequel les procédés peuvent s'enchaîner dans une filière de traitement, sont évalués dans ce type d'essai. À la fin des essais, la solution la plus prometteuse pour traiter un DMA fortement chargé en fer peut être identifiée.
4. Test en réacteur de 2 m^3. Ce test final permet de vérifier l'efficacité de la filière de traitement déterminée à l'étape précédente, dans une configuration plus réaliste. De plus, la quantité de matériaux utilisée dans le réacteur, la géométrie et le TRH servent de base pour les calculs servant à la conception d'un système grandeur réelle.
5. Construction de la filière de traitement grandeur réelle. Cette dernière étape fait la synthèse de toutes les observations obtenues durant les essais en laboratoire. Elle tient compte des propriétés chimiques et hydrogéologiques des matériaux.

La méthodologie présentée ci-dessus se retrouve donc dans la thèse à travers les cinq chapitres principaux. On présente dans ce qui suit les principales conclusions, contributions et recommandations de chacun de ces chapitres.

7.2 Chapitre 2

Dans cette étude, les matériaux utilisés pour concevoir les mélanges utilisés dans les BPSR pour le traitement d'un DMA fortement concentré en fer ont été caractérisés pour leur propriété de sorption du fer. Les essais de sorption ont montré principalement que les matières organiques (i.e. fumiers, boues des eaux usées municipales et le compost végétal) sont les substrats les plus performants pour enlever le fer. Plus précisément, la relation à l'équilibre entre le fer en solution et le fer adsorbé à la surface du solide est principalement proche du modèle de Freundlich (en d'autres termes, la sorption s'est produite sur une surface hétérogène) aux deux pH testés (3 et 6). La cinétique de réaction de sorption du fer peut être décrite pour la plupart des matériaux testés à pH 3 et 6, par une équation de pseudo-second ordre; modèle qui représente souvent une liaison forte entre la surface du matériau et les

cations métalliques (chimisorption). Toutefois, la cinétique de sorption est plus rapide à pH 6 qu'à pH 3.

Par la suite, huit mélanges différents pouvant constituer un BPSR ont été comparés pour leur capacité à traiter un drainage minier acide (pH 3.5 et [Fe] = 4000 mg/L) en utilisant des tests batch de 40 jours. Les essais batch ont été utilisés pour identifier rapidement (et de façon préliminaire) les meilleurs mélanges pour BPSR. Pour la plupart des mélanges testés, le pH augmente jusqu'à 7.5-8, le potentiel redox diminue en dessous de 0 mV après 10 jours d'essai et les concentrations de métaux dissous ont été réduites de plus de 99%.

Les principales conclusions des essais batch peuvent être résumées ainsi. Premièrement, les différents matériaux organiques (fumiers de poules, vaches, moutons et les boues municipales) pourraient être utilisés indifféremment sans affecter de manière significative les performances d'un BPSR. La présence de sédiments comme inoculum de bactéries n'est pas essentielle car d'autres matériaux contiennent déjà des bactéries sulfato-réductrices (fumier, compost végétal). De plus, l'ajout de 50% en masse d'agent structurant (calcite fine ou sable) pour améliorer les propriétés hydrauliques n'a pas affecté de manière significative l'efficacité de rétention des métaux. La réduction des sulfates n'est pas le mécanisme principal de traitement des métaux au début du test; la sorption joue un rôle important pendant les premières étapes du processus. Finalement, les mélanges les plus prometteurs (i.e. #1, #4 et #7, avec ou sans 50% d'agent structurant) ont été sélectionnés et ont été utilisés dans les essais en colonne afin d'évaluer leur comportement hydraulique et leur performance de rétention des métaux en conditions dynamiques.

En termes de contributions scientifiques, cette partie de la thèse présente pour une rare fois une caractérisation du pouvoir de sorption du fer des matériaux organiques utilisés dans les mélanges réactifs pour BPSR dans le cadre du traitement passif du DMA. De plus, par rapport aux travaux de Neculita (2008) et Potvin (2009), ce travail étudie l'effet de l'augmentation de la proportion d'agent structurant (jusqu'à plus de 50% en masse), l'impact d'ajouter ou non des sédiments comme source bactérienne, le remplacement d'un type de fumier par un autre et enfin l'utilisation ou non de nutriments comme l'urée.

Étant donné que la sorption est un phénomène grandement fonction du pH, de la température et de la force ionique de la solution, les principales recommandations sont d'effectuer plusieurs tests supplémentaires en variant les paramètres présentés précédemment, afin de mieux décrire la sorption des métaux à la surface des matériaux utilisés dans le biofiltre. Ces tests pourront d'ailleurs être réalisés en duplicata de façon à valider statistiquement leur qualité. De plus, la détermination du pH de la charge nulle de surface des matériaux permettrait aussi de comprendre pourquoi certains matériaux ont une mauvaise capacité de sorption dans les conditions acides du DMA (cas des copeaux et de la sciure). Enfin, une meilleure détermination des fonctions organiques présentes en surface des matériaux (par FTIR par exemple) permettrait de mieux comprendre la rétention des métaux par sorption.

7.3 Chapitre 3

Les efficacités à long terme (plus de 450 jours) de trois BPSR en colonne (10,7 L, mélanges #1, #4 et #7) ont été évalués pour le traitement d'un DMA ayant une concentration élevée en fer (entre 1000 et 4000 mg/L). Les résultats présentés dans ce chapitre montrent que la performance de traitement du fer avec les BPSR est limitée. Néanmoins, le pH en sortie des colonnes est augmenté à 6 en moyenne. Les métaux comme Al, Cd, Cr, Ni, Pb et Zn sont relativement bien retenus dans les colonnes mais le fer reste présent à une concentration élevée (environ 3190 mg/L à 3387 mg/L en moyenne). Cette concentration élevée en fer dans les effluents de BPSR conduit à une acidité élevée provoquant une diminution du pH de l'effluent après quelques heures d'exposition aux conditions de laboratoire (exposé à l'air). La méthode choisie pour comparer l'efficacité des colonnes a été de déterminer le pourcentage de la concentration en métal initiale qui a été retenue. Toutefois, d'autres méthodes de comparaisons auraient pu être utilisées tel le calcul de la masse de fer retenue par colonne.

Par ailleurs, aucune réelle différence n'a été observée entre les trois mélanges testés. L'efficacité de rétention des métaux a été légèrement affectée par le TRH. De plus, l'ajout de 50% en masse d'agent structurant (sable calcique ou sable) pour améliorer les propriétés hydrauliques n'a pas affecté de manière significative l'efficacité d'élimination de métaux comme dans les tests batch. Les mesures de conductivité hydraulique saturée ont montré aussi que l'ajout d'une proportion plus grande d'agent structurant n'a pas vraiment permis

d'améliorer les propriétés hydrauliques. Toutefois, la colonne #7 voit son k_{sat} diminué à la fin de la période d'essai. Cependant, aucun changement de texture n'a été observé lors du démantellement de la colonne. Cette diminution de k_{sat} pourrait provenir de bulles de gaz resultant de la décomposition de la matière organique dans la colonne (mauvaise saturation). Un test de traceur effectué en fin de test sur la colonne contenant le mélange #4 (composé de 50% en masse de mélange organique pour BPSR et 50% en masse de calcite fine) n'a démontré aucun changement significatif de la porosité, pour la période testée. Les différents résultats permettent donc de conclure que les phénomènes de colmatage n'ont pas été présents de façon significative dans les BPSR testés.

Enfin, la caractérisation des mélanges après démantèlement des colonnes a montré que le fer (l'élément le plus problématique à traiter dans le DMA) a été principalement retenu par la formation d'hydroxydes ou d'oxyhydroxydes et par précipitation de sulfures. Les extractions séquentielles réalisées pour fractionner les métaux retenus dans le biofiltre auraient pu être réalisées en plus du milieu sur le haut et le bas de la colonne. La literrature (e.g. Neculita et al., 2008b) montre d'ailleurs que les métaux ne sont pas distribués éagalement sur toute la longeur de la colonne (cas d'une colonne alimentée par le haut). Toutefois, en raison du nombre important d'analyses que cela aurait impliqué et de l'absence de preuve visuelle lors du démantèlement d'un comportement différent entre le haut et la bas du système, il a été jugé pertinent de faire les analyses uniquement sur le milieu de la colonne, qui représente alors une moyenne de ce que l'on retrouve dans le biofiltre.

La principale contribution de cette partie de la thèse est de démontrer que l'utilisation seule d'un BPSR pour traiter un drainage minier acide concentré en fer (dans ce chapitre entre 1000 et 4000 mg/L; concentrations nettement plus élevées que celles testées par les autres chercheurs dans la littérature, mais fréquemment retrouvées sur le terrain) n'est pas une option viable à long terme et ce, pour tous les mélanges testés. De plus, cette étude a permis de déterminer quel type de traceur (NaCl) peut être utilisé dans le BPSR afin de déterminer le TRH réel; on ne retrouve à notre connaissance pratiquement aucune tentative de ce genre dans la littérature. Enfin, les travaux ont montré que l'utilisation de colonnes ayant une alimentation en DMA du bas vers le haut prévient aussi le colmatage du système.

Ce chapitre montre que les BPSR intègrent plusieurs procédés pour le traitement des DMA. Tout d'abord, les phénomènes de rétention des métaux y sont très diversifiés (sorption, précipitation sous différentes formes, etc.). La caractérisation des matériaux après utilisation est ainsi difficile à réaliser étant donné que les phases minérales précipitées sont peu stables dans les conditions des analyses. Par exemple, les sulfures biogéniques risquent de s'oxyder très rapidement au contact de l'oxygène. L'analyse effectuée alors sur un échantillon sec (ce qui est le cas pour la plupart de nos analyses post-démantèlement) s'en trouvera biaisée si celui-ci n'est pas séché sous azote par exemple. C'est pourquoi on suggère de tester d'autres techniques d'analyse de surface des solides telle que la XPS (spectrométrie des photoélectrons X). Cela permettrait de mieux cerner les mécanismes de traitement. En outre, il sera alors plus facile de différencier la précipitation et la sorption en sachant avec quel type d'atome ou groupement le métal est associé. L'avantage des analyses XPS est que l'on peut pratiquer directement l'essai sur un échantillon congelé (prévenant ainsi l'altération des phases précipitées). Une autre recommandation de ce chapitre serait de mener une étude microbiologique de l'influence sur l'activité microbienne du biofiltre du sel utilisé lors du test de traceur.

7.4 Chapitre 4

Ce chapitre porte sur la caractérisation des cendres de bois vis-à-vis du traitement d'un DMA fortement chargé en fer. Les cendres de bois sont des matériaux à faibles coûts et disponibles localement. Les cendres sont aussi connues pour leurs propriétés de rétention des métaux et pour leur pouvoir neutralisant. Elles sont donc des matériaux ayant un bon potentiel d'utilisation dans une filière de traitement où son principal rôle est alors de réduire la concentration en fer avant un traitement final par BPSR. Au préalable, des tests sur plusieurs matériaux reconnus pour avoir de bonnes propriétés de rétention des métaux (exemple de la tourbe, voir Appendice C) ont montré que les cendres de bois avaient un potentiel de sorption supérieur.

Trois matériaux à base de cendres ont été testés : les cendres de bois (matériel initial), la partie riche en carbone des cendres (obtenue par flottation) et les cendres de bois fines (tamisées en dessous de 1,18 mm de diamètre). Les résultats de la caractérisation ont montré

que les cendres ont une surface spécifique élevée (entre 46 à 159 m^2/g), une haute teneur en carbone organique (entre 12 et 32%) et des pH de pâte élevés (jusqu'à 12,2).

Les isothermes de sorption du fer correspondent au modèle de Freundlich pour les cendres de bois, le carbone et les cendres de bois fines et ce, autant à pH 3 qu'à pH 6. Cependant, l'étape limitante lors de la sorption du fer dépend du matériel et du pH : réaction de pseudo-second ordre à la surface du matériau (pour la cendre et le carbone à pH 3, la cendre tamisée à 1,18 mm à pH 6) ou une diffusion interne (carbone à pH 6, la cendre tamisée à 1,18 mm à pH 3) et externe (la cendre à pH 6) du fer vers la surface du grain.

Par la suite, cinq colonnes de 1,7 L avec différents mélanges de cendres et de sable (cendres de bois, cendres de bois et 30% massique de sable, cendres de bois et 60% massique de sable, cendres de bois fines et carbone) ont été étudiées pour enlever les métaux d'un effluent de BPSR. Les colonnes ont permis de déterminer que les cendres de bois seules sont les plus efficaces pour retenir le fer; elles diminuent la concentration de fer au cours d'une période de plus de cent jours en dessous de 10 mg/L (99% d'élimination du fer).

Le fer est retenu principalement sous forme d'hydroxydes ou oxyhydroxydes. En effet, les analyses au microscope électronique à balayage (MEB) ont montré une superposition de fer et d'oxygène (possible pour des oxydes ou hydroxydes) et les résultats de l'analyse par diffraction des rayons X (DRX) proposent la formation de goethite. Enfin, l'extraction séquentielle met en évidence que le fer est principalement contenu (de 73,4 à 51,1%) dans une fraction réductible ou lié à des oxydes-hydroxydes de Fe-Mn. La sorption pourrait également jouer un rôle important puisque la fraction correspondant aux phases liées à de la matière organique n'est pas négligeable pour chaque matériau. Le deuxième élément important retenu dans les colonnes est le sulfate. En effet, la concentration de sulfate du DMA a diminué de manière significative (entre 43 et 51% de rétention selon la colonne), essentiellement par précipitation de sulfate de calcium (gypse ou anhydrite).

Enfin, le risque de colmatage du système est négligeable pour la période testée puisque la conductivité hydraulique saturée est restée stable durant la réalisation des essais, dans la gamme de $5{,}0 \times 10^{-3}$ cm/s à $3{,}1 \times 10^{-2}$ cm/s.

La contribution majeure de ce chapitre est l'étude de l'utilisation des cendres de bois d'une usine de cogénération afin de traiter un DMA. À notre connaissance, cette étude propose l'une des premières caractérisations détaillées de la capacité de traitement du fer par sorption dans un effluent de BPSR. De plus, des caractérisations utilisant différentes techniques minéralogiques (MEB, DRX), chimiques (extractions séquentielles, digestions acides), thermiques (thermogravimétrie), physiques (surface spécifique, granulométrie) et hydrauliques (conductivité hydraulique saturée) ont permis de décrire les mécanismes de rétention des métaux et le comportement hydraulique des colonnes.

Tout comme les matériaux organiques (chapitre 3), les techniques d'échantillonnage et de caractérisation à l'étape post-démantèlement peuvent faire changer la spéciation des éléments analysés même si un maximum de précautions est pris lors de la réalisation des tests. Dans le cas des phénomènes de sorption, l'analyse des surfaces par des techniques telles la XPS et la FTIR (spectroscopie infrarouge à transformée de Fourrier) pourrait être poussée davantage afin d'affiner la connaissance des mécanismes de rétention des métaux. De plus, la modélisation géochimique couplée avec ces nouveaux types d'analyses de surfaces permettrait de mieux différencier les phénomènes de précipitation et de sorption entrant en jeu dans la rétention des métaux. Enfin, des tests de traceur et des essais dans des colonnes plus grandes permettraient d'améliorer notre compréhension des propriétés hydrauliques des cendres de bois sur le long terme.

7.5 Chapitre 5

Comme il a été présenté au chapitre 3 et tel que mentionné par Neculita (2008) et Potvin (2009), les BPSR utilisés seuls ne sont pas suffisamment efficaces pour traiter un DMA contenant une forte concentration en fer (> 500 mg/L). Une filière de traitement incorporant plusieurs méthodes de traitement, serait probablement une bonne option pour traiter un tel DMA hautement contaminé.

Dans ce chapitre, l'évaluation des performances d'une filière de traitement pour un DMA fortement contaminé en fer (pH = 3; entre 2000 et 4000 mg/L de fer) est réalisée dans des colonnes placées en série (environs 10 L) et dans un réacteur compartimenté de 2 m^3 environ. La filière comprend trois sections séparées. La première section se compose d'un BPSR

contenant 50% en masse un mélange réactif (fumier, sciure, copeaux d'érable, compost, urée, sédiments et sable) et 50% de calcite fine. Son but premier est de neutraliser l'acidité et de retenir une partie des métaux dissous dans le DMA. La deuxième section contient des cendres de bois qui agissent comme un neutralisant et, surtout, comme un filtre pour le fer (la rétention du fer se fait par sorption et précipitation). La dernière section est composée d'un second BPSR (ayant 2% de calcite) afin d'éliminer les métaux résiduels.

Les résultats ont montré que le pH a augmenté en moyenne autour de 6 dans les colonnes et le réacteur et que le potentiel redox (Eh) a diminué de manière significative à -100 mV dans le second BPSR du réacteur et à approximativement 135 mV à la sortie des colonnes. Le fer a été réduit à environ 100 mg/L dans le réacteur tandis qu'il a été diminué à une moyenne de 712 mg/L dans le traitement en colonnes. Dans le cas du fer, la norme de rejet (3 mg/L) n'est pas respectée. Toutefois, ceci pourrait être corrigé en augmantant légèrement le temps de rétention ou en aérant l'effluent. Les concentrations en Al, Cd, Cr, Ni, Pb et Zn respectent quant à elles les normes de rejets de l'industrie minière.

L'une des différences principales en termes de performances entre les colonnes et le réacteur est le temps pour saturer en fer le système composé de cendres de bois. Pour les colonnes, le fer n'est très bien plus retenu (moins de 45% de rétention) à partir de 300 jours environ (avec un TRH de 19,6 jours). En ce qui concerne le réacteur de 2 m^3, après un an de fonctionnement au même TRH, le fer continue d'être retenu (rétention de plus de 98% à 364 jours d'opération). Ainsi, les résultats présentés dans ce chapitre montrent bien que l'échelle et la configuration de la filière de traitement a un impact sur les performances de traitement à long terme. Par contre, les mécanismes de rétention des métaux sont similaires que ce soit dans le réacteur ou dans les colonnes.

La principale contribution de cette partie est l'utilisation d'une filière de traitement (colonnes ou réacteur de $2m^3$) pour tester le traitement d'un DMA riche en fer (2000 à 4000 mg/L). De plus, une comparaison d'efficacité en fonction de la géométrie et de la taille du réacteur a permis de démontrer l'effet favorable d'un test en plus grand volume sur les performances à long terme des filières de traitement. Enfin, cette étape en réacteur de $2m^3$ permet d'évaluer les quantités de matériaux nécessaires pour la construction à grande échelle d'une telle filière.

Il est important de souligner qu'un test de traceur effectué dans le réacteur a indiqué la présence d'une zone d'écoulement préférentiel. Cela pourrait signifier que le débit d'effluent passant dans chaque piézomètre d'échantillonnage serait peut-être moindre et donc que le temps de rétention serait plus grand que celui théorique. Afin de valider ou rejeter cette possibilité, des tests de traceurs complémentaires pourraient aussi être menés dans chaque piézomètre. Le traceur utilisé ici est du NaCl. Toutefois, ce traceur n'est pas conservatif, c'est-à-dire qu'il est en partie retenu dans le système ce qui n'est pas souhaitable dans un test de traceur. Il serait alors intéressant de tester d'autre traceur tel les traceurs isotopiques par exemple.

7.6 Chapitre 6

Ce dernier chapitre présente la conception et la construction d'une filière de traitement sur le site minier Lorraine au Témiscamingue. La conception se base principalement sur les paramètres utilisés dans le réacteur de 2 m^3. Le système est composé de trois sections tout comme celui présenté au chapitre 5. La construction s'est déroulée sur une semaine en août 2011. Ce système fait 40 m de long sur 3 m de large et 1 m de haut (environ 120 m^3). Le système est dimensionné pour traiter un débit maximal de l'ordre de 5 L/min (temps de rétention hydraulique de 12 jours). Cette filière de traitement permettra ainsi de mieux évaluer l'impact des températures sur les performances de traitement, l'impact des variations de débits et de composition du DMA causées par les précipitations et l'influence du gel hivernal sur la reprise de l'activité bactérienne à la fonte des neiges. À la connaissance de l'auteur, il s'agit d'une première conception et construction d'une filière de traitement utilisant des cendres de bois pour un DMA fortement contaminé en fer dans un contexte climatique similaire à celui du Québec.

Les principales recommandations de ce chapitre sont principalement de suivre la qualité de l'eau en sortie de système afin de vérifier son efficacité, d'évaluer la qualité de l'effluent à la sortie du système d'un point de vue toxicologique (de même que pour le réacteur de 2m^3), d'évaluer l'effet de la température et des précipitations sur les performances du système, puis enfin de déterminer le TRH effectif et de caractériser le comportement hydraulique *in situ* par des essais de traceur.

7.7 Dernières remarques

Le choix d'un système de traitement simple ou d'une filière de traitement dépend beaucoup de la qualité du DMA à traiter et des matériaux disponibles localement. Pour le moment, il n'existe pas réellement de formule permettant de concevoir les systèmes; la conception reste encore essentiellement empirique. Dans le cas des DMA fortement contaminés en fer, les systèmes de traitement se saturent pour la plupart relativement rapidement. Il est donc recommandé d'utiliser ce type de traitement en parallèle avec des méthodes de contrôle qui limitent la génération de drainage minier acide. Par exemple, le site Lorraine au Témiscamingue possède trois traitements passifs (une filière de traitement de type BPSR-cendres-BPSR, et deux drains dolomitiques) qui ne pourraient fonctionner si le parc à résidu n'avait pas été restauré par une couverture à effet de barrière capillaire (CEBC) limitant les flux d'eau à traiter et la diffusion de l'oxygène vers les résidus très réactifs (et donc la production de DMA).

Pour finir, les systèmes passifs permettent d'utiliser des matériaux considérés souvent comme des déchets (fumier, sciure de bois, boues municipales). De tels systèmes peuvent alors devenir une alternative viable afin de recycler une partie ces matériaux. Toutefois, une fois que les systèmes de traitement sont saturés, il faudra alors gérer des matériaux potentiellement contaminés aux métaux lourds. Il serait alors utile de caractériser le comportement environnemental de ces matériaux de façon à les stocker de façon adéquate (Genty et al., 2012). Il serait aussi intéressant de développer des moyens pour récupérer les métaux ayant une valeur économique.

RÉFÉRENCES BIBLIOGRAPHIQUES

Cette liste de références concerne les articles et documents cités dans le résumé et les chapitres 1, 6 et 7. Les références des chapitres 2, 3, 4, 5 et des appendices A, B se trouvent à la fin de chacun des chapitres.

Akcil, A., Koldas, S., 2005. Acid mine drainage: causes, treatment and case studies, J. Clean. Prod. 14, 1139-1145.

Alvarez-Valero, A., Saez, R., Perez-Lopez, R., Delgado, J., Nieto, J.M., 2009. Evaluation of heavy metal bio-availability from Almagrera pyrite-rich tailings dam (Iberian Pyrite Belt, SW Spain) based on a sequential extraction procedure. J. Geochem. Explor. 102, 87-94.

Aubertin, M., Bussière, B., Bernier, L., 2002. Environnement et gestion des rejets miniers. Edition Presses Internationales Polytechnique, Montréal.

Bhattacharya, J., Ji, S.W., Lee, H., Choi, Y., 2008. Treatment of acidic coal mine drainage: design and operational challenges of successive alkalinity producing systems. Mine Wat. Environ. 27, 12–19.

Bédard, I., Comeau, Y, Aubertin, M., Bussière, B., 1997. Zone d'épanchement du parc à résidus miniers Aldermac : Étude des techniques de réhabilitation. Centre de développement technologique, Ecole Polytechnique Montréal, Montréal, 159 pp.

Bernier, L., 2002. Suivi du comportement de la couverture multicouche et des DAC au site minier de Lorraine. Centre de développement technologique, École Polytechnique Montréal, Montréal, Canada, 187 pp.

Bernier, L., 2005. The potential use of serpentinite in the passive treatment of acid mine drainage: batch experiment. Environ. Geol. 47, 670-684.

Blais, J.F., Dufresne, S., Mercier, G., 1999. État du développement technologique en matière d'enlèvement des métaux des effluents industriels. Revue des sciences de l'eau 12, 687-711.

Blowes, D.W., Ptacek, C.J., 1994. System for treating contaminated groundwater, in: U.S. Patent 5,362,394, filed March 3, 1992, issued Nov. 8, 1994.

Brown, P., Gill, S., Allen, J., 2000. Metal removal from wastewater using peat. Wat. Res. 34, 3907-3916.

Bussière, B., Aubertin, M., Zagury, G.J., Potvin, R., Benzaazoua, M., 2005. Principaux défis et pistes de solution pour la restauration des aires d'entreposage de rejets miniers abandonnées. Chaire industrielle CRSNG Polytechnique – UQAT en environnement et gestion des rejets minier, Rouyn-Noranda, Canada, 50 pp.

Bussière, B., Potvin, R., Dagenais, A.M., Aubertin, M, Maqsoud, A., Cyr J., 2009. Restauration du site minier Lorraine, Latulipe, Québec : Résultats de 10 ans de suivi. Déchets 54, 49-64.

Bussière, B., 2010. Restauration des sites miniers. Forum sur le développement minier en Abitibi-Témiscamingue, 20 mars 2010, Canada, 25 pp.

Champagne, P., Van Geel, P., Parker, W., 2005. A Bench-scale Assessment of a Combined Passive System to Reduce Concentrations of Metals and Sulphate in Acid Mine Drainage. Mine Wat. Environ. 24, 124-133.

Cocos, I.A., 2000. Sélection d'un mélange réactif utilise dans les biobarrières perméables pour le traitement des eaux souterraines contaminées par le drainage minier acide. Rapport de maitrise, Université de Montréal, Montréal, Canada, 102 pp.

Costa, M.C., Santos, E.S., Barros, R.J., Pires, C., Martins, M., 2009. Wine wastes as carbon source for biological treatment of acid mine drainage. Chemosphere 75, 831-836.

Cravotta, C.A., Trahan, M.K., 1999. Limestone drains to increase pH and remove dissolved metals from acidic mine drainage. Appl. Geochem. 14, 581-606.

Cravotta, C.A., 2003. Size and performance of anoxic limestone drains to neutralize acidic mine drainage. J. Environ Qual. 32, 1277-1289.

Cyr, J., 2005. Les sites miniers abandonnés au Québec: bilan et perspectives. Symposium 2005 sur l'environnement et les mines, 15-18 mai 2005, Rouyn-Noranda, Canada, 10 pp.

Cyr, J., 2008. La restauration du site minier Aldermac : un projet de 16,5 M$. Direction du développement et du milieu miniers, consulté le 26 janvier 2010, http://www.mrnf.gouv.qc.ca/mines/quebec-mines/2008-11/restauration.asp.

Dagenais, A.M., 2005. Techniques de contrôle du drainage minier acide basées sur les effets capillaires. Thèse de doctorat, École polytechnique Montréal, Montréal, Canada, 335 pp.

Dagenais, A.M., Aubertin, M., Bussière, B., Cyr, J. 2005. Performance of the Lorraine mine site cover to limit oxygen migration. SME Transactions, 318, 190-200.

Directive 019 sur l'industrie minière, 2005. Ministère du developpement durable, de l'environnement et des parcs. Consulté en novembre 2011 sur http://www.mddep.gouv.qc.ca/milieu_ind/directive019/index.htm

El-Khalil, H., El-Hamiani, O., Bitton, G., Ouazzani, N., Boularbah, A., 2008. Heavy metal contamination from mining sites in South Morocco: Monitoring metal content and toxicity of soil runoff and groundwater. Environ. Monit. Assess. 136, 147-160.

Espana, J.S., Pamo, E.L., Pastor, E.S., Ercilla, M.D., 2006. The acidic mine pit lakes of the Iberian Pyrite Belt: An approach to their physical limnology and hydrogeochemistry. Ap. Geochem. 23, 1260–1287.

Evangelou, V.P., Zhang, Y.L., 1995. A review: pyrite oxidation mechanisms and acid mine drainage prevention. Environ. Sci. Tech. 25, 141-199.

Figueroa, L., Miller, A., Zaluski, M., Bless, D., 2007. Evaluation of a two-stage passive treatment approach for mining influenced waters. National Meeting of the American Society of Mining and Reclamation, Gillette, WY, 30 Years of SMCRA and Beyond June (pp. 238-247). Barnishel, R.I., Lexington, KY.

Gazea, B., Adam, K., Kontopuolos, A., 1995. A review of passive systems for the treatment of acid mine drainage. Miner. Eng. 9, 23-42.

Genty, T., 2007. Traitement passif d'effluents miniers contaminés par le drainage minier acide à l'aide de drains calcaires anoxiques et biofiltres sulfato-réducteurs. MS thesis, UQAT, QC, Canada, 132

Genty, T., Bussière, B., Potvin, R., Benzaazoua, M., 2008. Neutralization of acid mine drainages in anoxic limestone drains: a laboratory study. Proceeding Post-Mining 2008, Nancy, France, 12 pp.

Genty, T., Bussière, B., Potvin, R., Benzaazoua, M., Zagury, G.J., 2011. Dissolution of different limestone in highly contaminated acid mine Drainage: Application to anoxic limestone drains. Submitted to Environ. Earth Sci.

Genty, T., Neculita, C.M., Bussière, B., Zagury, G.J., 2012. Environmental behaviour of sulphate-reducing passive bioreactor mixture. The 9th International Conference on Acid Rock Drainage (ICARD 2012), Ottawa, Canada, May 21-25, 2012.

Gibert, O., de Pablo, J., Cortina, J.L., Ayora, C., 2005. Municipal compost-based mixture for acid mine drainage bioremediation: Metal retention mechanisms. Ap.Geochem. 20, 1648-1657.

Gosselin, M., 2007. Étude de l'influence des caractéristiques hydrogéochimiques des résidus miniers réactifs sur la diffusion et la consommation de l'oxygène. Rapport de maîtrise, École Polytechnique de Montréal, Montréal, Canada, 246 pp.

Grout, J.A., Levings, C.D., 2001. Effects of acid mine drainage from an abandoned copper mine, Britannia Mines, Howe Sound, British Columbia, Canada, on transplanted blue mussels (Mytilus edulis). Mar Environ Res. 51, 265-88.

Gupta, B., Curran, M., Hasan, S., Ghosh, T.K., 2009. Adsorption characteristics of Cu and Ni on Irish peat moss. J. Environ. Manag. 90, 954-960.

Gusek, J.J., 2001. Why do some passive treatment systems fail? The Center for Environmental Health Sciences at Darmouth. http://www.leo.lehigh.edu/envirosci/enviroissue/amd/links/passive_fail.html. Accessed 25 February 2011.

Harris, M.A., Ragusa, S., 2001. Bioremediation of acid mine drainage using decomposable plant material in a constant flow bioreactor. Environ. Geol. 40, 1192-1204.

Hedin, R.S., Nairn, R.W., Kleinmann, R.L.P., 1994. Passive treatment of coal mine drainage, US Bureau of Mines, Pittsburgh, PA, 35 pp.

Hosten, G., Gulsun, M., 2004. Reactivity of limestone from different sources in Turkey. Miner. Eng. 17, 97-99.

Ji, S.W., Kim, S.J., 2008. Lab-scale study on the application of In-Adit-Sulfate-Reducing System for AMD control. J. Hazard. Mater. 160, 441–447.

Johnson, D.B., Hallberg, K.B., 2005. Acid mine drainage remediation options: a review, Sci. Total Environ. 338, 3-14.

Jong, D., Parry, C., 2006. Microbial sulphate reduction under sequentially acidic conditions in an upflow anaerobic packed bed bioreactor. Wat. Res. 40, 2561-2571.

Kalin, M., Fyson, A., Wheeler, W.N., 2006. The chemistry of conventional and alternative treatment systems for the neutralization of acid mine drainage. Sci. Total Environ. 366, 395–408.

Kleinmann, R.L.P., Crerar, D.A., Pacelli, R.R., 1981. Biogeochemistry of acid mine drainage and a method to control acid formation. Mining Eng. 300-304.

Kuyucak, N., St-Germain, P., 1994. In situ treatment of acid mine drainage by sulfate reducing bacteria in open pits: scale-up experiences, in: Proceedings of the International Land Reclamation and Mine Drainage Conference, pp 303-309.

Kuyucak, N., Chabot, F., Martschuk, J., 2006. Successful implementation and operation of a passive treatment system in an extremely cold climate, northern Quebec, Canada, in: Barnhisel, R.I. (Ed.), Proceedings of the 7th International Conference on Acid Rock Drainage (ICARD), American Society of Mining and Reclamation (ASMR), vol. 38. Lexington, KY, pp. 3131-3138.

La, H., Kim, K.H., Quan, Z.X., Cho, Y., Lee, S., 2003. Enhancement of sulfate reduction activity using granular sludge in anaerobic treatment of acid mine drainage. Biotechnol. Letters 25, 503–508.

Lapointe, F., 2006. Potentiel d'utilisation du bauxsol TM comme matériel réactif d'une barrière perméable pour contrôler le drainage minier acide. Thèses de l'université de Laval, Québec, Canada, chapitre 1 à 2.

Lei, L., Song C., Xie, X., Li, Y., Wang, F., 2010. Acid mine drainage and heavy metal contamination in groundwater of metal sulfide mine at arid territory (BS mine, Western Australia. Trans. Nonferrous Met. Soc. China 20, 1488-1493.

Luptakova, A., Kusnierova, M., 2005. Bioremediation of acid mine drainage contaminated by SRB. Hydrometallurgy 77, 97-102.

Ma, W., Tobin, J.M., 2004. Determination and modelling of effects of pH on peat biosorption of chromium, copper and cadmium. Biochem. Eng. J. 18, 33-40.

Mc Cauley, C., O'Sullivan, A., Milke, M., Weber, P., Trumm, D., 2009. Sulfate and metal removal in bioreactors treating acid mine drainage dominated with iron and aluminum. Wat. Research 43, 961-970.

Melanson, M., 2006. Analyse d'un système de traitement passif pour le site de la mine Eustis. Centre Universitaire de Formation en Environnement, Sherbrooke, Canada, 57 pp.

MEND, 1999. Review of passive treatment for treatment of acid mine drainage. Report 3.14.1, 197 pp.

Molson, J., Aubertin, M., Bussière, B., Benzaazoua, M., 2008. Geochemical transport modelling of drainage from experimental mine tailings cells covered by capillary barriers. Ap. Geochem. 23, 1-24.

Morin, K., Hutt, N. 1997. Prediction of mine site-drainage chemistry through closure using operational monitoring data. J.Geochem. Expl. 73, 123-130.

Neculita, C.M., Zagury, G.J., Bussiere, B., 2007. Passive treatment of AMD in bioreactors using SRB: critical review and research needs. J. Env. Qual. 36, 1-16.

Neculita, C.M., 2008. Traitement biologique passif du drainage minier acide : sources de carbone, mécanismes d'enlèvement des métaux et écotoxicité. Thèse de doctorat, École polytechnique de Montréal, Montréal, Canada, 244 p.

Neculita, C.M., Zagury, G.J., Bussiere, B., 2008a. Effectiveness of sulphate-reducing passive bioreactors for treating highly contaminated acid mine drainage: I. Effect of hydraulic retention time. Ap. Geochem. 23, 3442-3451.

Neculita, C.M., Zagury, G.J., Bussiere, B., 2008b. Effectiveness of sulphate-reducing passive bioreactors for treating highly contaminated acid mine drainage: II. Metal removal mechanisms and potential mobility. Ap. Geochem. 23, 3545-3560.

Perkins, E.H., Nesbitt, H.W., Gunter, W.D., St-Armand, L.C., Mycroft, J.R., 1995. Critical review of processes and geochemical models adaptable for prediction of acidic drainage from waste rock, in: Mine Environment Neutral Drainage (MEND), Report 1.42.1. CANMET secretariat, Ottawa, Ontario.

Potvin, R., 2009. Évaluation à différentes échelles de la performance de systèmes de traitement passif pour les effluents fortement contaminés par le drainage minier acide. Thèse de doctorat, Université du Québec en Abitibi-Témiscamingue, Rouyn-Noranda, Canada, 335 p.

Ritcey, G.M., 1989. Tailings Management, Problems and Solutions in the Mining Industry. Elsevier, Amsterdam.

Robinson-Lora, M.A., Brennan, R.A., 2009. Efficient metal removal and neutralization of acid mine drainage by crab-shell chitin under batch and continuous-flow conditions. Bioressour. Technol. 100, 5063-5071.

Rouhani, P., Champagne, P., Van Geel, P., 2003. Impacts of hydraulic and constituent loading on a combined passive system for the treatment of acid mine drainage. 8ième conférence spécialisée sur le génie de l'environnement et durable de la société canadienne de génie civil. Moncton, New-Brunswick, Canada, 4-7 juin 2003, 10 pp.

Santomartino, S., Webb, J.A., 2007. Estimating the longevity of limestone drains in treating acid mine drainage containing high concentrations of iron. Appl. Geochem. 22, 2344-2361.

Sheoran, A.S., Sheoran, V., Choudhary, R.P., 2010. Bioremediation of acid-rock drainage by sulphate-reducing prokaryotes: A review. Miner. Eng. 23 1073-1100.

Silveira, A., Silva, R., Rubio, J., 2009. Treatment of acid mine drainage (AMD) in south brazil : Comparative active processes and water reuse. Int. J. Miner. Process. 93, 103–109.

Skousen, J.G., Ziemkiewicz, P.F., 2005. Performance of 116 Passive Treatment Systems for Acid Mine Drainage, in: ASMR, 3134 Montavesta Rd. Publication, Proceeding of the National Meeting of the American Society of Mining and Reclamation, Breckenridge, Lexington.

St-Arnault, M., Bussiere, B., Potvin, R., Aubertin, M., 2004. Résultats des travaux de caractérisation réalisés sur les drains dolomitiques du site Lorraine., Chaire industrielle CRSNG Polytechnique – UQAT en environnement et gestion des rejets miniers, Rouyn-Noranda, Canada, 73 pp.

Tassé, N., Germain, D., 2002. Évaluation de la performance de divers types de résidus forestiers pour le traitement du drainage minier acide, in : Proceeding of the Symposium 2002 sur l'environnement et les mines, Rouyn-Noranda, Canada, 11 pp.

Teclu, D., Tivchev, G., Laing, M., Wallis, M., 2008. Bioremoval of arsenic species from contaminated waters by sulphate-reducing bacteria. Wat. Research. 42, 4885-4893.

Trumm, D., 2006. Methodology to Determine Management Strategies. document CRL Energy Ltd, 14 pp.

Ulrich, M. 1999. Non-metallic carbonous minerals in the passive treatment of mining wastewater in Slovenia. Chem. Engin. Process. 38, 249-258.

URS, Report, 2003. Passive and semi-active treatment of acid rock drainage from metal mines-state of the practice. Prepared for U.S. Army Corps of Engineers, Concord, Massachusetts, by URS Corporation, Portland.

Wilmoth, R., 2002. Final report – Sulfate reducing bacteria reactive wall demonstration. Mine waste technology program, activity III, project 12. IAG NO: DW89938870-01-1. Prepared for US environmental protection agency. 69 pp.

Zagury, G.J., Kulnieks, V., Neculita, C.M., 2006. Characterization and reactivity assessment of organic substrates for sulphate-reducing bacteria in acid mine drainage treatment. Chemosphere. 64, 944-954.

Zaluski, M.H., Trudnowski, J.M., Harrington-Baker, M.A., Bless, D.R., 2003. Post-mortem findings on the performance of engineered SRB field-bioreactors for acid mine drainage

control. The 6th International Conference on Acid Rock Drainage, Cairns, QLD, 845-853.

Zis, T., Ronningen, V., Scrosati, R., 2004. Minor improvement for intertidal seaweeds and invertebrates after acid mine drainage diversion at Britannia Beach, Pacific Canada. Mar. Pollut. Bull. 48, 1040-1047.

APPENDICE A

PASSIVE TREATMENT OF ACID MINE DRAINAGE: REPEATABILITY FOR SULPHATE REDUCING PASSIVE BIOREACTOR COLUMN EFFICIENCY TESTING

Cet article a été écrit pour la 11ième conférence de l'IMWA, 2011, Aachen, Allemagne (Editor : Rüde et al., pages 313-318).

Auteurs

Thomas Genty[1], Bruno Bussière[1], Carmen M. Neculita[2], Mostafa Benzaazoua[3], Gérald J. Zagury[4]

[1]Industrial Chair CRSNG Polytechnique-UQAT: Environment and mining wastes management, University of Québec in Abitibi-Témiscamingue, Rouyn-Noranda, Québec, Canada

[2]Division of Environmental Engineering and Sustainability, Department of Civil and Environmental Engineering, KAIST, Republic of Korea

[3]Laboratoire de Génie Civil et d'Ingénierie Environnementale, INSA de Lyon, Villeurbanne, France,

[4]Industrial Chair CRSNG Polytechnique-UQAT : Environment and mining wastes management, École Polytechnique, Québec, Canada

Abstract

This work presents an experimental method developed over the years to design, set-up, and operate columns that test sulphate reducing passive bioreactors (SRPBs) for acid mine drainage (AMD) treatment. Results obtained from identical columns with this experimental

approach are presented and interpreted for their statistical validity. The statistical analysis was based on the "paired-difference test" which allows comparing two sets of data in pairs by looking at the difference between the two sets of data. The three series of data showed a good repeatability (data within a confidence interval of 95%) for pH, oxydoreduction potential, alkalinity, total iron and sulphate concentrations. Hence, duplicate or triplicate column tests are not systematically required for assessing the performance of SRPBs, if the columns are designed, set-up, and operated as proposed by the authors.

Key words: passive treatment, sulphate-reducing passive bioreactor, statistical analysis, repeatability

A.1 Introduction

Preventing the formation of AMD is generally the preferred option for mine sites rehabilitation (Aubertin et al., 2002). In many cases, especially when the weathering process of metal sulphide minerals is already entailed, prevention alone is not sufficient and the collection and temporary treatment of contaminated mine water is also required. There are numerous available options to treat the AMD, which can be classified into chemical and biological systems that both mainly aim at increasing pH, neutralising acidity, and removing metals. Another classification differentiates the active systems, which require continuous input of resources to sustain the process, from passive systems, which in exchange, require relatively minimal maintenance during operation (Neculita et al., 2008, Potvin, 2009). Passive systems, together with an AMD control method, are the best option to rehabilitate abandoned mine sites. The present study focuses on SRPBs as sustainable biotechnology for AMD treatment. SRPBs permit to increase the pH, generate alkalinity and remove metals from contaminated water (Neculita et al., 2007, Potvin, 2009).

Passive systems for AMD treatment are often designed on the basis of column efficiency testing. However, the repeatability of these tests could be questionable due to the inherent heterogeneity of solid materials be used in the reactors and to differences in laboratory experimental test procedures. Performing duplicate or even triplicate column tests are often requested to obtain statistically valid results. The number of scenarios that could be tested for

AMD treatment is limited by the high costs involved (Demers et al., 2011). This study presents a laboratory methodology which was developed in order to set-up and to operate SRPBs laboratory columns, and to evaluate the repeatability of column tests.

A.2 Columns set-up and operation

SRPB duplicate (or triplicate) tests were performed under similar conditions (14 cm diameter x 70 cm height in Genty, 2007 and 2011, 10 cm diameter x 45 cm height in Neculita et al. 2008). Column reactors were built with transparent Plexiglas and equipped at the bottom side with a perforated plastic plate, which was covered with a geotextile to avoid the leaching of fine particles in the effluent. In addition, to prevent clogging and/or to allow a uniform flow distribution at the influent and effluent ports, column ends were filled with 5 cm heights of gravel (~ 1 cm diameter) in both the upper and bottom areas. SRPB mixture materials were firstly mixed and homogenized, and then packed in columns in 10 cm height layers (each layers should have similar weights and water content). Layer was slightly compacted before the addition of the next one. Then, an aluminum foil was laid around the column to prevent chemolithotrophic and phototrophic bacteria development. After the set-up, the bioreactors were saturated with Postgate B medium (Postgate, 1984), which was prepared using distilled water and had the following composition: 3.5 g/L sodium lactate; 2.0 g/L $MgSO_4 \cdot 7H_2O$; 1.0 g/L NH_4Cl; 1.27 g/L $CaSO_4 \cdot 2H_2O$; 1.0 g/L yeast extract; 0.5 g/L KH_2PO_4; 0.5 g/L $FeSO_4 \cdot 7H_2O$; 0.1 g/L thioglycolic acid, and 0.1 g/L ascorbic acid. Columns were then incubated for four weeks (acclimation period) before starting their operation. The individual volume of Postgate B medium was used to calculate the porosity of each column. Theoretically, the estimated porosity should be as close as possible for the duplicate (or triplicate) columns. AMD fed was started after the acclimation period; the column was considered ready for AMD treatment when the oxydoreduction potential decreased to values below -150 mV (Neculita et al., 2008). The AMD was pumped at selected flow rates to insure the reaching of the targeted hydraulic retention time (HRT). The flow direction was upward or downward, depending on the study. A schematic representation of an upward flow column design is presented in Figure A.1.

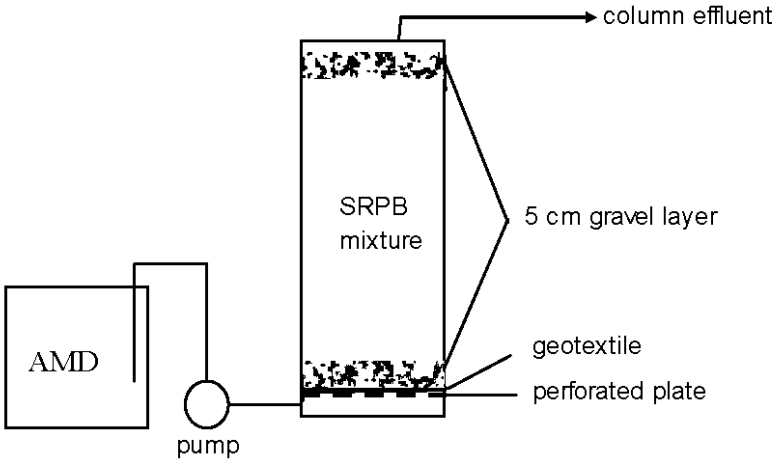

Figure A.1 Upflow column design

Slight differences existed between the three sets of experiments, which were used for the present statistical analysis. The first series of SRPB tests (Genty, 2011) was performed in four 10.7 L columns. The composition of two SRPB mixtures (#4 and #7), which were tested in duplicates columns, is given in Table A.1, previously optimized (Genty, 2011). The porosity was estimated at 0.41, for both columns filled with mixture #4, and at 0.40 and 0.39, for the duplicate columns filed with mixture #7. Artificial AMD 1 (see Table A.2) was pumped in upward flow, for 64 days, at an HRT of 5 days (0.6 mL/min).

The second series of tests (Genty, 2007) was performed using a similar design and set-up procedure, but the HRT was set at 10 days. The compositions of the filling mixture (#1) and of the artificial AMD 2 tested in these columns are presented in Table A.1 and Table A.2, respectively. Finally, the third series of tests used three 3.5 L columns filled with the same filling mixture #1 in triplicate and operated in downward flow at an HRT of 10 days for the treatment of the artificial AMD 3 (see Table A.2). More details about this last study are available in Neculita et al. (2008).

To assess the performance of all the tested columns, influent and effluent were weakly measured for pH, oxydoreduction potential (called ORP, and Eh if the ORP is corrected

relative to the standard hydrogen electrode), sulphates concentration, acidity, alkalinity, and metals concentrations.

Table A.1 Composition of SRPB mixtures (%, dry)

Mixture	#1	#4	#7
Celullosic wastes			
Maple chips	10	5	6
Sawdust	20	10	11
Organic wastes			
Chiken manure	10	5	8
Leaf compost	20	10	12
Inoculum			
Sediment	15	8	8
Inert structural agent			
Sand	20	10	50
Nutriment (Nitrogen)			
Urea	3	2	3
Neutralizing agent			
Calcium carbonate	2		2
Calcite		50	

Table A.2 AMD composition (mg/L, except for pH)

Elements	AMD 1	AMD 2	AMD 3
Al	7	7	0
Cd	0.5	1	9.8
Cr	1	2	1
Fe	4000	1600	1066 to 504
Mg	10	100	85.8
Mn	10	21	10.1
Ni	2	7	13.7
Pb	0.5	1	0.5
SO_4^{2-}	9000	4200	4022
Zn	0.5	2	14.5
pH	3.5	3.5	2.8 to 5.7

A.3 Repeatability evaluation

The aim of statistical analysis performed in the present study was to ascertain whether two sets of data from two similar column tests set-up and operated as proposed in this study, come from the same population. The statistical approach is similar to the one detailed in the work of Demers et al. (2011). The use of student's t distribution was justified by the relatively limited available data. To compare two series of data, the "Paired-difference test" and a two-tailed test at 95% confidence interval were used (Demers et al., 2011). The method hypothesis was that the difference between the two means (μ) of two series of data from two columns (1 and 2) was null.

[A-1] $$\mu_1 - \mu_2 = 0$$

The t test notation became:

[A-2] $$t = \frac{\bar{d}}{s_d / \sqrt{n}}$$

Where $\bar{d}$ was the mean of the paired differences, n was the number of paired differences and s_d was the standard deviation of the paired differences. For the calculation of s_d the following equation was used :

[A-3] $$s_d = \sqrt{\frac{\sum_{i=1}^{n}(d_i - \bar{d})^2}{n-1}}$$

The hypothesis (data come from the same population) was rejected when the t value obtained with the equation [A-2] was above a pre-determined value (determinated in statistical tables for a two-tailed test at 95% confidence interval, n-1 was the degree of freedom).

A.4 Selected results

A.4.1 First experiment set: Genty (2011)

Effluent quality (pH, ORP, alkalinity and total iron concentration) at the exit of duplicate SRPB columns with mixture #4 and #7 are presented in Figure A.2.

The pH of treated effluent steadily decreased during the first 30 days from values above 8 to between approximately 6 and 6.5 and then stabilized, without real difference between duplicate columns. Consistently, alkalinity values decreased from 11250 mg/L CaCO3 or 9333 mg/L CaCO3 to 504 mg/L CaCO3 or 450mg/L CaCO3, respectively for mixture #4 and mixture #7. During the same period, Eh increased constantly from negative values (as low as -120 mV) to 74-75 mV, regardless the mixture or duplicate reactors. Similar trend was recorded for the evolution of acidity (not presented here) and total iron, which concentration increased values up to 3500 mg/L (mixture #4) or to 3200 mg/L (mixture #7). Standard deviation of iron concentration (both mixtures) exceeded 1000 mg/L and indicated relatively high variability. Finally, sulphate concentrations (not shown in Figure 2) ranged from 6811 mg/L to 10054 mg/L (for mixture #4) and from 6270 mg/L to 11837 mg/L (for mixture #7).

Apparently, results from duplicate columns seemed comparable. However, a simple visual comparison of the data on effluent quality is not accurate enough to evaluate the repeatability of the tests and statistical calculations are required. Table A.3 presents results on repeatability calculation for the two tested columns: mixture #4 and #7.

During the first 64 days, calculated t values were below the t test value (2.45 or 4.3, depending on the parameter) for a confidence interval of 95%, except for the pH of column #7, for which the calculated t is very close to the t test value (2.46 vs. 2.45). This statistical analysis allowed the interpretation that the data could come from the same population, and thus from almost identical tests. Therefore, physicochemical parameters such as pH, Eh, alkalinity, iron and sulphate concentrations were repeatable for the two columns filled with the same mixture and treating the same AMD quality.

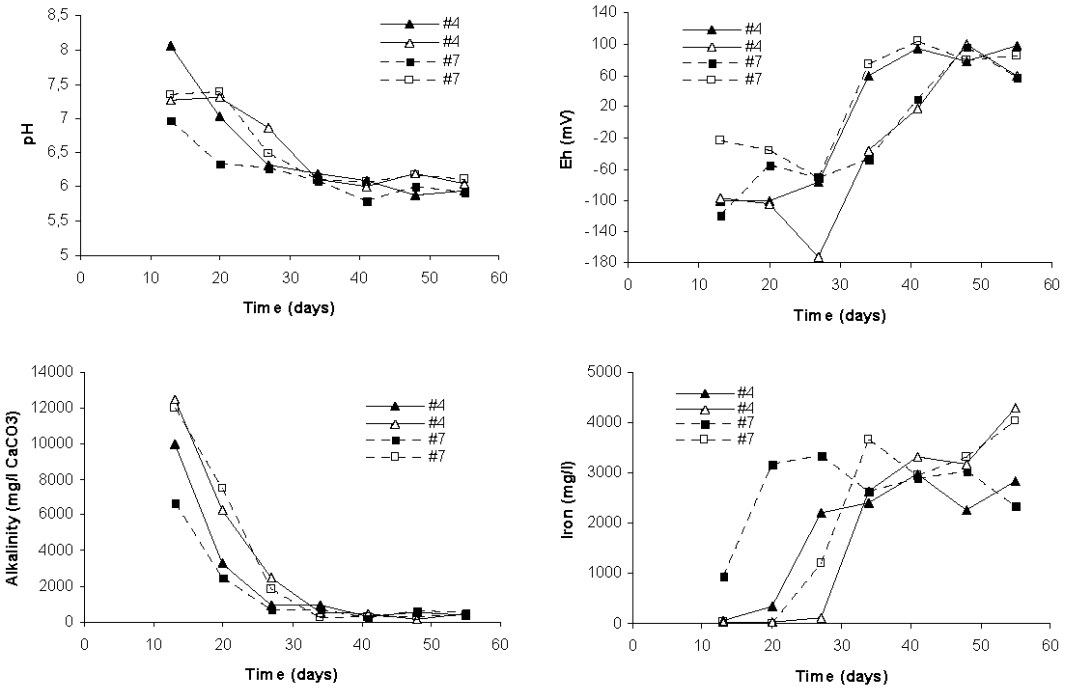

Figure A.2 Evolution of pH, Eh, alkalinity and iron concentration in treated effluent using mixtures #4 and #7

Table A.3 T-test statistics for physicochemical parameters for treated effluents using mixtures #4 and #7

Parameters	column	Average $\bar{d}$	Standard deviation s_d	Calculated t	t test value	Within 95% confidence interval
pH	# 4	0.040	0.43	0.23	2.45	yes
	# 7	0.33	0.328	2.46	2.45	no
Eh	# 4	40.93	49.30	2.03	2.45	yes
	# 7	45.16	51.83	2.13	2.45	yes
Alcalinity	# 4	912.00	1384.00	1.61	2.45	yes
	# 7	1508.43	2555.37	1.45	2.45	yes
Total iron	# 4	76.74	1124.19	0.17	2.45	yes
	# 7	448.76	1724.29	0.64	2.45	yes
Sulphate	# 4	178.70	2300.93	0.11	4.30	yes
	# 7	1705.46	3352.52	0.72	4.30	yes

A.4.2 Second experiment set: Genty (2007)

Figure A.3 presents the main quality parameters of the treated effluent of the two duplicate columns tested in the second study. The pH values continuously decreased from around 8 to 6.5, at the end of the experiments. However, Eh remained relatively low during the testing period with values between -80 and -130 mV; similar variations were recorded in the two columns. Iron concentrations decreased from approximately 1600 mg/L in influent AMD to values usually below 3 mg/L in treated water. Duplicate columns showed slightly different alkalinity, with final values of 1584 and 1676 mg/L of $CaCO_3$. Small differences were recorded between values measured at the same sampling time. Similarly to the first study, the results presented here seem, at least visually, comparable.

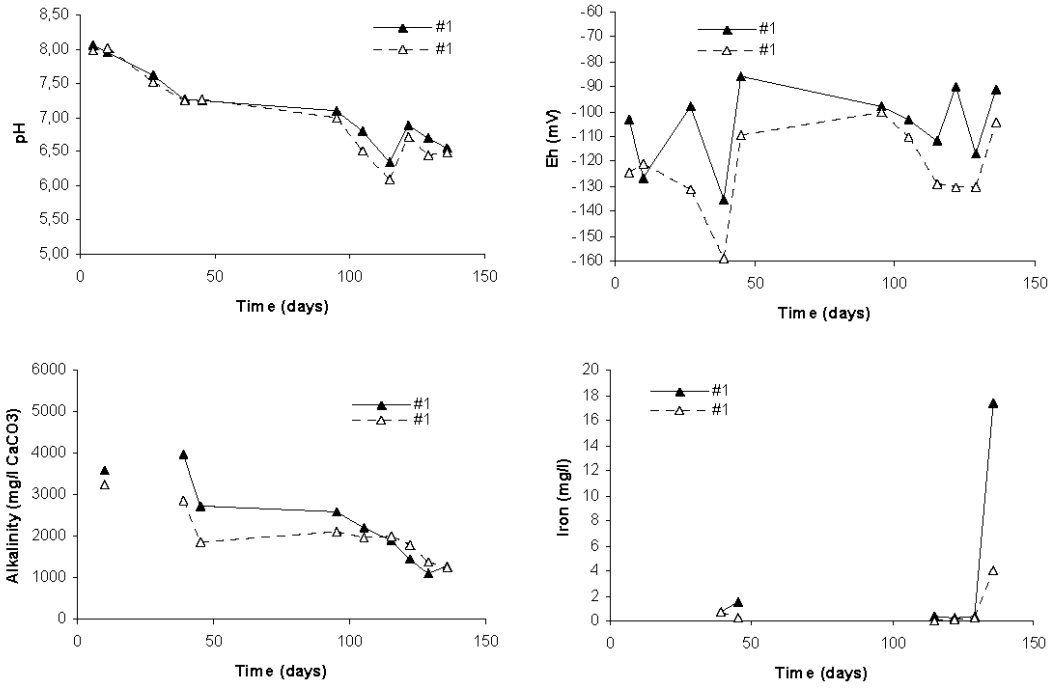

Figure A.3 Evolution of pH, Eh, alkalinity and total iron concentration in treated effluent using mixture #1

Table A.4 presents the statistical results for these last two column tests. As it can be seen, statistical interpretation of the data on pH, Eh, alkalinity, iron concentrations from Genty (2007) proved that the two column tests were repeatable within 95% confidence interval.

Table A.4 T-test statistics for physicochemical parameters for treated effluent using mixture #1 (source of original data: Genty, 2007)

Parameters	Average $\bar{d}$	Standard deviation	calculated t	t test value	within 95% confidence interval
pH	0.12	0.098	0.38	2.23	yes
Eh	18.02	11.65	0.47	2.23	yes
Alcalinity	2.53	5.35	0.19	2.57	yes
Total iron	428.00	353.18	0.40	2.31	yes

A.4.3 Third experiment set: Neculita et al. (2008)

Table A.5 presents statistical results of column tests performed with mixture #1 and AMD 3 (Neculita et al., 2008).

Table A.5 T-test statistics for physicochemical parameters treated effluent using mixture #1 (source of original data: Neculita et al., 2008)

Parameters	Columns tested	Average $\bar{d}$	Standard deviation	calculated t	t test value	within 95% confidence interval
pH	1 and 2	0.15	0.20	0.11	2.02	yes
	2 and 3	0.18	0.30	0.09	2.02	yes
	3 and 1	0.19	0.28	0.10	2.02	yes
ORP	1 and 2	16.93	18.08	0.14	2.02	yes
	2 and 3	23.18	22.56	0.15	2.02	yes
	3 and 1	22.73	20.09	0.17	2.02	yes
Total iron	1 and 2	44.49	89.51	0.07	2.02	yes
	2 and 3	53.48	75.68	0.11	2.02	yes
	3 and 1	46.69	94.39	0.07	2.02	yes
Sulphate	1 and 2	211.93	185.87	0.17	2.02	yes
	2 and 3	260.80	200.03	0.20	2.02	yes
	3 and 1	273.86	219.47	0.19	2.02	yes

Triplicate columns were compared two by two (columns 1 and 2, columns 2 and 3, and columns 1 and 3) for their repeatability. If each pair of columns was found repeatable, thus the three columns were repeatable too. Once again, the statistical analysis showed good repeatability for all selected parameters (pH, ORP, total iron and sulphate concentrations) with all data within the 95% confidence interval.

A.5 Conclusions

Results from three independent studies, which tested the performance of 9 SRPBs for the treatment of three qualities of artificial AMD were compared to evaluate the repeatability of the experimental procedure. Indeed, numerous factors (like analytical instruments, operator, sampling, material set up procedure, etc.) could affect the result of an experiment. Statistical analyses of the treated effluent quality showed good repeatability (within a confidence interval of 95%) for selected parameters (pH, ORP or Eh, alkalinity, total iron and sulphate concentrations). Based on these results, duplicate or triplicate column tests are not systematically required for assessing the performance of passive treatment systems such as SRPBs, providing that the columns are designed, set-up, and operated with a good methodology and a rigorous control of the boundary conditions.

Acknowledgements

This research was supported by the Canada Research Chair on Restoration of Abandoned Mine Sites and the Industrial NSERC Polytechnique-UQAT Chair in Environment and Mine Wastes Management.

References

Aubertin, M., Bussiere, B., Bernier, L., 2002. Environnement et gestion des rejets miniers. Manual on CD-ROM Presses internationales Polytechnique, Montréal, QC, Canada.

Demers, I., Bussière, B., Aachib, M., Aubertin, M., 2011. Repeatability evaluation of instrumented column tests in cover efficiency evaluation for the prevention of acid mine drainage. Water Air Soil Pollut. 219, 113-128.

Genty, T., 2007. Traitement passif d'effluents miniers contaminés par le drainage minier acide à l'aide de drains calcaires anoxiques et biofiltres sulfato-réducteurs. MS thesis, UQAT, QC, Canada, 132 p.

Genty, T., 2011. Comportement hydro-geochimiques des systèmes de traitement passif pour des effluents fortement contaminés par le drainage minier acide. PhD dissertation, UQAT, QC, Canada.

Neculita, C.M., Zagury, G.J., Bussiere, B., 2008. Effectiveness of sulphate-reducing passive bioreactors for treating highly contaminated acid mine drainage: I. Effect of hydraulic retention time. Appl. Geochem. 23, 3442-3451.

Neculita, C.M., Zagury, G.J., Bussiere, B., 2007. Passive treatment of AMD in bioreactors using SBR: critical review and research needs. J. Environ. Qual. 36, 1-16.

Postgate, J.R., 1984. The sulphate-reducing bacteria, Second Ed. Cambridge University Press, Cambridge.

Potvin, R., 2009. Évaluation à différentes échelles de la performance de systèmes de traitement passif pour des effluents fortement contaminés par le drainage minier acide. PhD dissertation, UQAT, QC, Canada, 365 p.

APPENDICE B

DISSOLUTION OF CALCITIC MARBLE AND DOLOMITIC ROCK IN HIGH IRON CONCENTRATED ACID MINE DRAINAGE: APPLICATION TO ANOXIC LIMESTONE DRAINS

Cet article a été soumis à la revue Environmental Earth Sciences, en novembre 2010. L'Article est en cours de révision.

Auteurs

Thomas Genty[1], Bruno Bussière[1], Robin Ptovin[2], Mostafa Benzaazoua[3], Gérald J. Zagury[4]

[1]Industrial Chair CRSNG Polytechnique-UQAT: Environment and mining wastes management, University of Québec in Abitibi-Témiscamingue, Rouyn-Noranda, Québec, Canada

[2] CÉGEP de l'Abitibi-Témiscamingue, Rouyn-Noranda, Québec, Canada

[3]Laboratoire de Génie Civil et d'Ingénierie Environnementale, INSA de Lyon, Villeurbanne, France,

[4]Industrial Chair CRSNG Polytechnique-UQAT : Environment and mining wastes management, École Polytechnique, Québec, Canada

Abstract

Oxidation of sulphide mining waste can generate acid mine drainage that has the potential to seriously affect the ecosystems. Acid mine drainage is characterised by a high acidity, high concentrations of sulphates and metals. To reduce environmental impacts of acid mine drainage, neutralisation using limestone drains is an option proposed in the literature and used around the world. The present study focuses on the influence of the carbonate rock

mineralogy and their particle size on the neutralising capacity. The tests were performed in two different anoxic conditions: in batch reactors, and in columns having a hydraulic retention time of 15 hours. The results showed that the neutralisation capacity of calcite was more important than for dolomitic rock, and smaller particle size gave higher alkalinity production (fine calcite dissolved faster in contact with AMD). A characterization of metal precipitate in sludge and in limestone coating was performed and demonstrated that gypsum, lepidocrocite and goethite were the predominant secondary minerals to be formed. Finally, this study underlines that anoxic limestone drain cannot be used alone to treat high iron concentrated acid mine drainage.

Keywords: mine water treatment, acid mine drainage, passive systems, anoxic limestone drains.

B.1 Introduction

B.1.1 Acid mine drainage formation and treatment with anoxic limestone drains

Mine drainage is the result of water movement through the components of a mine site such as mine openings, waste rock dumps, low grade ore piles, and tailings impoundments (e.g. Morin and Hutt, 2001). In absence of a sufficient neutralising potential from the mine waste, mine drainage can become acidic and is then called acid mine drainage (AMD). The production of AMD can be described by a series of chemical reactions catalyzed by bacterial activity (see the following references for more information on these reactions: Kleinmann et al., 1981; Blowes and Ptacek, 1994). Briefly, sulphide minerals oxidize and produce sulphuric acid that lowers the pH when the neutralization potential of the waste due to carbonates or silicates is absent or exhausted (Benzaazoua et al., 2004). The low pH of AMD also increases the solubility of some metals and metalloids that can be found in concentrations greater than current regulation criteria.

During mining operations, chemical agents are usually used to treat AMD collected from the mine site (Ritcey, 1989). However, in the context of sustainable development, active chemical treatment is not usually considered as a viable option for the long-term rehabilitation of AMD generating sites. The other water treatment options available are the

use of passive treatment methods such as bioreactors with sulphate-reducing bacteria (e.g. Neculita et al., 2007), wetlands (e.g. Skousen and Ziemkiewicz, 2005; Barley et al., 2005), and oxic and anoxic limestone drains (e.g. Cravotta 2003); this paper focuses on anoxic limestone drains (ALD) used to treat highly contaminated AMDs, typical of those found in many Canadian hard rock mines.

ALD are trenches filled with crushed limestone (or carbonate rock) with a high calcite content, covered with an impermeable material to ensure top sealing. The stream of contaminated effluent flows under anoxic conditions into the drain by gravity. The AMD dissolves the limestone leading to a calcium and bicarbonate release that reduces the acidity, and increases the pH and alkalinity of the effluent (Hedin et al., 1994; Cravotta and Trahan, 1999; Cravotta, 2003). The anoxic environment in ALD prevents oxidation of dissolved metals (mainly iron) inside the drain avoiding massive precipitation and drain clogging. Metal precipitates, such as iron oxyhydroxides, are consequently formed at the exit of the drain, due to the direct oxidation with oxygen.

B.1.2 Carbonate rocks used in ALD

The most important criteria to select the carbonate rock that constitutes the ALD are the alkalinity production and the neutralisation rate (Cravotta and Watzlaf, 2002; Cravotta, 2003; Cravotta et al., 2008). Hence, it is usually assumed that carbonate rock used in ALD must have the highest unit surface area possible and a high calcium carbonate content (more than 90% according to Watzlaf and Hedin, 1993); unit surface area depends mainly on particle size and internal rock porosity (Morse, 1983, suggested that carbonate rock should have a grain diameter below 5 cm). A high unit surface area allows a better neutralization of acidity (Morse and Arvidson, 2002) and a high purity in calcium carbonate induces faster neutralization rates (Hedin et al., 1994). However, the high purity of the limestone used in ALD can be detrimental in the long term. Indeed, gypsum precipitates could be formed at the surface and passivate the calcite (Hammarstrom et al., 2003; Huminicki and Rimstidt, 2008; Soler et al., 2008). To reduce the influence of this gypsum coating, Huminicki and Rimstidt (2008) recommend using dolomite to neutralize AMD with a very low pH. Although dolomite dissolves more slowly than calcite (Herman and White, 1985; Langmuir, 1997; Liu

et al., 2005), the production of dissolved calcium is less important, and the gypsum formation is reduced. The most successful ALD tests to neutralize AMD reported in the literature used calcite (Cravotta et al., 2008). However, Potvin (2009) showed that dolomite can also be used to neutralize a very acidic AMD.

B.1.3 Objectives and content

Anoxic limestone drains have been applied mainly for the treatment of AMD coming from coal mines (Hedin et al., 1994; Cravotta and Trahan, 1999; Cravotta, 2003). For this type of AMD, the existing literature shows that ALD can efficiently treat the contaminated water. However, there is only few data on the effectiveness of ALD to treat AMD from hard rock base metal mines, which usually contain higher concentrations of dissolved metals and sulphate (Aubertin et al., 2002) than AMD from coal mines (Bernier, 2005).

Therefore, the main objective of this paper was to evaluate, at the laboratory scale using batch and column (dynamic) tests, the lifetime and the capacity of ALD to treat highly contaminated AMD from hard rock base metal mines. The influence of different parameters on the performance of ALD was evaluated, namely particle size and mineralogy of the crushed carbonate rock, and the characteristics of AMD. The effect of coating on the neutralisation potential of the carbonate rock tested was also investigated.

Moreover, since the recent literature proposes to combine ALDs with other passive systems like sulphate reducing biofilters and peat biofilters to treat highly contaminated AMD (Champagne et al., 2005; Figueroa et al., 2007), the present study provides crucial information on the potential contribution of ALD in a multi-step passive treatment system as an alkalinity generating step.

B.2 Methods and Materials

B.2.1 Synthetic AMD solution tested

The tests (batch and columns tests) were carried out using two AMD having characteristics given in Table B.1. The metallic salts used in the preparation of AMD were dissolved in tap water. The AMD composition given in Table B.1 is representative of observed concentrations

near AMD generating sites located in Quebec and Canada (e.g. Aubertin et al., 2002). The oxydo-reduction potential of AMD was positive (>500 mV) in both cases. To illustrate the variability of AMD, a highly contaminated (based on a real case called AMD Lorraine; see Potvin 2009, for more details) and less contaminated (called AMD Light) AMD were tested. The AMD Lorraine had a pH of 3.5, a high iron concentration (above 6900 mg/L) and a sulphate concentration of 15000 mg/L. The AMD Light had a pH of 5.5, an iron concentration of approximately 1600 mg/L and a sulphate concentration around 4200 mg/L.

Table B.1 Characteristics of the two influent synthetic acid mine drainage solutions (in mg/L except pH)

Component	Used salt	AMD Light	AMD Lorraine
Al	$Al_2(SO_4)_3,18H_2O$	7	7
Cd	$CdSO_4,8H_2O$	1	1
Cr	$CrK(SO_4)_2,12H_2O$	2	2
Fe	$FeSO_4,7H2O$	1600	6900
Mg	$MgSO4,7H_2O$	100	100
Mn	$MnSO_4,H_2O$	21	21
Ni	$NiSO_4,6H_2O$	7	7
Pb	$Pb(NO_3)_2$	1	1
SO_4^{2-}	$Na_2SO_4,10H_2O$	4200	15000
Zn	$ZnSO_4,7H_2O$	2	2
pH	HCl/NaOH 1N	55	35

B.2.2 Batch experiment description

Batch tests are frequently used as a preliminary procedure before the construction of full scale mine water treatment plant (Bernier, 2005; Lindsay et al., 2008; Robinson-Lora and Brennan, 2009). This type of test allows determining which materials have the best capacity to treat a given AMD (Neculita and Zagury, 2008).

The experimental protocol used in this study was adapted from the one proposed by Bernier (2005). The main objective of this experiment was to compare the neutralizing potential of the different carbonate rocks and to observe the influence of particle size in batch tests. Each reactor consisted of a 1.5 L glass jar filled with AMD and the neutralizing material (calcite or dolomite). The reactor was hermetically sealed with a rubber seal and a top cap in order to

maintain an anaerobic environment. The targeted liquid to solid ratio was 0.4. The first batch test series were performed during 150 hours (≈6 days) under static anoxic conditions with AMD Lorraine to determine the time needed to reach a nearly constant pH. During this test, only the pH was measured. For the second series of batch test (41 h), the anaerobic environment was maintained for a period of 15 hours, which corresponds to an optimal hydraulic residence time (HRT) for ALDs (e.g. Hedin et al., 1994). After this period, the treated water was transferred into a open recipient to allow the contact with oxygen and to promote the precipitation of iron hydroxides and gypsum. Parameters such as pH, alkalinity, metals and sulphate concentrations were monitored throughout the entire testing period of 41 hours (at 0, 7, 15, 22, and 41 h). The last batch test series were made with coated carbonate rocks coming from column tests after dismantling (see section 2.3.); these tests were performed to quantify the effect of coating on the neutralization capacity of carbonate rocks. The operating conditions were the same as described previously (15 hours of anoxia with AMD Lorraine).

B.2.3 Column tests description

Column tests can provide information on the efficiency of treatment in a long term period and simulate more representative environmental conditions (compared to batch tests) that should be closer to a full scale plant (Neculita et al., 2008; Robinson-Lora and Brennan, 2009). Five Plexiglas columns of 14 cm diameter and 70 cm height (10.7 L) were filled with the four carbonate rocks described in Table B.2; one column (filled with calcite coarse) was run as a duplicate. According to the volume of liquid used to fill the columns, the porosities of the different columns was estimated to be 0.42 for the column with the fine calcite, 0.56 for columns with the calcite intermediate and coarse, and 0.53 for the column filled with the dolomite intermediate. Columns were fed from the bottom with AMD solution to allow constant anoxic conditions. A perforated plastic plate covered with a geotextile was placed at the bottom of the column to uniformly feed the column. The water upflow was set at 6 mL/min to ensure a hydraulic residence time in the column of approximately 15 h. The flow was controlled by a peristaltic pump and was monitored on a daily basis. At the exit of the column, the effluent was aerated with compressed air before being sent to a clarifier tank. These steps had approximately a hydraulic retention time of 2 hours for aeration and 27 hours

for clarification. As mentioned earlier, the last two stages were implemented to remove iron present in the effluent using the oxidation of ferrous iron to ferric iron, which then precipitate as iron hydroxides. Parameters such as pH, alkalinity, metals and sulphate concentrations were measured at the exit of the column and in the clarifier. A schematic representation of the setup is presented in Figure B.1. To assess the role of AMD characteristics on treatment efficiency, AMD Light and AMD Lorraine were used sequentially for one month on the same material.

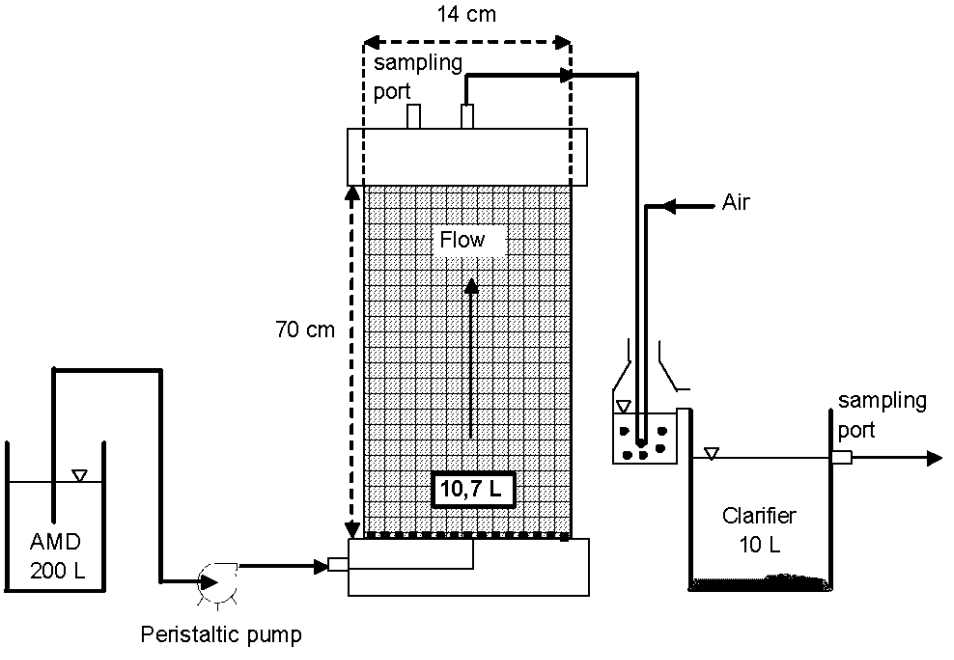

Figure B.1 Schematic diagram of the column laboratory setup (dimensions are not to scale)

Table B.2 Characteristics of carbonate rock used in the different columns (*column 3 and 4 are duplicates). Method Detection Limit (MDL) is 1% for XRD quantification

	Calcite			Dolomite
Type	Fine	Intermediate	Coarse	Intermediate
Mineral composition by XRD				
Calcite (wt%)	95	95	95	<MDL
Dolomite (wt%)	0	<MDL	<MDL	75
Quartz (wt%)	2.5	2.5	2.5	15
Hornblende (wt%)	2.5	2.5	2.5	0
Muscovite (wt%)	<MDL	<MDL	<MDL	9
Kutnahorite (wt%)	<MDL	<MDL	<MDL	0.5
Magnesite (wt%)	<MDL	<MDL	<MDL	0.5
Element abundance by ICP-AES				
Ca (wt%)	35	35	35	16.5
Mg (wt%)	0.5	0.5	0.5	8.7
Al (wt%)	0.01	0.01	0.01	0.9
Mn (wt%)	0.006	0.006	0.006	0.038
Fe (wt%)	0.07	0.07	0.07	0.7
S (wt%)	0.5	0.5	0.5	0.03
Physical characteristics				
Particle size minimum (cm)	0.03	0.8	1.3	0.8
Particle size maximum (cm)	0.8	1.9	3.8	1.9
Relative density of solid grain	2.72	2.67	2.69	2.54
Estimated unit surface area (m^2/m^3)	3283	224	120	312
Estimated unit surface area (cm^2/g)	12.07	0.84	0.45	1.23
Column characteristics				
Number	1	2	3, 4 *	5
Porosity	0.42	0.53	0.56	0.53
Carbonate rock mass (kg)	16.76	15.50	14.89	15.13

B.2.4 Sampling and analytical method for water quality evaluation

Water samples were taken twice a week at the exit of columns and clarifiers. Samples were analysed for pH, alkalinity and dissolved metals. The pH was measured with an Orion Triode sensor coupled with a Benchtop pH/ISE Meter Orion model 920 (relative precision +/- 0.01). The alkalinity concentration was obtained by titration with sulphuric acid 0.02N (precision of 1 mg $CaCO_3$/L) (APHA, 1995). Filtered water samples sent to the chemical analysis were preserved with 2% volume of nitric acid at 70% (w/w) before analysis; metal concentrations

were evaluated with Inductively Coupled Plasma-Atomic Emission Spectrometry (ICP-AES) technique using a Perkin Elmer OPTIMA 3100 RL (relative precision of 5%).

B.2.5 Sampling and characterisation of solids

An X-ray diffractometer (XRD; Bruker axs D8 ADVANCE) was used to characterize the mineralogy of solid samples. The instrument is equipped with a Cu anticathode and scintillation counter. Data treatment was done using Bruker axs EVA and TOPAS software packages. The proportion of minerals was estimated by the Rietveld method (precision of 0.5%). This method uses a least squares approach to refine a theoretical line profile until it matches the measured profile. At the end of the column experiments, coatings from carbonate rock were collected by scraping off the rocks. Recovered materials were then air-dried for one week at 35°C. Collected sludge from each clarifier was also air dried for the same period. Dry samples of the coating and the sludge were crushed to 10 µm before XRD analysis.

However, because the coating and the sludge could be constituted of amorphous minerals, a thermogravimetric analysis (TGA) coupled with a differential scanning calorimetric analysis (DSC) was also performed on both materials using a SDT Q600 TA. This equipment allows simultaneous registry of weight loss and heat flow along thermal treatment. Thermal behaviours were registered in an inert nitrogen atmosphere at a rate of 10°C/min from ambient temperature up to 600°C, and then to 1020°C at 20°C/minute. Tests were performed with approximately 35 mg of material placed in a 90 µl alumina cup and covered by an alumina lid. The thermal behaviour of a given material is directly related to his mineralogy (e.g. Prasad et al., 2006).

A Hitachi 3500-N scanning electron microscope (SEM) was used to characterize the microstructure and texture of coating samples. The main characteristics of the SEM-EDS during measurements on coatings were: voltage of 20 keV; amperage of 140 A; pressure of approximately 25 Pa; and work distance of 15 mm.

To determine the samples chemistry, solids were digested in HNO_3, Br_2 , HCl, and HF. Then, the liquid resulting from this treatment was analysed for metal by ICP-AES (relative precision of 5%).

Finally, saturation indices of the main secondary minerals that could influence the water quality at the exit of the columns and clarifiers were calculated using Vminteq version 3. Vminteq is a chemical equilibrium model used to calculate metal speciation and solubility equilibriums. It is probably the most widespread model for these purposes today, and it is renowned for its stability (KTH, 2010).

B.2.6 Carbonate rock characteristics

Calcitic marble (called calcite hereinafter) used in this study comes from the quarry of Perth, Ontario (Canada), while the dolomitic rock (called dolomite) comes from the Témiscamingue region in Quebec (Canada). This dolomitic rock contains some detrital silicated minerals. The main characteristics of the two type of carbonate rock are given in Table B.2. Particle size distribution was determined using different sieve sizes (see Figure B.2). The particle size analysis shows that dolomite intermediate and Calcite intermediate were relatively similar in term of grain size distribution (minimum and maximum particle size between 0.8 and 1.9 cm). This similarity was useful to compare the influence of the rock source towards treatment efficiencies. The calcite fine and calcite coarse had minimum and maximum particle sizes between 0.03 and 0.8 cm, and 1.3 and 3.8 cm respectively. The XRD analysis showed that the calcite used was 95% pure in $CaCO_3$, and contained a small proportion of quartz and hornblende. Dolomitic rock was mainly 75% composed of dolomite ($CaMg(CO_3)_2$), with 15% of quartz (SiO_2) and 9% of muscovite. Identified gangue minerals (quartz, hornblende and muscovite) were considered inert with respect to AMD neutralization. The elemental abundance showed that calcite contains approximately 35% of calcium and that dolomite contains 16.5% of calcium and 8.7% of magnesium.

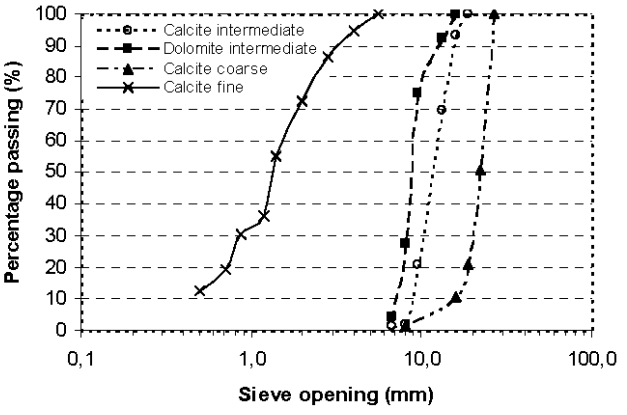

Figure B.2 Particle size distribution of materials

The unit surface area A_s can be determined using the distribution of particles size of carbonate rocks and the porosity n_p ($n_p = V_v / V_t$; V_v is the void volume and V_t the total volume).

The parameter A_s (m^2/m^3 or m^{-1}) can be approximated with equation [B-1] (Monoret, 2001):

[B-1] $$A_s = (1-n_p) \cdot \int_0^{+\infty} \frac{6}{d_p} \cdot f(d_p) \cdot dd_p$$

with d_p the diameter of a particle (m) and $f(d_p)$ the frequency of the diameter d_p observed in the particle size distribution (adimensional). Equation [B-1] can be simplified into equation [B-2] considering the diameter of two consecutive sieves and disregarding the residual part (Monoret, 2001):

[B-2] $$A_s = \frac{(1-n_p)}{\Gamma} \cdot \sum_i^n \frac{12}{(d_{i+1} + d_i)} \cdot \frac{m_i}{M}$$

with the following parameters : d_{i+1} and d_i the diameter of two consecutive sieves (m), Γ a form factor (adimensional), m_i mass of carbonate rock in the sieve *i* (g), M total mass of carbonate rock (g), and *n* the number of sieve.

According to Monoret (2001), the form factor for gravel could be approximated to 0.8. The estimation of the unit surface area by equation [B-2] gave the following results : 3283 m^2/m^3 for calcite fine (or 12.07 cm^2/kg considering a measured relative density of 2.71), 224 m^2/m^3 (or 0.84 cm^2/kg considering a measured relative density of 2.66) for calcite intermediate, 120 m^2/m^3 (or 0.45 cm^2/kg considering a relative measured density of 2.69) for calcite coarse and 312 m^2/m^3 (or 1.23 cm^2/kg considering a measured relative density of 2.54) for dolomite intermediate. Other approaches could have been used to estimate A_s (e.g. Chapuis and Légaré, 1992) but equation [B-2] was considered adequate in this study.

B.2.7 Carbonate rock dissolution model

Carbonate rock dissolution rate is an important data to assess the lifetime of an ALD. This kinetic data allows determining the carbonate rock weight loss with time, which is recognized as a better parameter than the alkalinity production rate to evaluate the performance of an ALD. Indeed, alkalinity can not be determined if the pH is below 4.5 and most of the time, calcium concentration is measured more accurately than alkalinity (Cravotta and Watzlaf, 2002).

Cravotta and Watzlaf (2002) propose to evaluate the dissolution kinetic constant assuming that the flow rate is constant between two measurements of calcium concentration in the effluent and influent of ALD. Therefore, the mass flux of dissolved carbonate rock J_{CaCO_3} in mol/day can be approximated by the following equation considering that 1 mol of dissolved carbonate is equal to 1 mol of calcium in water:

[B-3] $$J_{CaCO_3} = Q \cdot ([Ca]_e - [Ca]_i)$$

with Q in L/day, $[Ca]_e$ the calcium concentration in mol/L in the effluent and $[Ca]_i$ the calcium concentration in mol/L in the influent. Equation [B-3] allows estimating the daily carbonate rock mass loss.

In order to determine the kinetic constant for the carbonate rock dissolution, it is often assumed that a first order equation appropriately represents adequately the phenomenon (Cravotta and Watzlaf, 2002; Cravotta, 2003; Mukhopadhyay et al., 2007):

[B-4] $$\frac{dM}{dt} = -kM$$

with M the carbonate rock weight and k the kinetic constant. The integration of equation [B-4] gives:

[B-5] $$M_x(t) = M_0 e^{-kt}$$

with $M_x(t)$ the carbonate rock weight at the time t and M_0 the initial carbonate rock weight. Then, the kinetic constant k is determined by plotting the logarithm of M / M_0 versus time. Kinetic constant values are valid for a given carbonate rock, hydraulic retention time, temperature, and pressure.

B.2.8 Statistical validity of results

The aim of statistical analysis performed in the present section was to ascertain whether two sets of data from two similar column tests (columns 3 and 4) come from the same population. The statistical approach is similar to the one detailed in the work of Demers et al. (2011). The use of student's t distribution was justified by the relatively limited available data. To compare two series of data, the "Paired-difference test" as a two-tailed test at 95% confidence interval was used (Demers et al., 2011). The method hypothesis was that the difference between the two means of two series of data from two columns was null.

The t test notation became:

$$t = \frac{\bar{d}}{s_d / \sqrt{n}} \quad \text{[B-6]}$$

where $\bar{d}$ was the mean of the paired differences, n was the number of paired differences and s_d was the standard deviation of the paired differences. The hypothesis (data come from the same population) was rejected when the t value obtained with the equation [B-6] was above a pre-determined value (determined in statistical tables for a two-tailed test at 95% confidence interval, n-1 was the degree of freedom). Statistical analyses were performed on alkalinity concentration at the exit of the columns since this parameter is considered representative of carbonate rocks dissolution. Then, the Fischer-Snedecor (Mendelhall and Beaver, 1994) was used to compare calcite and dolomite columns (columns 2 and 5). Result were statically different if the ratio between the variance of alkalinity in column 3 and the variance of alkalinity in column 5 was higher than a predetermined value $F_{a,b}^{0.05}$ (function of a the degree of freedom of alkalinity in column 3, b the degree of freedom of alkalinity in column 5, and for a confidence interval of 95%) which can be found in statistical table.

B.3 Results

B.3.1 Batch tests

Figure B.3 presents the evolution of AMD Lorraine's pH after contact with the four types of carbonate rock during 150 hours (anaerobic conditions). The pH after 15 hours of anaerobic conditions reached 6.0 for calcite fine, 5.8 for calcite intermediate, 5.7 for calcite coarse, and 5.5 for dolomite intermediate. Between 15 and 150 hours, the pH did not evolve significantly. Hence, the value of 15 hours recommended in the literature (Hedin et al., 1994) as the optimal hydraulic residence time is in agreement with results obtained in the present study.

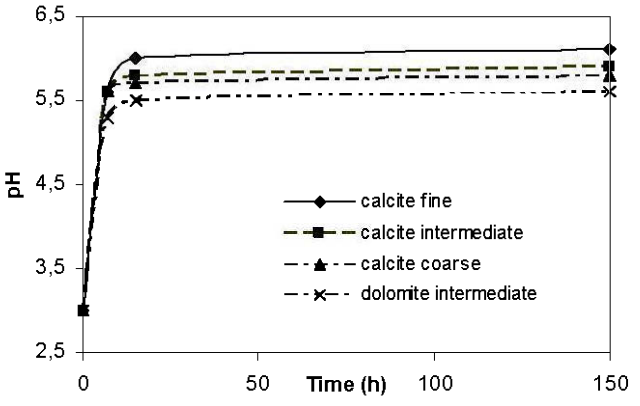

Figure B.3 pH evolution for treatment of AMD Lorraine for an anoxia period of 150 h for the batch test

The main results of the second series of batch tests, which include an aerobic period, performed with the different carbonate rocks and the two AMDs are presented in Figure B.4 and Figure B.5. With the AMD Lorraine (Figure B.4a), there was a rapid increase in pH during the first seven hours of anoxic conditions (from 3.3 to 5.6 for all calcite materials, and from 3.3 to 5.4 for the dolomite). Then, during the next eight hours, a difference in the neutralisation potentials between each calcite was observed; the water quality of the jar filled with calcite fine reached a pH of 6 while the jars filled with the calcite intermediate and calcite coarse reached a pH of 5.8 and 5.7 respectively. For the jar filled with dolomite, the pH reached 5.5 at the end of anoxic period (15 hours). After 40 hours of treatment (with 25 hours of aerobic treatment), the pH decreased to 5.1 for calcite fine, to 4.4 for calcite intermediate and coarse, and to 4.0 for dolomite intermediate. After 15 hours of anaerobic conditions (for the AMD Lorraine), the alkalinity (Figure B.4b) increased from 0 to 200 mg/L $CaCO_3$ for the calcite fine, from 0 to 160 mg/L $CaCO_3$ for the calcite intermediate, from 0 to 140 mg/L $CaCO_3$ for the calcite coarse, and from 0 to 20 mg/L $CaCO_3$ for the dolomite intermediate.

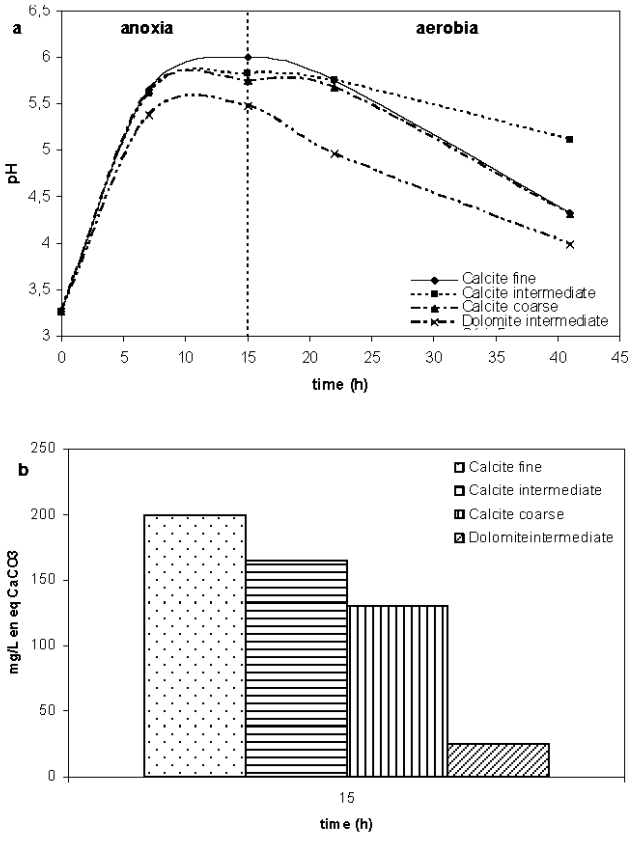

Figure B.4 Chemical parameters measured in batch test experiments for AMD Lorraine, (a) pH evolution and (b) alkalinity concentration (in mg/L $CaCO_3$) at the final time of anoxia t=15 hours (initial alkalinity was below method detection limit of 1 mg/L $CaCO_3$ in AMD)

For the AMD Light, the effluent pH (Figure B.5a) increased during the anoxic period from 5.6 to 6.2 for the calcite fine jar, to 6.0 for the calcite intermediate jar, to 5.9 for the calcite coarse jar, and to 5.7 for the dolomite intermediate jar. A pH decrease was observed after 15 hours (which corresponds to the beginning of the aerobic conditions). After 40 hours of treatment, the pH dropped to a value of 4.9 for calcite fine, of 4.7 for calcite intermediate and coarse, and to 4.6 for dolomite intermediate. The pH decrease was mainly attributed to the hydrolysis of metal and precipitation of iron hydroxide. These results confirmed that the neutralizing potential is higher for calcite than for dolomite. In addition, the finer the calcite particles were, the better was the neutralisation. For alkalinity (see Figure B.5b), a similar trend to the one of the AMD Lorraine was observed, but with lower alkalinity values:

between 140 and 40 mg/l $CaCO_3$ for the three calcites, and 20 mg/l $CaCO_3$ for the dolomite intermediate. These results confirm that a higher production of alkalinity is obtained with fine carbonate rocks, and that dolomite does not generate alkalinity as much as calcite when exposed to a less contaminated AMD (AMD Light).

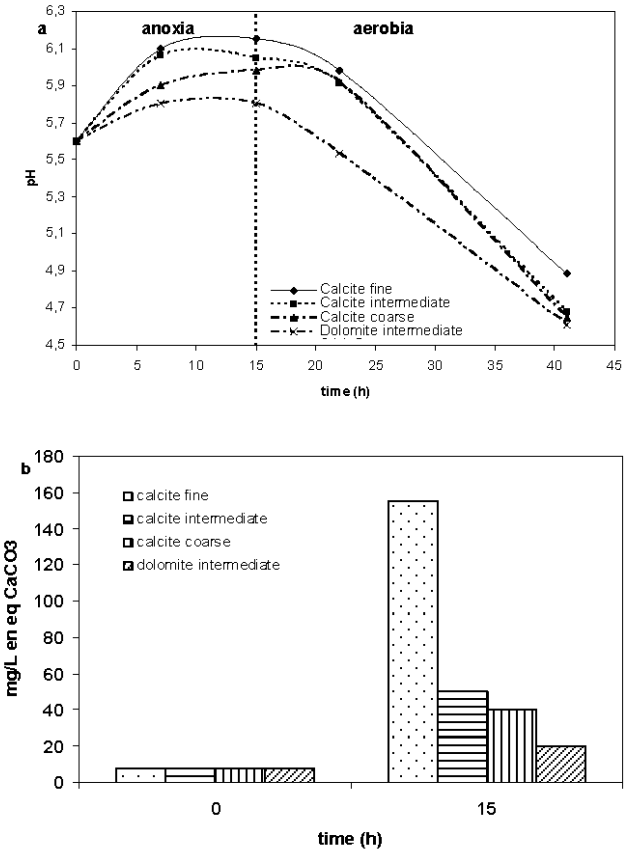

Figure B.5 Chemical parameters measured in batch test experiments for AMD Light, (a) pH evolution and (b) alkalinity concentration (in mg/L $CaCO_3$) at the initial time t=0 and final time of anoxia t= 15 hours

B.3.2 Columns tests

B.3.2.1 AMD Lorraine treatment

During the column tests, the dolomite could only increase the pH up to a value of 5.2. The pH increased to values up to 5.6, 5.8 and 6 for calcite coarse, calcite intermediate and calcite fine

respectively (Figure B.6a). These results also confirmed the impact of limestone grain size on the neutralizing capacity (the finer the calcite, the higher is the pH increase). They also showed the higher neutralizing potential of calcite compared to dolomitic rock. Moreover, the results in columns 3 and 4 (duplicate columns) indicated that the experiments were reproducible. Indeed, statistical results showed that the alkalinity concentration came from the same population for the two duplicate ($t = 0.71$, the theoretical values of t was found at 2.44 for a confidence interval of 95% and a degree of freedom of 6). The alkalinity at the columns' exit ranged between 212 and 346 mg/L $CaCO_3$ for the calcite fine, 124 and 280 mg/L $CaCO_3$ for the calcite intermediate, 56 and 100 mg/L $CaCO_3$ for the calcite coarse, and 26 and 50 mg/L $CaCO_3$ for the dolomite intermediate (Figure B.6b). As observed in batch tests, the production of alkalinity was higher for calcite than for dolomite, and fine calcite particles generated more alkalinity due to their higher unit surface area.

Results of pH evolution in the clarifier showed that the pH dropped to a value usually between 3 and 3.7 for all columns. This pH drop results from the precipitation of metals which acidified water by metal (iron mainly) hydrolysis. As a result, at the end of the treatment, the pH was comparable to the pH of the initial AMD (pH of approximately 3).

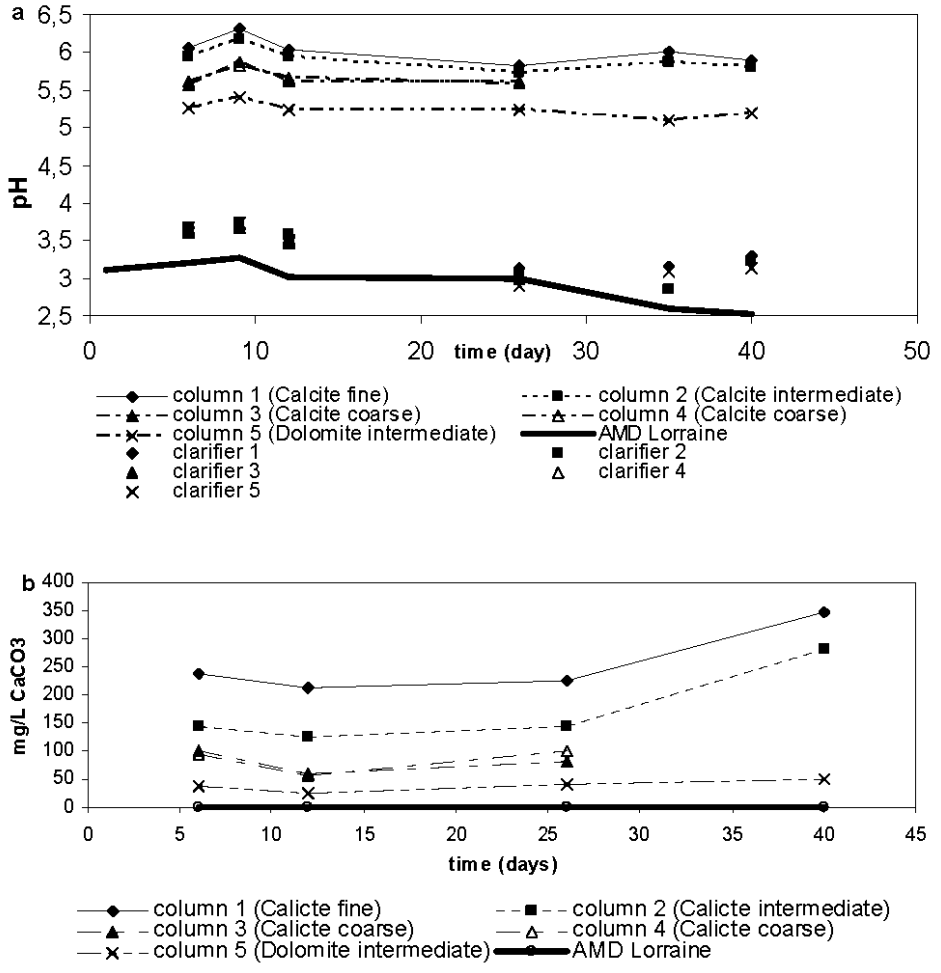

Figure B.6 Chemical parameters measured in column test experiments for AMD Lorraine: (a) pH (b) alkalinity concentration (in mg/L $CaCO_3$). Columns 1, 2, 3, 4, and 5 are filled respectively by calcite fine, calcite intermediate, calcite coarse, calcite coarse (duplicata), and dolomite intermediate. Clarifiers 1 to 5 are linked respectively to columns 1 to 5

B.3.2.2 AMD Light treatment

The pH in the column filled with the calcite fine increased from 5.5 to a maximum of 6.5 while calcite intermediate increased the pH up to a maximum of 6.4, calcite coarse to 6.3 and dolomite intermediate to 6 (Figure B.7a). The pH of columns 3 and 4 (duplicate columns) gave similar results and confirmed that the experiments were reproducible. The pH in each

clarifier varied from 3.7 to 4.8 whatever the type of carbonate rock; these values were lower than the initial AMD pH. AMD Light was prepared on a weekly basis and adjusted to pH 5.5. However, pH varied and decreased with time due to iron hydrolysis. The same observation was made by Neculita et al. (2008). The alkalinity reached a maximum concentration of 62 mg $CaCO_3$/L for calcite fine, 50 mg $CaCO_3$/L for calcite intermediate, 48 mg $CaCO_3$/L for calcite coarse and 24 mg $CaCO_3$/L for dolomite intermediate (Figure B.7b). Hence, the difference between each column towards the alkalinity production was less significant for AMD Light than for AMD Lorraine for calcite, but the difference between calcite and dolomitic rock stayed observable. In the case of AMD Light, the impact of particle size and carbonate rock mineralogy seemed to be less important than with AMD Lorraine.

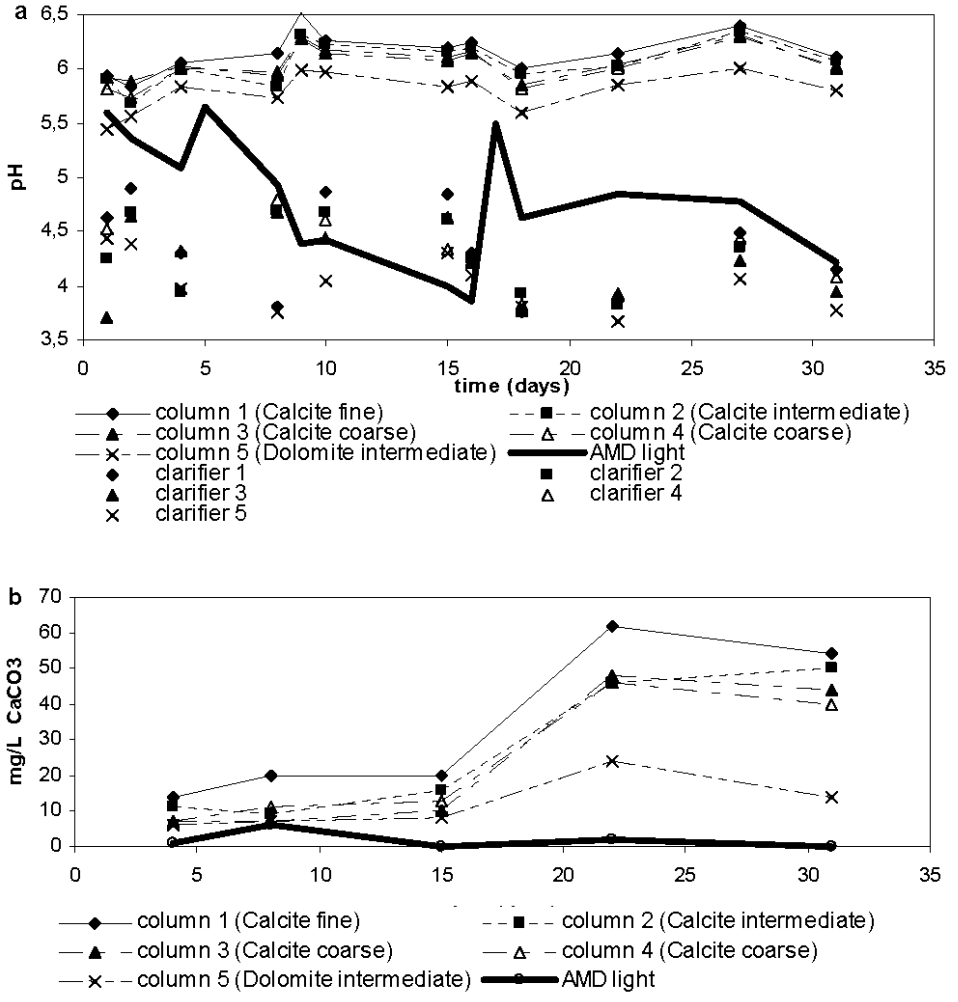

Figure B.7 Chemical parameters measured in column test experiments for AMD Light: (a) pH (b) alkalinity concentration (in mg/L $CaCO_3$). Columns 1, 2, 3, 4, and 5 are filled respectively by calcite fine, calcite intermediate, calcite coarse, calcite coarse (duplicata) and dolomite intermediate. Clarifiers 1 to 5 are linked respectively to columns 1 to 5

B.4 Results interpretation and discussion

B.4.1 Calcite and dolomite dissolution

Calcitic marble and dolomitic rock had not the same dissolution response toward AMD because alkalinity generation depends on the columns and on the AMD quality. This can be

observed in Figure B.6 to B.7, and is confirmed by statistical results that showed that alkalinity concentration at the exit of calcite intermediate and dolomite intermediate columns were significantly different. More specifically, the ratio between the variance of alkalinity in column 3 and the variance of alkalinity in column 5 (19.9) was greater than the theoretical values ($F_{7,7}^{0.05}$ = 3.8) for a confidence interval of 95% and two degrees of freedom of 7. Calcium concentration (in average) for AMD Light increased up to 181 mg/L for calcite fine, 114 mg/L for calcite intermediate, 91 mg/L for calcite coarse, 62 mg/L for dolomite intermediate. For AMD Lorraine, calcium concentration reached 324 mg/L for calcite fine, 285 mg/L for calcite intermediate, 265 mg/L for calcite coarse, and 149 mg/L for dolomite intermediate (results not shown). Figure B.8 represents the carbonate rock mass loss in each column during the experiment at 21°C. To calculate the carbonate rock mass loss, the following hypotheses were made: based on VMinteq modelling, precipitation of calcium as gypsum in ALD systems was considered negligible compared to the calcium dissolved (one mol of calcium in solution was equal to one mol of carbonate rock dissolved); and Ca concentration and water flow were stable between two measurements. A significant slope change at 57000 minutes (950 hours) was observed corresponding to the change of AMD treated, from AMD Light to AMD Lorraine. Whatever the type of carbonate rock or AMD, the curves were nearly linear and particle size did not seem to influence the dissolution rate.

However, as suggested in the literature, the weight decrease could be also approximated by equation [B-5] (see in section 2.7) which is an exponential correlation with a first order kinetic (Mukhopadhyay et al., 2007).

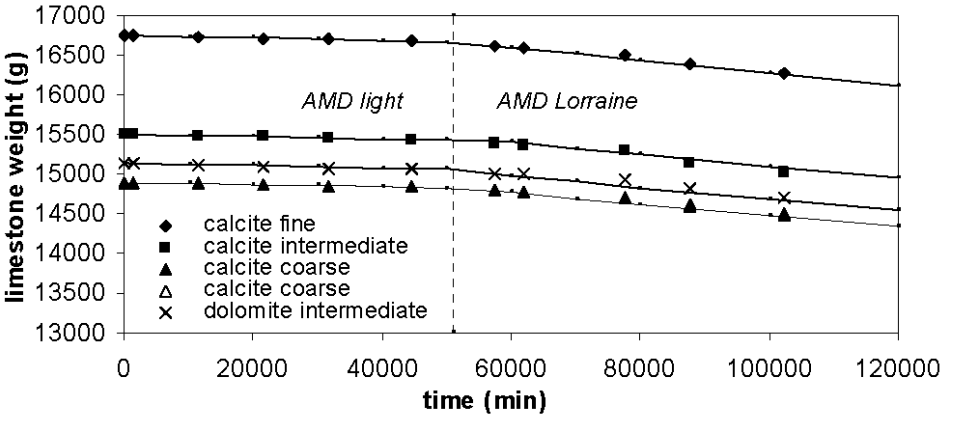

Figure B.8 Carbonate rock weight as a function of time. The calculation is based on the calcium concentration at the column exit (hypothesis: the number of moles of calcium at the column exit corresponds to the number of moles of dissolved carbonate rock). Continuous black lines represent the prediction of weight loss using equation 5 and kinetic constants given in section B.4.1

The kinetic constants k for AMD Light was 0.060 y^{-1} for calcite fine, 0.054 y^{-1} for calcite intermediate, 0.050 y^{-1} for calcite coarse and 0.048 y^{-1} for dolomite intermediate (with a correlation between experimental determination of carbonate rock mass and the first order kinetic model of R^2=0.99 for all tested materials). For AMD Lorraine, the k values were: 0.26 y^{-1} for calcite fine, 0.27 y^{-1} for calcite intermediate, 0.25 y^{-1} for calcite coarse and 0.24 y^{-1} for dolomite intermediate (with a correlation of R^2=0.98). Kinetic constant values determined by equation [B-5] showed the important role of particle size on the dissolution rate since smaller particles had higher kinetic constants. Values obtained in this experiment were in agreement with other values found in the literature. For example, Mukhopadhyay et al. (2007) show that carbonate rock dissolution can be approximated by a first order reaction and that the kinetic constant varies around 0.42 y^{-1} and Cravotta and Watzlaf (2002) found values between 0.044 y^{-1} and 0.13 y^{-1} for a number of ALDs.

Then, considering the previous values of k, it was possible to express the following order for the carbonate rock dissolution: calcite fine > calcite intermediate > calcite coarse; Perth calcitic marble > Témiscamingue dolomitic rock (for a similar particle size); Carbonate rock

dissolution in AMD Lorraine > carbonate rock dissolution in AMD Light. These previous conclusions are in accordance with the literature (e.g. Stumm and Morgan 1996; Langmuir 1997; Morse and Arvidson 2002; Hosten and Gulsun 2004; Liu et al. 2005; Potgieter et al. 2006).

Using equation [B-5], the carbonate rock weight lost with time in each column for both AMD was calculated. Calcite fine, intermediate and coarse, and dolomite intermediate would be totally dissolved (weight lost greater than 99%) after approximately 17.7, 17, 18.4, 19.2 years respectively with AMD Lorraine and after approximately 76.7, 85.3, 92.1, 95.9 years respectively with AMD Light.

B.4.2 Relation between carbonate rock dissolution and unit surface area

Results presented in the previous section showed that whatever the AMD, the finer the calcite, the better was the neutralization. This property to generate more alkalinity is essentially due to the higher unit surface area. Calcite fine had the highest unit surface area (approximately 3282 m^2/m^3 or 12.07 cm^2/g) while calcite intermediate and calcite coarse had respectively a unit surface area of 224 m^2/m^3 (0.84 cm^2/g) and 120 m^2/m^3 (0.45 cm^2/g). The dissolution of carbonate rock is governed by physicochemical surface phenomena such as diffusion, adsorption, and reaction of reagents to the surface of the solid (Morse and Arvidson, 2002). Thus, the dissolution rate of carbonate rock is greatly influenced by the unit surface area. Figure B.9 presents the daily alkalinity generated for the different columns and for the two AMDs. The influence of the unit surface area on the alkalinity production was more significant for the more acidic AMD. In this case, the finer calcite produced 2000 mg/day of alkalinity while the coarser calcite produced 650 mg/day of alkalinity. For AMD Light, the influence of unit surface area on alkalinity production was less significant. Indeed, the alkalinity production rate varied between 400 (for the calcite fine) and 200 mg $CaCO_3$/day (for the calcite intermediate and coarse).

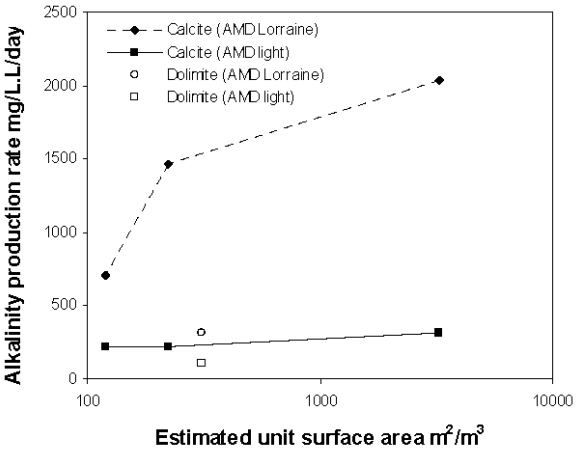

Figure B.9 Alkalinity production rate (in mg $CaCO_3$/day) versus the estimated unit surface area (in m^3/m^2)

The reactivity of carbonate rock was also a function of the AMD type and particularly of the AMD's pH. For a similar particle size, and thus for a similar unit surface area, the neutralizing potential was higher for calcite than for dolomite. Figure B.9 shows that calcite intermediate produced, in the case of AMD Lorraine, 1463 mg $CaCO_3$/day, while dolomite produced 317 mg $CaCO_3$/day (which corresponds to a ratio of 4.6). Stumm and Morgan (1996) show also that dissolution constant of calcite is higher than dolomite. It was also interesting to note that for AMD Light, the difference between the alkalinity produced by dolomite and calcite was less important than for the highly contaminated AMD Lorraine. The alkalinity produced by calcite intermediate was 221 mg $CaCO_3$/day while the one produced by dolomite intermediate was 105 mg $CaCO_3$/day (which corresponds to a ratio of 2.1).

B.4.3 Treatment of metals in ALD

ALD is usually used to treat AMD with low concentration of metals (Hedin et al., 1994). In the context of AMD from hard rock mines typically found in Canada, AMD contains high concentration of dissolved metals, which is typically treated through active lime treatment (Ritcey, 1989). Removal of metals contained in AMD was also assessed during the column tests. Results indicated that only lead, chromium, and aluminium were removed during AMD

treatment. The possible mechanisms of Pb and Cr removal could be sorption onto iron oxyhydroxides of the coating. Indeed, Voges et al. (2001) and Genç-Fuhrman et al. (2008) observed Pb and Cr sorption onto iron oxyhydroxides. Thermodynamic modeling using VMinteq v.2.53 showed that aluminium could be removed by precipitation as hydroxides. For the other metals (Fe, Zn, Mg, Mn, Ni, Cd), the acidic pH in the clarifier did not allow an effective precipitation. Only magnesium concentration increased in the last column due to the dissolution of dolomite. These observations confirmed that ALD should not be used alone to treat AMD with high dissolved metal concentrations.

After columns tests, precipitated sludge in each clarifier was collected for analysis. The XRD analysis identified the main sludge minerals: 8% of gypsum, 8% of lepidocrocite, and 84% of goethite. In addition, the thermal analysis by TGA-DSC confirmed the precipitation of secondary minerals by goethite dewatering at 250°C (Prasad et al., 2006). The precipitation of iron hydroxide was also confirmed by thermodynamic modeling. The saturation indices of goethite and lepidocrocite were both positive (ranging from 2 to 4) for all carbonate rocks studied. However, the thermodynamic modelling results (using the water quality in the clarifier) were not in agreement with the precipitation of gypsum (negative gypsum saturation index). In fact, gypsum formation was observed only at the interface between water and air. The evapo-concentration at this interface could explain gypsum precipitation. In summary, even if iron concentration did not significantly decrease in the ALD, some iron precipitated as sludge in clarifiers and as coating on carbonate rock grains.

B.4.4 Effect of particle coating on neutralization processes

Batch tests, similar to those presented in section 2.1, were performed to compare the reactivity of coated and uncoated material on the neutralization of AMD. The coated carbonate rocks came from each column used previously, after dismantling. The pH increased from an average of 3.2 at the beginning of the batch test to an average of 6 for calcite and 5.7 for dolomite after 15 hours for coated carbonate rocks. The comparison of pH results between the coated and uncoated materials showed that there was no significant change after 110 pore volumes (the test corresponded to two months or 110 pore volumes

including the treatment of AMD Light and Lorraine in column tests). Alkalinity values were similar for coated and fresh material, for both calcite and dolomite.

Coating of carbonate rock is a local precipitation phenomenon at the water-rock interface due to the acid neutralization process and alkalinity production (Santomartino and Webb, 2007). Figure B.10a and Figure B.10b presents images for coated calcite and dolomite obtained by SEM on a polished section (carbonate rocks are cut transversely and polished to allow coating descriptions). BSE images indicated that the coating was porous and thus did not really affect the alkalinity production or acidity neutralization for the tested period; similar observations were reported by Santomartino and Webb (2007). The porosity of coating was approximated by SEM picture analysis (pixels count on height pictures) to 45% for dolomite and 24% for calcite. Hence, calcite seemed to coat more easily than dolomite. This hypothesis is also suggested by many authors (e.g. Hedin et al., 1994; Booth et al., 1997; Hammarstrom et al., 2003; Huminicki and Rimstidt, 2008; Soler et al., 2008) who suggest that carbonate rock coating (due to metal hydroxide and gypsum precipitation within the drain) influence the reactivity in ALD systems. However, reactivity of carbonate rocks is not affected in the presented batch test conditions probably due to the porosity of coating.

Figure B.10a and Figure B.10b also show X-mapping of the main chemical elements observed on calcite and dolomite using the EDS technique. The X-mapping and corresponding EDS analysis indicated that the coating was mainly composed of iron oxides in both cases (calcite and dolomite), but there was also aluminium within the calcite coating. Calcium originates from the local gypsum precipitation and the aluminium presence could be explained by the precipitation of aluminium hydroxides like gibbsite during the neutralisation process (Santomartino and Webb, 2007).

XRD analyses of the precipitates (extracted by shaking coated carbonate rock between two sieves) showed the presence of iron hydroxide and gypsum. More precisely, a goethite proportion of 7%, 8%, 38%, 50% were obtained for calcite fine, intermediate, coarse, and for dolomite intermediate respectively. A lepidocrocite proportion of 4% was estimated for calcite fine, 2% for calcite intermediate, 6% for calcite coarse, 6% for dolomite intermediate. Higher gypsum concentrations were estimated by XRD analysis on coating fragments: 89%

for calcite fine, 90% for calcite intermediate, 56% for calcite coarse, and 44% for dolomite intermediate. Moreover, the thermal analysis by TGA-DSC confirmed the formation of gypsum by a weight loss peak at 125°C corresponding to the gypsum dewatering (Dweck et al., 2000). Geochemical modelling using VMinteq suggested that the conditions were favourable for the precipitation of goethite and lepidocrocite for all cases. Gypsum was close to equilibrium with a saturation index slightly lower than 0.

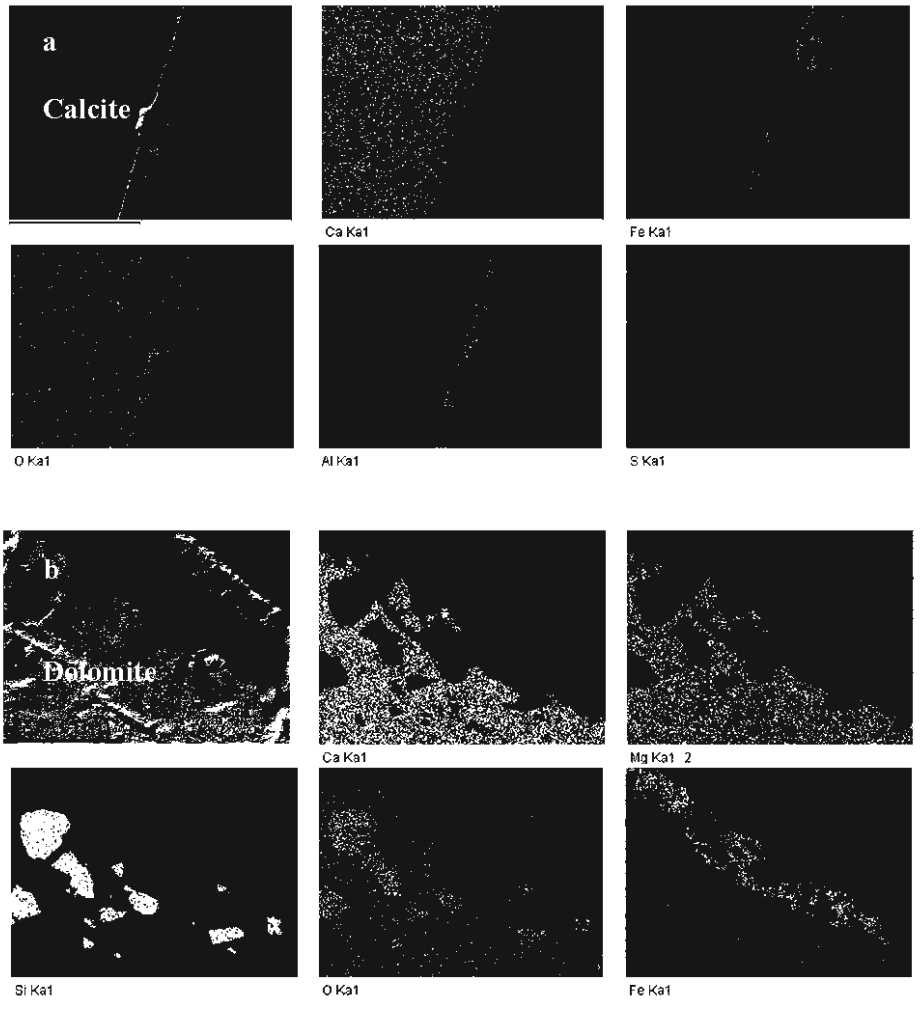

Figure B.10 SEM images of a cross section of coating and elemental maps (voltage of 20 keV, amperage of 140 A, pressure around 25 kPa, and work distance of 15 mm): (a) calcite grain and (b) dolomite grain

In agreement with the findings reported in the literature (e.g. Hammarstrom et al., 2003; Huminicki and Rimstidt, 2008; Soler et al., 2008), results obtained in this study confirmed that the use of dolomite can attenuate the risk of carbonate coating by gypsum.

B.4.5 ALD design considerations

Selection of an appropriate carbonate rock to treat AMD is a critical step for ALDs design. In this study, different particle sizes of carbonate and different mineralogy were tested to find the most efficient system. As seen in the previous section, the smaller the particle size, the greater was the alkalinity production. However, the coating contained more gypsum with fine particles of calcite than for coarse calcite. Although the coating did not affect the neutralisation performance during the present experiment, numerous authors suggest that coating, and particularly gypsum precipitation, may affect the treatment performance and could clog the system (Hedin et al., 1994, Booth et al., 1997; Hammarstrom et al., 2003; Huminicki and Rimstidt, 2008; Soler et al., 2008). Other carbonate rocks like dolomite could be used to neutralize AMD. Although the kinetics of dolomite dissolution was lower, the pH of highly contaminated AMD (AMD Light and Lorraine) was increased from 3.5 to 5.5 for a 15 hours retention time. Moreover, the alkalinity produced by dolomite was in the same order of magnitude than calcite for the AMD Light. These results suggest that anoxic dolomitic drains could be a viable alternative to anoxic calcite drains to neutralize a slightly contaminated AMD.

ALD using calcite or dolomite could not remove metals from a very contaminated AMD (see section 4.3). To respect governmental guidelines for mine water, ALD used alone is not an option. Some authors (e.g. Champagne et al., 2005, Figueroa et al., 2007), proposed a combination of ALD and sulphate reducing bacteria biofilters to treat AMD. Considering that sulphate reducing bacteria thrive at a pH near 5 (Neculita et al., 2007), Figueroa et al. (2007) propose to use ALD to increase the pH before the treatment in sulphate reducing bacteria biofilters. For the AMD tested in this study, dolomite or calcite could be used in ALDs before biofilters since both were able to increase the pH near 5. Consequently, the choice of carbonate rock would be mainly driven by the local availability of the material.

B.5 Conclusion

The role of an anoxic carbonate rock drain (ALD) aims mainly at increasing the pH and producing alkalinity. Results from batch and columns tests confirmed the capacity of the tested ALDs to do so. The AMD was neutralized to a pH between 5.5 and 6 whatever the type of carbonate rock used. Furthermore, all selected carbonate rocks were able to produce alkalinity, but at different rates. Calcite generated more alkalinity than dolomite for a similar grain size; the difference was more pronounced when a highly acidic AMD was treated. The grain size also significantly influenced the rate of alkalinity production. The finer the carbonate rock, the greater was the alkalinity production. Again, the influence of grain size on the alkalinity produced was a function of the acidity of the AMD to be treated. The impact of grain size was more significant for the highly contaminated (Lorraine) AMD than for AMD Light.

Results of this study demonstrated the importance of the carbonate rock source in an efficient ALD. Indeed, mineralogical and particle size properties played an important role in the neutralisation of AMD. A carbonate rock with a fine particle size tended to dissolve more rapidly than a coarser carbonate rock, so the lifetime of the drain would be shortened. The calcitic marble would also be more reactive than dolomitic rock for the same particle size. Hence, particle size of the carbonate rock was a critical parameter for the design of an ALD since it governs water flow (or the hydraulic retention time) and neutralisation capacity of the system. In our study, coatings formed in the drains (goethite, lepidochrocite and gypsum) did not seem to affect carbonate rock reactivity. Indeed, the alkalinity production rate with coated carbonate rocks was relatively similar to those obtained with fresh carbonate rocks.

It is worth mentioning that an ALD alone cannot successfully treat metal from a highly contaminated AMD that has a low pH and contains high concentrations of dissolved metals. A one step treatment in ALD was not efficient to significantly decrease the pollution of high iron concentrated AMD as AMD (Lorraine and Light). Indeed, iron present in the ALD effluent could decrease the pH due to the oxidation of ferrous ions and the precipitation of iron oxyhydroxides. Multi-step treatment is required in this case. Therefore, to be efficient,

ALD should be combined with other passive treatment methods such as sulphate-reducing bacteria bioreactors or engineered wetlands to remove metals.

Acknowledgements

This research was supported by the Natural Sciences and Engineering Research Council of Canada (NSERC) through the Industrial NSERC Polytechnique/UQAT Chair in Environment and Mine Waste Management. The authors gratefully acknowledge the industrial and governmental partners of the Chair for the funding of this study and the OMYA Company for providing carbonate rock material.

References

APHA, 1995. Alkalinity titration. In: Greenberg A (ed) Standard methods for the examination of water and wastewater, 19th edn. Washington DC.

Aubertin, M., Bussière, B., Bernier, L., 2002. Environnement et gestion des rejets miniers. Edition Presses internationales Polytechnique, Montréal.

Barley, W., Hutton, T.C., Brown, M.M.E., Cusworth, J.E., Hamilton, T.J., 2005. Trends in biomass and metal sequestration associated with reeds and algae at Wheal Jane Biorem pilot passive treatment plant. Sci. Total Environ. 345, 279-286.

Benzaazoua, M., Bussiere, B., Dagenais, A.M., Archambault, M., 2004. Kinetic tests comparison and interpretation for prediction of the Joutel tailings acid generation potential. Environ. Geol. 46, 1086-1101.

Bernier, L., 2005. The potential use of serpentinite in the passive treatment of acid mine drainage: batch experiment. Environ. Geol. 47, 670-684.

Blowes, D.W., Ptacek, C.J., 1994. Acid-neutralization mechanisms in inactive mine tailings. In: Jambor JL, Blowes DW (ed). Short Course Handbook on Environmental Geochemistry of Sulfide Mine-Waste, Mineralogical Association of Canada. Special Vol. 22, pp 272-292.

Booth, J., Hong, Q., Compton, R., Prout, K., Payne, R., 1997. Gypsum overgrowths passivate calcite to acid attack. J. Colloid. Interface Sci. 192, 207-214.

Champagne, P., Van Geel, P., Parker, W., 2005. A bench-scale assessment of a combined passive system to reduce concentrations of metal and sulphate in acid mine drainage. Mine Water Environ. 24, 124-133.

Chapuis, R.P., Légaré, P.P., 1992. A simple method for determining the surface area of fine aggregates and fillers in bituminous mixtures. In Meininger RC (ed) Effects of aggregates and mineral fillers on asphalt mixture performance, ASTM STP 1147. Philadelphia, pp 177–186.

Cravotta, C.A., Ward, S.J., Hammarstrom, J.M., 2008. Downflow limestone beds for treatment of net acidic, oxic, iron-laden drainage from a flooded anthracite mine, Pennsylvania, USA-2. Laboratory evaluation. Mine Water Environ. 27, 86-99.

Cravotta, C.A., 2003. Size and performance of anoxic limestone drains to neutralize acidic mine drainage. J. Environ Qual. 32, 1277-1289.

Cravotta, C.A., Watzlaf, G., 2002. Design and performance of limestone drains to increase pH and remove dissolved metals from acidic mine drainage. In: Naftz DL, Morrison SJ, Fuller CC, Davis JA (Ed), Handbook of groundwater remediation using permeable reactive barriers, Academic press, Amsterdam, pp 19-66.

Cravotta, C.A., Trahan, M.K. 1999. Limestone drains to increase pH and remove dissolved metals from acidic mine drainage. Appl. Geochem. 14, 581-606.

Demers, I., Bussière, B., Aachib, M., Aubertin, M., 2011. Repeatability evaluation of instrumented column tests in cover efficiency evaluation for the prevention of acid mine drainage. Wat. Air Soil Pollut. 219, 113-128.

Dweck, J., Buchler, P.M., Vieira Coehlo, A.C., Cartledge, F.K., 2000. Hydration of a Portland cement blended with calcium carbonate. Thermochimica Acta 346, 105-113.

Figueroa, L., Miller, A., Zaluski, M., Bless, D., 2007. Evaluation of a two stage passive treatment approach for mining influenced water. In: RI Barnishel (Ed) National meeting of the ameriacan society of mining and reclamation, Gillette, WY, 30 years of SMCRA and Beyond June 2-7, 2007, Lexington, pp 238-247.

Genç-Fuhrman, H., Wu, P., Zhou, Y., Ledin, A., 2008. Removal of As, Cd, Cr, Cu, Ni and Zn from polluted water using an iron based sorbent. Desalination 226, 357-370.

Hammarstrom, J.M., Sibrell, P.L., Belkin, H.E., 2003. Characterization of limestone reacted with acid-mine drainage in a pulsed limestone bed treatment system at the Friendship Hill National Historic Site Pennsylvania, USA. Appl. Geochem. 18, 1705-1721.

Hedin, R.S., Nairn, R.W., Kleinmann, R.L.P., 1994. Passive treatment of coal mine drainage. US Bureau of Mines IC 9389, Pittsburgh.

Herman, J.S., White, W.B., 1985. Dissolution kinetics of dolomite-Effects of lithology and fluid flow velocity. Geochem. Cosmochem. Acta 49, 2017-2026.

Hosten, G., Gulsun, M., 2004. Reactivity of limestone from different sources in Turkey. Miner. Eng. 17, 97-99.

Huminicki, D.M.C., Rimstidt, J.D., 2008. Neutralization of sulfuric acid solutions by calcite dissolution and the application to anoxic limestone drain design. Appl. Geochem. 23, 148-165.

Kleinmann, R.L.P., Crerar, D.A., Pacelli, R.R., 1981. Biogeochemistry of acid mine drainage and a method to control acid formation. Miner. Eng. 81, 300-304.

KTH, 2010. Visual MINTEQ A free equilibrium speciation model, version 3.0, beta version. http://www.lwr.kth.se/English/OurSoftware/vminteq/index.html. Accessed 15 September 2010.

Langmuir, D., 1997. Aqueous Environmental Geochemistry. Prentice-Hall, USA.

Lindsay, M., Ptacek, C., Blowes, D., Gould, D., 2008. Zero-valent iron and organic carbon mixtures for remediation of acid mine drainage: Batch experiments. Appl. Geochem. 23, 2214-2225.

Liu, Z., Yuan, D., Dreybrot, W., 2005. Comparative study of dissolution rate determinating mechanisms of limestone and dolomite. Environ. Geol. 49, 274-279.

Mendelhall, W., Beaver, R.J., 1994. Introduction to probability and statistics, Duxbury Press, Belmont.

Monoret, C., 2001. Traitement d'effluent concentrés par culture fixée sur gravier ou pouzzolane. PhD thesis, University de Montpellier II.

Morin, K., Hutt, N., 2001. Prediction of minesite-drainage chemistry through closure using operational monitoring data. J. Geochem. Explor. 73, 123-130.

Morse, J.W., Arvidson, R.S., 2002. Dissolution kinetics of major sedimentary carbonate minerals. Earth Sci. Rev. 58, 51-84.

Morse, J.W., 1983. The kinetics of calcium carbonate dissolution and precipitation. Rev. Mineral Geochem. 11, 227-264.

Mukhopadhyay, B., Bastias, L., Mukhopadhyay, A., 2007. Limestone drain design parameters for acid rock drainage mitigation. Mine Water Environ. 26, 29-45.

Neculita, C.M., Zagury, G.J., 2008. Biological treatment of highly contaminated acid mine drainage in batch reactors: Long-term treatment and reactive mixture characterization. J. Hazard. Mater. 157, 358-366.

Neculita, C.M., Zagury, G.J., Bussière, B., 2008. Effectiveness of sulfate-reducing passive bioreactors for treating highly contaminated acid mine drainage: I Effect of hydraulic retention time. Appl. Geochem. 23, 3442-3451.

Neculita, C.M., Zagury, G.J., Bussière, B., 2007. Passive treatment of acid mine drainage in bioreactors using sulphate-reducing bacteria: critical review and research needs. J. Environ. Qual. 36, 1-16.

Potgieter, V.S.S., Potgieter, J.H., Monama, P., Van Grieken, R., 2006. Comparison of limestone, dolomite and fly ash as pre-treatment agents for acid mine drainage. Miner. Eng. 19, 454-462.

Potvin, R., 2009. Évaluation à différentes échelles de la performance de systèmes de traitement passif pour des effluents fortement contaminés par le drainage minier acide. PhD dissertation, UQAT, QC, Canada, 365 p.

Prasad, P.S.R., Prasad, S., Krishna, V., Babu, E.V.S.S.K., Sreedhar, B., Ramana, S., 2006. In situ FTIR study on the dehydration of natural goethite. J. Asian Earth Sci. 27, 503-511.

Ritcey, G.M., 1989. Tailings Management, Problems and Solutions in the Mining Industry. Elsevier, Amsterdam.

Robinson-Lora, M., Brennan, R., 2009. Efficient metal removal and neutralization of acid mine drainage by crab-shell chitin under batch and continuous-flow conditions. Appl. Geochem. 23, 2214-2225.

Santomartino, S., Webb, J.A., 2007. Estimating the longevity of limestone drains in treating acid mine drainage containing high concentrations of iron. Appl. Geochem. 22, 2344-2361.

Skousen, J.G., Ziemkiewicz, P.F., 2005. Performance of 116 Passive Treatment Systems for Acid Mine Drainage. In: National meeting of the american society of mining and reclamation, Breckenridge, CO, June 19-23, 2005, Lexington, pp 1100-1133.

Soler, J.M., Boi, M., Mogollon, J.L., Cama, J., Ayora, C., Nico, P.S., Tamura, N., Kunz, M., 2008. The passivation of calcite by acid mine water: Column experiments with ferric sulfate and ferric chloride solutions at pH 2. Appl. Geochem. 23, 3579-3588.

Stumm, W., Morgan, J., 1996. Aquatic chemistry. 3rd edn. Wiley Interscience Publication, New York.

Voges, L., Mark, P.E., Benjamin, M., Chang, Y., 2001. Use of iron oxides to enhance metal removal in crossflow microfiltration. J. Environ. Eng. Sci. 41, 1-419.

Watzlaf, G.R., Hedin, R.S., 1993. A method for predicting the alkalinity generated by anoxic limestone drains. In: 14th annual meeting Surface Mine Drainage Task Force, West Virginia University, Morgantown.

APPENDICE C

RÉSULTATS DES ESSAIS DE TRAITEMENT DU DMA AVEC DE LA TOURBE

Dans cet essai préliminaire, une colonne (14 cm de diamètre et 70 cm de hauteur) contenant de la tourbe de sphaigne (dont les propriétés principales sont présentées au Tableau C.1) a été alimentée par un DMA riche en fer (autour de 4000 mg/L). Le temps de rétention de la colonne est d'approximativement 3 jours. Les Figures C.1 et C.2 présentent respectivement l'évolution du pH et de la concentration en fer en sortie de colonne. Il est alors possible de remarquer que le pH après traitement est similaire à celui du DMA et que le fer n'est pas retenu. Ainsi, la tourbe n'a pas été retenue pour une étude en filière de traitement.

Tableau C.1 Caractéristiques de la tourbe

Densité	Humidité	Carbone organique total	Azote total Kjeldahl	Capacité échange cationique (meq/100 mg)	BSR (Cellules /100ml)	pH de pâte
1,47	42%	48%	0,9%	111,2	<2	5,5

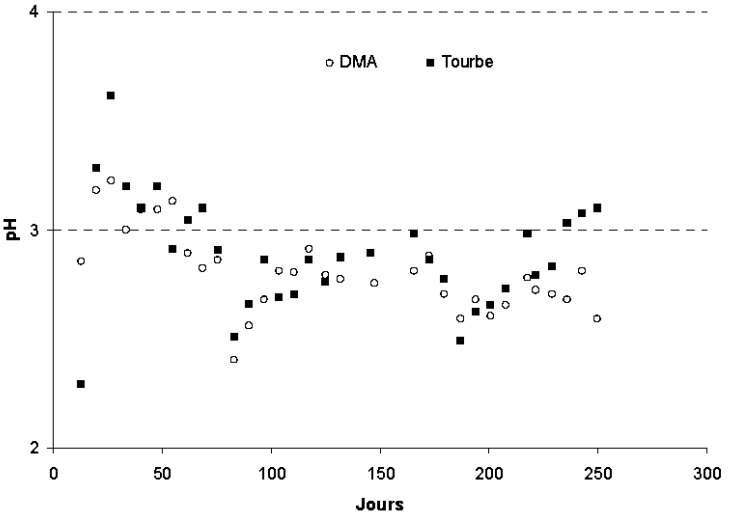

Figure C.1 Évolution du pH en sortie de colonne

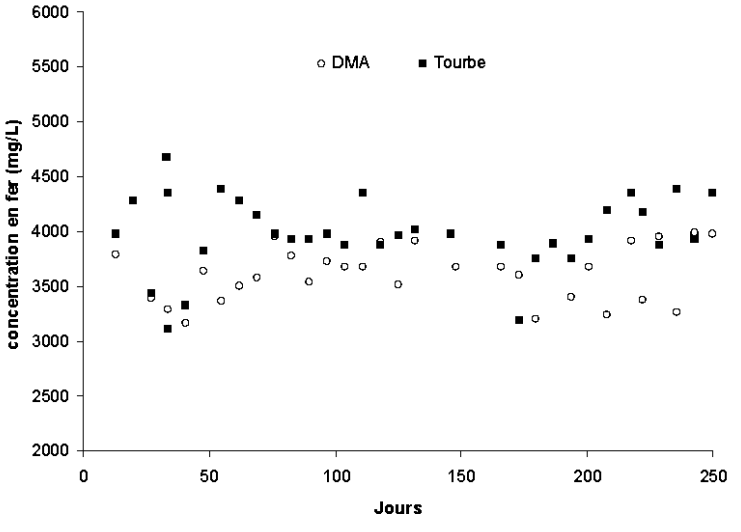

Figure C.2 Évolution de la concentration en fer en sortie de colonne

APPENDICE D

PHOTOGRAPHIES DES ESSAIS EN LABORATOIRE

(Sur CD-ROM)

APPENDICE E

RÉSULTATS BRUTS DES ESSAIS EN BATCH ET LEURS CARACTÉRISATIONS

(Sur CD-ROM)

APPENDICE F

CARACTÉRISATION INITIALE DES MATÉRIAUX UTILISÉS

(Sur CD-ROM)

APPENDICE G

RÉSULTATS BRUTS DES ESSAIS DE SORPTION

(Sur CD-ROM)

APPENDICE H

RÉSULTATS BRUTS DES ESSAIS EN COLONNES

(Sur CD-ROM)

APPENDICE I

RÉSULTATS BRUTS DE L'ESSAI EN MODÈLE INTERMÉDIAIRE

(Sur CD-ROM)

APPENDICE J

RÉSULTATS BRUTS DE LA CARACTÉRISATION APRÈS DÉMANTELLEMENT DES COLONNES ET DU MODÈLE

(Sur CD-ROM)